

University of Fort Hare
Together in Excellence

**Grain size analysis, coastal hydrodynamics and erosion
protection: a case study from Knysna and Plettenberg Bay,
South Africa**



Ayabulela Raymond Pezisa

(201516104)

University of Fort Hare
Together in Excellence

A dissertation submitted in fulfilment of the requirements for the Degree of

Master of Science in Geology

Department of Geology, Faculty of Science and Agriculture

University of Fort Hare

Supervisor: Professor Ken Liu

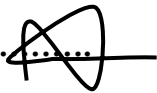
December 2022

DECLARATION

I, Ayabulela Raymond Pezisa with the student number: 201516104 hereby declare that the research project represented in this dissertation was conducted by myself under the supervision of Professor Ken Liu in the Department of Geology, University of Fort Hare. The research reported in this thesis, except where otherwise indicated, contains the original research results and has not been previously accepted or concurrently submitted to any other university for any degree award or examination purposes. I am conscious of the University of Fort Hare's policy on plagiarism and I have laid hold of each precaution to comply with the regulations.

I, therefore, submit the dissertation for examination and award of the Degree of Master of Science (Geology) at the University of Fort Hare.

Signature



At the Department of Geology
Faculty of Science and Agriculture
University of Fort Hare
South Africa



Date: 28 November 2022

University of Fort Hare
Together in Excellence

ACKNOWLEDGEMENTS

The major core I would like to thank is God and my Ancestors (Maduna noo Tolo) for protecting me, the inner strength and energy I got during the process and, the determination to complete the research project. I extend my gratitude to my supervisor Prof Ken Liu who supported, motivated and consistently revealed interest in this research project. In addition, with the humility he showed me precious advice and supervision, I sincerely thank him from the bottom of my heart.

I am deeply grateful for the emotional support, encouragement, and financial assistance from my parents and siblings at all times. I would like to thank National Research Foundation (NRF) and South African Institute for Aquatic Biodiversity (SAIAB) for the funds for this research project.

I would like to thank the staff of the Department of Geology, the University of Fort Hare for their support and contributions to my research project.

Last but not least, I would like to appreciate Lutho Best for his presence and, being helpful during the field trip. I wish to acknowledge the help of Mr. Michael Katwire in preparing the thin-sections for the analysis.



University of Fort Hare
Together in Excellence

ABSTRACT

The modern beach sands and Cretaceous Knysna Formation distributed along the coast of Plettenberg Bay and Knysna coast in the Western Cape Province of South Africa, have been examined and studied in the field outcrops and laboratories via grain-size analysis, XRD, SEM, EDX and microscope petrography analyses.

This study looked into the coastal hydrodynamics and environment protection. The project aims to investigate the sediment distribution, grain-size variation, sedimentary structures, coast erosion and mitigation in the Plettenberg and Knysna coast to address environmental issues in the south coast of South Africa. The research will provide new insight onto coastal sedimentation, hydrodynamic condition, coastline erosion and the safety of the coastal environment and human property. The study will promote government attention on the sea level change, which caused flooding and environmental disaster along the south coastal area of South Africa.

The rock sequence in the inland side of the study areas belongs to Cretaceous Knysna Formation, which comprises seven upward fining sequences. The stratigraphic sequence is underlain by the Table Mountain quartzite of the Cape Supergroup, and is overlain by Tertiary sediments and modern coastal dune sands. The Knysna Formation at the research area consists of massive conglomerate, sandstone and minor mudstone of mainly fluvial dominated sediments.

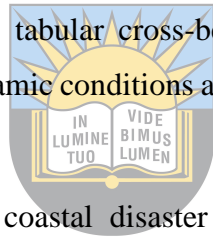
The grain size analysis reveals that the modern fluvial channels at Plettenberg Bay and Knysna areas are of dominant coarse sands with minor silt and mud, which defines the sediments were deposited by moderate to high energy currents. Whilst the beach zones in Plettenberg Bay are predominated by fine to medium-grained marine sands. Grain-size analyses of beach sands show well-sorted, fine to coarse skewed in grain size distribution, indicating a relative lower to medium uniform energy condition during transportation and deposition. The bivariate plots of grain-size distribution demonstrate of the shallow agitated marine environment with the influence of tide and aeolian processes. Hydrodynamic condition in the beach area was more persistent and less variation compared to the river environment.

The mineralogy and petrology studies revealed that in Plettenberg Bay and Knysna sediments are predominantly consisted of minerals quartz, feldspar, calcite, muscovite, aragonite, clay minerals,

and salts (halite). Skeletal carbonate minerals (shell and coral fragments) are more than chemical precipitated carbonate minerals.

The microtextures detected on the surface of the fluvial and marine sand grains involve V-shaped pits, upturn pits, dissolution pits and secondary mineral precipitation that were created by chemical and mechanical processes formed via sea-water dissolution, corrosion, and transport crashing. Whereas the boring holes and burrows created by activity of microorganisms boing into the surface of the grains. These microtextures of the river and beach sands exhibit a shallow marine and fluvial environments with medium to high energy conditions and active organic activities.

Several sedimentary structures were detected in the coastal environments, including various types of ripple marks and dunes, burst bubble-hole, swash line, rill marks, rhomboid marks, burrows, boring and bioturbation, planar lamination and gravel pavement. In addition, sedimentary structures were also identified in the Cretaceous Knysna Formation such as air/water escape hole, convolute bedding, lenticular bedding, tabular cross-bedding and load cast. The sedimentary structures closely linked with hydrodynamic conditions and therefore can be used as indicators for depositional environments.



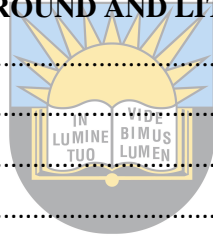
Flooding and erosion had become a coastal disaster that results in sediment redistribution throughout the coastal system and therefore caused landscape reform like coastal cliffs and sharpened dunes in erosive areas. Particularly, coastal hazards become more and more serious in recent years due to climate and sea level changes. Thus, to recognise coastal erosion and disaster and make a management strategy is of significant importance to compete against coastline retreat and to protect infrastructure and human safety in the coast area.

The author had proposed a number of mitigation methods for environmental protection and for combating coastal erosion, including breakwaters, groins, jetties, vertical walls, rock armour, vegetation, boundary hardening, and revetment etc, which are the effective ways for protection of coast retreat, property damage and human safety.

Keywords: Grain-size analysis, coastal hydrodynamics, grain surface texture, sedimentary structures, coast erosion, environment protection.

TABLE OF CONTENTS

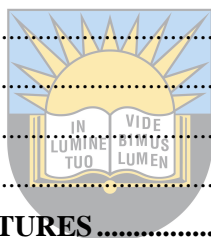
DECLARATION	ii
ACKNOWLEDGEMENTS	iii
ABSTRACT	iv
TABLE OF CONTENTS	vi
LIST OF FIGURES	xii
LIST OF TABLES	xviii
CHAPTER 1: INTRODUCTION	1
1.1 Coastal hydrodynamics and erosion	1
1.2 Background of the Plettenberg Bay and Knysna Area	2
1.3 Study areas and geological map.....	3
1.5 Aims and objectives of the study	6
1.6 Research questions and the significance of the study	7
CHAPTER 2: GEOLOGICAL BACKGROUND AND LITERATURE REVIEW	9
2.1 Uitenhage Group.....	9
2.1.1 Enon Formation	9
2.1.2 Kirkwood Formation.....	11
2.1.3 Sundays River Formation.....	13
2.1.4 Knysna Formation.....	14
2.2 Quaternary Sediments.....	15
2.2.1 Distribution of sediments in the Keurbooms estuary (Plettenberg Bay).....	16
2.2.2 Distribution of sediments in the Knysna estuary	16
2.3 Cross-shore sediment transport.....	17
2.4 Types of coast	18
2.4.1 Cliff coast.....	18
2.4.2 Clayey bank coast	19
2.4.3 Muddy coast.....	20
2.4.4 Dune/Sandy coast.....	21
2.5 Processes of coastal erosion.....	23
2.6 Erosional landforms	23
2.7 Causes of Coastal Erosion	24
2.7.1 Tide currents	24
2.7.2 Sea-Level-change	24



University of Fort Hare
Together in Excellence

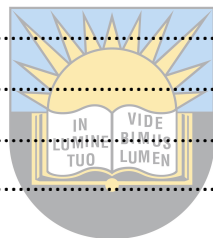
2.7.3 River Mouth Changes	25
2.7.4 Aeolian (wind) erosion and wave action.....	25
2.7.5 Climate change.....	27
2.7.6 Cross-shore sand loss	27
2.8 Coastal flooding.....	28
CHAPTER 3: METHODOLOGY.....	30
3.1 Introduction.....	30
3.2 Desktop study	30
3.3 Fieldwork method	30
3.4 Laboratory methods	33
3.4.1 Grain-size analysis	33
3.4.1.1 Grain-size parameters	34
3.4.1.2 Grain-size Sieving Analysis.....	36
3.4.2 Classification of grain-size and grain-size distribution.....	38
3.4.3 X-Ray Diffraction Analysis (XRD Analysis)	40
3.4.4 Scanning Electron Microscopy (SEM) and Energy-Dispersive X-Ray Spectrometer (EDX/EDS) Analysis	41
3.5 Geological apparatus used during the field and lab research include:	42
CHAPTER 4: STRATIGRAPHY OF KNYSNA FORMATION.....	44
4.1 Rock types of the Knysna Formation.....	44
4.2. Stratigraphic profile of the Knysna Formation.....	45
CHAPTER 5: GRAIN SIZE ANALYSIS	53
5.1 Introduction.....	53
5.2 Grain size measurements	54
5.3 Moderately to Well sorted River samples.....	57
5.4 Poorly sorted River samples	60
5.5 Grain size parameters for river sample analysis	64
5.5.1 Discussion on grain size parameters	66
5.6 Beach sample analysis (Well sorted samples)	67
5.7 Grain size statistical parameters of beach sediments	71
5.7.1 Discussion.....	74
5.8 Inter-relationship of grain size parameters (Bivariate plots).....	78
5.8.1 Discussion.....	78
5.9 Conclusion	84
CHAPTER 6: PETROGRAPHY AND MINERALOGICAL COMPOSITION	85

6.1 Introduction.....	85
6.2 Mineral and fossil compositions	85
6.2.1 Quartz (SiO ₂).....	86
6.2.2 Feldspar.....	87
6.2.3 Muscovite.....	90
6.2.3 Organic pellet.....	90
6.2.4 Lithic fragments.....	91
6.2.5 Calcite (CaCO ₃)	91
6.2.6 Sponge.....	93
6.3 X-ray diffraction (XRD) results.....	93
CHAPTER 7: GRAIN SURFACE TEXTURE AND MORPHOLOGY.....	97
7.1 Introduction.....	97
7.2 V-shape pits	97
7.3 Upturned plates	98
7.4 Secondary mineral precipitation	99
7.5 Dissolution pits/pores	102
7.6 Burrow and boring holes.....	102
7.7 Mineral recrystallization	104
CHAPTER 8: SEDIMENTARY STRUCTURES	105
8.1 Introduction.....	105
8.2 Flow regime	105
8.3 Beach sedimentary-structures	106
8.3.1 Ripple mark and dune	106
8.3.1.1 Catenary ripples	108
8.3.1.2 Straight ripples	108
8.3.1.3 Sinuous ripples.....	109
8.3.1.4 Lunate/linguoid ripples	109
8.3.1.5 Rhomboid marks	110
8.3.2 Groove mark	111
8.3.3 Swash line	112
8.3.4 Disc-shaped pebble	112
8.3.5 Burrows.....	113
8.4 River sedimentary structures.....	114
8.4.1 Boring and bioturbation	114



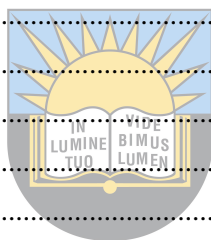
University of Fort Hare
Together in Excellence

8.4.2 Planar lamination	115
8.4.3 Gravel pavement	115
8.5 Cretaceous Knysna Formation sedimentary-structures.....	116
8.5.1 Air escape holes	116
8.5.2 Bedding structure	117
8.5.2.1 Lenticular bedding	118
8.5.2.2 Tabular cross-bedding.....	118
8.5.2.3 Deformation bedding	119
8.5.2.4 Load cast	120
CHAPTER 9: COASTAL EROSION	122
9.1 Introduction.....	122
9.2 Causes of erosion	122
9.3 Impacts of erosion.....	123
9.4 Types of coastal erosion.....	123
9.4.1 Water erosion	123
9.4.2 Wind erosion	125
9.5 Damages of coastal erosion	125
9.5.1 The shoreline erosion	126
9.5.2 The wave-cut platform cliff	127
CHAPTER 10: MITIGATION METHODS FOR COASTAL EROSION.....	129
10.1 Introduction.....	129
10.2 Hard engineering solution.....	129
10.2.1 Groins.....	129
10.2.2 Jetties.....	131
10.2.3 Breakwaters.....	131
10.2.4 Seawalls	132
10.2.5 Revetments.....	132
10.2.6 Rock armour (rip-rap)	133
10.3 Soft engineering solution	134
10.3.1 Dune restoration/vegetation	134
10.3.2 Beach nourishment.....	136
CHAPTER 11: DISCUSSION AND CONCLUSION.....	138
RECOMMENDATIONS.....	142
REFERENCES.....	143



University of Fort Hare
Together in Excellence

APPENDICES	166
APPENDIX A: GRAIN SIZE ANALYS	166
A.1 Sample P2	166
A.2 Sample P3	167
A.3 Sample P4	168
A.4 Sample P6	169
A.5 Sample P9	170
A.6 Sample K2.....	171
A.7 Sample K3.....	172
A.8 Sample P15	173
A.9 Sample P16	174
A.10 Sample P17	175
A.11 Sample P18	176
A.12 Sample P19	177
A.13 Sample P20	178
A.14 Sample P21	179
A.15 Sample P22	180
A.16 Sample P23	181
A.17 Sample P24	182
A.18 Sample P25	183
A.19 Sample P26	184
A.20 Sample P27	185
A.21 Sample P28	186
A.22 Sample P29	187
A.23 Sample P30	188
A.24 Sample P31	190
A.25 Sample P32	191
A.26 Sample P33	192
A.27 Sample P34	193
A.28 Sample P35	194
A.29 Sample P36	195
A.30 Sample P37	196
A.31 Sample P38	197
A.32 Sample P39	198
A.33 Sample P40	199



University of Fort Hare
Together in Excellence

A.34 Sample P41	200
A.35 Sample P42	201
A.36 Sample P43	202
A.37 Sample P44	203
A.38 Sample P45	204
A.39 Sample P46	205
A.40 Sample P47	206
A.41 Sample P48	207
A.42 Sample P49	207
A.43 Sample P50	208



University of Fort Hare
Together in Excellence

LIST OF FIGURES

FIGURE 1.1: GEOGRAPHIC MAP SHOWING THE STUDY AREAS, KNYSNA AND PLETTENBERG BAY OF WESTERN CAPE PROVINCE OF SOUTH AFRICA.	4
FIGURE 1.2: GEOLOGICAL MAP SHOWS THE AREAS WHERE UITENHAGE GROUP OUTCROP (ROBERT ET AL., 2015).	5
FIGURE 1.3: TYPICAL BEACH PROFILE (HTTP://THEBRITISHGEOGRAPHER.WEEBLY.COM/COASTS-OF-EROSION-AND-COASTS-OF-DEPOSITION.HTML).....	6
FIGURE 2.1: PHOTOGRAPH SHOWING AN OUTCROP OF ENON FORMATION CONGLOMERATE FORMED BY ALLUVIAL CHANNEL IN THE GAMTOOS VALLEY, EASTERN CAPE, SOUTH AFRICA.	11
FIGURE 2.2: PHOTOGRAPH SHOWING INTERBEDDED POROUS MEDIUM TO COARSE-GRAINED SANDSTONE WITH BROWNISH FINE CONGLOMERATE LAYER (TOP) OF KIRKWOOD FORMATION.....	12
FIGURE 2.3: PHOTOGRAPH SHOWING SUNDAYS RIVER FORMATION DOMINATED BY MUDSTONE WITH ALTERNATED SILTSTONE AND SANDSTONE LAYERS.	14
FIGURE 2.4: PHOTOGRAPH SHOWING AN OUTCROP OF KNYSNA FORMATION ALONG THE N2 ROAD AT KNYSNA.	15
FIGURE 2.5: PHOTOGRAPH SHOWING HARD ROCK “CLIFF COAST” (ONLINE GOOGLE SEARCH PHOTO).	19
FIGURE 2.6: PHOTOGRAPH SHOWING SEMI-HARD ROCK “CLAYEY BANK” COAST.	20
FIGURE 2.7: PHOTOGRAPH SHOWING THE MUDDY COAST AT PLETTENBERG BAY AT WESTERN CAPE.	21
FIGURE 2.8: PHOTOGRAPH SHOWING SANDY COAST AND SWASH-LINE AT THE BEACH OF PLETTENBERG BAY.	22
FIGURE 2.9: PHOTOGRAPH SHOWS WAVE EROSION ALONG THE SHORE OF SOUTH COAST OF SOUTH AFRICA.	26
FIGURE 2.10: AERIAL IMAGE REVEALING COASTAL FLOODING IN PORT ELIZABETH, SOUTH AFRICA.	29
FIGURE 3.1: LOCATION OF THE SAMPLING STATIONS IN PLETTENBERG BAY ALONG WITH THE KEURBOOMS RIVER AND BEACH ENVIRONMENT (ONLINE GPS IMAGE).	31
FIGURE 3.2: PHOTOGRAPH SHOWING DOLERITE BLOCK TO PROTECT EROSION ALONG THE GARDEN ROUTE COAST OF KNYSNA.	32

FIGURE 3.3: PHOTOGRAPH SHOWING THE KNYSNA ESTUARINE FLOODPLAIN.	32
FIGURE 3.4: LOCATION OF THE SAMPLING STATIONS ALONG KNYSNA ESTUARY (ONLINE GPS IMAGE)...	33
FIGURE 3.5: EQUIPMENT AND METHODS FOR GRAIN-SIZE SIEVE ANALYSIS.	38
FIGURE 3.6: CLASSIFICATION OF SEDIMENTS AND SEDIMENTARY ROCKS BASED ON THE GRAIN SIZE (FRIEDMAN & SANDERS, 1978; BLOTT & PYE, 2001).....	39
FIGURE 3.7: JEOL JSM-6390 LV MODEL OF SCANNING ELECTRON MICROSCOPE.....	42
FIGURE 4.1: FIELD OUTCROP OF THE KNYSNA FORMATION ALONG THE ROAD N2 GARDEN ROUTE AT KNYSNA. (A) TYPICAL CLAST-SUPPORTED CONGLOMERATE, AND (B) RED-BROWNISH SANDSTONE INTERCALATED WITH THIN MUDSTONE.....	44
FIGURE 4.2: CLAST-SUPPORTED CONGLOMERATE WITH LENTICULAR BROWNISH SANDSTONE OF KNYSNA FORMATION.....	46
FIGURE 4.3: THICK-BEDDED RED-BROWNISH SANDSTONE WITH CONGLOMERATE (TOP) IN KNYSNA FORMATION.....	47
FIGURE 4.4: TWO UPWARD FINING CYCLES WITH EROSION SURFACES AT THE BOTTOM ALONG KNYSNA FORMATION OUTCROP.....	48
FIGURE 4.5: A MEASURED STRATIGRAPHIC SECTION OF THE KNYSNA FORMATION WITH LEGEND AT THE BOTTOM.....	51
FIGURE 5.1: HISTOGRAM (LEFT) AND CUMULATIVE CURVE (RIGHT) FOR SAMPLE P5.....	58
FIGURE 5.2: HISTOGRAM (LEFT) AND CUMULATIVE CURVE (RIGHT) FOR SAMPLE P7.....	59
FIGURE 5.3: HISTOGRAM (LEFT) AND CUMULATIVE CURVE (RIGHT) FOR SAMPLE P8.....	60
FIGURE 5.4: HISTOGRAM (LEFT) AND CUMULATIVE CURVE (RIGHT) FOR SAMPLE P1.....	61
FIGURE 5.5: HISTOGRAM (LEFT) AND CUMULATIVE CURVE (RIGHT) FOR SAMPLE P10.....	63
FIGURE 5.6: HISTOGRAM (LEFT) AND CUMULATIVE CURVE (RIGHT) FOR SAMPLE K1.....	64
FIGURE 5.7: HISTOGRAM (LEFT) AND CUMULATIVE CURVE (RIGHT) FOR SAMPLE P11.....	68
FIGURE 5.8: HISTOGRAM (LEFT) AND CUMULATIVE CURVE (RIGHT) FOR SAMPLE P12.....	69
FIGURE 5.9: HISTOGRAM (LEFT) AND CUMULATIVE CURVE (RIGHT) FOR SAMPLE P13.....	70
FIGURE 5.10: HISTOGRAM (LEFT) AND CUMULATIVE CURVE (RIGHT) FOR SAMPLE P14.....	71
FIGURE 5.11: BIVARIATE SCATTER PLOT SHOWING STANDARD DEVIATION/SORTING VERSUS MEAN. THE STANDARD DEVIATION/SORTING VERSUS MEAN GRAPH DEMONSTRATES THAT THE SEDIMENTS ARE FINE TO MEDIUM GRAINED AND VERY WELL-SORTED TO MODERATELY SORTED. BEACH SANDS ARE FINER THAN FLUVIAL SANDS AND BEACH SANDS ARE WELL SORTED THAN FLUVIAL SANDS.....	79
FIGURE 5.12: BIVARIATE SCATTER PLOT SHOWING SKEWNESS VERSUS MEAN. THE GRAPH SKEWNESS AGAINST MEAN PLAYS A SIGNIFICANT ROLE TO IDENTIFY DEPOSITIONAL ENVIRONMENTS. BEACH SANDS ARE MORE SYMMETRIC OR COARSE SKEWED, WHILE FLUVIAL SANDS ARE MUCH DISPERSIVE	

WIDELY FROM STRONGLY COARSE-SKEWED TO FINE-SKEWED. ALSO SHOWING BEACH SANDS ARE FINER THAN FLUVIAL SANDS.....	80
FIGURE 5.13: BIVARIATE SCATTER PLOT SHOWING KURTOSIS VERSUS MEAN. THE PLOT BETWEEN MEAN AND KURTOSIS SHOWS THAT MOST SEDIMENTS ARE FINE-GRAINED FOR BEACH SANDS, WHILE FLUVIAL SANDS ARE MORE VARIABLE IN SIZE. ALSO SHOWING BEACH SANDS ARE MOSTLY MESOKURTIC AND PLATYKURTIC, WHEREAS FLUVIAL SANDS HAVE A WIDE DESPISE DISTRIBUTION FROM LEPTOKURTIC TO VERY PLATYKURTIC.....	81
FIGURE 5.14: BIVARIATE SCATTER PLOT SHOWING KURTOSIS VERSUS SKEWNESS. THE FIGURE SHOWS THAT BEACH SANDS ARE MORE CONCENTRATED IN THE PLATYKURTIC TO MESOKURTIC CATEGORIES, WHEREAS THE FLUVIAL SANDS ARE WIDELY DISPERSED FROM VERY PLATYKURTIC TO VERY LEPTOKURTIC. THESE CHARACTERISTICS CAN BE USED TO DISTINGUISH PALEO-DEPOSITION ENVIRONMENT AND WATER ENERGY FOR SEDIMENTS AND SEDIMENTARY ROCKS.	82
FIGURE 5.15: BIVARIATE SCATTER PLOT SHOWING SKEWNESS VERSUS STANDARD DEVIATION/SORTING. THE BIVARIATE PLOT OF THE SORTING AND SKEWNESS INDICATES THAT BEACH SANDS FALL INTO WELL SORTED TO VERY WELL SORTED CATEGORY, AND NEAR SYMMETRIC TO COARSE SKEWED CATEGORY. WHEREAS FLUVIAL SANDS FALL INTO WIDE AREA AND SHOW A DISPERSIVE SORTING..	83
FIGURE 5.16: BIVARIATE SCATTER PLOT SHOWING KURTOSIS VERSUS STANDARD DEVIATION/SORTING. THE BIVARIATE PLOT SHOWS THAT BEACH SANDS ARE MUCH CONCENTRATED IN THE VERY WELL-SORTED TO WELL SORTED CATEGORY, WHILE FLUVIAL SANDS ARE MUCH WIDELY DISTRIBUTED THAN THE BEACH SANDS. THE PROJECTED POINTS ARE SCATTERED WIDELY, INDICATING A WORSE SORTING.	84
FIGURE 6.1: PHOTOMICROGRAPHS SHOWING QUARTZ GRAINS (QTZ, WHITE), SHELL FRAGMENT (SH) AND SPONGE FRAGMENT (SP).....	86
FIGURE 6.2: PHOTOMICROGRAPHS OF SEM+EDX ANALYSES SHOWING QUARTZ MINERALS. THE AU PEAK WAS DUE TO GOLD COATING. THE EDX IMAGES SHOW HIGH CONTENT OF OXYGEN AND SILICA, WITH LITTLE OTHER CHEMICAL COMPONENTS.	87
FIGURE 6.3: PHOTOMICROGRAPHS SHOWING VARIOUS GRAINS OF FELDSPAR (FS), QUARTZ (QTZ) AND CALCITE (CAL). QUARTZ HAS NO CLEAVAGE, WHILE FELDSPAR (FS) SHOWS CLEAR CLEAVAGE IN THE CRYSTALLINE GRAIN INDICATED BY ARROWS.	88
FIGURE 6.4: SEM AND EDX ANALYSES FOR ALBITE GRAIN (TOP) HAVING SILICA, ALUMINIUM AND SODIUM CHEMICAL COMPOSITIONS (TOP); AND CA-PLAGIOCLASE GRAIN SHOWING SILICA, ALUMINIUM AND CALCIUM COMPOSITIONS (BOTTOM). AU PEAK WAS DUE TO GOLD COATING FOR THE SAMPLE.....	89
FIGURE 6.5: PHOTOMICROGRAPHS OF VARIOUS SAND GRAINS SHOWING ORGANIC PELLET (OP), QUARTZ (QTZ) AND MUSCOVITE (MSVT).	90

FIGURE 6.6: PHOTOMICROGRAPHS OF VARIOUS SAND GRAINS SHOWING. QUARTZ (QTZ), CALCITE (CAL), AND SEDIMENTARY LITHIC FRAGMENT (FR). BLUE ARROWS INDICATE ROUNDED ORGANIC PELLETS (DARK COLOURED).	91
FIGURE 6.7: SEM AND EDX ANALYSIS SHOWING CALCITE MINERAL WITH HIGH CALCIUM AND OXYGEN CONTENTS. ALSO CONTAIN SMALL AMOUNT OF QUARTZ (SI RICH). THE AU PEAK WAS DUE TO GOLD COATING FOR THE SAMPLE.	92
FIGURE 6.8: XRD PATTERNS FOR ALL THE SAMPLES P1, P2, P5, P19, P30, P47, K1 AND K2. THE DOMINANT MINERALS ARE QUARTZ, CALCITE, ARAGONITE AND MUSCOVITE.	96
FIGURE 7.1: SEM PHOTOMICROGRAPH SHOWING (A) TINY V-SHAPED PITS (UP-LEFT ON THE PHOTO), WITH SECONDARY MINERAL PRECIPITATED ON THE MIDDLE OF THE PHOTO; AND (B) TINY V-SHAPED PITS DUE TO COLLISION ON THE GRAIN SURFACE. NOTE SOME OF THE PITS ARE DISSOLUTION PORE, NOT V-SHAPED PITS.	98
FIGURE 7.2: SEM PHOTOMICROGRAPH SHOWING (A) A RELATIVE LARGE V-SHAPED PIT WITH SECONDARY MINERALS PRECIPITATED INSIDE THE PIT; AND (B) UPTURNED PLATES WITH STEPPED CRUSHING IMPACTS ON THE GRAIN SURFACE; ALSO SHOWING TINY V-SHAPED PITS ON THE SMALL GRAIN SURFACE (BOTTOM LEFT),	99
FIGURE 7.3 SECONDARY MINERAL PRECIPITATED ON THE GRAIN SURFACE.	100
FIGURE 7.4: SEM AND EDX IMAGE SHOWING SECONDARY MINERAL OF QUARTZ (SiO ₂) PRECIPITATED ON THE GRAIN SURFACE. THE AU PEAK DUE TO GOLD COATING FOR SAMPLE.	100
FIGURE 7.5: SECONDARY MINERAL OF CALCITE (CaCO ₃) PRECIPITATED ON THE GRAIN SURFACE. THE AU PEAK IS DUE TO GOLD COATING FOR SAMPLE.	101
FIGURE 7.6: SECONDARY MINRAL OF SALT (NaCl) PRECIPITATED ON THE GRAIN SURFACE. THE AU PEAK IS DUE TO GOLD COATING FOR SAMPLE.	101
FIGURE 7.7: SEM PHOTOMICROGRAPH SHOWING (A) GRAIN WITH DISSOLUTION PORES ON THE SURFACE AND (B) A GRAIN WITH IRREGULAR DISSOLUTION PORES ON THE SURFACE (UP-MIDDLE)	102
FIGURE 7.8: SEM PHOTOMICROGRAPH SHOWING A SMALL ROUNDED BORING HOLE ON THE GRAIN SURFACE (LEFT GRAIN), ALSO A DISSOLUTION HOLE ON THE RIGHT GRAIN, WHICH IS MUCH SHALLOWER.	103
FIGURE 7.9: SEM PHOTOMICROGRAPH SHOWING ROUNDED BORING HOLES ON THE GRAIN SURFACE CREATED BY ORGANISM (SUCH AS WARMS) THROUGH CORROSION AND BORING (RED ARROWS). ALSO SHOWING DISSOLUTION HOLES CREATED BY CHEMICAL DISSOLUTION WHICH ARE MORE IRREGULAR IN SHAPE AND RELATIVE SHALLOW IN DEPTH (BLACK ARROWS) COMPARED TO BORING HOLES. NOTE ALSO SECONDARY MINERAL (BLUE ARROW) PRECIPITATED ON THE GRAIN SURFACE AND IN THE DISSOLUTION HOLES.	103

FIGURE 7.10: SEM PHOTOMICROGRAPH SHOWING RECRYSTALLIZATION OF QUARTZ ON THE GRAIN SURFACE.....	104
FIGURE 8.1: SEDIMENTARY STRUCTURES FORMED IN DIFFERENT FLOW REGIMES (AFTER SELLEY, 2000).	106
FIGURE 8.2: THE STOSS AND THE LEE SIDE OF A RIPPLE AND THE CURRENT FLOW DIRECTION (SELLEY, 2000).	107
FIGURE 8.3: CATENARY RIPPLES CREATED BY VARIATION OF THE STRONG CURRENTS IN THE SANCTUARY BEACH, PLETTENBERG BAY.	108
FIGURE 8.4: STRAIGHT RIPPLES FORMED WHEN A RIPPLE CREST IS SPLIT BY CURRENT FLOWING IN THE LOOKOUT BEACH, PLETTENBERG BAY.	108
FIGURE 8.5: SINUOUS RIPPLES CREATED BY THE INTERFERING PROCESS OF THE SECOND TIME OF RIPPLES IN THE CENTRAL BEACH, PLETTENBERG BAY.....	109
FIGURE 8.6: LUNATE/LINGUOID RIPPLES CREATED BY VERY FAST FLOW ON THE BEACH. NOTE ALSO THE FLAT TOP OF THESE RIPPLES, CAUSED BY EROSION OF RIPPLE CREST IN A VERY SHALLOW WATER ENVIRONMENT IN THE BEACON BEACH, PLETTENBERG BAY.	110
FIGURE 8.7: RHOMBOID MARKS ARE RHOMBOHEDRAL FORMED BY TIDAL FLOW AND EBB CURRENTS DOWN A BEACH SLOPE IN THE LOOKOUT BEACH, PLETTENBERG BAY.....	111
FIGURE 8.8: GROOVE MARKS CAUSED BY STRONG WATER EROSION ALONG BEACH SURFACE IN THE ROBERG BEACH, PLETTENBERG BAY.....	111
FIGURE 8.9: A SWASH LINE IN PLETTENBERG BEACH (HOBIE BEACH) AFTER WATER REACHED THE HIGHEST POINT, DUMPED ALL THE MATERIALS AND THEN RETREATED INTO SEA.....	112
FIGURE 8.10: THE DISC-SHAPED PEBBLE RESULTED FROM TIDAL WATER OF ROUTINE TRANSPORTATION AND ABRASION IN THE CENTRAL BEACH, PLETTENBERG BAY.	113
FIGURE 8.11: PHOTOGRAPH SHOWING VERTICAL BURROWS CREATED BY ORGANISM LIVING IN A SHALLOW WATER ENVIRONMENT IN THE KEURBOOMS RIVER LAGOON, PLETTENBERG BAY.....	114
FIGURE 8.12: BORING AND BIOTURBATION STRUCTURES IN THE MODERN RIVER SURFACE FORMED BY ORGANISMS IN KNYSNA RIVER MOUTH.....	114
FIGURE 8.13: PLANAR LAMINATION IN THE RIVER SURFACE, ELABORATING A QUIET WATER STAGE OF LOWER ENERGY ENVIRONMENT AT KEURBOOMS RIVER (PLETTENBERG BAY).	115
FIGURE 8.14: A PHOTOGRAPH SHOWING THE GRAVEL MATERIALS AT KNYSNA RIVER MOUTH.....	116
FIGURE 8.15: AIR ESCAPE-HOLE STRUCTURE ON BEDDING SURFACE OF THE CRETACEOUS ROCK IN ROBERG FORMATION, PLETTENBERG BAY. NOTE THE ROUNDED AIR ESCAPE HOLES HAD BEEN FILLED WITH SAND AND MUD IN THE HOLE CENTRE AT LATER STAGE (LEFT), WHILE THE HOLES AT	

RIGHT SIDE ARE EMPTY DUE TO THE CENTRE MATERIAL WAS DISSOLVED OR TAKEN OFF. HAMMER HEAD FOR SCALE (BOTTOM RIGHT).	117
FIGURE 8.16: LENTICULAR BEDDING SHOWS “LENS-LIKE” SANDSTONE ALTERNATED WITH MUDSTONE. THE THICKNESS OF SANDSTONE IS UNSTABLE, AND DIES OUT ON ONE SIDE OR BOTH SIDES, SUNDAYS RIVER FORMATION.....	118
FIGURE 8.17 TABULAR CROSS BEDDING IN ENON FORMATION. THE DIP DIRRECTION OF THE CROSS BEDDING INDICATES PALEOCURRENT DIRECTION. IN THIS PHOTO, THE PALEOCURRENT WAS FLOWING FROM RIGHT TO LEFT.....	119
FIGURE 8.18: DEFORMATION BEDDING IN THE KNYSNA FORMATION.....	120
FIGURE 8.19: LOAD CAST (MIDDLE) IN THE CRETACEOUS ROCKS OF KNYSNA FORMATION.	120
FIGURE 9.1: THE PHOTOGRAPH SHOWS A TARRED ROAD WASHED AWAY BY WATER EROSION IN DURBAN.	124
FIGURE 9.2: PHOTOGRAPH SHOWS ACTIVE WIND EROSION ON A SANDY BEACH RESULTING IN TIRE TRACKS, PE IN COLCHESTER.	125
FIGURE 9.3: PHOTOGRAPH SHOWS SHORELINE EROSION ALONG THE BEACH IN DURBAN, SOUTH AFRICA.	127
FIGURE 9.4: PHOTOGRAPH SHOWS THE WAVE-CUT PLATFORM ON THE CLIFF RESULTING IN SHORELINE EROSION, KEURBOOMS RIVER LAGOON.....	128
FIGURE 10.1: PHOTOGRAPH DEMONSTRATING A SERIES OF SMALLER GROINS IN PORT ELIZABETH, SOUTH AFRICA.	130
FIGURE 10.2: PHOTOGRAPH DISPLAYING A COASTAL SEAWALL TO PROTECT INFRASTRUCTURES ALONG KNYSNA COAST.	132
FIGURE 10.3: PHOTOGRAPH SHOWING REVETMENT OF DOLOSSE BLOCKS IN PORT ELIZABETH, SOUTH AFRICA.	133
FIGURE 10.4: PHOTOGRAPH DEMONSTRATING RIPRAP STRUCTURES WITH PEBBLE-AND-BOULDER QUARTZITE ALONG THE RIVERBANK AT KNYSNA.....	134
FIGURE 10.5: PHOTOGRAPH ILLUSTRATING DUNES REHABILITATION MANAGING COASTAL EROSION IN CENTRAL BEACH, PLETTENBERG BAY.	135
FIGURE 10.6: PHOTOGRAPH SHOWING RECONSTRUCTION OF WETLANDS IN THE RIVERBANKS TO PREVENT EROSION, KNYSNA RIVER MOUTH.....	136
FIGURE 10.7: PHOTOGRAPH SHOWING SOFT ENGINEERING SOLUTION (BEACH NOURISHMENT) TO PREVENT FLOODING, KNYSNA IN SOUTH AFRICA.	137

LIST OF TABLES

TABLE 3.1: GRAPHIC PARAMETERS FOR GRAIN-SIZE DISTRIBUTION AND CALCULATION (FORK & WARD, 1957).....	34
TABLE 3.2: CRITERIA FOR SORTING, SKEWNESS AND KURTOSIS CALCULATION IN ϕ SCALE (FOLK, 1974).	35
TABLE 5.1: CATEGORIZATION OF GRAIN SIZE ANALYSIS PARAMETERS (AFTER FRIEDMAN, 1961; BLOTT & PYE, 2001).....	54
TABLE 5.2 PARAMETER VALUES FOR 53 SAMPLES ANALYZED.....	55
TABLE 5.3: RETAINED AND CUMULATIVE PERCENTAGE FOR SAMPLE P5.....	57
TABLE 5.4: RETAINED AND CUMULATIVE PERCENTAGE FOR SAMPLE P7.	58
TABLE 5.5: RETAINED AND CUMULATIVE PERCENTAGE FOR SAMPLE P8.....	59
TABLE 5.6: RETAINED AND CUMULATIVE PERCENTAGE FOR SAMPLE P1.....	61
TABLE 5.7: RETAINED AND CUMULATIVE PERCENTAGE FOR SAMPLE P10.....	62
TABLE 5.8: RETAINED AND CUMULATIVE PERCENTAGE FOR SAMPLE K1.....	63
TABLE 5.9: GRAIN-SIZE STATISTICAL PARAMETERS OF RIVER SAMPLES FROM P1-P10 AND K1-K3.....	64
TABLE 5.10: RETAINED AND CUMULATIVE PERCENTAGE FOR SAMPLE P11.....	67
TABLE 5.11: RETAINED AND CUMULATIVE PERCENTAGE FOR SAMPLE P12.....	68
TABLE 5.12: RETAINED AND CUMULATIVE PERCENTAGE FOR SAMPLE P13.....	69
TABLE 5.13: RETAINED AND CUMULATIVE PERCENTAGE FOR SAMPLE P14.....	70
TABLE 5.14: GRAIN-SIZE STATISTICAL PARAMETERS OF BEACH SAMPLES FROM P11 TO P50.	71
TABLE 6.1: PERCENTAGES OF MINERALS FROM SAMPLE P1 TO SAMPLE K2.....	93
TABLE 8.1: TERMINOLOGY OF BED THICKNESS (AFTER GREENSMITH, 1989).....	117

CHAPTER 1: INTRODUCTION

1.1 Coastal hydrodynamics and erosion

In the Plettenberg Bay and Knysna region, the study of coastal hydrodynamics and erosion is crucial because of current requirements for urban and industrial expansion. This study is a part of a major environmental research project in the South African south coast, and is aimed at unravelling the coastal hydrodynamics and sedimentation processes in order to provide first hand data and new insight for coastal environment protection.

Coastal erosion in many cases is referred to as shoreline retreat, which caused the loss of coastal lands, and damage of infrastructures due to the net removal of sediments or bedrock from the shoreline. Coastal erosion can be either occur very quickly, a period of days to weeks, and that is known as "rapid-onset hazard" or occurring over many years, or decades to centuries, and that process is called "slow-onset hazard" (Nordstrom, 2004). Coastal erosion is a natural phenomenon that can be increased by human activities and natural hazards (storms and tsunamis). Shoreline retreat is commonly directed by currents and wave actions; however, by mass wasting activities on coast slope, especially on the muddy coast slope (Harrison et al., 2001).

University of Fort Hare
Together in Excellence

Coastal erosion problems become critical because coastal zone for population concentration, and urbanization in recent years. Further, coast zone in South Africa had attracted many tourists from world wide, and is the localies for National Roads and industry development, thus protection of environment, and coast erosion is particularly important tasks for South Africa (Barragan & Andreis, 2015). Thus, such processes can be driven to undercut cliffs and steep slopes on coastal headlands and assist to mass wasting.

Coastal erosion may be a process that happens whenever material move far away from the shoreline is not stabilized by new material being deposited towards the coastline. Several coastal landforms generally undergo asymmetrical pattern cycles of erosion and accretion on time scales of days to years. It is particularly noticeable on sandy landforms like dunes, beaches, dunes, and arbitrarily closed and open lagoon entrances (Bird, 1985). Thus, human events also can powerfully impact the movement of landforms to erode, as an example, coastal structures (like seawalls and

breakwaters) will modify alongshore sediment transport pathways, leading to erosion in various localities and accretion in others (Qian, 1984). The discharge of sediments via the coastal system (for instance dredging or sand mining) or depletion within the supply of sediments (such as the regulation of rivers) also can be related to unintended erosion. At macro scales, natural and man-made-induced climate change can alter the probability and rate of coastal erosion. Sedimentary variation is the principal issue showing to immoderate erosion rates spotted, which then are related in sand mining (Rangel-Buitrago et al., 2015a,b; Vallejo et al., 2016), dams (Rangel-Buitrago & Posada, 2005), location of coastal engineering structure (Rangel-Buitrago et al., 2011, 2015a,b), and ecosystem devastation (Botero & Salzwedel, 1999; Vilarity et al., 2011). Coastal erosion becomes risky once society does not modify its results on individuals, the built environment, and infrastructure (Gutman, 1979).

1.2 Background of the Plettenberg Bay and Knysna Area

Plettenberg Bay is a well-known coastal town situated along the Garden Route on the Southern Cape coast. The number of people residing in Plettenberg Bay is more than 100,000 people. There is extensive increment during Easter and December occasion periods when massive influxes of travellers flock to the area, expanding by 45 000 and 75 000 individuals separately (Becke, 2003). Plettenberg Bay is supported by this region's high biodiversity and attractive natural beauty. Now, the town has developed into one of South Africa's most famous towns for an area of holidays for both international and national tourists.

Knysna is a well-known coastal town and a scenic natural town with more than 100,000 residents in the Western Cape Province of South Africa and is part of the Garden Route. Knysna derived from the Khoisan a long time ago, which means "place of wood or fern leaves" (Von Breitenbach, 1974; Van der Merwe, 1998).

The Knysna Municipality has governed the Eden district to maintain the whole economic performance. Knysna is the leading financial sector because of tourism. However, it plays a prominent role as a significant driver in the trade sector and occupies a macroscale component of the Knysna economy, 31% than the Province of 11% (Coetzee et al., 1997).

1.3 Study areas and geological map

Plettenberg Bay is located in the part of the Western Cape Province, which is an area where some of the oldest and youngest rocks in the world can be found near each other. It is situated at about 203 km west of Port Elizabeth, along the south coast of South Africa. By the geographical interpretation, the Plettenberg is positioned at $34^{\circ}03'09''\text{S}$, $23^{\circ}22'17''\text{E}$ and the altitude is approximately 77 m in figure (1.1).

The Knysna is situated on the Northern side of a shallow lagoon-like estuary. The current landscape altered through the Late Pleistocene, the Holocene Epochs, along with a series of variations in sea level, and climate change. By the geographical interpretation, the Knysna is positioned at $34^{\circ}02'08''\text{S}$, $23^{\circ}02'56''\text{E}$ figure (1.1).



University of Fort Hare
Together in Excellence

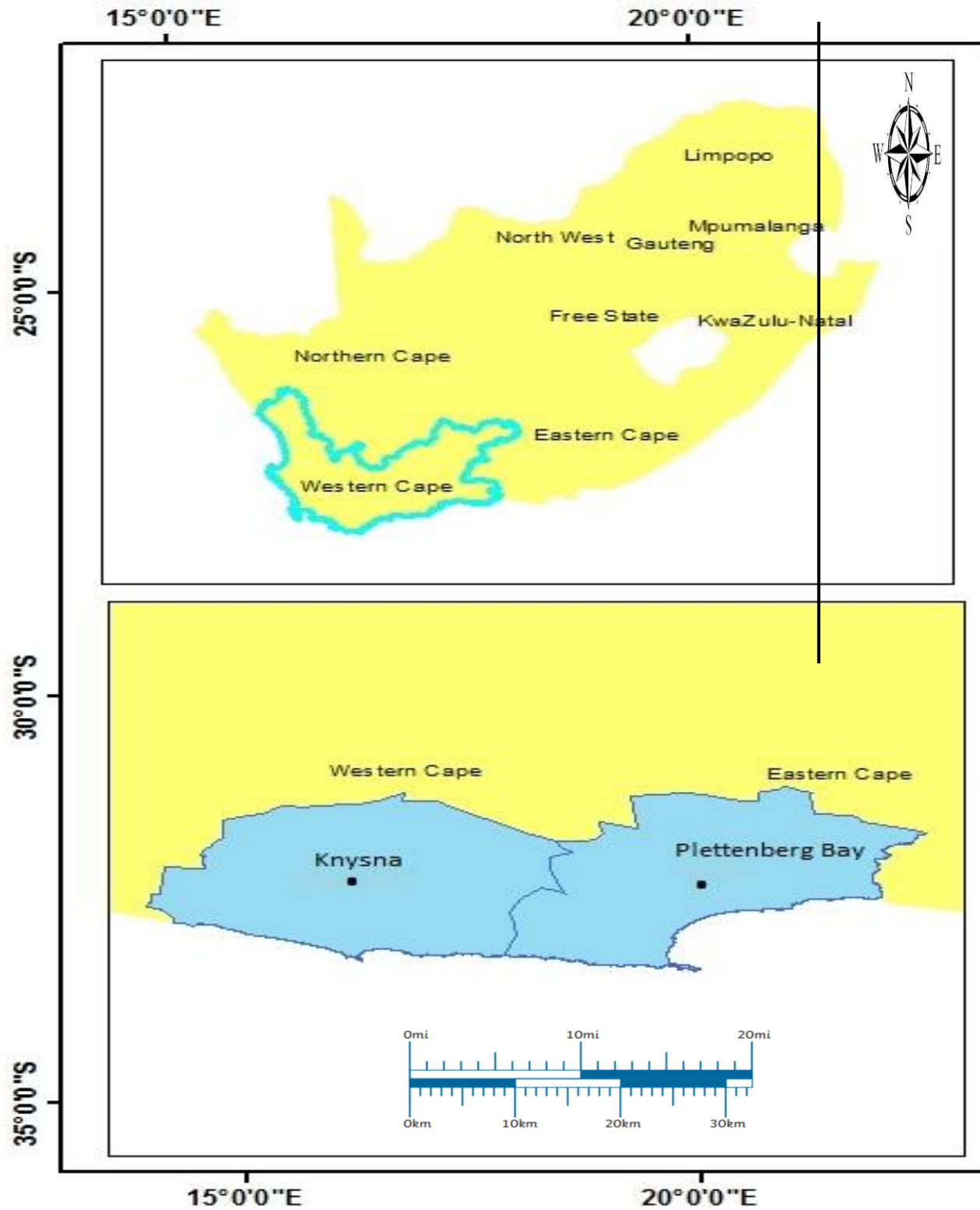


Figure 1.1: Geographic map showing the study areas, Knysna and Plettenberg Bay of Western Cape Province of South Africa.

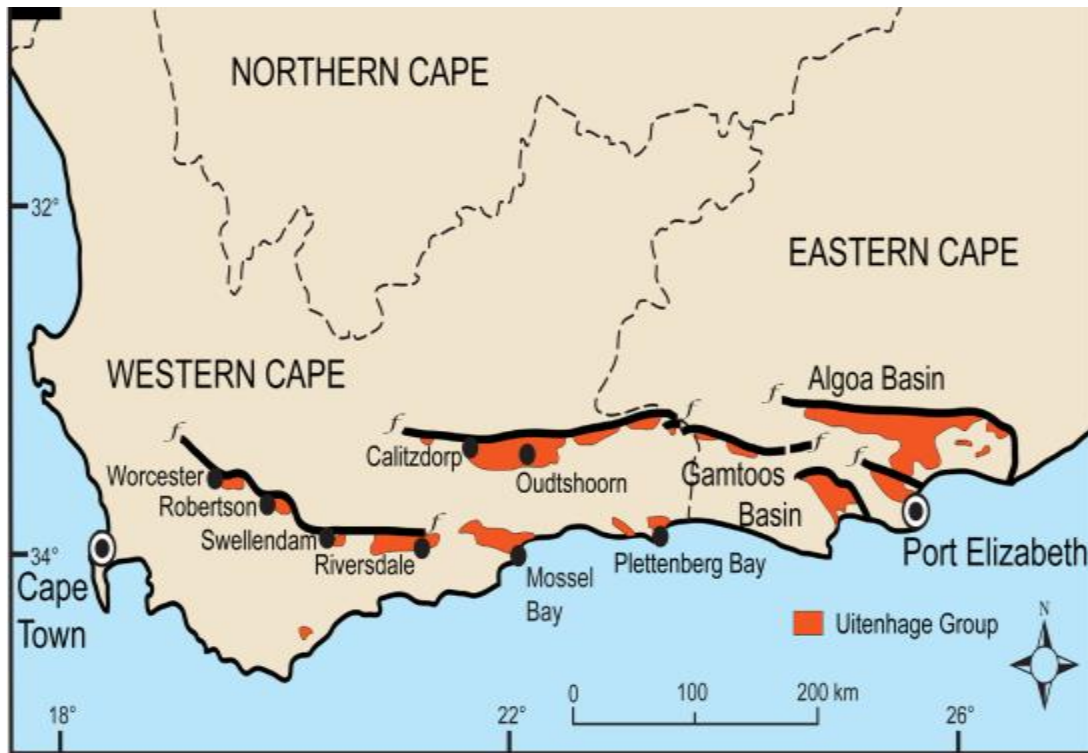


Figure 1.2: Geological map shows the areas where Uitenhage Group outcrop (Robert et al., 2015).

1.4 Littoral zonation of coastline area

Beaches are energetic landforms that offer important habitats, pastime sites, and superstorm safety alongside the world's coasts (Komar, 1998). As low-lying coastal landforms, seashores could be exceptionally liable to erosion and flooding in the future sea-level rise deriving from climate change (Vitousek et al., 2017). The beaches additionally reply to supplies, losses, and exchanges of sediment, mass stability this is typically called the littoral cell "sediment budget," and modification to sediment budgets may have tremendous results on coastline role and morphology (Limber et al., 2008; Anthony et al., 2014, 2015). For many coasts, particularly those in active tectonic settings, essential origins of littoral sediment occur from rivers and streams (Milliman & Farnsworth, 2013). Numerous dynamic tectonic margin settings are sustained by approximately small rivers (watershed regions much more minor than 100,000 km²), which integrate to contribute the majority of sediment to the world's oceans (Milliman & Syvitski, 1992).

Changes in river sediment resources will alternate the trajectory of deltas and littoral cells as proven with the aid of using each discount of sediment discharge (Anthony et al., 2014, 2015;

Pratellesi et al., 2018) and will rise in sediment discharge (Warrick et al., 2019; Nienhuis et al., 2020). However, the river sediment is discharged from time to time and the motion of sediment in coastal cells is usually extra regular and pushed by ocean waves, explicit ranges arise within the evolution of river mouth sediment deposits (East et al., 2018; Measures et al., 2020). Since river sediment is removed from time to time and the motion of sediment in littoral cells is usually extra regular and pushed by ocean waves, precise ranges arise within the evolution of river mouth sediment deposits (Kuenzi et al., 1979; Hicks & Inman, 1987; Cooper, 1993; Giosan & Bhattacharya, 2005; Barnard & Warrick, 2010; East et al., 2018; Measures et al., 2020). Rivers supply critical sediment inputs to several littoral cells, thereby recharging the sand and gravel of beaches across the world. However, there may be restrained records of approximately the styles and methods of littoral-grade sediment transfer from rivers into coastal systems (Warrick, 2020).

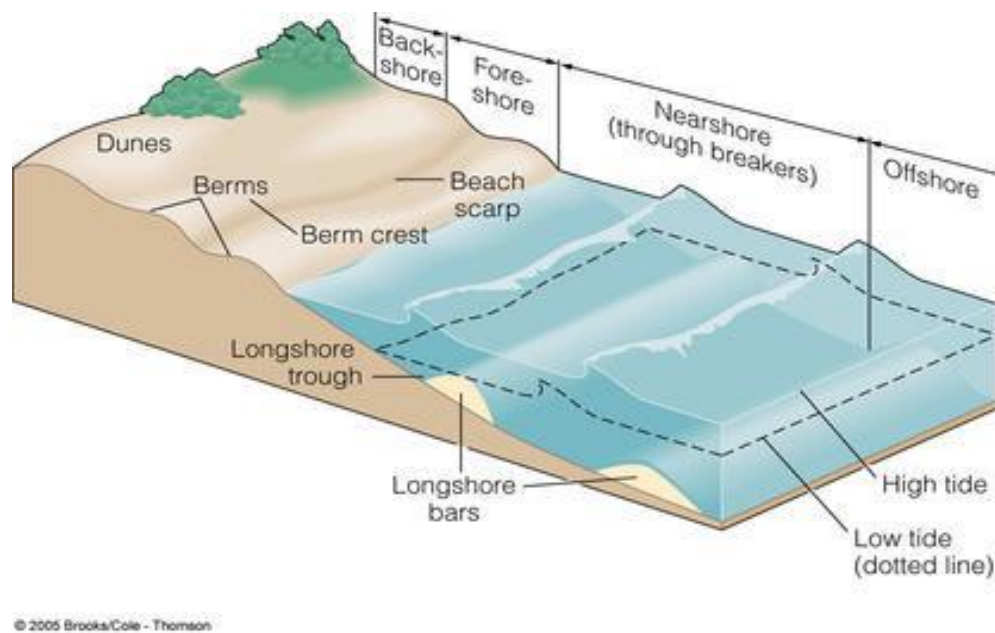


Figure 1.3: Typical beach profile (<http://thebritishgeographer.weebly.com/coasts-of-erosion-and-coasts-of-deposition.html>).

1.5 Aims and objectives of the study

This project aims to investigate the sediment characteristics and the hydrodynamic condition in the Plettenberg and Knysna coast in order to address coastal erosion and the environment

protection, particularly human life and property safety. Therefore, the study will highlight coastal hydrodynamic energy, including coastal configuration and bathymetry. It will further indicate sea level change could cause environmental change and sediments redistribution. .

The specific objectives were:

- To investigate sediments deposited along the coast;
- To study hydrodynamics and water energy in the coast area;
- To analyze grain-size variation and distribution of sediments;
- To study sedimentary structures and depositional environments;
- To investigate the mineral compositions along the south coast;
- To find mitigation methods and engineering structures to prevent coast erosion and environmental damage;

1.6 Research questions and the significance of the study

According to the objectives of this research project, the author will address a number of research questions which closely linked to the research objectives in the study areas.

What types of sediments and rocks are present in Plettenberg Bay and Knysna area?

What is the characteristics of the sediment grain-size distribution in study areas?

What types of minerals are found in these sediments, and where do they originate from?

Is there a link between grain-size variation and hydrodynamic energy?

What types of sedimentary structures formed on the beach and coast river environments? Does each sedimentary structure indicate a specific depositional environment?

Is there any erosion along the coast and did it caused environment and property damage?

What kind of mitigation methods which can effeciently prevent coast erosion?

The author will try to address the above questions which closely links to the research aim and objectives.

There are limited previous research work and publications on the characteristics of sediments distributed along the Plettenberg Bay and Knysna coast, and thus we try to provide new insight on the coast sedimentation, hydrodynamic mechanism, erosion and environmental protection, Particularly, it could have economic significance in the protection of coastline property and human safety.



University of Fort Hare
Together in Excellence

CHAPTER 2: GEOLOGICAL BACKGROUND AND LITERATURE REVIEW

2.1 Uitenhage Group

The rock stratigraphy in the research area belongs to Uitenhage Group of Cretaceous sediments of approximately 130 Ma in age (Johnson, 1994; Muir et al., 2017). Several geological activities took place in the Late Jurassic/ Early Cretaceous, such as the rifting within the continent and local uplift generated by volcanic activities (Gust et al., 1985). However, the blocking fault and the erosion of the younger southern African continent led to the rapid deposition of massive amounts of silty, sandy conglomeratic alluvial made by the rivers and the beaches (Gust et al., 1985).

Uitenhage Group is composed of three formations, i.e. Enon Formation at the bottom, upward by Kirkwood Formation and Sundays River Formation. The Enon Formation was deposited by thick alluvial fan and braided fluvial conglomerates (Muir, 2018). The Uitenhage sequence becomes younger towards the northeast. Enon Formation consists of a noticeable thickness >1 km from the core data of the fluvial conglomerates and was overlaid by the multicoloured alluvial siltstones and the pebble channel sandstones of the Kirkwood Formation (Montgomery, 2010). This Uitenhage sequence thickens and randomly becomes fine-grained sediments towards the southeast (Dinis, 2018). The reddish-brown colour of the Enon conglomerates and calcrete-rich palaeosols surrounded by the Kirkwood alluvial frequently indicates that the areas were semi-arid. Resulting, warmer to hot and with minimum seasonal rainfall within the Uitenhage Group, no fossil remains were recorded in the beds (Montgomery, 2010).

The Uitenhage Group is quite cramped to the erosional residue of several rift basins offshore has subsurfaces distributions and onshore of the southern Cape (McMillan et al., 1997; Muir et al., 2017a,b). The Uitenhage Group comprises primarily the continental conglomerates of red beds (feldspar-rich) and white beds (Kaolinite-rich). Equal to Enon Formation at Knysna area, it was also called as Knysna Formation.

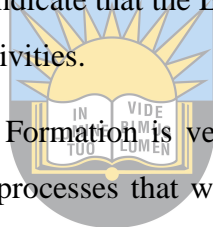
2.1.1 Enon Formation

The Enon Formation is the Late Jurassic to Early Cretaceous. It exists in many offshore and onshore Mesozoic rift basins formed by Gondwana breaks occurring in the Western to Eastern South Africa (Lock et al., 1975; Dingle et al., 1983; Fouche et al., 1992). The Enon is the basal

unit of the Uitenhage Group, and the description applies only to the exposures of the Enon. Atherstone (1857) used the name conglomerate of Enon to distinguish the coarse clastic deposits in the area of the Enon, exposed at the Sundays River Valley, 160 km north of Port Elizabeth.

As the research conducted at a later stage, some authors uniformly cited the deposits as Enon Stage, "Enon conglomerate," and "Enon Beds" (Roger, 1905; Haughton, 1928; Engelbrecht et al., 1962; Joubert & Johnson, 1998). However, the Enon Formation is the oldest and primarily adjacent formation occupying the Mesozoic basins of South Africa. The Enon Formation is thickly bedded, with a poorly sorted pebble to cobble conglomerate with sub- and well-rounded clasts with subordinate sandstone and mudstone. The geological beds are often structureless internally and the local clasts could be imbricated (Muir et al., 2017). The derivation of the Enon Formation was from the eroded Cape Fold Belt; hence is commonly classified by clasts that differ strongly from immediate Palaeozoic basement rocks (Hill, 1972). The Enon Formation characteristics (such as coarse clasts sizes, massive beds, etc.) indicate that the Enon Formation was entirely deposited in an energetic alluvial and debris flow activities.

The topographic gradient in the Enon Formation is very steep and necessary for high-energy transportation of continental sediment processes that were likely prolonged by normal faulting along the rift basin margin. The deposition of fluvial probable by braided rivers or braid plains, scree deposits on an immature and alluvial fan depositional environments (Shone, 1976; Holzforster, 2007; Van der Linde, 2007). In the Enon Formation, the pebbles vary in size and age from place to place. Typically this geological phenomenon occurs due to a marine transgression or regression. Muir et al. (2017b) documented that the Enon Formation locally displays a laterally gradational, contact, and interfingering with Kirkwood Formation. The braided fluvial conglomerate of the Enon Formation within the Uitenhage Group the thick alluvial are quite nearly all very poorly sorted (Shone, 2006).

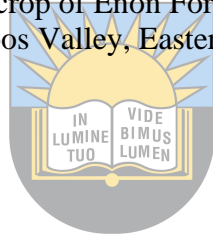


University of Fort Hare
Together in Excellence



Figure 2.1: Photograph showing an outcrop of Enon Formation conglomerate formed by alluvial channel in the Gamtoos Valley, Eastern Cape, South Africa.

2.1.2 Kirkwood Formation



The Kirkwood Formation comprises of the grey-olive to yellowish medium to coarse grained sandstones of changeable sideways and the vertical extent of interbedded with various colours such as grey, red, and pale-greenish siltstone and mudstone with a thickness of 30 m up, this formation is quite calcrete-rich palaeosols, with irregular fragments of conglomerates (sporadic conglomerates) with other volcanic tuffs (McLachlan & McMillan, 1976; Viljoen, 1992; Frost, 1996; Shone, 2006). The gradational and locally interfingering nature that separates the contact between Enon Formation and Kirkwood Formation is complicated to identify in the field (McLachlan & McMillan, 1976; Dingle, 1973).

Rigassi & Dixon (1972) and Shone (1976) overviewed the Kirkwood Formation that is mainly originated from the fluvial deposit; however, Dingle et al. (1983) came up with valid evidence suggesting that Kirkwood Formation is formed moderately in shallow marine and lacustrine depositional settings. Frost (1996) stated that the climate was semi-arid with a warm to hot temperature under low seasonal rainfall of 100-500 mm/annual. After a decade, Shone (2006)

documented that within the lower part of the Kirkwood Formation are indicative of changes in the sea level and adjacency of the fluvial system to the marine shorelines during the Early Cretaceous.

The Kirkwood Formation is the Late Jurassic and Early Cretaceous age by McLachlan & McMillan, 1976; Gomez et al., 2002 and Shone, 2006. The research based on the Kirkwood Formation made a crucial contribution to the Early Cretaceous floras of Africa (Muir et al., 2015). The Kirkwood Formation of South Africa has not been acknowledged the appearance of charcoal in conglomerate deposits within the formation; in the Kirkwood Formation, the sediments of Early Cretaceous fluvial to estuarine carry rare lignite and carbonaceous clays. There are flat-lying to gentle dipping beds with massive lenticular or planar bedding also flat-lamination with cross-bedding (Almond, 2013). Kirkwood Formation consists of lenticular pebbly conglomeratic which are quite seen among poorly-consolidated channel sandstone. In the Kirkwood Formation, the mudstone and sandstone generally dominates conformably overlies, although locally interfingers with the Enon (Muir et al., 2017).



Figure 2.2: Photograph showing interbedded porous medium to coarse-grained sandstone with brownish fine conglomerate layer (top) of Kirkwood Formation.

2.1.3 Sundays River Formation

The uppermost part of the Uitenhage Group within the Algoa Basin is occupied by the Sundays River Formation, overlying and interfingering with bottom Kirkwood Formation. There is a probability that an unconformity divides them and can not be dismissed (Winter, 1973; McLachlan & McMillan, 1976; Shone, 1978). McMillan (2003) emphasizes that regardless of the stratigraphic relations of this unit undetermined, its depositional age which is well-constrained to Lowermost Valanginian-Hauterivian based on foraminifera-ammonite assemblages.

The Sundays River Formation is determined from the underlying and partial lateral correspondent, the Kirkwood Formation, comprising mainly the greenish-grey laminated mudstones differentiated to the red-spotted paleosol-rich mudstones of the latter. However, within the Sundays River Formation, there are infinite marine invertebrate fossils that are quite not present from the Kirkwood Formation (Kitchin, 1908; Spath, 1930; McLachlan & McMillan, 1976, 1979; Cooper, 1983). Cenozoic Algoa Group overlay unconformably is commonly conglomerate-dominated and sandstone instead of the mainly argillaceous Sundays River Formation and can be identified based on the grain-size difference (Muir, 2018). The Sundays River Formation thickness is highly inconstant due to the structure of the Algoa Basin and erosion (Shone, 1976).

The lithology of the Sundays River Formation consists of greyish to olive-grey of very fine-to-medium grained sandstone beds interbedded with a variation of mudstone dominant, suggested by Shone (1976). Mudstone is very dominant with a range of (70-90%) and consists of olive- to dark-green and spotted purple/green mudstone (McMillan, 2003). However, there are calcareous layers present in small quantities. Those shell fragments and whole calcareous invertebrate body fossils are usually found both isolated throughout and as discrete calcareous interbeds in the sand- and mudstone (McMillan, 2010).

It is hypothesized that the continental Bufferliskloof Formation correlates with the Sundays River Formation (Viljoen, personal communication 2016); however, this argument is found on the lithostratigraphic grounds. In addition only points out that the conglomeratic unit, similarly to the Sundays River Formation, occupies an uppermost position of respective rift basin stratigraphy.



Figure 2.3: Photograph showing Sundays River Formation dominated by mudstone with alternated siltstone and sandstone layers.

2.1.4 Knysna Formation

Knysna Formation is correlate to Enon Formation in age, and occurs only in Knysna-Pletenberg area. It is exposed along the N2 highway in the Garden Route, and the Knysna Formation lies between latitude $23^{\circ}03'34''$ and longitude $34^{\circ}02'36''$ (Otunola & Liu, 2019). Along the South African coastline, the Cretaceous sediments were deposited nearby the boundary between KwaZulu-Natal and Eastern Cape with dispersed outcrops from Port Elizabeth to George in the southern part (Reddering, 2000; Norman & Whitefield, 2006). The Knysna Formation is formally recognized by Jacobs (1992) and consists of sands of fine-grained muddy lignitic sand and lignites with a thickness of 30 m. Their respective ancient time and palaeoecological importance were quickly acknowledged (Phillips, 1927; Du Toit, 1956).

In the Early Knysna Formation, aeolian, including lignite deposits, appear in pockets on the coastal platform of Knysna Formation (Jacobs, 1992). Otunola & Liu (2019) analyzed the Knysna Formation as well-sorted to moderately well-sorted from a fluvial-beach depositional environment. Furthermore, the Knysna Formation is Cretaceous in age with Cretaceous sediments (Liu, personal communication 2021). The Knysna Formation comprises mainly conglomerates and

sandstones that unconformably excessively on the metamorphosed Cape Supergroup rocks (Reddering, 2000). Compared to Enon Formation, Knysna Formation contains more lenticular sandstone in the pebble dominated sequence.



Figure 2.4: Photograph showing an outcrop of Knysna Formation along the N2 Road at Knysna.

University of Fort Hare
Together in Excellence

2.2 Quaternary Sediments

Quaternary sediments are the most identified in the outcrop due to their deficit of uniformity in rocks and by interrelation, with landforms illustrating depositional processes (shorelines, river terraces, moraines, etc.). Quaternary sediments are created by the various processes of deposition. They are witnesses to the changes in climate and geography that have structured the landscapes linked with an impact on human evolution. In these deposits, the fossils are very correlated to modern life forms, however, it is possible that these climates illustrated warmer or cooler conditions. Quaternary sediments are easiest to be identified, mostly not being cemented, including loose sands such as modern beach and river sands and sand dunes.

2.2.1 Distribution of sediments in the Keurbooms estuary (Plettenberg Bay)

The Keurbooms estuary sediments mainly consist of fine-grained quartz (silt and sand) with organic material and clay. Derived from Tertiary to Quarternary marine and partly calcareous sand and estuarine terrace gravel, the Keurbooms River and the lower reaches of the Bitou River are underlying onto (Duvenage & Morant, 1984). The gradual up-estuary variation of hydrodynamics and sedimentary conditions profoundly influences the behaviour of burrowing organisms. The Keurbooms estuary contains less clay, and the sand is incoherent and easily regenerated by tidal currents and the small wind-driven waves (Reddering & Rust, 1997).

According to Reddering & Esterhuysen (1983), environmental and recreational terms in flood tide-dominated Keurbooms Estuary indicate that the sediment accumulation is undesirable. Quite often, tidal resonance results from the flood tide domination caused by a net marine sediment movement into these estuaries. Reddering & Esterhuysen (1983) further elaborated that the estuary where marine sediment enters is deposited on the flood tidal deltas. A coastal barrier separates the lower estuary from the sea, and the barrier through a tidal inlet provides tidal connections between the sea and the estuary. According to Reddering (1999) the bay of Plettenberg Bay is classified by a wave-dominated shoreline where very high longshore sediment transport rates are recorded southeasterly storms. The primary source of sediments in the estuary is the surf zone (Reddering, 1999).

2.2.2 Distribution of sediments in the Knysna estuary

The substratum of the estuary comprises mainly unconsolidated sandy sediments of marine, aeolian, and fluvial origin (Reddering & Esterhuisen, 1984; 1987). The Knysna Estuary is situated along a portion of rocky terrain where the longshore sediments are high transport capacity exceeds supply. According to Chunnnett (1965) and Zwamborn (1980), only micro volumes of marine sediments are transported into the estuary. The middle reaches of the estuary specify that the grain size, shape, and chemical composition of the surface sediments comprise almost entirely of aeolian material, which most probably originated from the Brenton dune on the southern bank of the estuary (Reddering & Esterhuisen, 1987). Duvenhage (1983) verified that the Knysna Estuary is an S-shaped stretch of water of 1 633 ha in dimension, with a channel estimated at 19 km long and 2 km wide. The Knysna Estuary has a tidal reach of approximately 17 km (Reddering &

Esterhuisen, 1984). The hills with steep slopes surround almost the entire estuary. The estuary's upper reaches with angularity and poorly sorted sand grains indicate that these sediments are mostly fluvially derived (Reddering & Esterhuisen, 1987).

Marker (2000) stated that flood occurrence had been revealed to play a prominent role in the sediment dynamics of the estuary, causing the deposition of the fine sediments in the middle reaches of the system. However, the deposition of the sediments is related to evolves of the hydrodynamics the loss of habitat (salt marsh vegetation and water quality clarity) for both vertebrates and invertebrates (Maree, 2000). The sediment loads deriving from the catchment area in the order of 100-150 t/km²y (Roosenboom, 1978). Chunnet (1965) demonstrated that siltation in the estuary from exterior sources has been essentially absent over the past centuries, with recognized siltation being the interior movement of material. Grindley (1985) indicated that siltation problems typically appear where artificial structures have been constructed. CSIR (1989) concluded an increase in sedimentation rate within the Green Hole region due to the Leisure Island causeway and George Rex Drive. In general low sediment input into the estuary was confirmed by Reddering (1994), who discovered small-scale evidence of sediment influx in recent years.

2.3 Cross-shore sediment transport

Sediment budgets illustrated such onshore transport turned a vital effect early during the post-event morphodynamics, hence it is very important to review why this transport turned in massive half unidirectional during this early phase of the coastal action. Expanding theoretical data of these cross-shore transport configurations is also done via scaling from, for instance, cross-shore and longshore transport or diffusivity relations (Nienhuis et al., 2015; Ortiz & Ashton, 2016). Unfortunately, numerous relations are developed for absolute beach profiles, comprising of subaerial, intertidal, and submarine segments of the profile. These impede operation to the river mouths discovered here as a result of, as explicit on top of and exactly below, the profiles to begin with doing currently not have coast or subaerial sections (i.e., the shapes do currently not have foreshores). Higher data of the physical techniques are required to develop theoretical data of these settings.

Cross-shore sediment transport actions of surf zones are naturally complex owing to 3-dimensional (3-D) topography and hydrodynamics together with 3-dimensional uneven oscillatory flows, wave

grouping, and related energy transformation into infragravity frequencies, wave- and bathymetric brought on vortices, turbulence added through wave breaking and dissipation, and undertow sequences (Aagaard, 2014; Wei et al., 2017). Investigations of cross-shore sediment transport are usually restricted to sandy beach settings and targeted on situations that purpose beach alteration, inclusive of coastline erosion or bar formation (Masselink et al., 2008). Research of the physical outcomes of waves at river mouth settings has typically targeted wave impacts on river plume formation and initial river mouth bar formation in embayed environments without littoral zones (Gao et al., 2018) or patterns of littoral sediment bypassing of river mouths (Nienhuis et al., 2016b). Research currently does no longer deal with the transforming of river mouth bar sediment towards the beach. They are steady in suggesting that the outcomes of waves at the timing and geometry of sediment delivery may be complicated (Nienhuis et al., 2016b; Gao et al., 2018).

2.4 Types of coast

Coastlines consist of the natural borderline area among the ocean and the land. Their natural characteristics rely through the form of the rocks revealed alongside the coastline, the movement of natural methods, and the effort of animals and vegetation (De Vries et al., 2010). The severity of natural activities shaped their source both as erosional or depositional properties. The geological structure of a coastal area identifies the uniformity of the soil, even the degree of rocky material and their discharge and breakdown (De Vries et al., 2010).

2.4.1 Cliff coast

Cliff coast is also classified to be a “hard” coast as a result it had been made up of resistant materials, that embrace volcanic or sedimentary rocks. This coast structure ordinarily incorporates a short shore platform, usually exposed in low tide. Natural erosion is due to slope fluctuation, weathering, and wave motion and ends in the deterioration of the shoreline. As shown in Figure 2.5, intense wave things, together with tsunamis and storm waves, will have a far less erosive impact during this coast structure (Mangor et al., 2004).



Figure 2.5: Photograph showing hard rock “Cliff coast” (online Google search photo).



2.4.2 Clayey bank coast

This coast could also be referred to as a “semi-hard” coast and compatible soil; usually on the estuarine coastlines and often has vertical banks ranging from 1-5 m on top. The abrasion rate is comparatively excessive contrasted to the rugged coast as a result of it consisted of weaker and far less resistant material. Erosion is mostly due to coastal actions, weathering, and shortage of vegetation cover (ARC, 2000). For strenuous activities, as well as tsunamis and storms, as shown in Figure 2.6, vegetation cover performs an important role in defending the coast from inundation and flooding via decreasing wave amplitude and energy and decreasing wave flow momentum; thus, erosive forces and inundation distance area unit reduced (De Vries et al., 2010).



Figure 2.6: Photograph showing semi-hard rock “Clayey bank” coast.

2.4.3 Muddy coast

University of Fort Hare
Together in Excellence

This coast is described as a fine-grained sedimentary deposit, dominantly silt, and clay material through the rivers; it should be defined as a “soft” coast (it is named as soft coast due to the accumulation of fine sediments). It is a considerable moderate seaward slope, known as an intertidal mudflat, whereby mangrove forests, saltmarshes, shrubs, and different trees area units are detected (De Vries et al., 2010). Various erosion is made in river damming that decreases sediment supply, reduces vegetation cover (normally salt marshes and mangroves), and shows vegetation roots through reducing the mudflat in figure (2.7), resulting in their very last slump. Through cyclones, healthful and heavy coastal forest/vegetation areas and trees will perform obstacles and reduce storm amplitude, in addition to providing a few preservations to the location at the rear of them. Within the occurrence of coastal forests, trees, and tsunamis will lower amplitude and tsunami inundation speed to a point whether the forest area is heavy and intensive sufficient. Each strenuous activity will purpose extreme erosion and scrub on the coast and at the river mouth (Mangor et al., 2004).



Figure 2.7: Photograph showing the muddy coast at Plettenberg Bay at Western Cape.

2.4.4 Dune/Sandy coast

University of Fort Hare
Together in Excellence

This coast includes loose material, mostly sand, few pebbles together with shells; it will be classified as a soft coast. Since it has a moderate seaward slope referred to as dissipative seashores with intensive fine sand and steady steep slopes on the fore-dunes/backshore. The profile of this coastal form depends upon waveform and wind direction and energy; thus, profiles may be changed to offer mainly structured methods of dissipating incoming wave energy (De Vries et al., 2010). In conclusion, this sort of coast undergoes short-time period fluctuation or cyclic erosion accretion, and long-time period evaluation has to perceive erosion as trouble here. Usually, accumulation and sand dune reconstruction take lots longer than erosional activities, and therefore the seashore has inadequate time to reconstruct earlier than the subsequent erosive action happens (De Vries et al., 2010). Erosional characteristics are a diminished seashore profile slope and therefore the insufficiency of a berm, nearshore bar, and erosional scarps aboard the fore-dune. Typically, erosion is a difficulty once the dunes deplete their vegetation cover that ambushes wind-

borne sediment within the course of reconstruction, develops slope uniformity, and cements the sand. In excessive activities, including tsunamis and storms (Figure 2.8), this kind of coast is a fence for the situation within the back of the dunes. Vegetation cover within the dunes are extraordinary natural protective standards towards tsunami inundation and coastal flooding (Sowmya et al., 2019).

In addition, this coastal form includes loose material, primarily sand from the rivers and eroded headlands, broken coral branches (coralline sand), and the shells from the edging reefs. It is going to be classified as a soft coast with a reef shielding offshore. The beach incline differs from moderate steep slopes relying upon the ability of natural intensity (in explicit waves) showing on them. Coconut trees, waru (*Hibiscus tiliaceus*), tree catappa, pandanus, pine trees, and different beach solid ground trees square measure standard here. Numerous erosion could be a result of a deficit of (1) the protective feature of the coastal environment, primarily coral reefs (wherein they will be detected) that shield the coast against wave activity; and (2) coastal trees that shield the coast against massive winds. Through extreme actions (Figure 2.8), healthy coral reefs and trees shield coasts to a degree via manner of suggests that of decreasing wave height and strength additionally to excessive coastal erosion (Mangor et al., 2004).



Figure 2.8: Photograph showing sandy coast and swash-line at the beach of Plettenberg Bay.

2.5 Processes of coastal erosion

The mixed impact of waves, currents, and tides brings about several gradational actions acting within the coastal zone (Mangor et al., 2004). Mangor et al. (2004) explained how coastal erosion occurs in the shape of hydraulic action, corrosion (or) abrasion, attrition, corrosion (or) solution, and water pressure. Hydraulic action is the impact of transferring water at the coastal rocks. It is because of the straight collision of waves at the coasts. In depth, pressures will construct as air and water compacted within the rock fractures. The most crucial type is abrasion. Abrasion (or) corrosion is a type of erosion that takes place with the assistance of erosion tools. Within water suspension, boulders, cobbles pebbles, and coarse sands are used by the waves to strike the coastal rocks. Attrition is an action wherever mechanical wear and tear will damage some rock mass among fragments. The mutual impact ensuing from rip and backwash currents is a good tool for coastal erosion. Corrosion (or) Solution is the chemical modification of rocks that will be soluble attributable to their contact with the seawater. The result is regionally important, mostly wherever soluble rock is shown on the shore (De Vries et al., 2010).

According to periodic drying and wetting, several chemical activities occur at the coastal rocks, that cause every physical disintegration and chemical decomposition. Fluctuate freeze and defrost also can create those rocks to be damaged with no challenge with the help of using the waves. The movement of these ocean waves shapes coastal characteristics. Coastal sediments are difficult to over one episode of transportation, erosion, and deposition, even if net seaward movement happens on a worldwide scale. The deep ocean floor changes the resting location for terrene sediment eroded from the coastline (De Vries et al., 2010; Sowmya et al., 2019). However, the beach accumulates pathways sand grains aboard the beach as waves strike the shore at an associate indirect angle. Sediment is transported landwards whereas water rushes throughout the beach as swash. Sediment is transported came within the direction of the ocean as backwash. The persistent uprush and backwash incorporates sand in a very zig-zag-like motion aboard the shore.

2.6 Erosional landforms

The major erosional landforms of the coasts are:

- A sea cliffs is a vertical precipice set due to waves crashing at once on a steeply inclined slope (Sowmya et al., 2019). These steep to vertical bedrock cliffs vary from a few metro masses above sea level. Their vertical kind results from wave-prompted erosion close to the sea level and the subsequent disintegration of rocks at a higher height (De Vries et al., 2010). Hydraulic action, abrasion, and chemical precipitation are all efforts to reduce a notch on the excessive water level near the bottom of the cliff. Continuous undercutting and erosion create the cliffs to retreat landward (Mangor et al., 2004).
- Sea caves shape alongside lines of weak points in cohesive, however well-jointed bedrock. Sea caves are prominent headlands in which wave refraction strikes the shore.
- Sea Arches shapes while sea caves consolidate from contrary sides of a headland. If the arch falls, a rock pillar stays in the back of a sea stack (Mangor et al., 2004).
- For sea stacks, wave-cut notches and, wave-built terrace are categorized as seaward of the locomoting cliffs, wave erosion creates a vast erosional platform called a wave-cut bench or wave-cut platform (De Vries et al., 2010). After the steady grinding and battering, the eroded fabric is transported to adjoining bays to end up beaches or seaward coming to rest a wave-constructed terrace (Sowmya et al., 2019).

2.7 Causes of Coastal Erosion

University of Fort Hare
Together in Excellence

2.7.1 Tide currents

The tides can increase the zone over which destructive waves can erode the beach (Subba Rao, 2002). High tide obstructs the premature breaking of the waves on the offshore sand bars, which vanish some of their energy at that position. Subba Rao (2002) stated that the waves shatter closer to the shore, which erodes the beach material. Consequently, locations with a high tidal range are more likely to erode (Subba Rao, 2002).

2.7.2 Sea-Level-change

A sea level would straightly result in the proportionality of higher shift the zone of wave action on the beach. This phenomenon would be visible in a shoreline recession which will be greater on the milder slopes (Bruun, 1983). Bruun (1962, 1983) has introduced a theory that determines the shoreline recession for a given rise in sea level. According to this evaluation, every millimetre rise

of sea-level results in a shoreline retreat of about a meter (Bruun, 1962). The global scale regarding the sea level is rising at 1.0 to 1.5 mm/y. Part of the main greenhouse effect may minimally escalate the rate of sea-level rise (Subramanya & Rao, 1991). Observations of the beach profile over a long period, such as a decade or more, are attained before an inevitable conclusion of retreat can be made.

2.7.3 River Mouth Changes

The river mouth certainly the sand spits on either side appear tough migration tendencies. However, these movements do not follow any uniform pattern (Subba Rao, 2002). A particular portion of these sand spits of affiliated sand expands for long distances with the river on one side and sea on the other side Bruun (1983).

The issues related to the river mouth are the following:

1. The migration of sand spits would include erosion at one end and deposition across from the other. The human encroachment has withdrawn on these poorly sand spits (sand bars), which are highly vulnerable. To secure the land and property, evaluate protection works are involved. Furthermore, sufficient space is not accessible for the proper of these works, creating them more exposed to failure (Bruun, 1962).

2. The long and narrow sand spits are extremely vulnerable regions as they comprise sand which can be simply operated by the water of both the sea and the river. In certain areas on the spit, the coastal erosion endangers to cut off the road. Therefore, it becomes essential to supply protection to sustain the only link roads (Subramanya & Rao, 1991).

2.7.4 Aeolian (wind) erosion and wave action

Wind erosion could be a natural occurrence during which wind generation moves the soil from another site to a different one. It is the potential to form substantial economic and environmental damage. A lightweight wind that soil fragments over the surface to a robust wind that pushes a major volume of soil fragments into the air to create dust storms are all exemplars of wind erosion. Whereas wind erosion is quite common in the deserts and on the beaches and coast's sand dunes,

it also can take place in agricultural places because of specific land situations. Wind erosion of soils is one of the most important environmental and agriculture problems, affecting several fields (Movahedan et al., 2012).

The wind waves influence the beaches in two ways,

1. The strong waves generate the beach to erode by taking away the material.
2. When waves move from deep to shallow waters, the circumstance occurs, and expected, wave orthogonal may diverge or converge on the beach. At locations of divergence, a relatively still water manages, and moderate deposition takes place (Subba Rao, 2002), at the location of convergence, the energy gets reduced, and the erosion exists.



Figure 2.9: Photograph shows wave erosion along the shore of south coast of South Africa.

Strong monsoon waves create the offshore motion of sand, while long-low expand waves in the non-monsoon months create the onshore action of the sand. If the offshore activity dominates, then coastal erosion occurs, and if onshore motion dominates, the beach will escalate (John, 1984; Lima et al., 2020). The wave heights which probable to generate dominant offshore activity will be a function of beach slope, wave period, and beach sediment size. So the waves, as they move from deeper waters regarding the coast, go through transformations due to many causes; however, the

one that could form extreme changes in the wave heights is the phenomenon called wave refraction (Lima et al., 2020).

2.7.5 Climate change

Climate change can affect coastal erosion in numerous ways. Here the purpose of interest is at the sea-level rise; other possible effects are related to variation in environmental conditions-temperature, wind, and precipitation. Variation among the precipitation pattern can affect the sediment removal of the rivers and also the succeeding sand supply to the coast. Utmost things of strong rain and long durations of drought are anticipated to emerge as bigger frequent (Wooldridge et al., 2016). The temperature also can operate its impact on soil erosion. Temperature changes can have an effect on all life forms in the coastal region (Mangor et al., 2004). Coastal erosion is especially sensitive to changes in coastal vegetation ridge plantation, as an example. Mangrove coasts are certain to temperature variation; but, additionally to sea-level rise (Subba Rao, 2002; Sowmya et al., 2019). Modification inside the wind pattern and wave climate can alternate the alongshore and cross-shore sand distribution. The alongshore sand distribution could also be liable to the littoral drift, which highly depends upon wave orientation. The cross-shore coastal form is massively affected through wave accumulate vital for storm events' excessive waves and water levels. Due to climate change, significant uncertainty exists concerning local modifications in wind regime and wave climate (Mangor et al., 2004).

2.7.6 Cross-shore sand loss

Sand loss due to the active coastal region in an exceedingly cross-shore route will arise throughout entire processes. The loss of material through the extended environment to at least 1 or 2 sides may be a natural motive of coastal erosion (Neal et al., 2018). They typically turn up at till/sandstone headlands, within which fine eroded material is removed away because of the currents, and coarse material is moved offshore or alongshore afar from the natural elevation. Very often, some semi-hard seaward-concave part of the coastline can bear erosion just in case of an inadequate provide of the sand via the rivers (Neal et al., 2018). The natural kind of this form of coastline is erosion and straightening; the straightened shoreline is named as a simplification coast. In marine deposit coastlines ejected among eroding away headlands (till or arenaceous rock, as an example) can move equally. The headlands have anciently furnished with material for constructing

up the matter coastlines, and therefore the ejected outline depends on the presence of the headlands. Thus, as a result of the headlands' retain to erode, the matter coastlines can imitate in spite of accumulative forms. This development could be a part of the simplification coast (Subba Rao, 2002).

2.8 Coastal flooding

High water levels are needed for coastal flooding for occurrence, mainly in which coastal hinterlands are fronted through protection structures (Harvey et al., 2021). High water levels tend to be related to high-energy hydrodynamic environments so that erosional effects may coincide with coastal flooding activities. Demonstrating erosion–flooding interactions throughout those actions is vital because low frequency, massive magnitude occasions can group disproportionate erosive and flooding potential (Callaghan et al., 2008; Harvey et al., 2021). The geomorphic state transitions, indicating the existence of threshold(s) in the geomorphic system that ought to be exceeded in providing state change (Harvey et al., 2021).

Breaking and overwash constitute a direct pathway via which water flows can propagate, ensuing in potentially high water levels in back-barrier regions representing a supply of flood hazards for landward receptors. Several morphological manages on barrier breaching, and overwash has been recognized (Sallenger et al., 2006). The morphology of alluvial channels and floodplains may be very unusual exaggerated excessive discharge (Sallenger, 2011). Consequently, floods are probably seemed to supply marked geomorphological modifications in the vast oceans, which might be furnished through coastal regions (Phillips et al., 2021). The effects of the substantial floods on the sea/ beaches are inadequately recorded to the quantity of this uncommon occurrence. Such floods in long-time sedimentation and stratigraphic facts are not consistently recognized clearly (Sallenger, 2011).



Figure 2.10: Aerial image revealing coastal flooding in Port Elizabeth, South Africa.



University of Fort Hare
Together in Excellence

CHAPTER 3: METHODOLOGY

3.1 Introduction

To achieve the aims and objectives of this research project, several methods were used to complete this dissertation. Three methods were used firstly, desktop study, secondly, field investigation, and thirdly laboratory method. For desktop, the study involves searching for documents that correlate with the project and finding previous work or historical background of geological activities of the study areas. The field investigation includes collecting samples and recognizing geological aspects such as lithostratigraphy, geological structures (sedimentary structures), sedimentary texture, and fluvial and marine (coastal) environments. However, the data was collected and recorded during the field trip. The laboratory technique involves the most crucial methods such as grain-size sieving of collected samples, microscopic or petrographic analysis of the sand samples, X-Ray Diffraction (XRD) and Scanning Electron Microscope (SEM).

3.2 Desktop study

The relevant journals, articles, e-books, and past research papers were used to find the study areas that the project is situated. Citation of those sources was made thoroughly and correctly. This method contributed mainly to the write-up of the literature search and review and built valid adequate information about the location of the study areas. Furthermore, the capturing of grain-size analysis results in the Microsoft Excel 2013 and recording the data resulting from the sieving per sample such as the weight retained, % weight retained, and cumulative frequency. Therefore, histograms were resulted and plotted using Microsoft Excel 2013.

3.3 Fieldwork method

In June 2019, the fieldwork was conducted in both study areas (Plettenberg Bay and Knysna). The river sediments were collected in Keurbooms River in 3 different places the East Bank (Outer bank), Point Bar (Inner bank), and the Middle Channel Bar at Knysna; sediments were collected ay Knysna Estuary. Sand sediments were also collected from the different beach zones in Plettenberg Bay, and those other beach regions will be named onwards.

Sediments were put into the sample bags and marked in ascending order from P1 to P50 for sediments collected at Plettenberg Bay and K1 to K3 at the Knysna area to avoid the sample

reputation and mixing the sediments. Those sand samples were then dried using an oven at 35°C in temperature. After that, they were taken to the laboratory for grain-size analysis to determine the grain-size distribution of the beaches zone in Plettenberg Bay. Along the Keurbooms river, two samples (P1-P2) were collected from the East bank, five samples (P3-P7) from the Point bar, and three samples (P8-P10) were collected from the Middle channel bar. Sand samples (P10-P40) were collected from the discrete beach sections at Plettenberg Bay. However, these sand samples were collected from several beaches: Sanctuary Beach and Robberg Beach, Beacon Beach, Central Beach, Hobie Beach, The Wedge Beach, and Lookout Beach. Sand samples were collected in those beach zones shown in figure (3.1); further, in the Lookout Beach, two rows were created. Five sand samples were collected in each beach zone in a linear sequence beginning from the low tide area (near the beach) to the supratidal section.

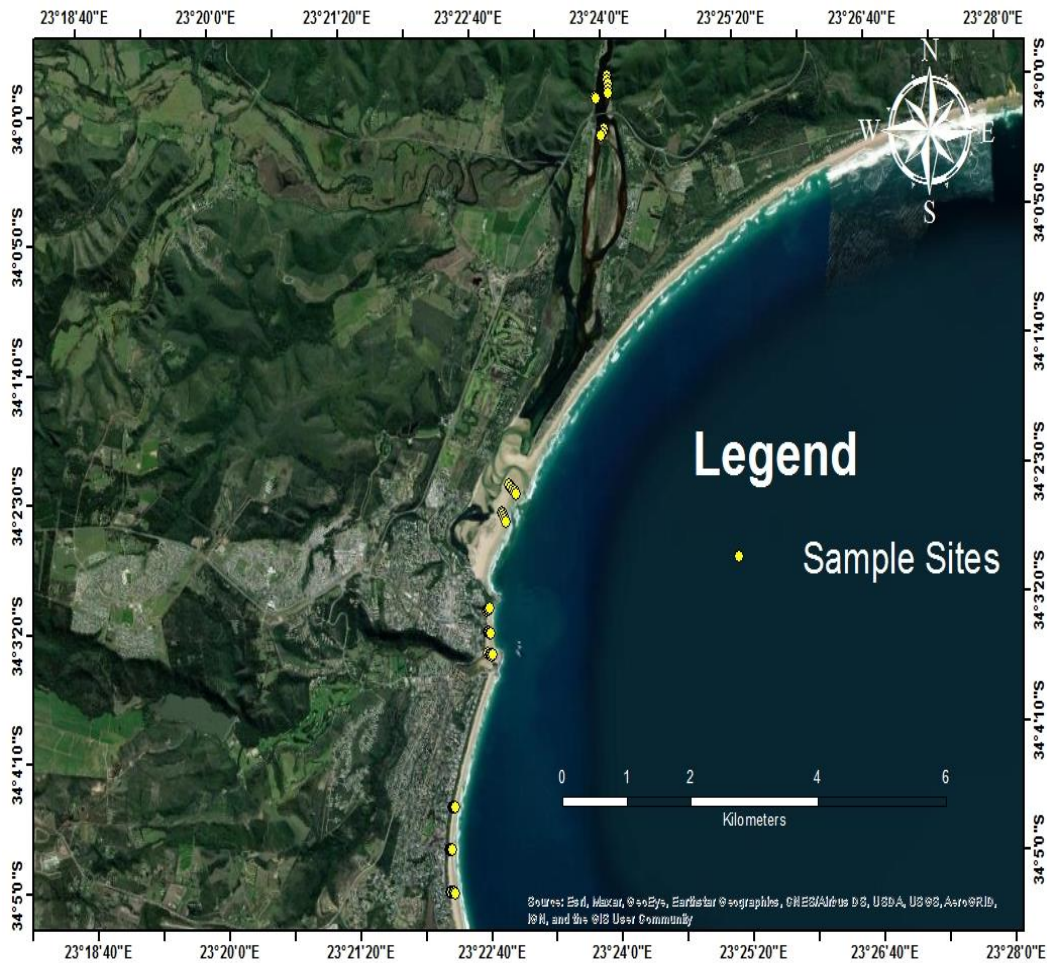


Figure 3.1: Location of the sampling stations in Plettenberg Bay along with the Keurbooms River and Beach environment (online GPS image).

In the Knysna area along the Road N2 in Garden Route, one sample (K1) of the Cretaceous sediment was collected near the river (Figure 3.2). However, two samples (K2-K3) were collected in the Knysna estuary; one sample was near the river, and another was on the flood plain shown in figure (3.3).



Figure 3.2: Photograph showing dolerite block to protect erosion along the Garden Route coast of Knysna



Figure 3.3: Photograph showing the Knysna Estuarine floodplain.

The Knysna Formation outcrops were mapped by observing and identifying lithologies, sedimentary structures, and the rocks' colour. Description of the sedimentary structures was made, and photographs were taken using an advance digital camera.



Figure 3.4: Location of the sampling stations along Knysna Estuary (online GPS image).

3.4 Laboratory methods

3.4.1 Grain-size analysis

Sedimentologists have commonly and widely used grain-size analysis to categorize and classify hydrodynamic conditions and sedimentary environments. Grain size is an elementary characteristic of siliciclastic sediments; hence it is suggested to be the significant detailed properties of sedimentary rocks. Several factors affect the grain size, such as source rock, climate, topography, transport mechanism, the distance from the river, and the distance from the shoreline. Thirteen river sediments and forty beach sediments were under review of grain-size analysis;

however, the grain-size parameters bivariate analysis were captured sequentially to unfold the hydrodynamic conditions, depositional settings, transportation history, and deposition environments.

3.4.1.1 Grain-size parameters

Grain-size parameters, namely graphic mean grain-size (M_Z), inclusive graphic sorting or standard deviation (σ_I), inclusive graphic skewness (SK_I), and graphic kurtosis (K_G) calculated according to the statistical measures of Folk & Ward (1957).

Grain-size parameters are quite a practical section for engineering geology, production of moulding materials, ecological safety, ballast, etc., however in explaining fundamental problems such as palaeogeographic, lithological, geochemical, etc. mineralogical.



Table 3.1: Graphic parameters for grain-size distribution and calculation (Folk & Ward, 1957).

Measure	Equation
Graphic mean	$M_Z = \frac{\phi_{16} + \phi_{50} + 84\phi}{3}$
Inclusive graphic standard deviation (sorting)	$\sigma_I = \frac{\phi_{84} - \phi_{16}}{4} + \frac{\phi_{95} - \phi_{15}}{6.6}$
Inclusive graphic skewness	$SK_I = \frac{\phi_{16} + \phi_{84} - 2(\phi_{50})}{2(\phi_{84} - \phi_{16})} + \frac{\phi_{5} + \phi_{95} - 2(\phi_{50})}{2(\phi_{95} - \phi_{5})}$
Graphic kurtosis	$K_G = \frac{\phi_{95} - \phi_{5}}{2.44(\phi_{75} - \phi_{25})}$

Median (M_d)

The median grain size is the value that emerges in the medial of the cumulative curve. However,

statistical is demonstrated in phi (ϕ) or millimetres (mm). The median is $M_d = \phi_{50}$ (Trask, 1932; Rashedi & Siad, 2016).

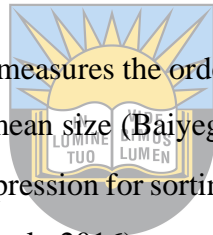
Mean (M_z)

Graphic mean grain size is the often used grain-size distribution because it acts as a benchmark of the average energy of the transportation medium and is controlled by the source of supply, transportation mechanism, and environment of deposition (Folk & Ward, 1957; Passega, 1964).

Furthermore, the mean grain size is the math norm scale of all grain particles that appear in a sample. In addition, the mean grain size shows the standard range of the sediment in terms of energy which relies on the speed of the transporting medium (Okeyode & Jibiri, 2013; Parthasarathy et al., 2016).

Standard Deviation or Sorting (σ)

Sorting grain size or standard deviation measures the order of grain size existing and the degree of scatter or spread of these sizes around mean size (Baiyegunhi et al., 2017). The inclusive graphic standard deviation is the arithmetical expression for sorting grain size (σ). Represents the velocity of the depositing agent (Parthasarathy et al., 2016).



University of Fort Hare
Together in Excellence

Skewness (SK_I)

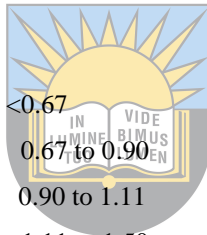
Skewness is a value of the degree symmetry of the grain-size distribution; skewness is the detailed parameter that highly causes the most of the grain-size measurement inclusive graphic skewness. However, it is a characteristic of the environmental conditions due to its direct relationship to the fine and coarse tails of the grain-size distribution (Haider, 2016).

Kurtosis (K_G)

Kurtosis measures peakedness or sharpness of the grain-size frequency curve and proportion between sorting in the 'tails' of the curve and the mean of the sorting (Parthasarathy et al., 2016). The unique part of calculating kurtosis is comparing the spread/ tails in the middle part of a distribution to the spread in the tails.

Table 3.2: Criteria for sorting, skewness and kurtosis calculation in ϕ scale (Folk, 1974).

SORTING	
Very well sorted	< 0.35
Well sorted	0.35 to 0.50
Moderately well-sorted	0.50 to 0.71
Moderately sorted	0.71 to 1.00
Poorly sorted	1.00 to 2.00
Very poorly sorted	2.00 to 4.00
Extremely poorly sorted	> 4.00
SKEWNESS	
Coarse-skewed	-1.00 to -0.30
Strongly coarse-skewed	-0.30 to -0.10
Near-symmetrical	0.10 to -0.10
Fine-skewed	0.30 to 0.10
Strongly fine-skewed	1.0 to 0.30
KURTOSIS	
Very platykurtic	< 0.67
Platykurtic	0.67 to 0.90
Mesokurtic	0.90 to 1.11
Leptokurtic	1.11 to 1.50
Very leptokurtic	1.50 to 3.00
Extremely leptokurtic	> 3.00



University of Fort Hare
Together in Excellence

3.4.1.2 Grain-size Sieving Analysis

The grain-size analysis is the simplest and most common method used to assort the powders according to their physical and chemical properties by applying the sequence of punch plates sieves. However, this procedure is also used to gauge the particle-size distribution of organic and non-organic granular matters comprising rock fragments (lithics), sands, and major minerals (clay minerals, feldspar, quartz), according to McGlinchey (2005).

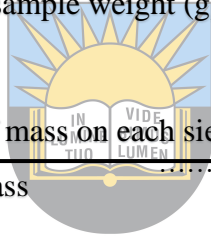
The oven was used to dry up the collected sand samples at 35⁰C; it was an average temperature level because some organic matters may extinct in higher temperatures more than the selected temperature. Subsequently, the parched sand samples were set into marked beakers, and now the

sieve analysis in the laboratory was the following step to be taken. Weighing balance was used to weigh each sand sample's mass in the laboratory accordingly. Sand samples were divided into different sized sieves, and the mass that remained during the sieving method was also recorded on the different sized sieves. For accurate results, the sieves were cleaned before resuming to another sample. The sieves size assorted from -1ϕ to $+5\phi$.

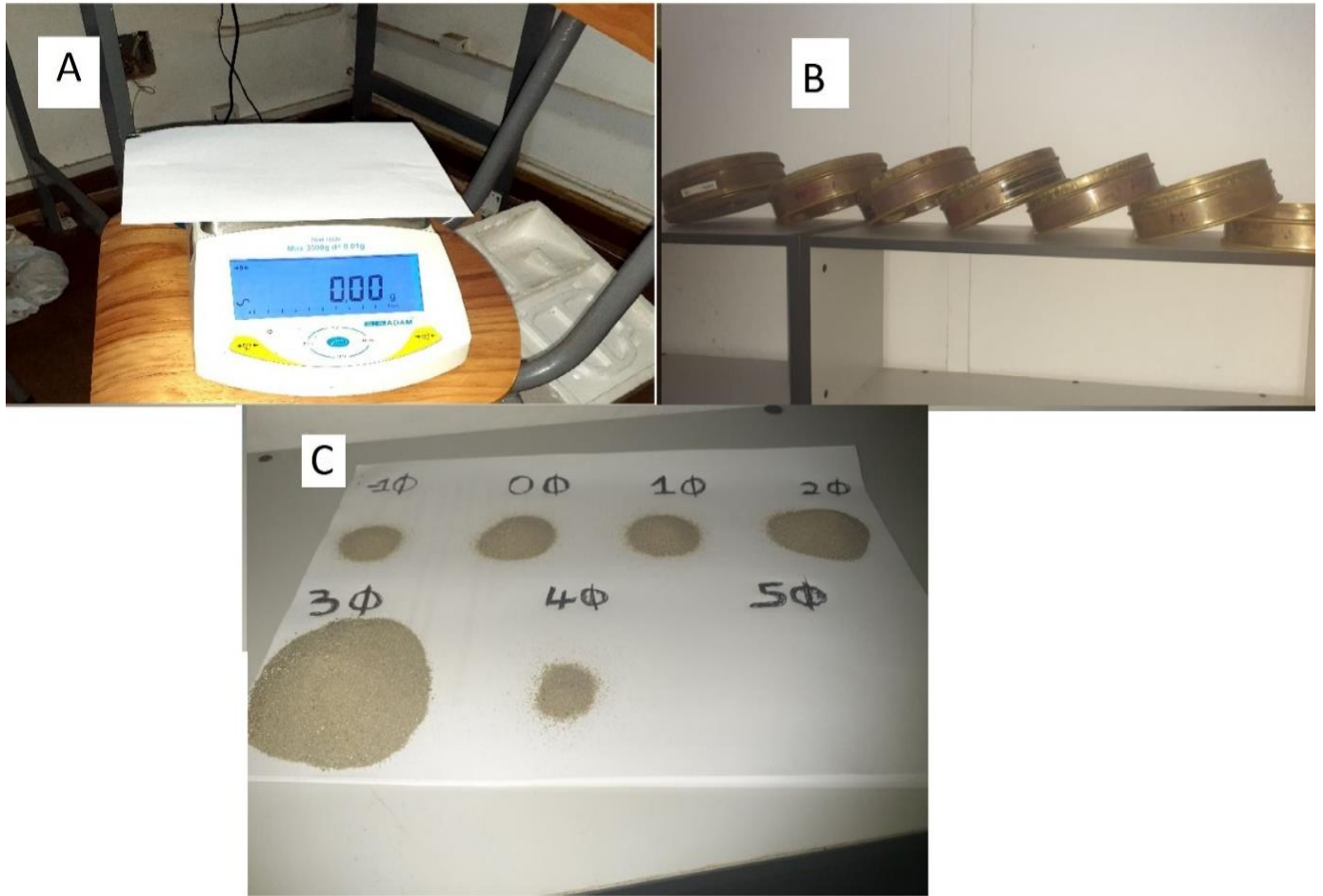
Furthermore, the mass retained on each sieve was recorded. Human errors were present; however, for valid results, the process was repeated on every sand sample that was weighed and sieved. The spreadsheet in Microsoft Excel was used to record all the sieve analysis outcomes. The percent weight retained, the cumulative weight percent, and the standard errors were calculated from the obtained results.

$$\% \text{ weight retained} = 100\% \times \frac{\text{weight retained on each sieve (g)}}{\text{original sample weight (g)}} \dots\dots\dots(1)$$

$$\text{Error} = 100\% \times \frac{\text{Aliquot mass} - \text{sum of mass on each sieve}}{\text{Aliquot mass}} \dots\dots\dots(2)$$



University of Fort Hare
Together in Excellence



University of Fort Hare
Togoloza P. M. M. M.
 Figure 3.5: Equipment and methods for grain-size sieve analysis.

3.4.2 Classification of grain-size and grain-size distribution

Historically Krumbein (1934) developed the hypothesis of grain-size analysis firstly. Various authors established the sieve method used to derive (GSD) grain-size distribution (Krumbein & Pettijohn, 1938; Folk, 1966; and others). Nevertheless, Johnson (1994) suggested that the grain-size distribution can be derived from the thin sections via microscopic studies. Dyer (1986), the most broadly and regularly used method to represent the grain-size data to acquire the sediments and their depositional environment involves the histogram, frequency distribution versus log diameter, the cumulative frequency curve, and probability distribution curve.

In addition, Udden (1914) and Wentworth (1922) established the “Udden-Wentworth grade scale,” which is frequently used to discover the grain-size categories, where the proportion of grain-sizes

in millimetres was converted to phi scale by $\phi = -\log_2 D$, Where ϕ is the phi-size and D is the diameter (in mm) of the particle or grain.

Grain size		Descriptive terminology		
phi	mm/ μ m	Udden (1914) and Wentworth (1922)	Friedman and Sanders (1978)	GRADISTAT program
			Very large boulders	
-11	2048 mm		Large boulders	Very large
-10	1024		Medium boulders	Large
-9	512	Cobbles	Small boulders	Medium
-8	256		Large cobbles	Small
-7	128		Small cobbles	Very small
-6	64			
-5	32			Very coarse pebbles
-4	16	Pebbles	Coarse pebbles	Coarse
-3	8		Medium pebbles	Medium
-2	4		Fine pebbles	Fine
-1	2	Granules	Very fine pebbles	Very fine
0	1	Very coarse sand	Very coarse sand	Very coarse
1	500 μ m	Coarse sand	Coarse sand	Coarse
2		Medium sand	Medium sand	Medium
3		Fine sand	Fine sand	Fine
4		Very fine sand	Very fine sand	Very fine
5	31		Very coarse silt	Very coarse
6	16	Silt	Coarse silt	Coarse
7	8		Medium silt	Medium
8	4		Fine silt	Fine
9	2	Clay	Very fine silt	Very fine
			Clay	Clay

Figure 3.6: Classification of sediments and sedimentary rocks based on the grain size (Friedman & Sanders, 1978; Blott & Pye, 2001).

Thin sections are usually calculated using statistical parameters such as mean grain-size, sorting, skewness, and kurtosis (Blott & Pye, 2001). Folk & Ward (1957) recommended the most proper and frequently used formulas to compute statistical parameters for grain size. The grain-size

analysis indicates essential hints to the sediment transport history, origin of the sediment, and depositional setting (Bui et al., 1990). Edwards (2001) emphasized that grain size and sorting are extensively used to distinguish the texture of the sediments and the depositional environments. The grain size is a textural parameter of sediments, and it comprises an essential aid infer analogous ancient sedimentary environments and hydrodynamic conditions (Friedman, 1961a; Andrews & Van Der Lingen, 1968; David, 1970; Dickinson, 1974; Ingersoll, 1990). Several sedimentologists derived the bivariate plots of the textural parameters to strengthen the depositional environments (Otunola & Liu, 2019). The method of bivariate analysis is used to interpret the energy, environment, and transportation mode (Alsharhan & El-Sammak, 2004); however, it is concluded that variations in the fluid-flow mechanism can be reflected in statistical parameters (Essien et al., 2016).

3.4.3 X-Ray Diffraction Analysis (XRD Analysis)

The X-Ray Diffraction is the fast analytical technique mainly used for period identification of crystalline matters and can issues the details on unit cell dimensions. XRD is a rapid and valid tool that provides for a procedure of mineral identification. However, it plays a prominent role in measurements of sample purity.

The X-ray powder diffraction works as it relates to the principle of Bragg's law. Moreover, the principle of Bragg's law states that when incident X-rays strike the surface of the crystal, they become scattered by atom, which implies that the angle of incident is equal to the angle of scattering (Dann, 2002; Skoog et al., 2007).

Eight fine powder samples (about 10 grams each) were sent to the X-Ray Diffraction Analytical and Consulting cc Laboratory at Pretoria by Dr Sabine Verryn for analysis. The samples were analyzed using a PANalytical X'Pert Pro powder diffractometer in 2 θ configuration with an X'Celerator detector and variable divergence and fixed receiving slits with Fe filtered Co-K α radiation ($\lambda=1.789\text{\AA}$). The phases were identified using X'Pert High score plus software. The scanning speed is 1^o 2 θ /minute. The samples were prepared for XRD analysis using a back loading preparation method, thus, a quantitative and qualitative XRD analysis was performed. Diffractograms were obtained using a Malvern Panalytical Aeris diffractometer with PIXcel

detector and fixed slits with Fe filtered Co-K α radiation. The phases were identified using X'Pert Highscore plus software.

3.4.4 Scanning Electron Microscopy (SEM) and Energy-Dispersive X-Ray Spectrometer (EDX/EDS) Analysis

The Scanning Electron Microscopy is the essential instrument used to identify clay minerals that usually have an exclusive morphology. Mainly, the SEM exerts a focused electron beam to initiate a clear image at the surface of solid specimens. The SEM analysis plays a prominent role in evaluating the correlations between the textures and shapes of fine-grained minerals.

The sample interconnected with the primary electron initiating numerous radiations that can be used to attain certain information about the surface structure and the composition of the sample (Steinmetz, 1984). SEM-EDX analyses were used to achieve the information about the surface textures of the beach sands.

Four sand samples were performed using the SEM in the Botany Department of the University of Fort Hare. The SEM model is Joel JSM-6390LV which uses 15KV to run the analysis. SEM was used to identify grain morphology, texture, cement types, detrital and authigenic minerals, pore filling and pore-lining clays, and other diagenetic changes such as replacement and recrystallization for the sand samples. The SEM analysis was coupled with the Energy Dispersive X-Ray (EDX) to determine the mineral types and chemical compositions.

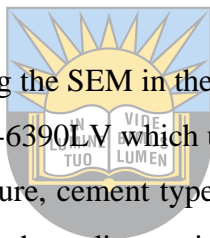




Figure 3.7: JEOL JSM-6390 LV model of Scanning Electron Microscope.

3.5 Geological apparatus used during the field and lab research include:

- Global Positioning System (GPS);
- Hammer;
- Digital camera for taking photos during the fieldwork;
- Compass;
- Weighing balance;
- Sieve sets (-1 ϕ to 5 ϕ);

- Scanning Electron Microscopy (JEOL JSM-6390 LV model) equipped with Energy Dispersive X-Ray Spectrometer;
- X-ray diffraction machine.
- Petrographic Microscope;
- Jaw crusher machine.
- Tape measure



University of Fort Hare
Together in Excellence

CHAPTER 4: STRATIGRAPHY OF KNYSNA FORMATION

4.1 Rock types of the Knysna Formation

The Cretaceous Knysna Formation distributes along the southern segment of South Africa during the drifting of Gondwana when there was extensive erosion of rocks from the Cape Fold Belt and Karoo sequence. The geological succession of the Knysna Formation distinguishes from the Table Mountain Quartzite (TMQ) of the Cape Supergroup at the basement with prevalent brown-maroon colouration and semi-hardening appearance. The bottom of the succession consists of medium to coarse conglomerate which in turn overlain by thin medium-bedded sandstone intercalated with thin mudstone. These lithologies are shown in Figure 4.1.

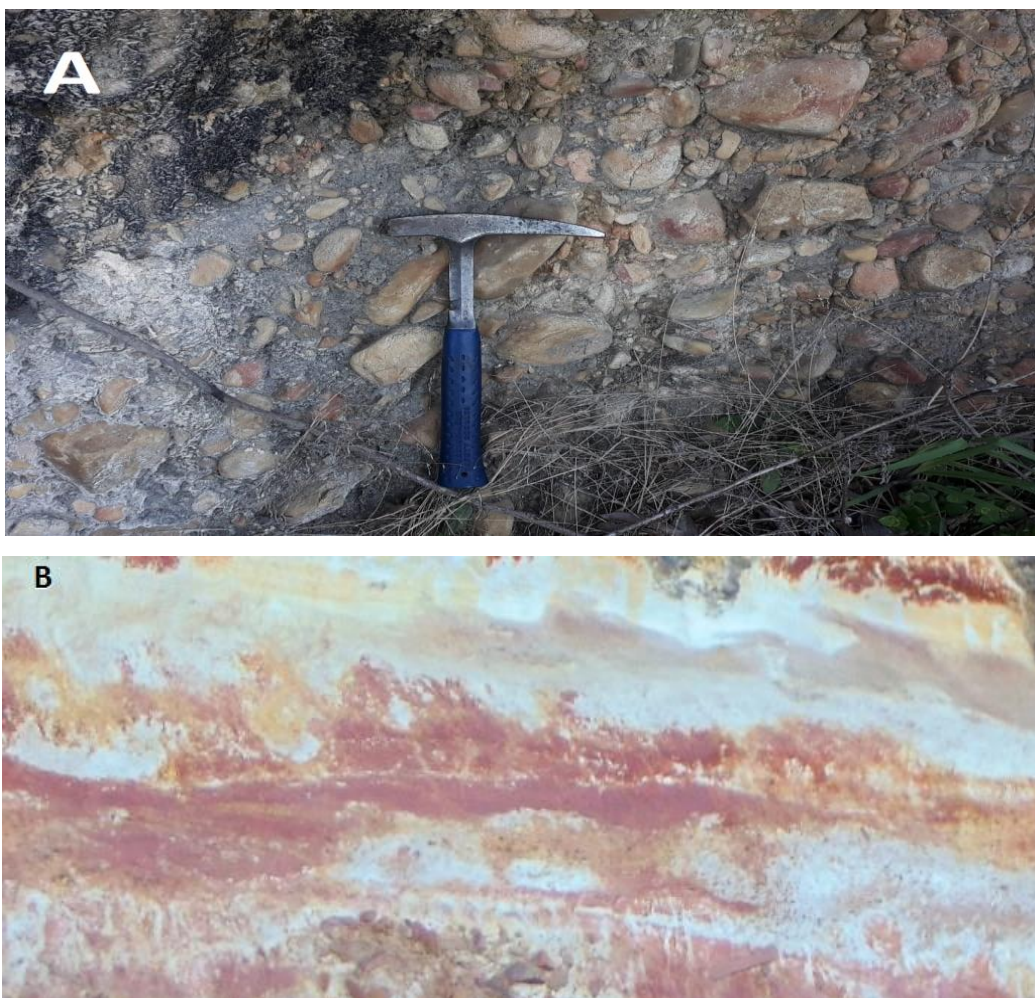


Figure 4.1: Field outcrop of the Knysna Formation along the Road N2 Garden Route at Knysna. (A) Typical clast-supported conglomerate, and (B) Red-brownish sandstone intercalated with thin mudstone.

4.2. Stratigraphic profile of the Knysna Formation

The stratigraphic section measured at field comprises a series upward-fining cycled clastic sediments. Each cycle is composed of conglomerate at the bottom overlain by brownish sandstone with minor red brownish mudstone at the top (Figure 4.5). The bottom sequence is dominated mainly by a clast supported, poorly to medium sorted pebbly conglomerate with thick to massive bedding structure of upto 12.4 m thick (Figure 4.2); the top is red bedded sandstone-mudstone sequence of upto 25.60 m (Figure 4.3). Clast-supported conglomerate comprises the pebbles of quartzite, igneous clasts and unmetamorphic sandstone clasts which probably came from surround Cape Supergroup and Karoo Supergroup source rocks.

The conglomerate of the Knysna Formation comprises sub-rounded and subangular pebbles of quartzite clasts, and cemented or semi-cemented together by quartz silt and clay matrix. The sub-rounded and subangular pebbles show that the pebbles have not been transported for a long distance from their source, and the red brownish colouration of sandstone-mudstone implies those sediments were formed in an oxidic fluvial environment, not marine sediments. The pebble size is approximately from 1 cm to 8 cm in diameter with an average size of 4-5 cm in diameter. The conglomerate and coarse sandstone were probably deposited in fluvial channels, whereas the mudstone was mostly deposited in an overbank or fluvial plain environment. Laterally, the channel conglomerate and sandstone are not stable, and are narrowly distributed, which means they were probably braided river channel deposits and the channels were very variable and could be freely shedding in the space.

In the Knysna Formation, the sandstone grain size is very variable from very coarse to fine arenaceous sands, and also comprises fine-grained to medium-grained. The colour of sandstone differs from red-brownish to brown-whitish colour. The sandstone becomes red-brownish in colour, which means that the environment is oxidizing, not reducing. Therefore, it is not possible for marine sediments but fluvial sediments. From the colour, even lithology is richer in feldspar, and that means it is not quartz-arenite, but it is arkosic sandstone (richer in feldspar). If sandstone is rich in feldspar and exposed in weathering and hydrolysis alters the sandstone to kaolinite, then becomes brown-whitish. The brown-whitish sandstone is rich in hematite, silicate, and iron oxide

due to the oxidation process. The load-cast present in the sandstone occurred because of the process of dissolution. Sandstone was deposited onwards more energetic water eroded the sandstone resulted in fragments which formed intraclasts. Sandstone clasts were coming up from the bottom or close, thus they were not transported very far, and because of water erosion, they become broken, fragmented, and deposited. Intraclasts are coming from inside the basin, not outside the basin. The grains are relatively round, that means were transported not far away from the bottom. The thinly to thickly-bedded sandstone is from around an average of (15 cm-10 m). They compose various sedimentary structures such as lenticular bedding, air escape structure, and load cast. These sedimentary structures are discussed in Chapter 8.

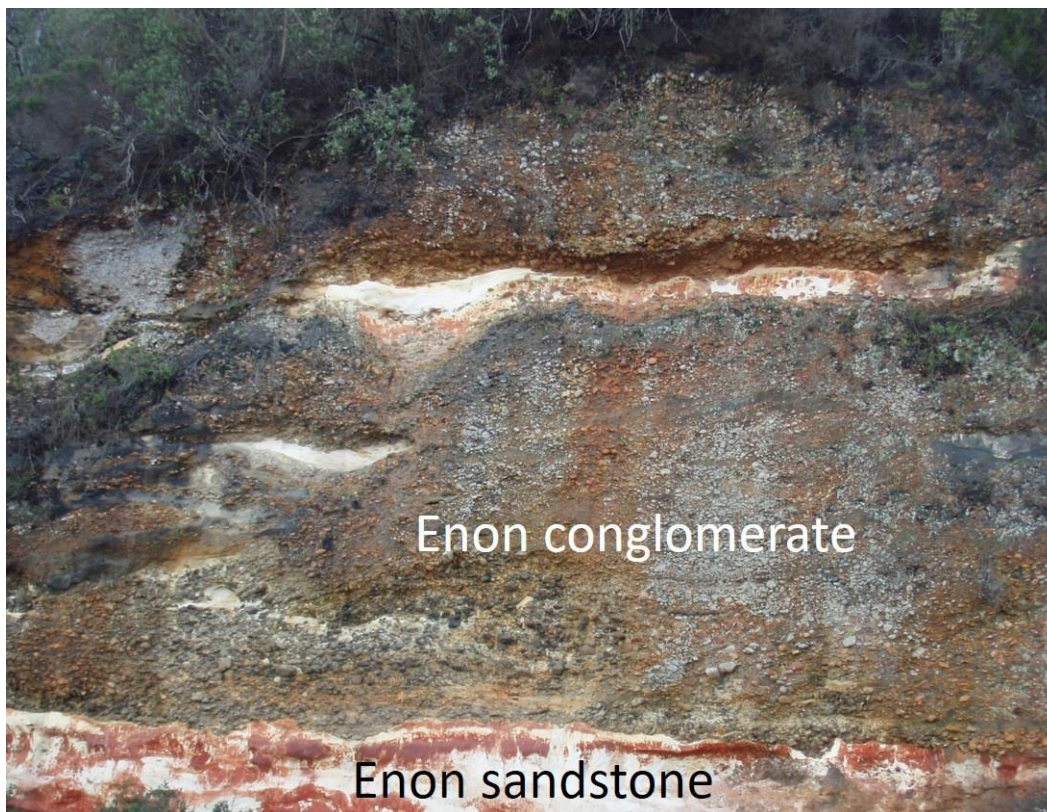


Figure 4.2: Clast-supported conglomerate with lenticular brownish sandstone of Knysna Formation.



Figure 4.3: Thick-bedded red-brownish sandstone with conglomerate (top) in Knysna Formation.

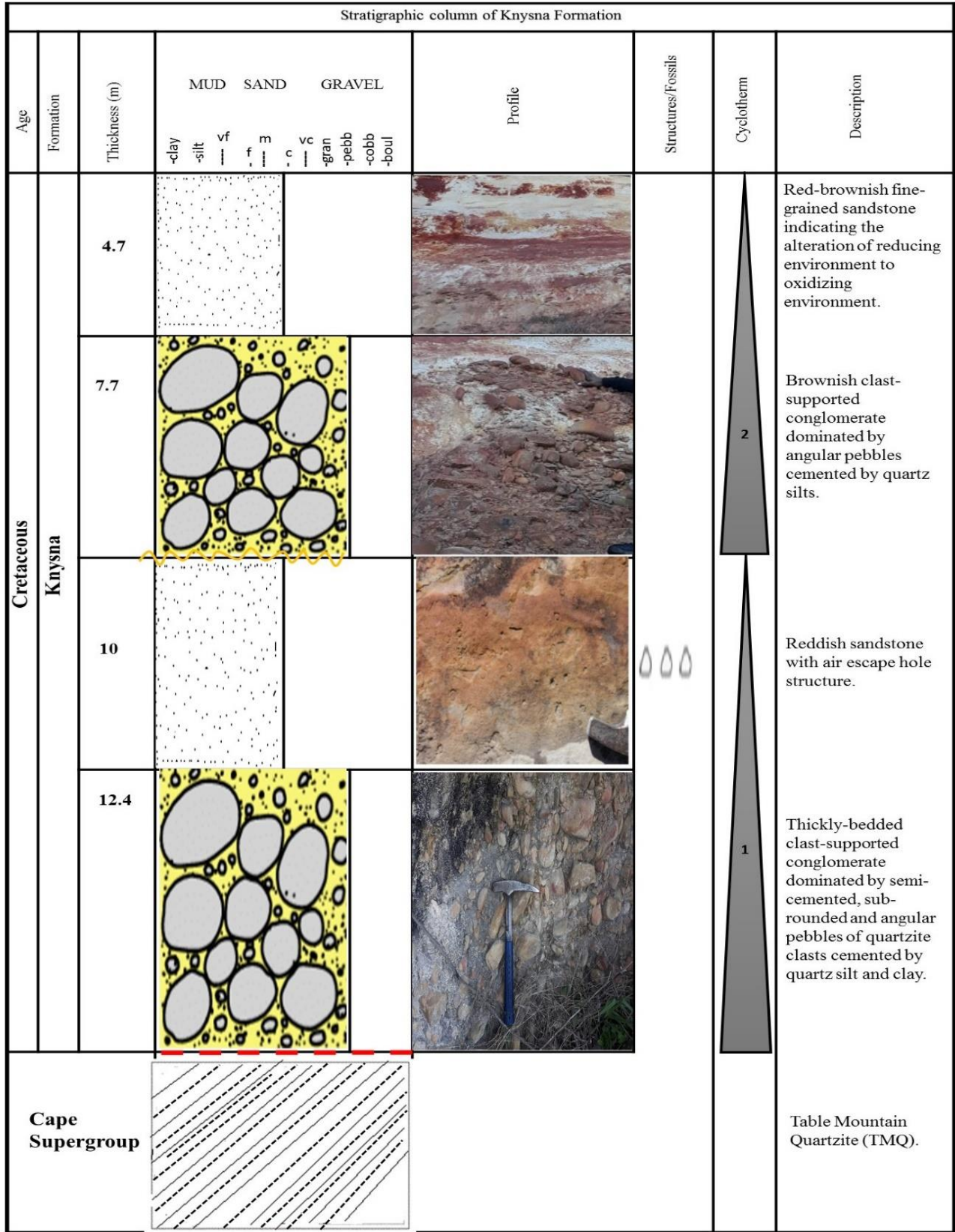


Figure 4.4: Two upward fining cycles with erosion surfaces at the bottom along Knysna

Formation outcrop.
University of Fort Hare
Together in Excellence

Stratigraphic column of Knysna Formation									
Age	Formation	Thickness (m)	MUD SAND GRAVEL			Profile	Structures/Fossils	Cyclothem	Description
			-clay -silt	vf f m	vc -gran -pebb -cobb -boul				
Cretaceous	Knysna	6.5						7	Whitish sandstone with cut off material.
		3.5							Very thickly-bedded oligomictic conglomerate.
		4.7						Subordinate whitish sandstone.	
		4.6						6	Clast-supported conglomerate.
		4.9						Thinly sandstone deposited in between conglomerate.	
		6.8						5	Clast-supported conglomerate.
		4.4						Deformed sandstone bedding resulted lenticular bedding.	
		9.2						4	Massive clastic-supported conglomerate with dispersed well-rounded and rounded quartzite pebbles surrounded by quartz silt and clay matrix.
		5						Whitish sandstone in between conglomerates	
11.7						3	Crushed angular conglomerate resulted along the normal faulting zone.		

(Continue on the next page)



Legend

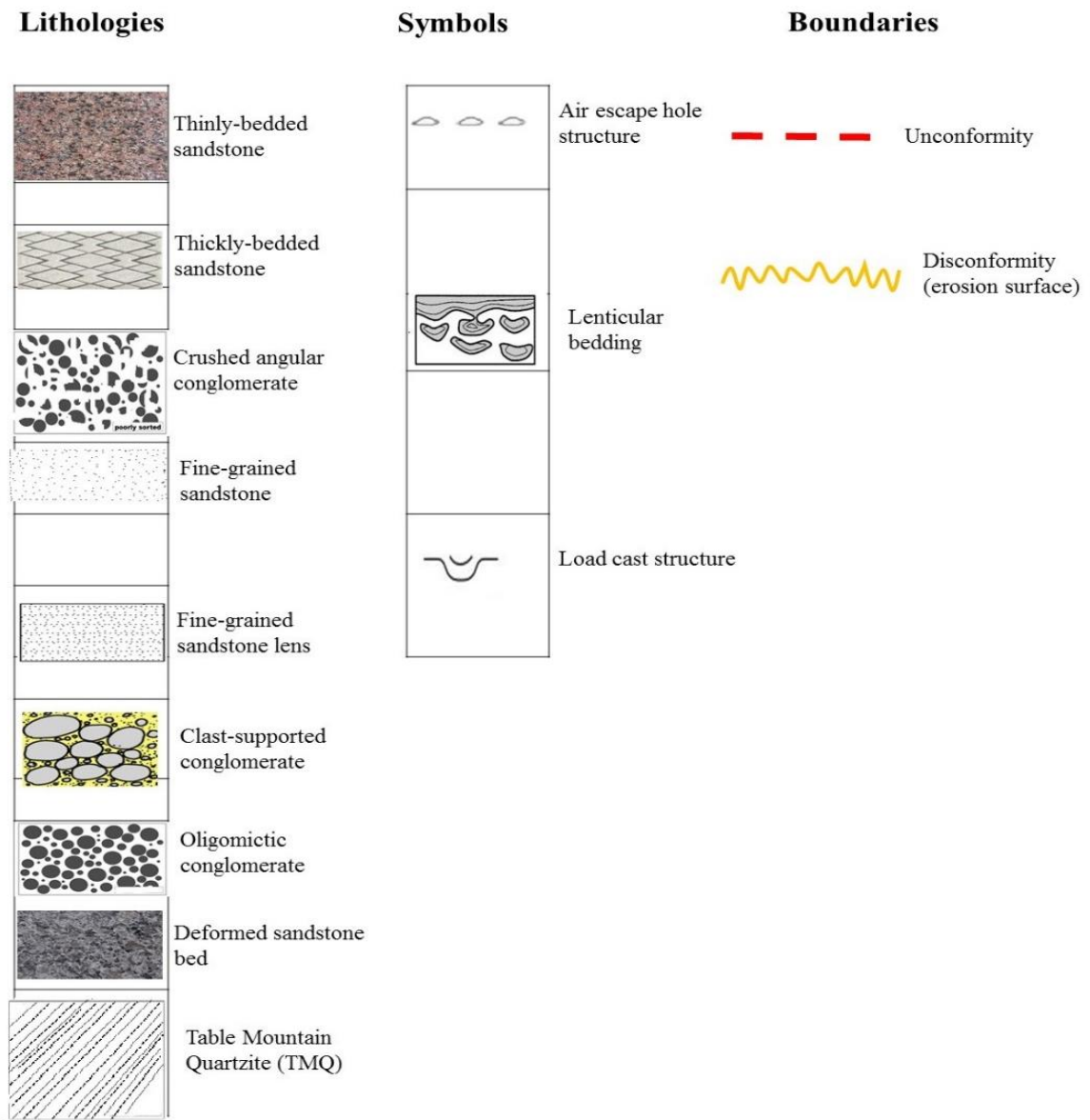
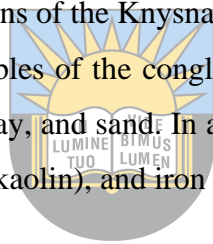


Figure 4.5: A measured stratigraphic section of the Knysna Formation with legend at the bottom.

The stratigraphic correlation is made up of seven upward-fining cycles. Cycle 1 is overlain by the TMQ of the Cape Supergroup. It entirely consists of a thickly-bedded clast-supported

conglomerate (12.4 m), which creates the unconformity boundary with the basement. Hence, in turn, creates the unconformity boundary with the basement overlain with an air escape hole reddish sandstone (10 m). Cycle 2 comprises a brownish clast-supported conglomerate with a thickness of 7.7 m overlain by red-brownish fine-grained sandstone of 4.7 m in thickness. Cycle 3 is the zone of faulting; a series of normal faults results in horst and graben blocks. However, the massive clast-supported conglomerate (11.7 m) crushed and formed angular pebbles underlying whitish sandstone deposits (5 m) with flame structure along the faulting zone. Cycle 4 comprises a massive clast-supported conglomerate with deformed sandstone bed forming lenticular bedding. Cycle 5 is composed of a clast-supported conglomerate with a thinly whitish sandstone bed, while cycle 6 consists of a clast-supported conglomerate with a subordinated brown-whitish sandstone lens. Cycle 7 is the last cycle composed of a thickly-bedded oligomictic conglomerate with a dissolving material in the whitish sandstone forming a load-cast or cut-off structure within the sandstone.

According to the stratigraphic correlations of the Knysna Formation, it is mostly predominated by clast-supported conglomerate. The pebbles of the conglomerate are sub-rounded to angular and semi-cemented mostly by quartz silt, clay, and sand. In addition, the sandstone comprises mostly of quartz, feldspar, mica, clay mineral (kaolin), and iron oxide.



University of Fort Hare
Together in Excellence

CHAPTER 5: GRAIN SIZE ANALYSIS

5.1 Introduction

Grain size, shape and sorting are sensitive to hydrodynamic condition and thus grain size parameters can be used to indicate the hydrodynamic environments. The vital feature of sedimentary rock, particular the siliciclastic sedimentary rock is composed of particles/grains, therefore grain-size analysis had been widely used in the geological research to recognise the hydrodynamic medium, and the wind or water current energy conditions. Obviously, the coarser grains are transported by fast-flowing high energy currents, while finer grains accumulate in quieter, slow-moving lower energy water environment. So grain size analysis had demonstrated that it was a widely used, meaningful research tool in reflecting hydrodynamic condition, transportation medium and depositional environments (Blott & Pye, 2001; Bui et al., 1990; Edwards, 2001; Folk & Ward, 1957; Friedman & Sanders, 1978; Liu & Greyling 1996; Otunola and Liu 2019).

Grain size can be measured in millimeter scale or can be measured in the Phi (ϕ) scale. The relationship between millimeter and Phi scale is shown in Figure 3.6, i.e.

$\phi = -\log_2 D$, Where ϕ is the phi-size, and D is the diameter (in mm) of the particles or grains.

Phi scale is a logarithmic scale, the classification scheme of the grain size was proposed by Udden (1914) and Wentworth (1922), and laterly modified by Friedman (1967). The scale was almost universally used by sedimentologists in the world. The Udden-Wentworth scale is classified into four major size categories (clay, silt, sand, and gravel), further subdivided into more subclasses.

Sorting is used to describe the grain size distribution of uniform grade, reflecting the stability of water energy and depositional process. Sorting can be divided into poorly, moderate, and well sorting. Sorting is usually presented in terms of graphs and statistical presentations.

The grain size is the essential physical characteristic of sediment; thus, it is used to analyze trends in the transportation and deposition processes associated with the dynamic conditions of energy (Blatt et al., 1972).

Main grain diameter is the most commonly used grain-size parameter to measure the average energy of transportation medium (Folk & Ward, 1957; Passega, 1964). However, most sediment particles are composed of several sizes and mean diameter describes the simplest method to issue a granulometric characterization of sediment via a single value. The median grain-size, sorting (standard deviation), and skewness of the grain-size data are the widest sediment parameters surveyed when trying to distinguish the direction of sediment transport and the correlated sedimentary process of deposition (McLaren & Bowles, 1985; Pedreros et al., 1996; Simms et al., 2006; Hajek et al., 2010).

5.2 Grain size measurements

Based on the Standard deviation (Sorting coefficient), Friedman (1961) and Blott and Pye (2001) proposed a classification for grain sorting grade and the related depositional mechanisms table (5.1). In the case of the Knysna and Plettenberg Bay, the sediments were dominantly by moderately to well-sorted category, which means that the sediments were deposited on the river and beach environments with moderate to relatively higher hydrodynamic conditions. The calculated parameters for all the collected 53 samples are listed in the Table 5.2 as below.

Table 5.1: Categorization of grain size analysis parameters (after Friedman, 1961; Blott & Pye, 2001).

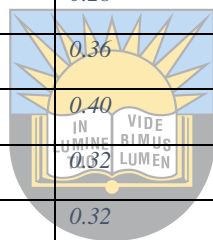
Ranges of standard deviation	Sorting class	Depositional machinism and formation environments
<0.35	Very well sorted	Coastal and lake dunes; beaches (foreshore), common on a shallow marine shelf.
0.35-0.50	Well sorted	Most beaches (foreshore); shallow marine shelf, many inland dunes.
0.50-0.80	Moderately well sorted	Most inland dunes; most rivers; most lagoons, distal marine shelf.
0.80-1.40	Moderately well sorted	Glacio-fluvial settings; rivers; some lagoons; some distal marine shelf.
1.40-2.00	Poorly sorted	Glacio-fluvial settings.
2.00-2.60	Very poorly sorted	Glacio-fluvial settings

>2.60	Extremely poorly sorted	Some glacio-fluvial settings
-------	-------------------------	------------------------------

Table 5.2 Parameter values for 53 samples analyzed.

Sample No	$M_d (\phi)$	$M_z (\phi)$	σ_1	SK_1	K_G
P1	1.39	1.27	1.12	0.01	0.52
P2	2.00	2.03	0.80	-0.11	0.99
P3	2.00	2.00	0.62	-0.01	0.81
P4	1.55	2.00	0.49	1.23	1.05
P5	1.82	2.10	0.54	0.56	0.95
P6	2.38	1.84	1.18	-0.48	1.21
P7	2.35	2.20	0.97	-0.49	2.40
P8	2.35	2.12	0.99	-0.54	1.37
P9	2.19	1.47	1.11	-0.48	0.90
P10	0.18	0.95	0.39	0.89	0.65
K1	0.98	1.25	1.30	0.40	0.67
K2	2.29	1.73	1.33	-0.36	0.88
K3	2.20	1.68	1.24	-0.40	0.43
P11	1.90	2.02	0.65	0.16	0.78
P12	2.25	2.15	0.66	-0.23	0.71
P13	2.49	2.50	0.46	-0.16	1.74
P14	2.50	2.54	0.33	0.09	0.82
P15	2.50	2.55	0.34	0.10	0.80
P16	2.40	2.31	0.54	-0.32	1.05
P17	2.45	2.45	0.34	-0.01	1.02
P18	2.42	2.37	0.48	-0.25	1.19
P19	2.29	2.21	0.61	-0.20	0.83
P20	2.48	2.47	0.50	-0.23	1.23
P21	2.30	2.20	0.58	-0.22	0.80
P22	2.40	2.43	0.45	-0.07	1.15

P23	2.50	2.53	0.32	0.04	0.76
P24	2.50	2.52	0.31	0.04	0.77
P25	2.45	2.49	0.38	-0.92	1.03
P26	2.45	2.48	0.40	-0.07	1.21
P27	2.50	2.52	0.34	-0.04	0.89
P28	2.50	2.52	0.31	0.04	0.82
P29	2.50	2.52	0.81	0.03	0.50
P30	2.50	2.52	0.31	0.04	0.41
P31	2.50	2.52	0.34	-0.04	0.89
P32	2.50	2.52	0.39	-0.13	1.11
P33	2.50	2.53	0.27	0.20	0.64
P34	2.49	2.53	0.37	-0.04	1.02
P35	2.50	2.53	0.28	0.13	0.73
P36	2.50	2.53	0.36	-0.08	0.97
P37	2.48	2.49	0.40	-0.13	1.01
P38	2.50	2.53	0.62	0.05	0.71
P39	2.50	2.53	0.32	0.09	0.78
P40	2.30	2.20	0.59	-0.25	0.83
P41	2.50	1.90	1.18	-0.63	1.87
P42	2.50	2.53	0.32	0.07	1.17
P43	2.50	2.53	0.33	0.07	0.75
P44	2.45	2.50	0.38	-0.04	1.08
P45	2.49	2.51	0.34	-0.12	1.21
P46	2.48	2.51	0.38	-0.11	1.19
P47	2.50	2.53	0.36	-0.01	0.98
P48	2.30	2.18	0.61	-0.30	0.87
P49	2.45	2.44	0.47	-0.18	1.08
P50	2.50	2.47	0.30	0.07	0.80



University of Fort Hare
Together in Excellence

5.3 Moderately to Well sorted River samples

This category of grain-size analysis of the river samples were shown as histograms and cumulative frequency curves e.g. figure (5.1). Three representative samples of this group sediments are discussed as below figures (5.1-5.3). For the reason of save text space, the other samples of this group are listed in the Appendix.

Sample P5

Aliquot mass = 242.68g

Table 5.3: Retained and cumulative percentage for Sample P5.

Sieve size (ϕ)	Mass retained (g)	% retained	Cumulative %
-1	0.95	0.39	0.39
0	2.87	1.18	1.57
1	21.09	8.70	10.27
2	117.96	48.63	58.90
3	96.30	39.70	98.40
4	2.02	0.83	99.43
5	1.36	0.56	99.99
Total mass	242.55		

Error = 0.05%

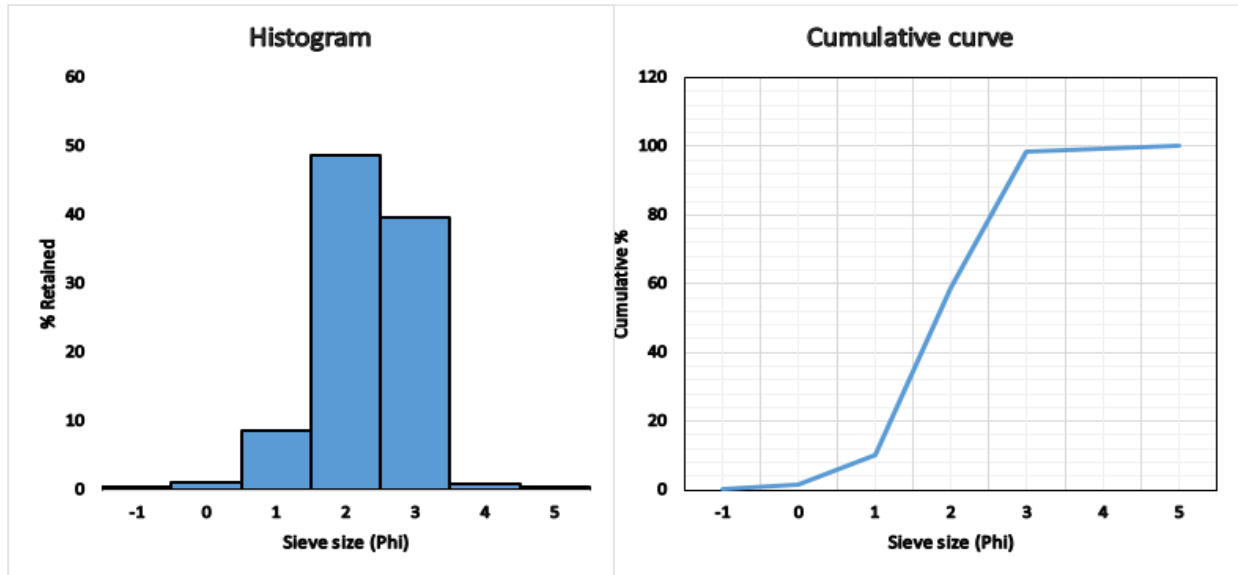


Figure 5.1: Histogram (left) and cumulative curve (right) for Sample P5.

The dominant sediment grain size ranges from 2 ϕ (0.25mm) and 3 ϕ (0.125 mm) followed by a small percentage at 1 ϕ (0.5mm). According to the Wentworth scale, this grain size range falls into medium to fine sand class for the Sample; with very little other coarser or finer particles mixing.

Sample P7

Aliquot mass = 211.59g

Table 5.4: Retained and cumulative percentage for Sample P7.

Sieve size (ϕ)	Mass retained (g)	% retained	Cumulative %
-1	9.29	4.41	4.41
0	7.95	3.77	8.18
1	6.81	3.23	11.41
2	23.86	11.32	22.73
3	153.67	72.89	95.62
4	3.92	1.86	97.48
5	5.32	2.52	100.00
Total mass	210.82		

Error = 0.36%

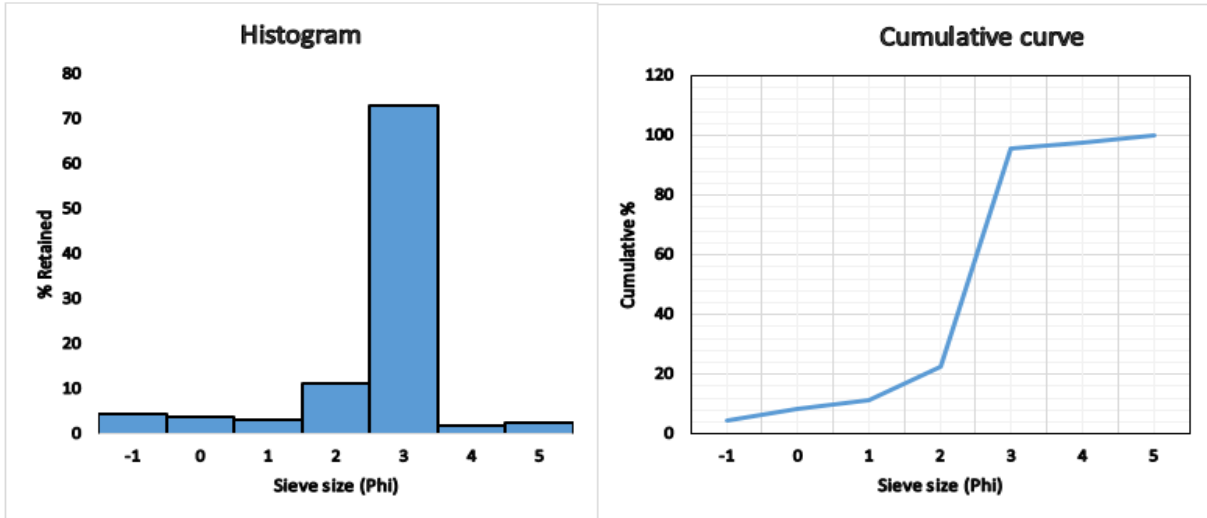
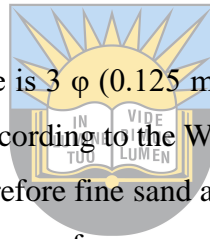


Figure 5.2: Histogram (left) and cumulative curve (right) for Sample P7.

The dominant sediment grain size range is 3 ϕ (0.125 mm) followed by 2 ϕ (0.25 mm) and small percentages of the remaining sieves. According to the Wentworth scale, this grain size range falls into fine to medium sand class, and therefore fine sand and medium sand are dominant in sample P7. This sample contains small percentage of coarser sands of seashells and fine silts of quartz grains.



University of Fort Hare
Together in Excellence

Sample P8

Aliquot mass = 196.94g

Table 5.5: Retained and cumulative percentage for sample P8.

Sieve size (ϕ)	Mass retained (g)	% retained	Cumulative %
-1	7.78	3.95	3.95
0	8.02	4.08	8.03
1	8.45	4.29	12.32
2	40.86	20.77	33.09
3	125.50	63.78	96.87
4	3.40	1.73	98.60

5	2.75	1.40	100.00
Total mass	196.76		

Error = 0.09

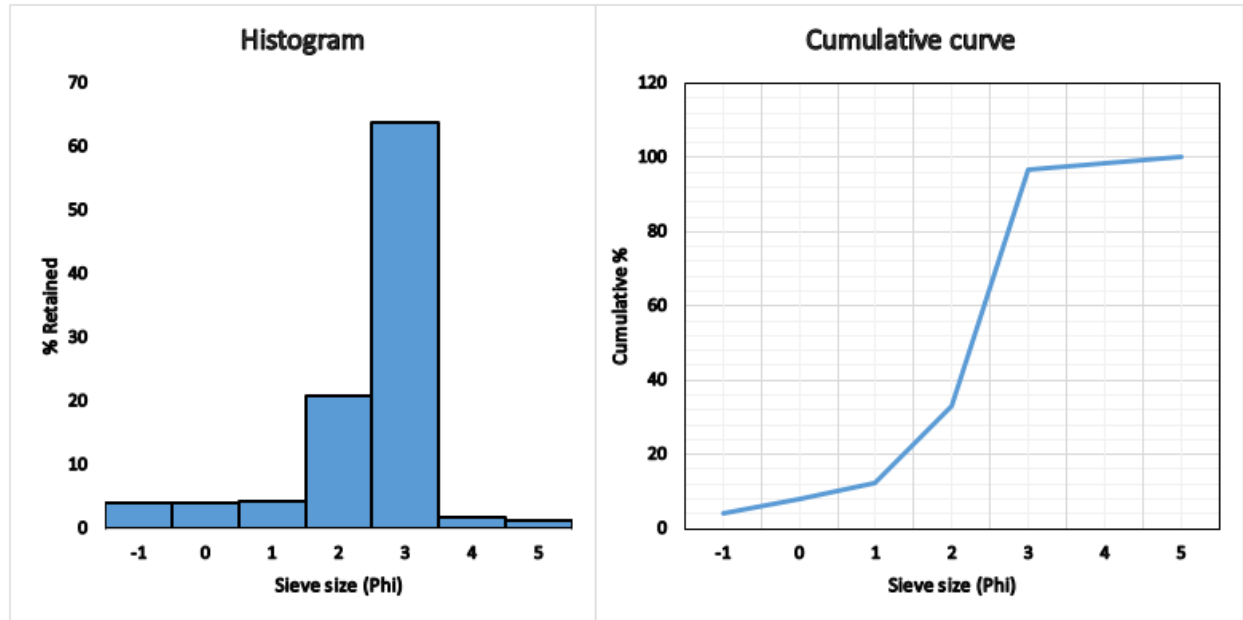


Figure 5.3: Histogram (left) and cumulative curve (right) for Sample P8.

The dominant sediment grain size range is 2 ϕ (0.25 mm) to 3 ϕ (0.125 mm), followed by small percentages of the remained coarser and finer particles. According to the Wentworth scale, this grain size range falls into fine to medium sand class. The coarser particles in the sample are mainly shell fragments such as oyster, mollusca and gastropoda fragments, and coral fragments as well.

5.4 Poorly sorted River samples

This category of samples show a wide range of grain size distribution, which scattered from -1 ϕ (2 mm) to 5 ϕ (0.031mm). Comparing to moderate and well sorted samples, these samples have a wide range of grain size distribution, and the grain size scattered from coarse sands to very fine silts and mud-sized materials, which indicate a poorly grain sorting and the hydrodynamic energy of sediment transportation was lower. Three representative poorly sorted river samples are discussed at below figures (5.4-5.6). The other samples of this group are listed in the Appendix.

Sample P1

Aliquot mass = 239.01g

Table 5.6: Retained and cumulative percentage for Sample P1.

Sieve size (ϕ)	Mass retained (g)	% retained	Cumulative %
-1	64.71	27.09	27.09
0	20.49	8.58	35.67
1	17.98	7.53	43.20
2	40.88	17.12	60.32
3	83.03	34.76	95.08
4	6.50	2.72	97.80
5	5.26	2.20	100.00
Total mass	238.55		

Error = 0.19%

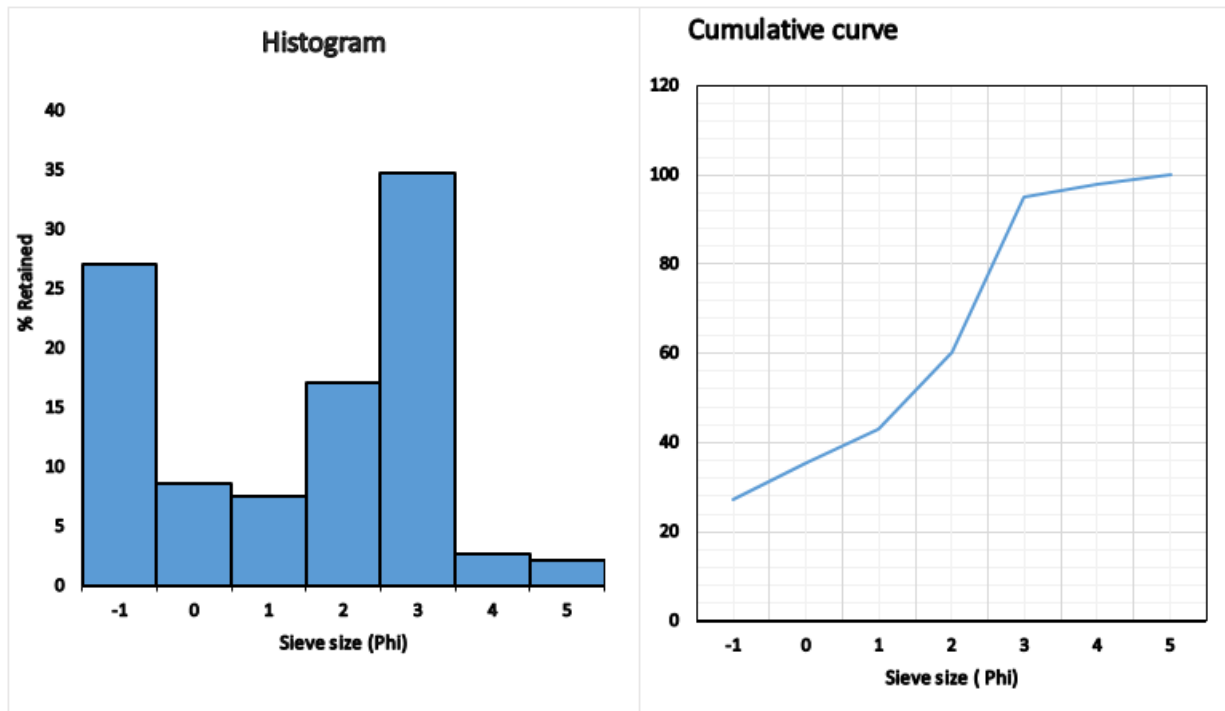
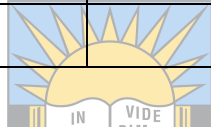


Figure 5.4: Histogram (left) and cumulative curve (right) for Sample P1.

The dominant sediment grain size range is 3 ϕ (0.125 mm), -1 ϕ (2mm) and 3 ϕ (0.50 mm), but the size distribution was scattered very wide from -1 ϕ until to 5 ϕ , indicating a very poor grain size sorting. According to the Wentworth scale, this grain size range falls into a fine to very coarse arenaceous grain size distribution. Poorly sorted grain size distribution means the sediments were deposited in a low energy of hydrodynamic environment, and the water energy was not competent to sort the sediments, hence resulting fine grains and coarse grains were mixed together.

Sample P10

Aliquot mass = 117.39g

Table 5.7: Retained and cumulative percentage for sample P10.

Sieve size (ϕ)	Mass retained (g)	% retained	Cumulative %
-1	43.65	37.36	37.36
0	13.48	11.54	48.90
1	9.00	7.70	56.60
2	12.94	11.07	67.67
3	28.22	24.15	91.82
4	3.26	2.79	94.61
5	6.29	5.38	99.99
Total mass	116.84		

Error = 0.47%

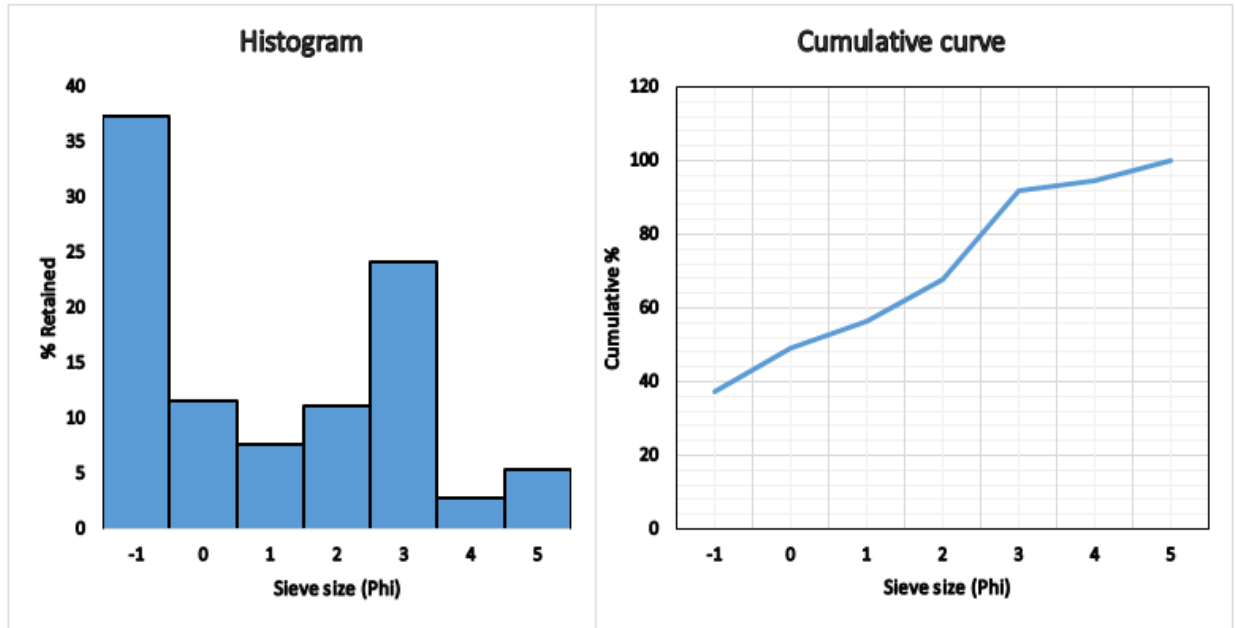


Figure 5.5: Histogram (left) and cumulative curve (right) for Sample P10.

The grain size distribution is very wide from -1ϕ to 5ϕ , hence it is very scatter. The dominant sediment grain size range is -1ϕ (2 mm), 3ϕ (0.125 mm), followed by 0ϕ , 2ϕ and 1ϕ , with some at 4ϕ in the sample. These characteristics of grain size distribution indicate a poorly sorting, and the sediments were deposited in a low energy hydrodynamic environment.

Sample K1

Aliquot mass = 274.49g

Table 5.8: Retained and cumulative percentage for sample K1.

Sieve size (ϕ)	Mass retained (g)	% retained	Cumulative %
-1	83.20	30.41	30.41
0	27.52	10.06	40.47
1	26.46	9.67	50.14
2	42.15	15.41	65.55
3	65.19	23.83	89.38
4	15.18	5.55	94.93

5	13.90	5.08	100.00
Total mass	273.60		

Error = 0.32%

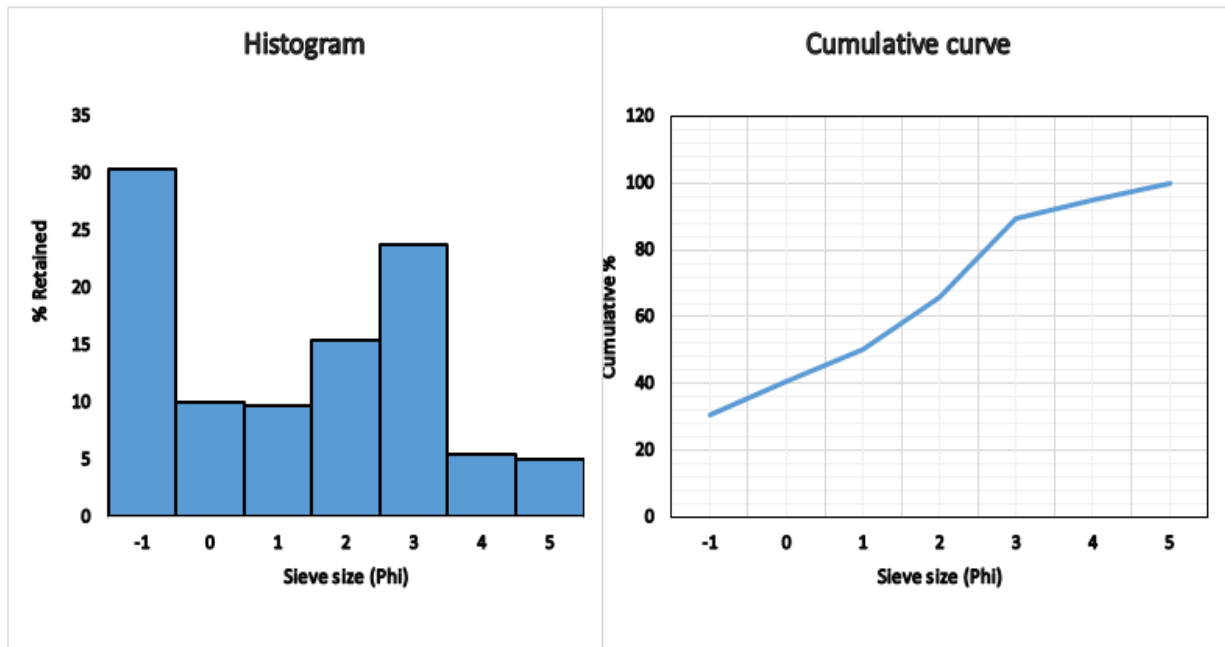


Figure 5.6: Histogram (left) and cumulative curve (right) for Sample K1.

University of Fort Hare
Together in Excellence

Similar to Sample 10, the grain size distribution of Sample K1 is also very scatter, the size ranges from -1ϕ to 5ϕ , indicating a poor sorting of grain size. The dominant sediment grain size range is -1ϕ (2 mm), 3ϕ (0.125 mm), followed by 2ϕ , 0ϕ , 1ϕ with more less percentage at 4ϕ and 5ϕ in the Sample K1.

5.5 Grain size parameters for river sample analysis

The grain-size analysis was accomplished on thirteen river samples accumulated from the Plettenberg Bay river (Keurbooms River) and Knysna Estuary (Floodplain) shown in Figure 3.1;3.3. Equations in Table 3.1 were used to calculate the statistical parameters of the mean (M_z), sorting (σ_I), skewness (SK_I), and kurtosis (K_G) presented in Table 5.2 and Table 5.9.

Table 5.9: Grain-size statistical parameters of River samples from P1-P10 and K1-K3.

Sample No	$M_d (\phi)$	$M_z (\phi)$	σ_1	SK_I	K_G	Explanation
P1	1.39	1.27	1.12	0.01	0.52	Fine and very coarse sand, very poorly-sorted, near symmetrical, and very platykurtic.
P2	2.00	2.03	0.80	-0.11	0.99	Fine and medium sand, poorly-sorted, strongly coarse-skewed, and mesokurtic
P3	2.00	2.00	0.62	-0.01	0.81	Fine and medium sand, moderately-sorted, near symmetrical, and platykurtic.
P4	1.55	2.00	0.49	1.23	1.05	Medium and fine sand, well-sorted, strongly fine-skewed, and mesokurtic.
P5	1.82	2.10	0.54	0.56	0.95	Medium and fine sand, moderately-sorted, strongly fine-skewed, and mesokurtic.
P6	2.38	1.84	1.18	-0.48	1.21	Fine and very coarse sand, very poorly-sorted, coarse-skewed, and leptokurtic.
P7	2.35	2.20	0.97	-0.49	2.40	Fine and medium sand, poorly-sorted, coarse-skewed, and very leptokurtic.
P8	2.35	2.12	0.99	-0.54	1.37	Fine and medium sand, poorly-sorted, coarse-skewed, and leptokurtic.
P9	2.19	1.47	1.11	-0.48	0.90	Fine and very coarse sand, very poorly-sorted, coarse-skewed, and platykurtic.
P10	0.18	0.95	0.39	0.89	0.65	Granule gravel, well-sorted, strongly fine-skewed, and very platykurtic.
K1	0.98	1.25	1.30	0.40	0.67	Granule gravel, very poorly-sorted, strongly fine-skewed, and very platykurtic.
K2	2.29	1.73	1.33	-0.36	0.88	Fine and very coarse sand, very poorly-sorted, coarse-skewed, and platykurtic.

K3	2.20	1.68	1.24	-0.40	0.43	Fine and very coarse sand, very poorly-sorted, coarse-skewed, and very platykurtic.
----	------	------	------	-------	------	---

5.5.1 Discussion on grain size parameters

A) Mean grain-size (M_z)

Mean values for the samples collected in Keurbooms River (sample P1 to P10) varies from 0.95 to 2.20 with an average value of 1.80, and the mean's distribution for those collected in Knysna Estuary (sample K1 to K3) differs from 1.25 to 1.73 with an average value of 1.60. Therefore, based on the Udden-Wentworth grade scale, sediments for both Keurbooms River and Knysna Estuary are medium-grained sands. It gives a hint of medium to fairly energy conditions. Sediments, in most cases, turn into coarser material with an increase in the energy of the transporting agent (Folk, 1974).



B) Median (M_d)

The median is the diameter with partial grains by weight finer and partial grains by weight coarser. It corresponds to the fifty percentile (ϕ_{50}) on a cumulative frequency curve. Thus, the median diameter of the Keurbooms River samples varies from $\phi_{0.18}$ - $\phi_{2.38}$ and Knysna Estuary varies from $\phi_{0.98}$ - $\phi_{2.29}$.

C) Sorting coefficient (σ_1)

The examined Keurbooms River samples indicate that the standard deviation varies from 0.39 to 1.18, with an average value of 0.82. Therefore, the average value shows that the area is dominant in poorly-sorted sediments. In comparison, the sorting of the Knysna Estuary samples differs from 1.24 to 1.33, with an average value of 1.29. Thus, the average value shows that the area is dominant in very poorly-sorted sediments. According to Friedman (1961b) and Blott & Pye (2001) spotted that several ranges of sorting in sand deposits define several depositional environments of the sands shown in table (5.1).

5.6 Beach sample analysis (Well sorted samples)

Grain-size sieve analysis was carried out on the forty beach samples collected from Plettenberg Bay beaches (Beacon, Robberg, Central, Hobie, Wedge, Sanctuary, and Lookout beach shown in figure (3.1). Statistical parameters (mean, sorting, skewness, and kurtosis) captured using the equation in Table 3.1 are tabulated in Table 5.2 and Table 5.14. Four representative samples are discussed in the text as below figures (5.7-5.10), the other samples of this group are listed in the Appendix to save text space and to avoid repetition.

Sample P11

Aliquot mass = 330.48g

Table 5.10: Retained and cumulative percentage for sample P11.

Sieve size (ϕ)	Mass retained (g)	% retained	Cumulative %
-1	1.89	0.57	0.57
0	2.11	0.64	1.21
1	5.19	1.57	2.78
2	177.80	53.95	56.73
3	142.35	43.19	99.92
4	0.25	0.08	100.00
5	0.00	0.00	100.00
Total mass	329.59		

Error = 0.27%

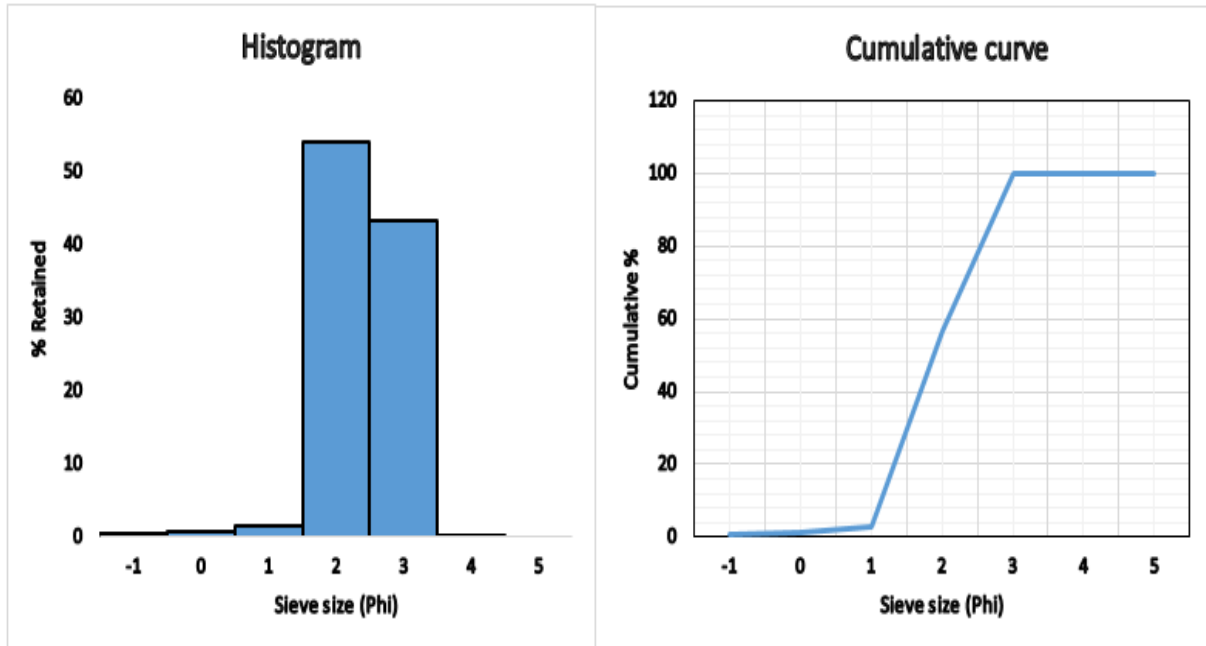


Figure 5.7: Histogram (left) and cumulative curve (right) for Sample P11.

The dominant sediment grain size range is 2 ϕ (0.25 mm) to 3 ϕ (0.125 mm), followed by a small percentage at 1 ϕ . According to the Wentworth scale, this grain size range falls into the medium sand and fine sand class, and therefore, medium and fine sands are dominant in the Sample P11. There are no seashell fragments present.

Sample P12

Aliquot mass = 387.17g

Table 5.11: Retained and cumulative percentage for sample P12.

Sieve size (ϕ)	Mass retained (g)	% retained	Cumulative %
-1	1.99	0.52	0.52
0	2.29	0.59	1.11
1	4.79	1.24	2.35
2	149.19	38.63	40.98
3	227.83	58.99	99.97
4	0.15	0.04	100.01
5	0.00	0.00	100.01

Total mass	386.24		
------------	--------	--	--

Error = 0.24%

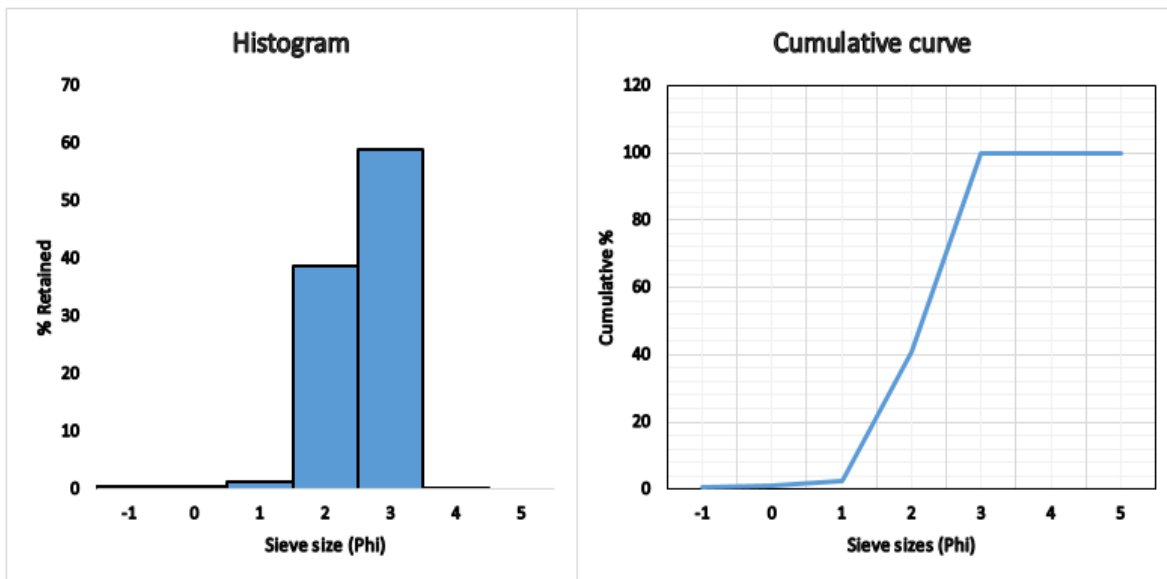


Figure 5.8: Histogram (left) and cumulative curve (right) for Sample P12.

The dominant sediment grain size range is 3 ϕ (0.125 mm) 2 ϕ (0.25 mm), followed by a small percentage of the grain size range of 1 ϕ . According to the Wentworth scale, this grain size range falls into fine sand and medium sand class and therefore fine and medium sand are dominant in sample P12, and some seashells are present.

Sample P13

Aliquot mass = 317.22g

Table 5.12: Retained and cumulative percentage for sample P13.

Sieve size (ϕ)	Mass retained (g)	% retained	Cumulative %
-1	0.00	0.00	0.00
0	0.52	0.16	0.16
1	1.32	0.42	0.58
2	32.49	10.25	10.83
3	282.10	89.02	99.85
4	0.45	0.14	99.99

5	0.00	0.00	99.99
Total mass	316.88		

Error = 0.11%

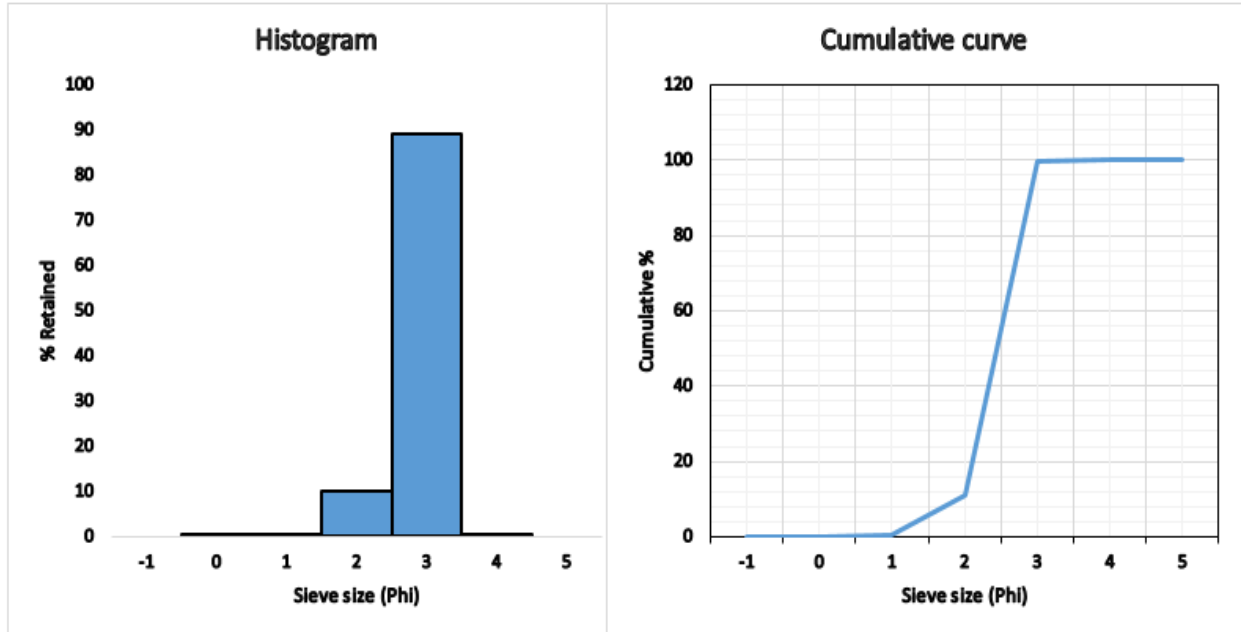


Figure 5.9: Histogram (left) and cumulative curve (right) for Sample P13.

The dominant sediment grain size range is 3 ϕ (0.125 mm), followed by small percentages of a grain size range of 2 ϕ (0.25 mm). According to the Wentworth scale, this grain size range fall into fine sand and medium sand class, and therefore fine and medium sand are dominant in sample P13.

Sample P14

Aliquot mass = 399.02g

Table 5.13: Retained and cumulative percentage for sample P14.

Sieve size (ϕ)	Mass retained (g)	% retained	Cumulative %
-1	0.50	0.13	0.13
0	0.16	0.04	0.17
1	0.23	0.06	0.23
2	7.21	1.81	2.04
3	389.69	97.67	99.71

4	0.70	0.18	99.89
5	0.49	0.12	100.01
Total mass	398.98		

Error = 0.01%

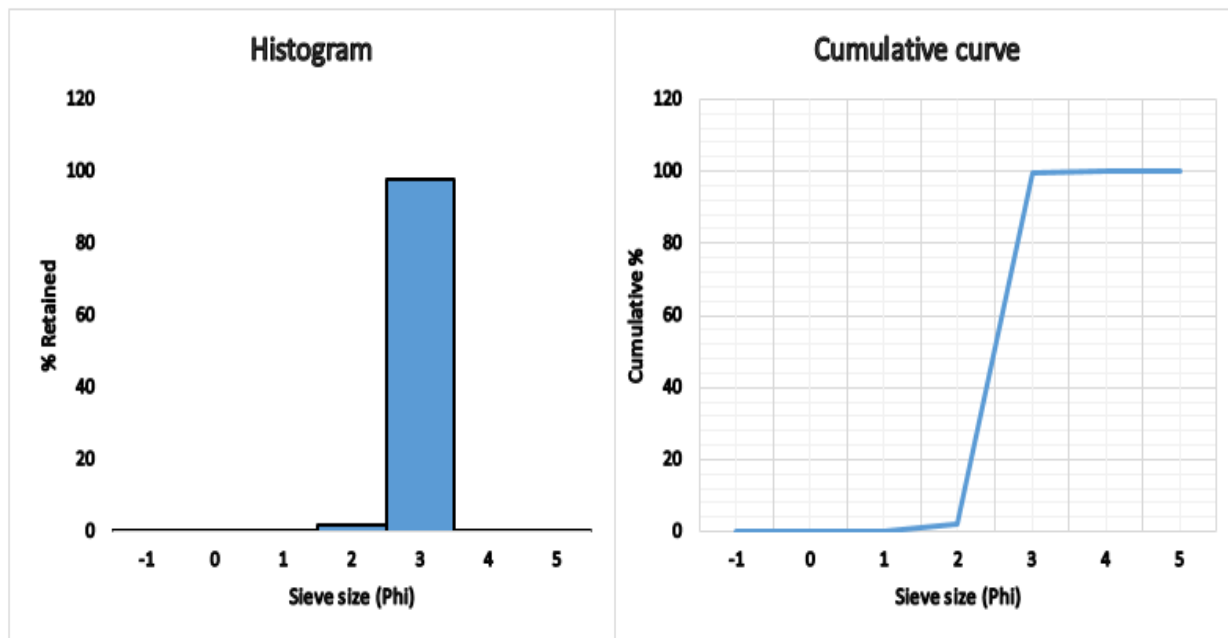


Figure 5.10: Histogram (left) and cumulative curve (right) for Sample P14.

University of Fort Hare
Together in Excellence

The grain size distribution area is very narrow and very concentrated. The dominant sediment grain size range is 3 ϕ (0.125 mm), and no much other size category is present. According to the Wentworth scale, this grain size range falls into a fine sand class for sample P14.

5.7 Grain size statistical parameters of beach sediments

Table 5.14: Grain-size statistical parameters of Beach samples from P11 to P50

Sample No	M_d (ϕ)	M_z (ϕ)	σ_1	SK_1	K_G	Explanation
P11	1.90	2.02	0.65	0.16	0.78	Medium and fine sand, moderately-sorted, fine-skewed, and platykurtic.

P12	2.25	2.15	0.66	-0.23	0.71	Fine and medium sand, moderately-sorted, strongly coarse-skewed, and platykurtic.
P13	2.49	2.50	0.46	-0.16	1.74	Fine and medium sand, well-sorted, strongly coarse-skewed, and very leptokurtic.
P14	2.50	2.54	0.33	0.09	0.82	Fine sand, very well-sorted, near symmetrical, and platykurtic.
P15	2.50	2.55	0.34	0.10	0.80	Fine sand, very well-sorted, near symmetrical, and platykurtic.
P16	2.40	2.31	0.54	-0.32	1.05	Fine and medium sand, moderately-sorted, coarse-skewed, and mesokurtic.
P17	2.45	2.45	0.34	-0.01	1.02	Fine and medium sand, very well-sorted, near symmetrical, and mesokurtic.
P18	2.42	2.37	0.48	-0.25	1.19	Fine and medium sand, well-sorted, strongly coarse-skewed, and leptokurtic.
P19	2.29	2.21	0.61	-0.20	0.83	Fine and medium sand, moderately-sorted, strongly coarse-skewed, and platykurtic.
P20	2.48	2.47	0.50	-0.23	1.23	Fine and medium sand, well-sorted, strongly coarse-skewed, and leptokurtic.
P21	2.30	2.20	0.58	-0.22	0.80	Fine and medium sand, moderately-sorted, strongly coarse-skewed, and platykurtic.
P22	2.40	2.43	0.45	-0.07	1.15	Fine and medium sand, well-sorted, near symmetrical, and leptokurtic.
P23	2.50	2.53	0.32	0.04	0.76	Fine sand, very well-sorted, near symmetrical, and platykurtic.
P24	2.50	2.52	0.31	0.04	0.77	Fine and medium sand, very well-sorted, near symmetrical, and platykurtic.
P25	2.45	2.49	0.38	-0.92	1.03	Fine and medium sand, well-sorted, coarse-skewed, and mesokurtic.
P26	2.45	2.48	0.40	-0.07	1.21	Fine and medium sand, well-sorted, near symmetrical, and leptokurtic.

P27	2.50	2.52	0.34	-0.04	0.89	Fine and medium sand, very well-sorted, near symmetrical, and platykurtic.
P28	2.50	2.52	0.31	0.04	0.82	Fine sand, very well-sorted, near symmetrical, and platykurtic.
P29	2.50	2.52	0.81	0.03	0.50	Fine and medium sand, poorly-sorted, near symmetrical, and very platykurtic.
P30	2.50	2.52	0.31	0.04	0.41	Fine and medium sand, very well-sorted, near symmetrical, and very platykurtic
P31	2.50	2.52	0.34	-0.04	0.89	Fine sand, very well-sorted, near symmetrical, and platykurtic.
P32	2.50	2.52	0.39	-0.13	1.11	Fine and medium sand, well-sorted, strongly coarse-skewed, and leptokurtic.
P33	2.50	2.53	0.27	0.20	0.64	Fine sand, very well-sorted, fine-skewed, and very platykurtic.
P34	2.49	2.53	0.37	-0.04	1.02	Fine and medium sand, well-sorted, near symmetrical, and mesokurtic.
P35	2.50	2.53	0.28	0.13	0.73	Fine sand, very well-sorted, fine-skewed, and platykurtic.
P36	2.50	2.53	0.36	-0.08	0.97	Fine and medium sand, well-sorted, near symmetrical, and mesokurtic.
P37	2.48	2.49	0.40	-0.13	1.01	Fine sand, well-sorted, strongly coarse-skewed, and mesokurtic.
P38	2.50	2.53	0.32	0.05	0.71	Fine sand, very well-sorted, near symmetrical, and platykurtic.
P39	2.50	2.53	0.32	0.09	0.78	Fine sand, very well-sorted, near symmetrical, and platykurtic.
P40	2.30	2.20	0.59	-0.25	0.83	Fine and medium sand, moderately-sorted, strongly coarse-skewed, and platykurtic.
P41	2.50	1.90	1.13	-0.63	1.87	Fine-sand, moderately-sorted, strongly coarse-skewed, and leptokurtic.

P42	2.50	2.53	0.32	0.07	1.17	Fine-sand, very-well sorted, near symmetrical, and leptokurtic.
P43	2.50	2.53	0.33	0.07	0.75	Fine sand, very well-sorted, near symmetrical, and platykurtic.
P44	2.45	2.50	0.38	-0.04	1.08	Fine and medium sand, well-sorted, near symmetrical, and mesokurtic.
P45	2.49	2.51	0.34	-0.12	1.21	Fine and medium sand, very well-sorted, strongly coarse-skewed, and leptokurtic.
P46	2.48	2.51	0.38	-0.11	1.19	Fine and medium sand, well-sorted, strongly coarse-skewed, and leptokurtic.
P47	2.50	2.53	0.36	-0.01	0.98	Fine sand, well-sorted, near symmetrical, and mesokurtic.
P48	2.30	2.18	0.61	-0.30	0.87	Fine and medium sand, moderately-sorted, coarse-skewed, and platykurtic.
P49	2.45	2.44	0.47	-0.18	1.08	Fine and medium sand, well-sorted, strongly coarse-skewed, and mesokurtic.
P50	2.50	2.47	0.30	0.07	0.80	Fine sand, very well-sorted, near symmetrical, and platykurtic.

5.7.1 Discussion

A) Mean-grain size (M_z)

The mean values for the samples compiled by Beacon Beach (P11 to P15) range from 2.02 to 2.55 with an average value of 2.35. The mean values for the samples collected from Robberg Beach (P16 to P20) range from 2.21 to 2.47 with an average mean of 2.36, and the mean distribution for those collected from Central Beach (P21 to P25), ranges from 2.20 to 2.53 with an average value of 2.43.

The mean value for the samples collected from Hobie Beach (P26 through P30) range from 2.48 to 2.52 with an average value of 2.51, and the mean value for the samples collected from Wedge Beach (P31 to P35) range from 2, 52 to 2.53 with an average value of 2.53, the average values for

the samples collected from the Sanctuary beach (P36 to P40) range from 2.2 to 2.53 with an average value of 2.46. In contrast, the mean values for the samples collected from Lookout beach (P41 to P50) range from 1.90 to 2.53, with an average value of 2.43.

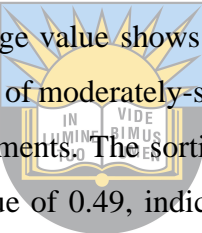
As stated by the Udden-Wentworth grade scale, this suggests that all those samples in the Plettenberg Bay beach where the research was conducted are fine-grained sands. However, it means that the energy of the transportation medium was constant and relative stronger (Folk, 1974; Nelson, 2015).

B) Median (M_d)

The median diameter of the beach samples extent from $\phi 1.90$ to $\phi 2.50$.

C) Sorting coefficient (σ)

The evaluated Beacon beach samples reveal that the sorting ranges from 0.33 to 0.65, with an average value of 0.45. Hence, the average value shows that the area is dominant in well-sorted sands. The Beacon beach comprises 40% of moderately-sorted sediments, 40% of very well-sorted sediments, and 20% of well-sorted sediments. The sorting values of the Robberg beach extents from 0.34 to 0.61, with an average value of 0.49, indicating well-sorted sands. Robberg beach consists of 40% of moderately-sorted sediments, 40% of very well-sorted sediments, and 20% of well-sorted sediments as well.



University of Port Harcourt
Together in Excellence

The sorting values of the Central beach extents from 0.31 to 0.58, with an average value of 0.41. Thus, the average value shows that the area is dominant in well-sorted sands. The Central beach comprises 40% of very well-sorted sediments, 40% of well-sorted sediments, and 20% of moderately-sorted sediments. The sorting values of the Hobie beach extents from 0.31 to 0.81, with an average value of 0.43, suggesting that the area is predominant of well-sorted sands. The Hobie beach comprises 50% of very well-sorted sediments, 25% of well-sorted, and 25% of poorly-sorted sediments.

The sorting values of the Wedge beach range from 0.27 to 0.39, with an average value of 0.32. Therefore, the average value shows that the area is dominant in very well-sorted sands. The beach comprises 75% of very well-sorted sediments and 25% of well-sorted sediments. The sorting values of the Sanctuary beach extents from 0.32 to 0.59, with an average value of 0.40, indicating

well-sorted sands. The Sanctuary beach consists of 40% of well-sorted sediments, 40% of very well-sorted sediments, and 20% of moderately-sorted sediments. The sorting values of the Lookout beach extents from 0.30 to 1.13, with an average value of 0.45. The average value shows that the area is dominant in well-sorted sands. Lookout beach comprises 40% of well-sorted sediments, 40% of very well-sorted sediments, and 20% of moderately-sorted sediments.

Friedman (1961) recorded that the extent in sorting anticipates several environments for deposition of sands in table (5.1). The predominance of very well-sorted sediments corroborates that the sediments were quite often deposited on beach environments or shallow marine environments where wave currents settle the sediments by size (Friedman, 1961b; Blott & Pye, 2001). The very well-sorted sediments are dominant in the beaches where the research was conducted (Plettenberg Bay), hinting that the beach sediments were revealed to a high energy state.

D) Skewness (SK_I)

The skewness values for the Beacon beach samples extents from -0.23 to 0.10, with an average value of -0.008, suggesting a near symmetrical nature of sediments. The skewness values of the Robberg beach extents from -0.32 to -0.01, with an average value of -0.202, indicating a strongly coarse-skewed nature of sediments. The skewness values of the Central beach extents from -0.32 to 0.04, with an average value of -0.106. Thus, the average value shows that the area is dominant in the near-symmetrical nature of sediments. The skewness values of the Hobie beach extents from -0.07 to 0.04, with an average value of 0, suggesting that the area is predominant of near-symmetrical nature of sediments.

The skewness values of the Wedge beach ranges from -0.13 to 0.20, with an average value of 0.024. Therefore, the average value shows that the area is dominant in the near-symmetrical nature of sediments. The skewness values of the Sanctuary beach extents from -0.25 to 0.09, with an average value of -0.064, indicating a near symmetrical nature of sediments. The skewness values of the Lookout beach extents from -0.63 to 0.07, with an average value of -0.11. The average value shows that the area is dominant of a strongly coarse skewed nature of sediments

The Beacon beach comprises 40% near-symmetrical, 40% strongly coarse-skewed, and 20% of fine-skewed sands. Robberg beach consists of 60% strongly coarse-skewed, 20% coarse-skewed, and 20% near symmetrical sands. The central beach is made up of 60% near-symmetrical, 20%

strongly coarse-skewed, and 20% of coarse-skewed sands. The Hobie beach is comprised of 100% of near-symmetrical sands. The Wedge beach comprises 40% fine-skewed, 40% near-symmetrical, and 20% of strongly coarse-skewed sands. The Sanctuary beach consists of 60% near-symmetrical and 40% strongly coarse-skewed sands. Lookout beach comprises 50% near-symmetrical, 40% strongly coarse-skewed, and 20% of coarse-skewed sands.

The majority of the beach samples are considered near symmetrical nature of sediments. Okeyode & Jibiri (2013) stated that the positive values suggest skewness in grain sizes. In contrast, the negative values specify that the skewness is towards the coarser grain sizes. The sand samples were made up of a uniform amount of positive and negative values based on the results. Therefore, the skewness characterises that the sediments were not revealed to strong, energetic environments such as strong tidal washing, storm surges, and wave-breaking.

E) Kurtosis (K_G)

The Beacon beach samples show that the kurtosis extents from 0.71 to 1.74, with an average value of 0.97. Thus, the average value shows that the area is dominant of mesokurtic nature in the sediments. The Beacon beach outlines 80% of platykurtic and 20% of very leptokurtic nature. The kurtosis values of the Robberg beach extents from 0.83 to 1.23, with an average value of 1.064, suggesting that the area is predominant of mesokurtic nature of sediments. The Robberg beach serves 40% mesokurtic, 40% leptokurtic, and 20% platykurtic nature.

The kurtosis values of the Central beach ranges from 0.76 to 1.23, with an average value of 0.90. Therefore, the average value shows that the area is dominant of platykurtic nature in the sediments. The Central beach defines 60% of platykurtic and 40% of leptokurtic nature. The kurtosis values of the Hobie beach extents from 0.41 to 1.21, with an average value of 0.766, indicating a platykurtic nature in the sediments. The Hobie beach indicates 40% of very platykurtic, 40% of platykurtic, and 20% of leptokurtic. The kurtosis values of the Wedge beach range from 0.64 to 1.11, with an average value of 0.878. Therefore, the average value shows that the area is dominant of platykurtic nature in the sediments. The Wedge beach profiles 40% of platykurtic, 20% of very platykurtic, 20% of mesokurtic, and 20% of leptokurtic nature.

The kurtosis values of the Sanctuary beach extents from 0.71 to 1.01, with an average value of 0.704, indicating a platykurtic nature in the sediments. The Sanctuary beach serves 60% of

platykurtic and 40% of mesokurtic nature. The kurtosis values of the Lookout beach extents from 0.75 to 1.87, with an average value of 1.104. The average value shows that the area is dominant of mesokurtic nature in sediments. Lookout beach profiles 50% leptokurtic, 30% mesokurtic, and 20% platykurtic nature. The predominance of platykurtic and mesokurtic nature of sediments shows an irregular assemblage of fine and medium sediments after sorting and remaining of an actual high energy nature throughout deposition (Avramidis et al., 2012).

5.8 Inter-relationship of grain size parameters (Bivariate plots)

Bivariate plots formed from various geomorphological parameters to discover depositional environments (Friedman, 1967). However, the bivariate plots are quite established through the notion that statistical parameters genuinely reflect variances in the fluid-flow mechanisms of sediment transportation and deposition (Sutherland & Lee, 1994). Al-Ghadban (1990), Sutherland & Lee (1994), Srivastava & Mankar (2009), Srivastava et al. (2010), and Srivastava et al. (2012) have demonstrated and recorded that the bivariate plots assist as reliable tools for classifying mechanisms of several environments of sedimentation. Folk & Ward (1957), Stewart (1958), Friedman (1967) and Moiola & Weiser (1968) outlined that the bivariate plots are very significant and mostly used plots, and these plots have been aimed to distinguish between the river and beach sands. In conclusion, the bivariate plot of graphic mean versus standard deviation/sorting figure (5.11); graphic mean versus skewness figure (5.12); graphic mean versus kurtosis figure (5.13); skewness versus kurtosis figure (5.14); standard deviation/sorting versus skewness figure (5.15); and standard deviation/sorting versus kurtosis figure (5.16) were applied to determine between several depositional settings.

5.8.1 Discussion

A) Graphic mean versus standard deviation (sorting)

The correlation between the graphic mean and standard deviation (sorting) exhibits that the river sands are fine-grained to medium-grained and are mainly moderately sorted in figure (5.11). The beach sands are frequently fine-grained and very well-sorted to well-sorted sand. Therefore, the substantial numeral of well-sorted to moderately-sorted sediments in the river samples and beach

sands suggest constant alteration of the sediments by waves and currents (Moiola & Weiser, 1968). For mean grain size and standard deviation (sorting) are hydraulically controlled, defining that the well-sorted sediments have mean value in the fine sand size range (Griffth, 1967; Chauhan et al., 2014; Rashedi & Siad, 2016). In conclusion, the beach sediments are prime-sorted compared to the river sediments.

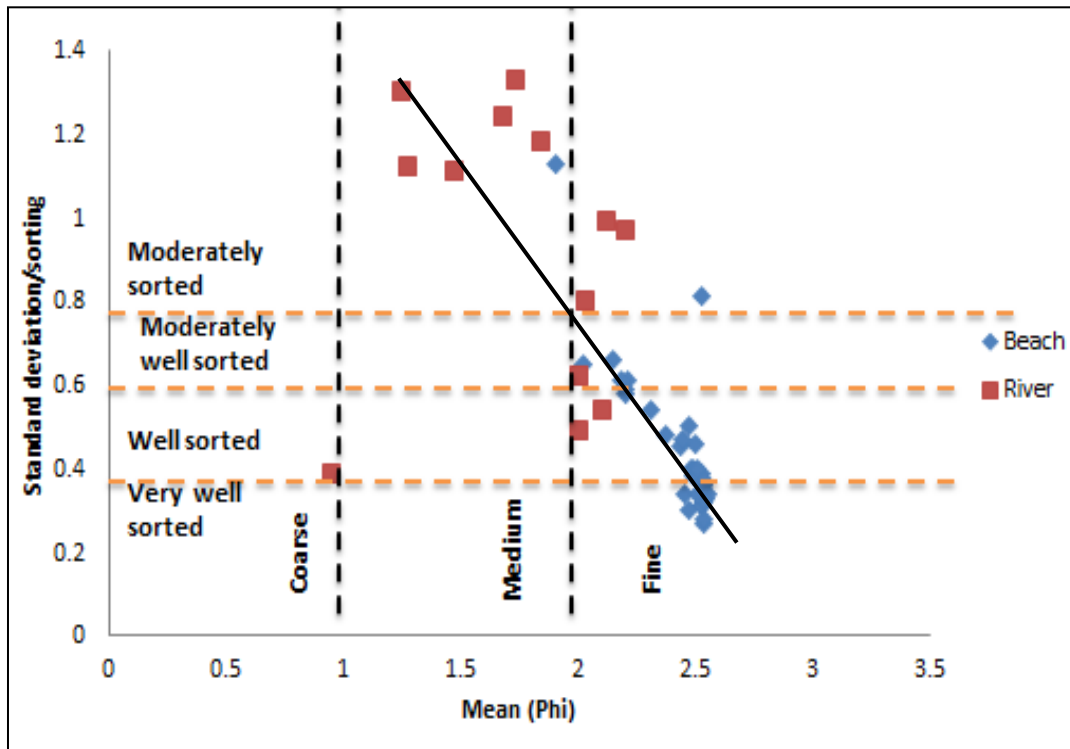


Figure 5.11: Bivariate scatter plot showing standard deviation/sorting versus mean. The standard deviation/sorting versus mean graph demonstrates that the sediments are fine to medium grained and very well-sorted to moderately sorted. Beach sands are finer than fluvial sands and beach sands are well sorted than fluvial sands.

B) Graphic mean versus skewness

The correlation between the graphic mean versus skewness figure (5.12) exhibits that in the river, sands are coarse-skewed to strongly coarse-skewed, although the beach sands are near-symmetrical and coarse-skewed in nature.

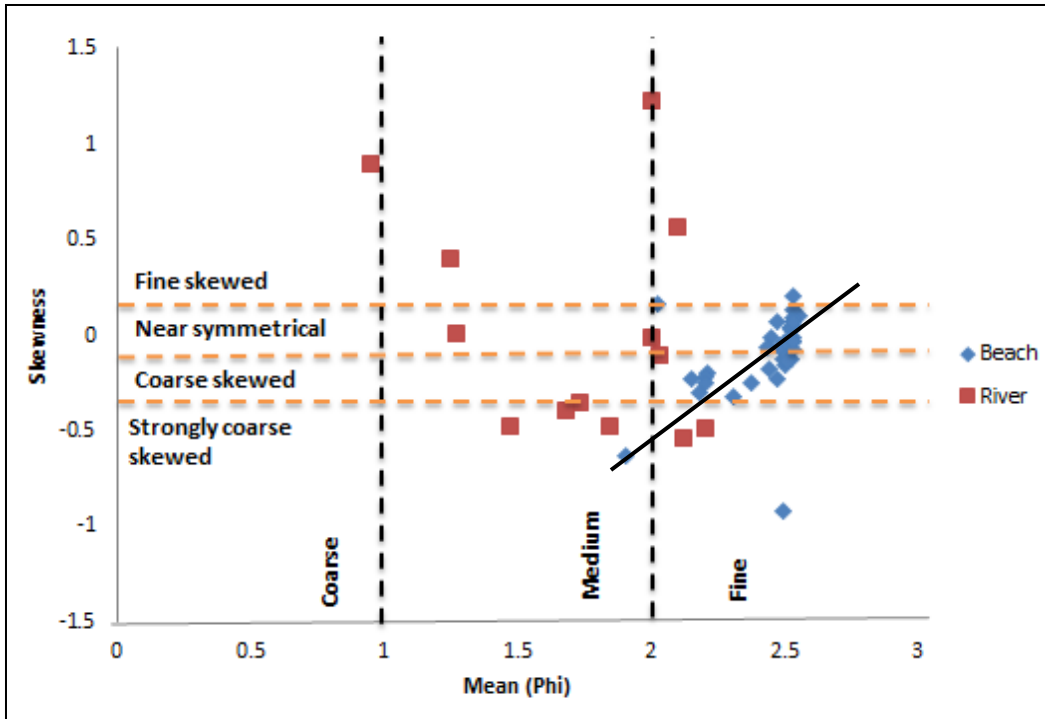


Figure 5.12: Bivariate scatter plot showing skewness versus mean. The graph skewness against mean plays a significant role to identify depositional environments. Beach sands are more symmetric or coarse skewed, while fluvial sands are much dispersive widely from strongly coarse-skewed to fine-skewed. Also showing beach sands are finer than fluvial sands.

University of Fort Hare
Together in Excellence

C) Graphic mean versus kurtosis

The bivariate plot of the graphic mean versus kurtosis figure (5.13) reveals that almost all the medium-grained river sands are mesokurtic, and the beach sands are purely platykurtic and mesokurtic in nature.

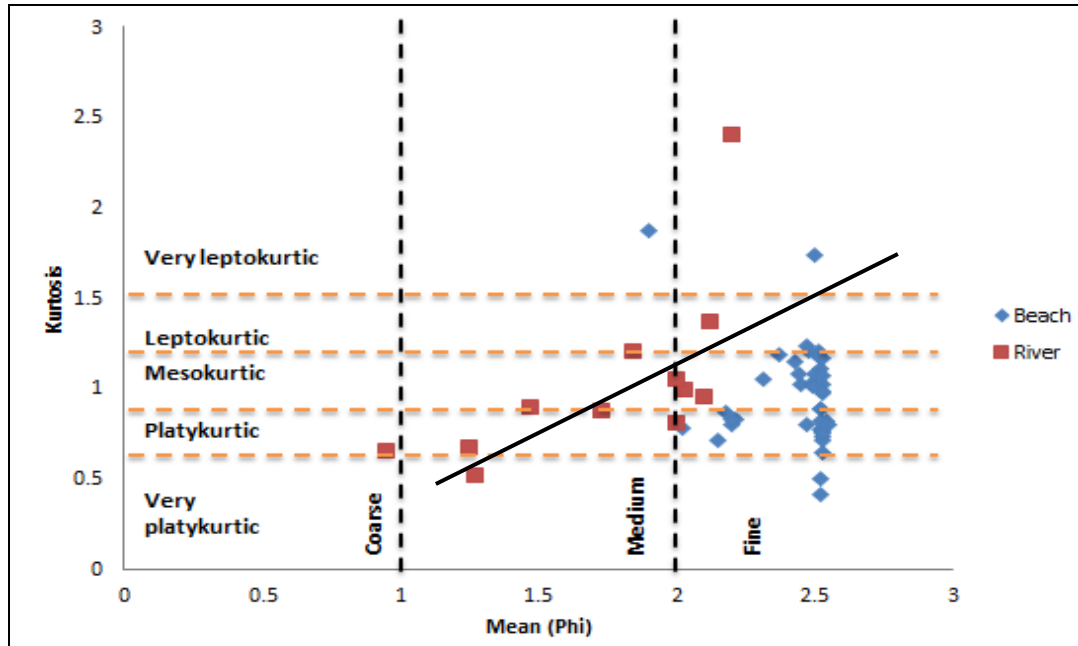
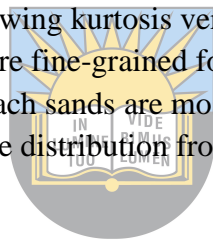


Figure 5.13: Bivariate scatter plot showing kurtosis versus mean. The plot between mean and kurtosis shows that most sediments are fine-grained for beach sands, while fluvial sands are more variable in size. Also showing beach sands are mostly mesokurtic and platykurtic, whereas fluvial sands have a wide despise distribution from leptokurtic to very platykurtic.



D) Graphic skewness versus kurtosis
 University of Fort Hare
Together in Excellence

Friedman (1967) outlined that the bivariate plot of skewness versus kurtosis of a specified sediment distribution effectively differentiates between depositional environments. The correlation between graphic skewness and kurtosis figure (5.14) shows that the river sands are platykurtic and mesokurtic in nature. They are mostly intensed in the coarse-skewed fine-skewed sphere. The beach sands are revealed as platykurtic and mesokurtic and are nearly symmetrical.

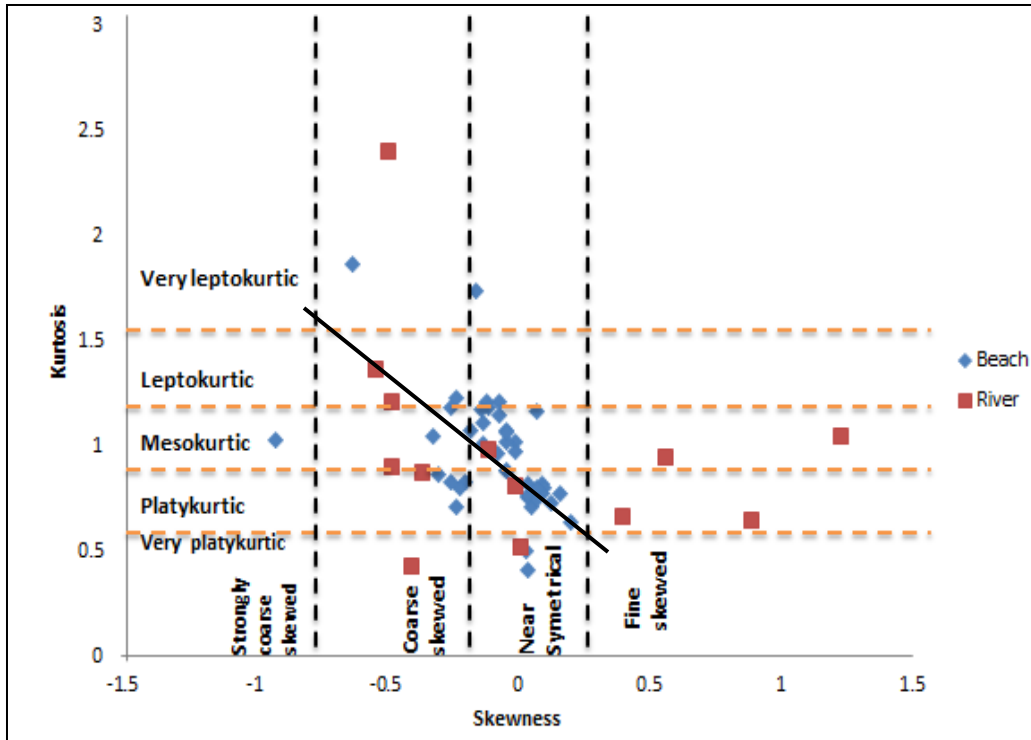
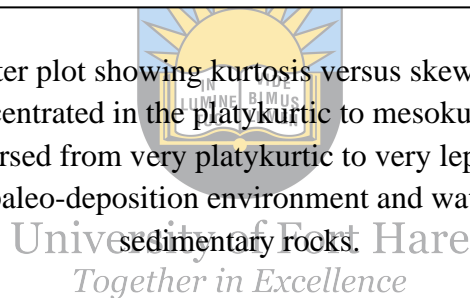


Figure 5.14: Bivariate scatter plot showing kurtosis versus skewness. The figure shows that beach sands are more concentrated in the platykurtic to mesokurtic categories, whereas the fluvial sands are widely dispersed from very platykurtic to very leptokurtic. These characteristics can be used to distinguish paleo-deposition environment and water energy for sediments and sedimentary rocks.



E) Graphic standard deviation (sorting) versus skewness

The bivariate plot of graphic standard deviation (sorting) versus skewness displays that most river sands are moderately-sorted and strongly coarse-skewed figure (5.15). In contrast, the beach sands are very well-sorted and well-sorted, congregated around the near-symmetrical and coarse-skewed area.

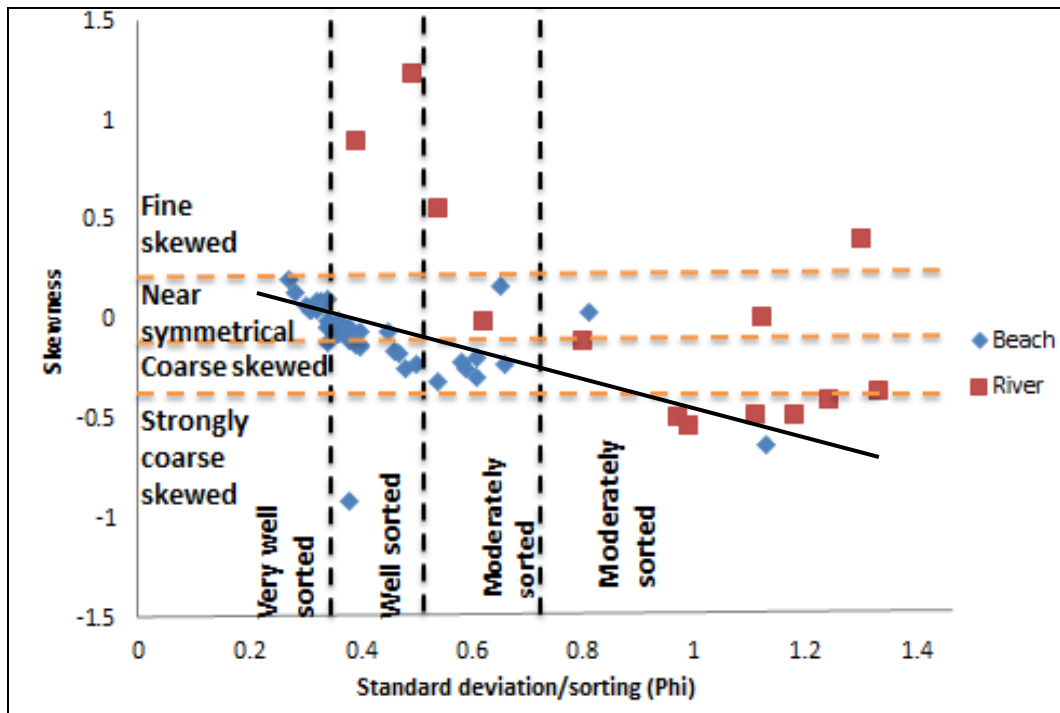


Figure 5.15: Bivariate scatter plot showing skewness versus standard deviation/sorting. The bivariate plot of the sorting and skewness indicates that beach sands fall into well sorted to very well sorted category, and near symmetric to coarse skewed category. Whereas fluvial sands fall into wide area and show a dispersive sorting.

University of Fort Hare
Together in Excellence

F) Graphic standard deviation (sorting) versus kurtosis

The bivariate plot of graphic standard deviation (sorting) versus kurtosis figure (5.16) shows that most river sands are moderately-sorted and scattered in the field. The beach sands are very well-sorted to well-sorted, concentrated at platykurtic, mesokurtic, and leptokurtic fields.

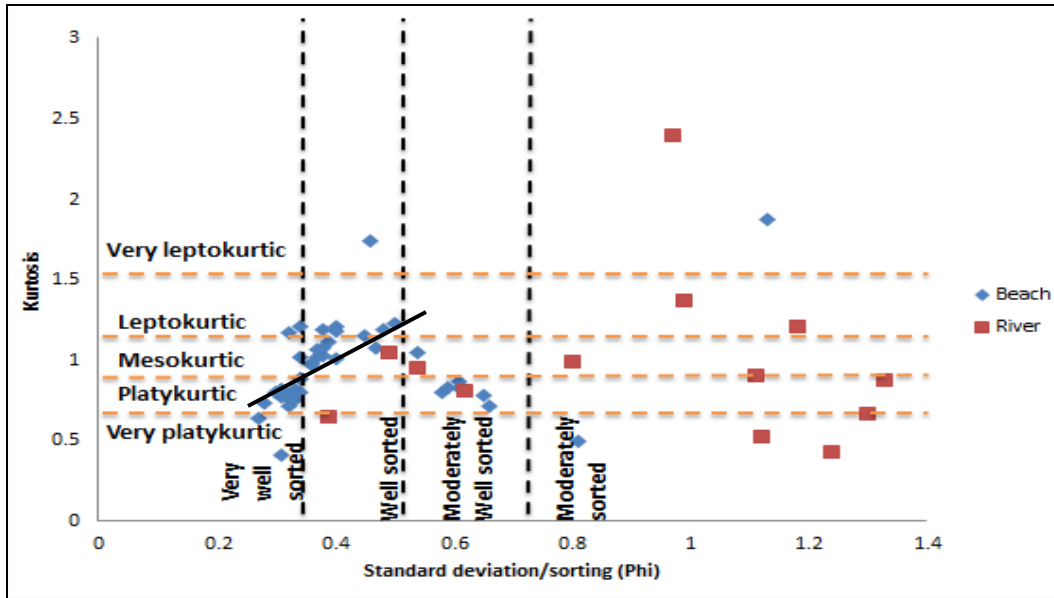
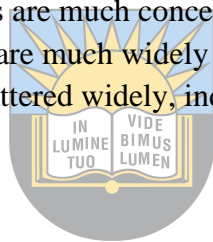


Figure 5.16: Bivariate scatter plot showing kurtosis versus standard deviation/sorting. The bivariate plot shows that beach sands are much concentrated in the very well-sorted to well sorted category, while fluvial sands are much widely distributed than the beach sands. The projected points are scattered widely, indicating a worse sorting.



5.9 Conclusion

These bivariate scatter diagrams show that beach sands are much well sorted comparing to river sands. All the parameters for beach sands are more concentrated in certain area, whereas river sands show a wider distribution parameters and more dispersive features. These characteristics imply that hydrodynamic condition in beach environment was more persistent, and the water energy was more stable than fluvial environment.

Beach samples are mostly well sorted to very well-sorted, and the grain size is more uniform. Whereas river sediments have more variable grain sizes and more dispersive skewness, kurtosis and standard deviation parameters in the studied areas. Thus grain size analysis and the parameters can be used to distinguish deposition environment and hydrodynamic conditions.

CHAPTER 6: PETROGRAPHY AND MINERALOGICAL COMPOSITION

6.1 Introduction

The purpose of this chapter is to identify the mineralogical compositions of the sediments, and as well as fossil contents. The method of discovery of the mineralogical composition of sediments requires the results captured from the various procedures, which involve advanced techniques for clay mineral identification. The common techniques used include petrographic microscope, X-ray diffraction (XRD) and Scanning electron microscopy (SEM), plus Energy dispersive X-ray spectrometer (EDX) to analyse the sand samples.

X-ray diffraction (XRD) is considered one of the best effective analytical approaches used in a quantitative and qualitative study (Ross & Kerr, 1931). Mainly, the mineral composition of sediments issues mineral features into the origin region and the depositional environment (Maity & Maiti, 2016). XRD analysis is appropriate for quantitative analysis as it relates to other single techniques, and accurate quantitative mineral analysis is crucial for mineralogical studies (Bish & Post, 1993; Zhou et al., 2018). Quantitative analysis of specific minerals, for example, clay minerals, are regarded as a prime obstacle due to several chemical compositions, endorsed orientation, structural disorder and structural diversity of clay minerals (Zwell & Danko, 1975; Zhou et al., 2018). However, various factors affect the accuracy of mineral analysis (Reynolds, 1989; Snyder & Bish, 1989; Moore & Reynolds, 1997). In conclusion, other techniques such as Scanning electron microscopy (SEM + EDX) is required to support XRD.

Scanning electron microscopy (SEM) scrutinizes a focused electron beam over a surface to produce an image. Scanning electron microscope (SEM) with Energy-Dispersive X-ray (EDX) is an essential technique with a typical chemical composition (Xu, 2002; Leng et al., 2005; Pye & Croft, 2007; Okrusch & Frimmel, 2020).

6.2 Mineral and fossil compositions

Mineral analysis under petrographic microscope shows the existence of quartz, feldspar, calcite, chlorite, aragonite, muscovite, organic carbon (carbonaceous pellets) and clay minerals. Quartz is

the most predominating mineral in each and every sample present in the study areas, followed by feldspar and calcite minerals while other minerals present only in a small amount.

6.2.1 Quartz (SiO_2)

According to the petrographical studies, quartz is the most dominating mineral in river and beach samples at Plettenberg Bay and Knysna area. Quartz under microscope emerges to be colourless and lower interference colour. It composed of monocrystalline and polycrystalline quartz grains. Polycrystalline quartz grains are more dominant than monocrystalline quartz grains, probably reflecting came from metamorphic source rock from surround Cape Supergroup of metamorphic quartzite or Karoo Supergroup of quartz arenite. Quartz differs from angular to rounded in shapes, revealing different energy levels during transportation processes.

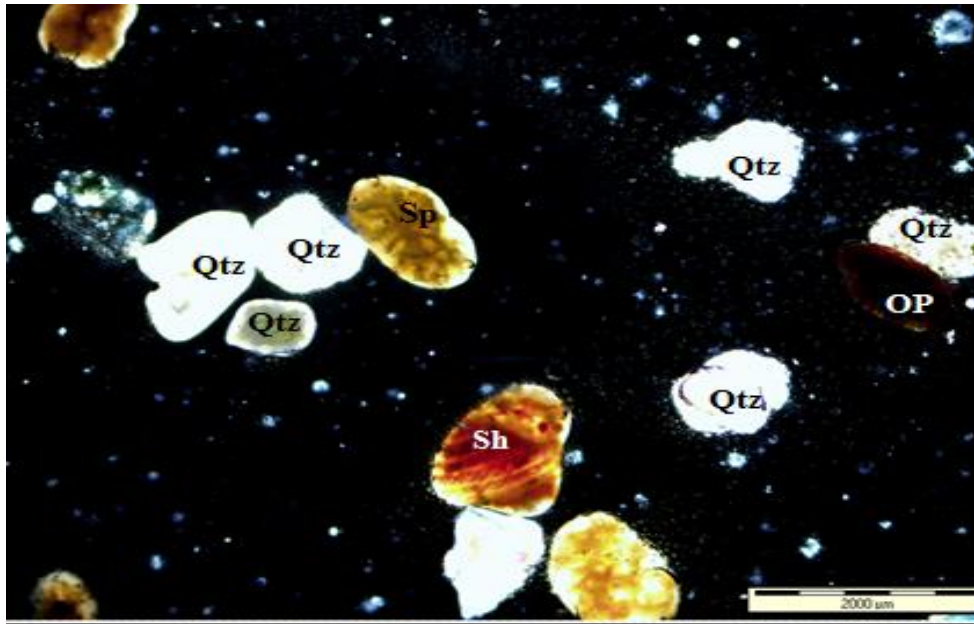


Figure 6.1: Photomicrographs showing quartz grains (Qtz, white), shell fragment (Sh) and sponge fragment (Sp).

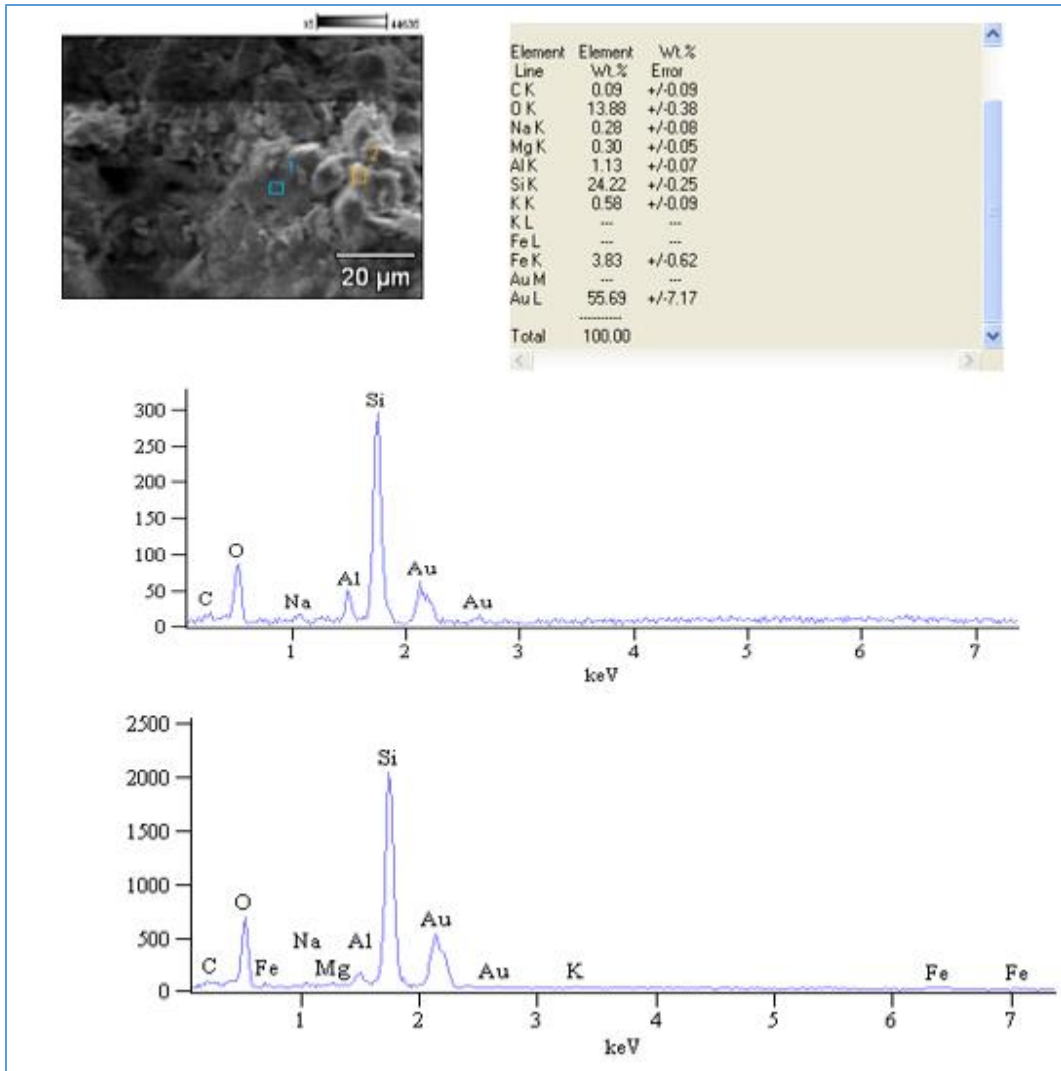


Figure 6.2: Photomicrographs of SEM+EDX analyses showing quartz minerals. The Au peak was due to gold coating. The EDX images show high content of oxygen and silica, with little other chemical components.

6.2.2 Feldspar

Orthoclase (KAlSi₃O₈)

Albite (NaAl Si₃O₈)

Plagioclase (CaAl₂Si₂O₈)

Feldspars are aluminosilicate minerals that are found in igneous, metamorphic, and sedimentary rocks and include potassium, sodium, and calcium varieties, thus are classified as orthoclase (microcline), albite and plagioclase figure (6.3). The most abundant feldspars in the study areas

are commonly orthoclase and plagioclase with an estimation percentage of 15-25%. Feldspars occur as both detrital and authigenic forms with the former is more abundant than the later. The feldspar minerals plagioclase, and orthoclase normally show low birefringent and interference colour. Despite the fact that feldspars are the most common minerals in igneous and metamorphic rocks, they are less stable in sedimentary rocks. The majority of feldspar has been altered to clay minerals or has been totally destroyed during weathering and dissolution as indicated by grey arrows in Figure 6.3. Microcrystalline clay minerals progress along the cleavage planes of feldspar is an indicator for feldspar alteration. Feldspar grains are medium to coarse grained and texturally sub-rounded to sub-angular figure (6.3) in the samples. Orthoclase is typically cloudy, with some grains showing a perthitic texture or simple twinning. In some instances, the potassium feldspar is also easily identified by its sericitization. Plagioclase is typically elongated and is identified by its polysynthetic or albite twinning of black and grey stripes, whereas microcline is distinguished by its cross twinning.

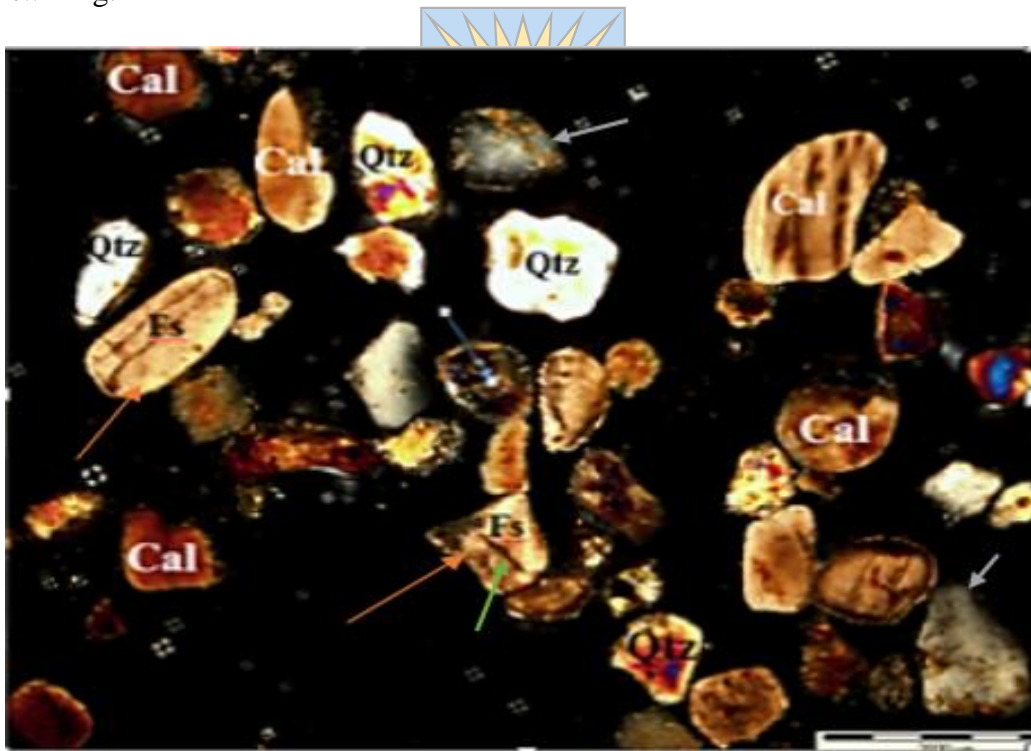


Figure 6.3: Photomicrographs showing various grains of Feldspar (Fs), Quartz (Qtz) and Calcite (Cal). Quartz has no cleavage, while feldspar (Fs) shows clear cleavage in the crystalline grain indicated by arrows.

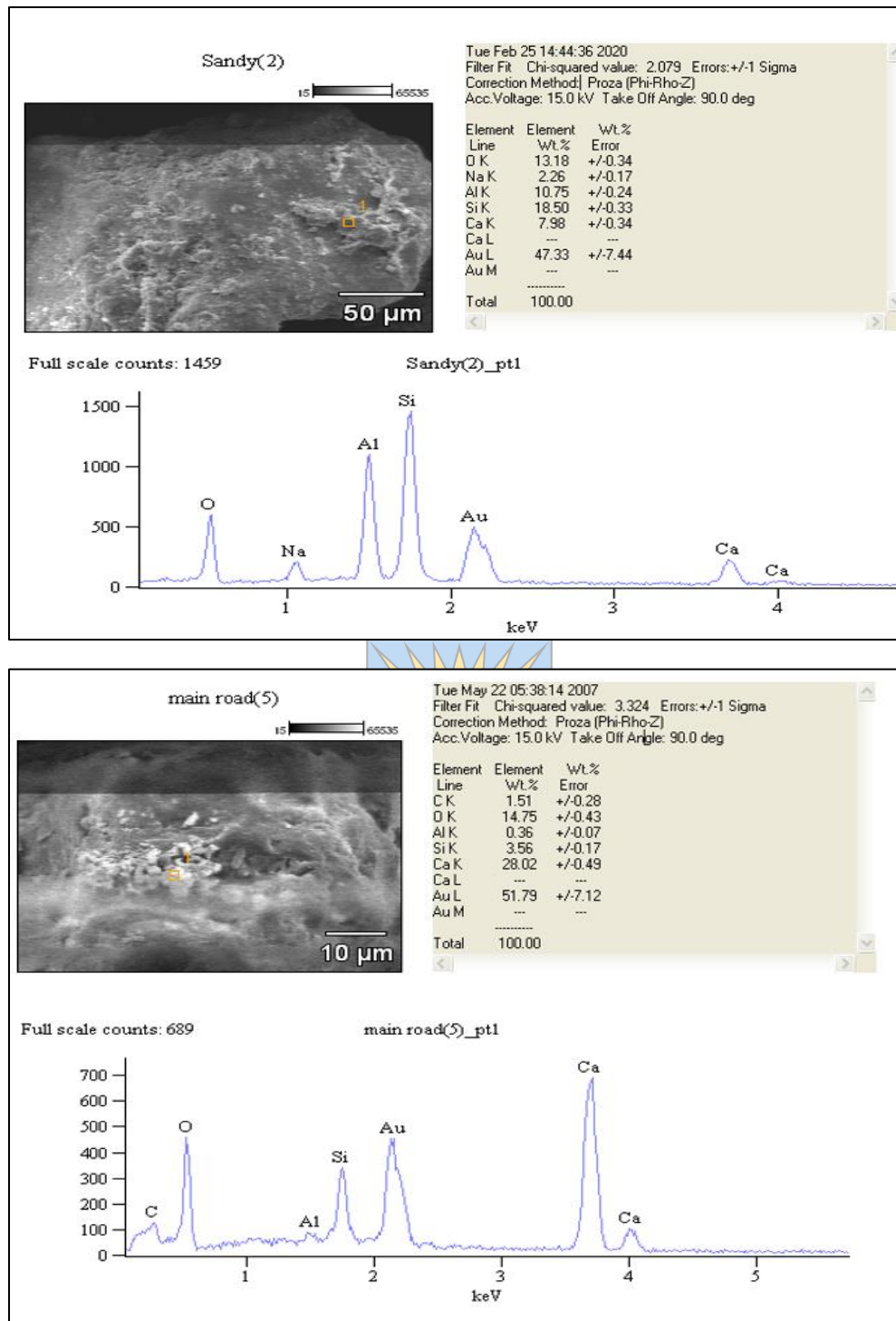


Figure 6.4: SEM and EDX analyses for Albite grain (top) having silica, aluminium and sodium chemical compositions (top); and Ca-plagioclase grain showing silica, aluminium and calcium compositions (bottom). Au peak was due to gold coating for the sample.

6.2.3 Muscovite

Muscovite is the main ordinary mineral of the mica family. Muscovite has the perfect cleavage; a unique lustre is relatively durable and is generally detrital in origin subjected to erosion and transportation, leading to the destruction of the original source minerals. Muscovite was noticed in certain sand samples figure (6.5) below.

6.2.3 Organic pellet

Organic pellets are tiny spherical to oval shaped or rod-shaped grains. They compose either of the aggregated carbonate mud, or the precipitated calcium carbonate, or sometimes the mixture of organic and chemical precipitation. Quite often, they consist either of calcite or aragonite mixing with organic carbon therefore are dark in colour. They were usually formed during early diagenetic stage in reduce environments. They originate due to organic and chemical cohesion where they combine together. Organic pellets are common dark in colour, but sometimes brown to pinkish in colours figure (6.5).

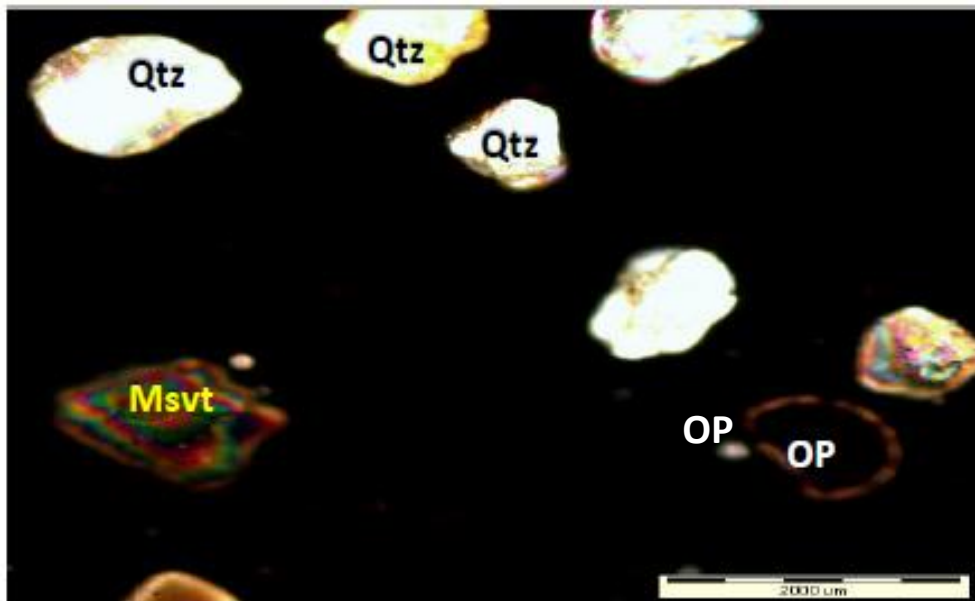
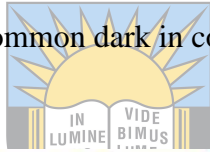


Figure 6.5: Photomicrographs of various sand grains showing organic pellet (OP), quartz (Qtz) and muscovite (Msvt).

6.2.4 Lithic fragments

Lithic fragments are pre-existing rocks that turned into consolidated tephra during eruption, deposition or transportation. However, the lithic fragments are also called rock fragments, which can be obtained from an extensive variation of lithotypes and ordinarily have a source of specific texture. The composition can be determined through thin sections. The lithic fragments are often sub-rounded, rounded to angular shape in terms of shapes. The rock fragments are defined as unstable in sedimentary environments; thus, if present in a sandstone, display good hints to the provenance of the grains. During the microscopic analysis of the study areas, the samples show that the lithic fragments resulted from Karoo Supergroup sandstone and siltstone figure (6.6).

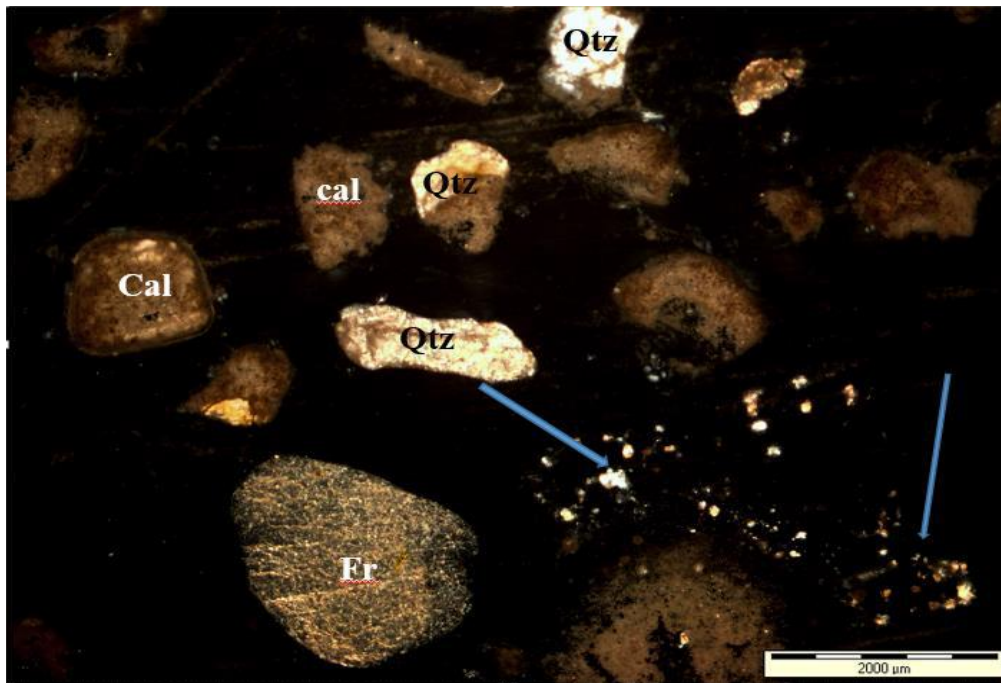


Figure 6.6: Photomicrographs of various sand grains showing. Quartz (Qtz), calcite (Cal), and sedimentary lithic fragment (Fr). Blue arrows indicate rounded organic pellets (dark coloured).

6.2.5 Calcite (CaCO_3)

Calcite is a carbonate mineral and is a common mineral in the beach sands. Calcite is a stable polymorph of calcium carbonate (CaCO_3) comparing to aragonite which has the same chemical composition with calcite but much unstable. Calcite is the primary component of limestone and

marble. Thus, calcite is one of the main widespread minerals in marine sediments (Dziadkowiec, 2019).

There are two types of calcite found in the beach environment, one is chemical precipitated calcite, and another one is organic calcite which constitute most of organic skeletons such as shell and coral fragments (Barclay et al., 2020). Calcite is insoluble in cold water, actually calcite is stable only in an alkaline environment. In acidic environment, it is easily soluble, and replaced by other mineral such as quartz. The crystal system of calcite is hexagonal with vitreous lustre and perfect rhomboic cleavage (Barclay et al., 2020). Calcite is usually white or colourless, sometimes brownish figure (6.3, 6.6 and 6.7).

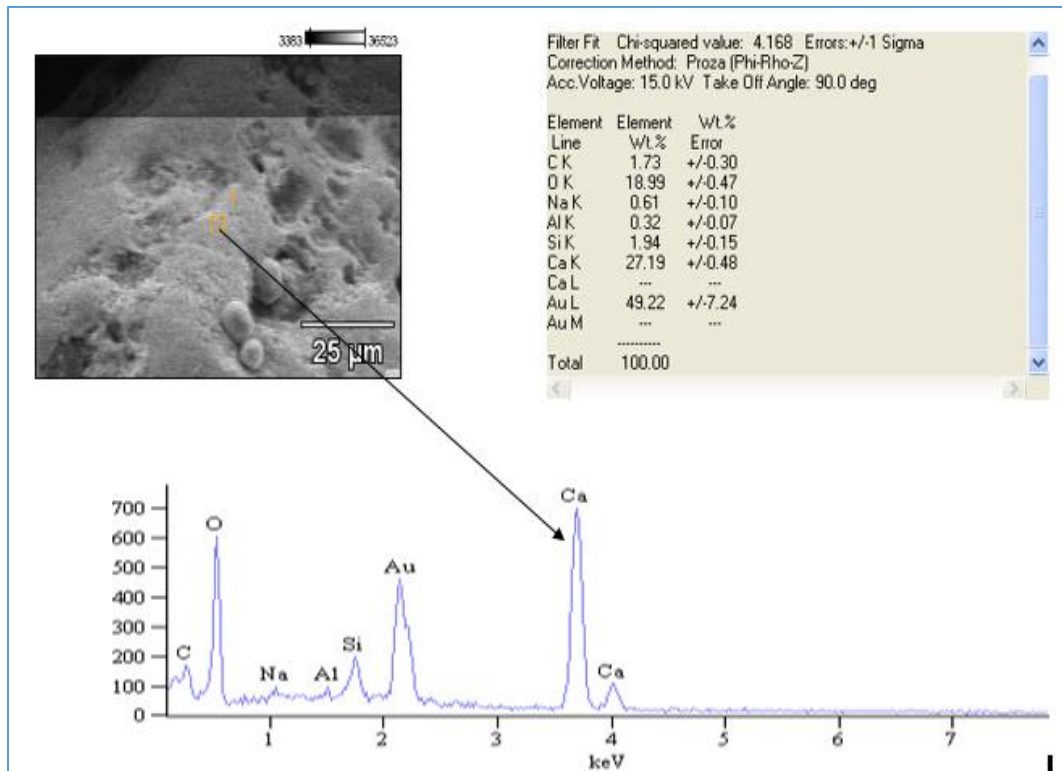


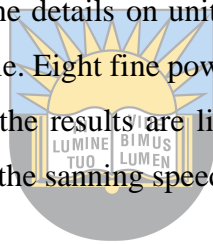
Figure 6.7: SEM and EDX analysis showing calcite mineral with high calcium and oxygen contents. Also contain small amount of quartz (Si rich). The Au peak was due to gold coating for the sample.

6.2.6 Sponge

Sponges are motionless organisms illustrating the aquatic issue in the surroundings with sizable filter particles and a nominal size variety filtering capability than different benthic invertebrates (Andus et al., 2016). Figure 6.1 shows a sponge fragment, and the primary sponge structure is still visible under microscope figure (6.1). Sponges was an old organism and can be traced to Cambrian age, but it still alive in modern environment. Sponge needs warm and clean water environment, and is a good indicator for unpolluted, high quality water environment.

6.3 X-ray diffraction (XRD) results

The X-Ray Diffraction (XRD) is a fast analytical technique mainly used for period identification of crystalline matters and can issues the details on unit cell dimensions and is used to identify mineral compositions present in a sample. Eight fine powder samples (about 10 grams each) were scanned by X-Ray Diffract-meter and the results are list in the Figure 6.9 and Table 6.1. The scanning range was from 1° to 80°, and the sanning speed was 1° 2θ/minute.



University of Fort Hare
Together in Excellence

Table 6.1: Percentages of minerals from sample P1 to sample K2.

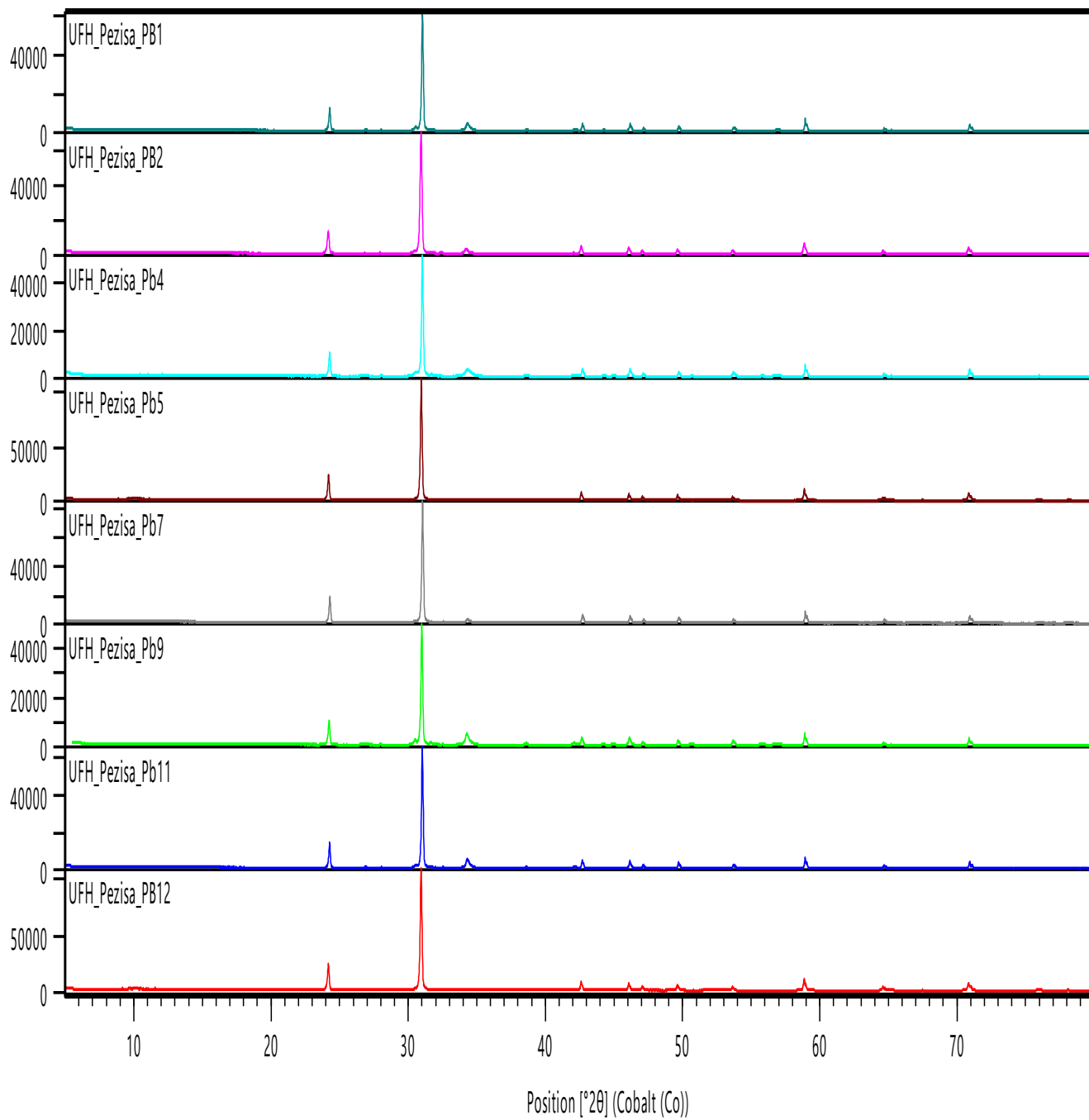
	P19		K1		K2		P2
	wt%		wt%		wt%		wt%
Quartz	79.4	Quartz	89.4	Quartz	77.4	Quartz	99.7
Calcite	12.7	Calcite	7.3	Calcite	14.8	Calcite	0
Aragonite	7.9	Aragonite	2.6	Aragonite	7.8	Aragonite	0
Muscovite	0	Muscovite	0.7	Muscovite	0	Muscovite	0.3
	P1		P47		P30		P5
	wt%		wt%		wt%		wt%
Quartz	92.9	Quartz	68	Quartz	80.2	Quartz	99.9
Calcite	4.8	Calcite	20.3	Calcite	14.1	Calcite	0

Aragonite	2	Aragonite	11.7	Aragonite	5.7	Aragonite	0
Muscovite	0	Muscovite	0	Muscovite	0	Muscovite	0.1



University of Fort Hare
Together in Excellence

Counts



Peak List
Quartz low; O2 Si1
Calcite; C1 Ca1 O3
Aragonite; C1 Ca1 O3
Muscovite 2M1; H2 Al2.83 Fe0.07 K0.92 Mg0.07 Na0.08 O12 Si3.03 Ti0.02

Figure 6.8: XRD patterns for all the samples P1, P2, P5, P19, P30, P47, K1 and K2. The dominant minerals are Quartz, Calcite, Aragonite and Muscovite.

XRD analysis shows the phenomenon of quartz, calcite, aragonite and muscovite present in sand grains of the study areas. According to the XRD analysis results, quartz is the predominant mineral composition in Plettenberg Bay and Knysna areas. . Both quartz and feldspar are detrital minerals, and they came from inland side and transported by river water to beach after weathering and erosion. Whereas aragonite and calcite are marine sourced minerals, they came from marine and transported by wave and tide to beach. These two sources of minerals, and grains got together on the beach through different medium and transportation process. Aragonite and calcite mainly came from dead marine organisms such as shells and corals, Other minerals such as muscovite and heavy minerals present only in a small amount, also mainly detrital origin.



University of Fort Hare
Together in Excellence

CHAPTER 7: GRAIN SURFACE TEXTURE AND MORPHOLOGY

7.1 Introduction

The surface texture or roughness of grains has been examined with scanning electron microscope in the Centre for Electronic Laboratory in the University of Fort Hare. Data and electronic images obtained can reflect the transportation and post-depositional alterations and the relevant sedimentary environment. Through the grain surface textures, one can trace various changes caused by physical, chemical or biological actions during grain transportation to post-deposition history (Kanori, 1980). Grain surface textures had been successfully used in the geological researches, various grain surface textures were caused by various mechanisms, it could be physical, chemical or biological factors. V-shaped pits reflected physical collision during particle transportation, boring holes on the grain surface reflected active activity by organism after deposition, and solution pores recorded a change by chemical alteration (Krinley & Doornkamp, 2011; Hodel et al., 1988; Mahaney, 1995).

A scanning electron microscope (SEM) demonstrates grain surface images of samples was used, the SEM is equipped with an Energy Dispersive X-ray (EDX) detector for analyse mineral composition and the percentages, respectively. Spherical and sub-circular shapes are substantiation images issued under the SEM analysis. By using the SEM + EDX analysis, various grain surface micro-textures were obtained and studied.

7.2 V-shape pits

The SEM results exhibited that many grains have V-shaped pits figure (7.1). V-shaped pits are frequently detected on the sand grain surface like quartz and feldspar, and are categorized as strong current environment like beach environment. The collision between particles during water transportation caused V-shaped prints on the grain surface. Basically, V-shaped pits formed due to physical collision, not chemical process. It is usually a tiny concave pits, but it could be a little larger although they are still belong to micro-texture and are SEM images. Hence, these characteristics take place throughout the crushing of grains, which are results of grain to grain collision occurred during water transportation process under high energy water conditions (Madhavaraju et al., 2006; Margolis & Kennett, 1971).

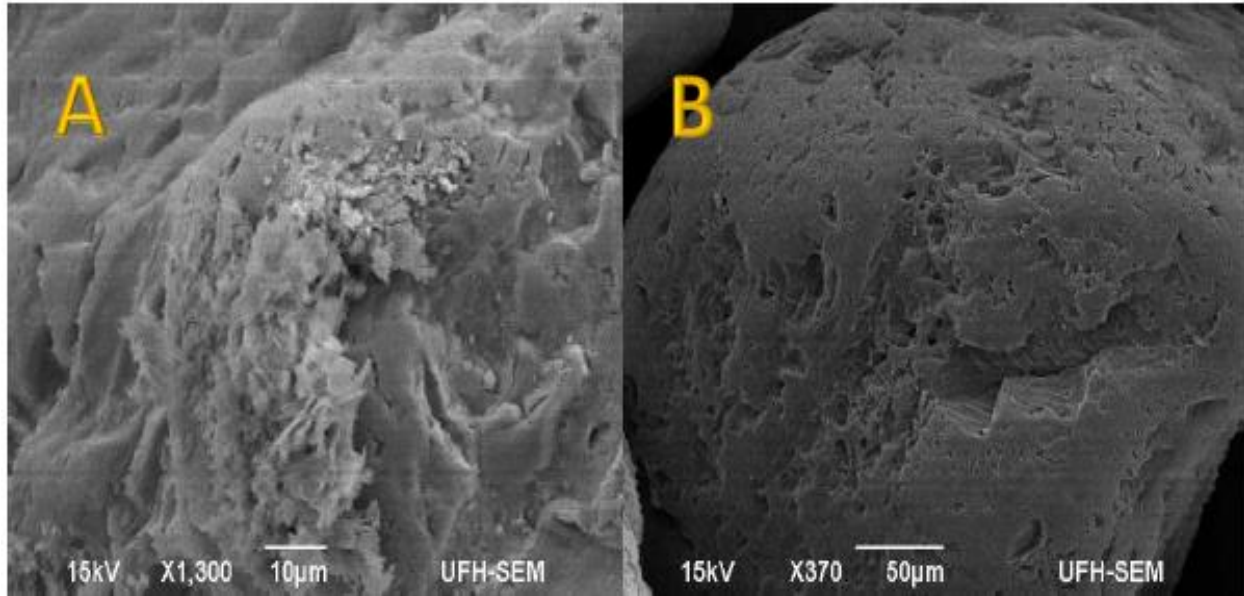
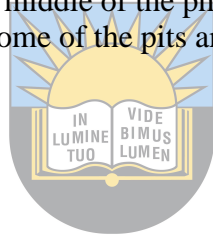


Figure 7.1: SEM photomicrograph showing (A) Tiny V-shaped pits (up-left on the photo), with secondary mineral precipitated on the middle of the photo; and (B) Tiny V-shaped pits due to collision on the grain surface. Note some of the pits are dissolution pore, not V-shaped pits.



7.3 Upturned plates

Upturned plates are formed also due to mechanical crushing and collision during transportation. Relatively soft sand grains move like creeping or saltating along the bottom bed and undergoing a sequence of high-velocity impacts at the grain surface. During the impact, the kinetic energy of each particle is a minimum of partially transformed into elastic energy among the grains. Once normal current or aeolian speeds of grain movement becomes fast, collision or fraction between grains becomes stronger, hence upturn plates created (Bagnold, 1941; Blumberg & Greeley, 1993; Dong et al., 2002). Upturned plates are correlated with velocities of aqueous or aeolian transport, outcomes of those energetic elastic collisions appear to be "abrasion fatigue" (Lucchi & Casa, 1968), and also the upturned plates area unit the motion of being succeeding in cleavage scarps. These plates are frequently modified in arid environments via precipitation and solution (Margolis & Krinsley, 1971). Basically, upturned plate are the most effective hint of high-energy transported by the high speed of water or winds figure (7.2 B).

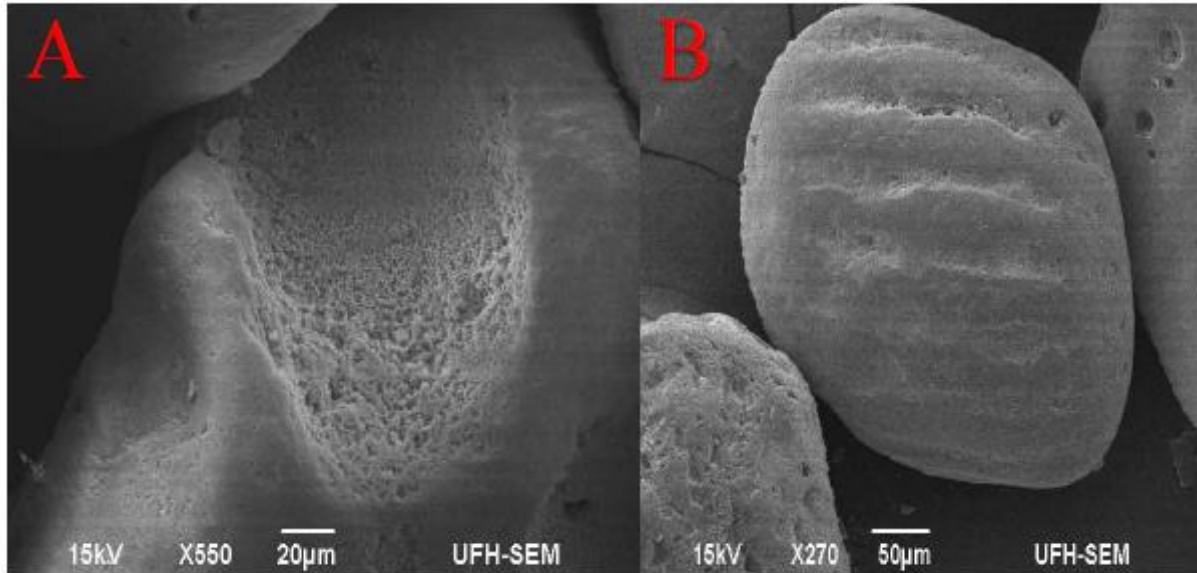
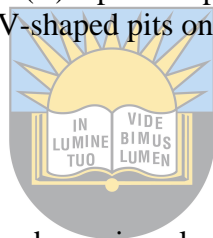


Figure 7.2: SEM photomicrograph showing (A) A relative large V-shaped pit with secondary minerals precipitated inside the pit; and (B) Upturned plates with stepped crushing impacts on the grain surface; also showing tiny V-shaped pits on the small grain surface (bottom left),

7.4 Secondary mineral precipitation



It is a very common fact that lots of secondary minerals precipitated on the particle surface figure (7.3-7.6). With the aid of EDX, we found that most of the secondary minerals are quartz (SiO_2) figure (7.4) and calcite (CaCO_3) figure (7.5). We also found secondary mineral of salt (NaCl) figure (7.6), which exists only in rare causes.

Quartz precipitates only in an acidic environment, whereas calcite precipitated only in an alkaline environment (Niu et al., 2018). Salt precipitated in a higher saline environment, usually in a high concentration of marine environment. Quartz can replace calcite in an acidic environment; while calcite can replace quartz in an alkaline environment. Therefore different secondary minerals can indicate different deposition environment in different Eh and pH conditions (Niu et al., 2018).

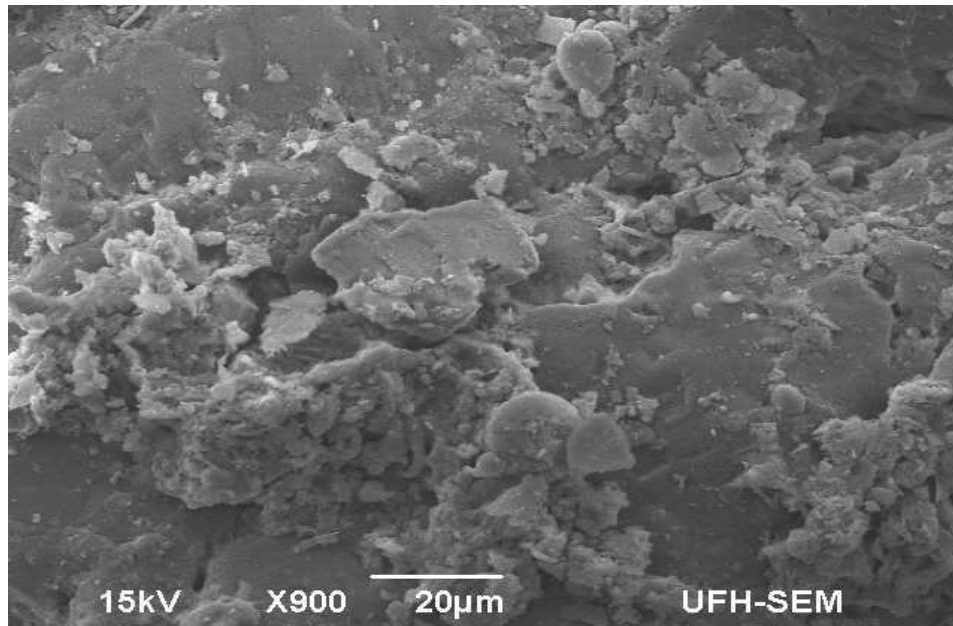


Figure 7.3 Secondary mineral precipitated on the grain surface.

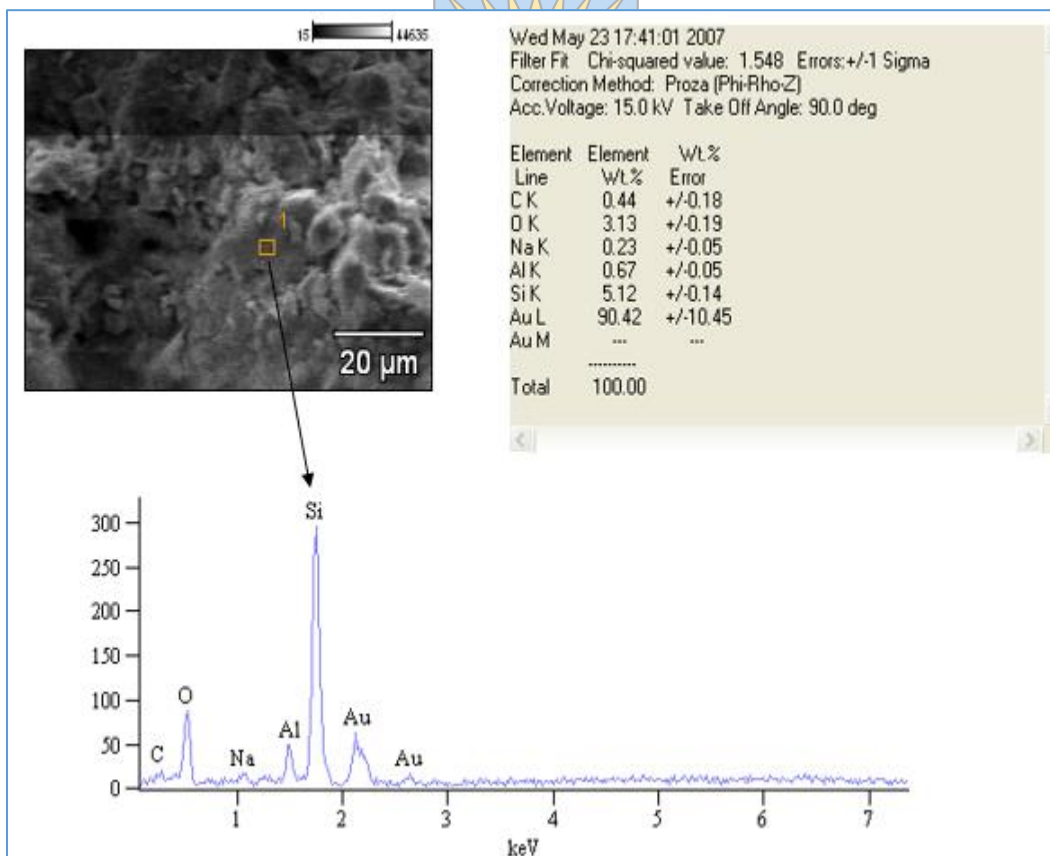


Figure 7.4: SEM and EDX image showing secondary mineral of quartz (SiO₂) precipitated on the grain surface. The Au peak due to gold coating for sample.

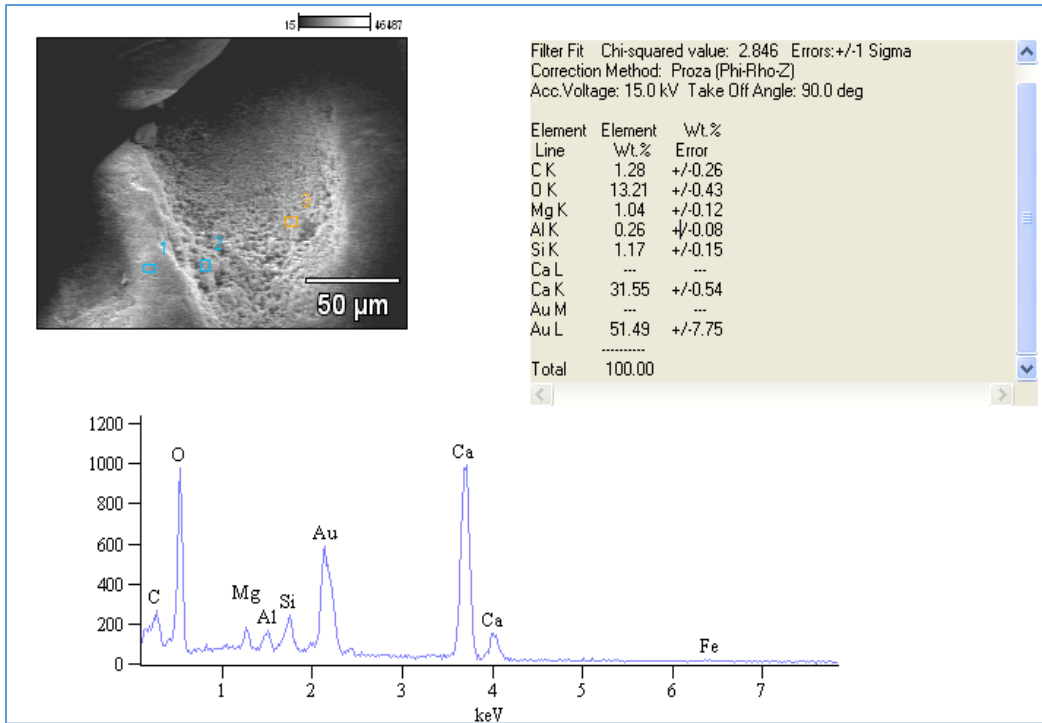


Figure 7.5: Secondary mineral of calcite (CaCO_3) precipitated on the grain surface. The Au peak is due to gold coating for sample.

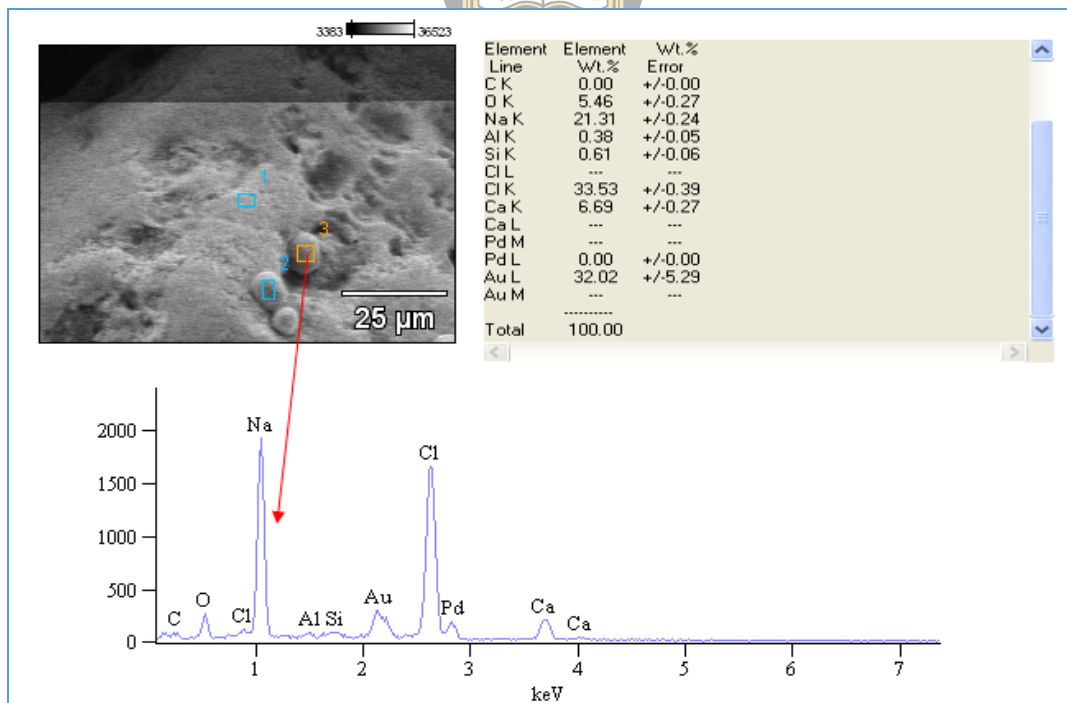


Figure 7.6: Secondary mineral of salt (NaCl) precipitated on the grain surface. The Au peak is due to gold coating for sample.

7.5 Dissolution pits/pores

The dissolution pits/pores are very common on the grain surface through SEM scanning. Dissolution pores are formed due to chemical instability in a new environment. Like the precipitation of secondary minerals, dissolution is just opposite to the precipitation. In an acidic environment, quartz becomes stable, and calcite becomes unstable, therefore quartz replaces calcite (Su et al., 2021). Whereas in an alkaline environment, calcite becomes stable and quartz becomes unstable, therefore, calcite replaces quartz. Also in an oxidic environment, hematite becomes stable, whereas pyrite becomes unstable, thus hematite replaces pyrite, or pyrite becomes weathered and remained with pores (Su et al., 2021). In an opposite reduce environment, pyrite becomes stable, and hematite becomes unstable, thus pyrite replaces hematite. All these replacement and dissolution could be created dissolution pores or pits, which can increase porosity and permeability of reservoir rocks and favour the formation of a good reservoir for hydrocarbon (oil and gas) or groundwater (Jew et al., 2022).

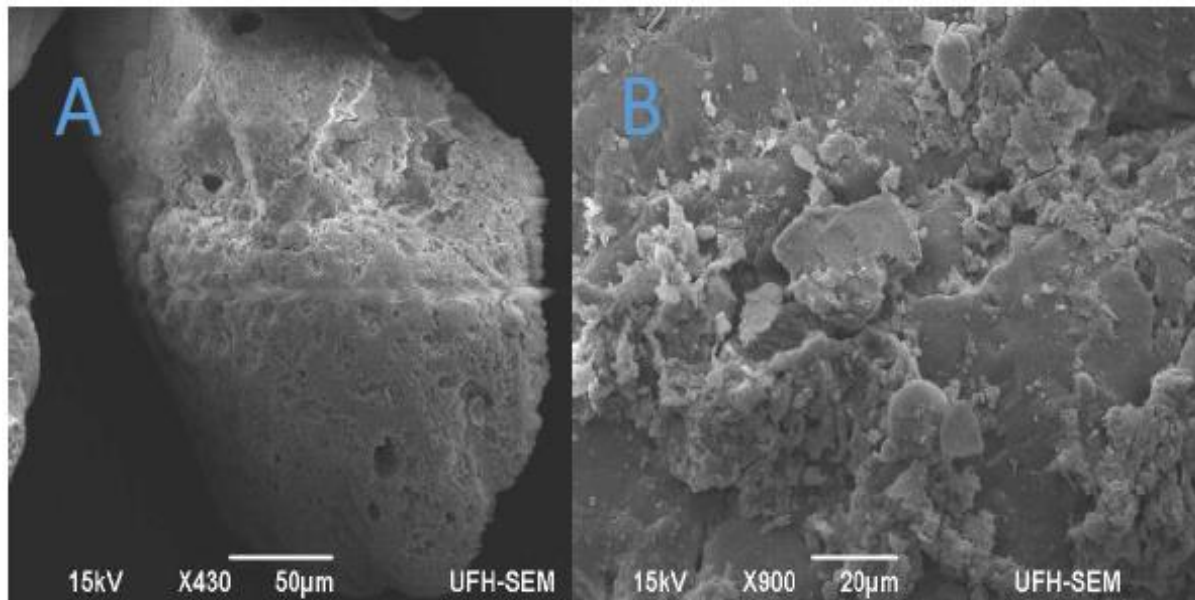


Figure 7.7: SEM photomicrograph showing (A) grain with dissolution pores on the surface and (B) A grain with irregular dissolution pores on the surface (up-middle).

7.6 Burrow and boring holes

Burrow and boring holes are created by activity of organism, particularly micro-organism. These holes are different with dissolution holes, and they are much regular or rounded in shapes, and also relatively deeper than dissolution holes. Micro-organisms, such as worms and algae, can bore into grain surfaces, thus creating rounded holes on the surface figure (7.8-7.9).

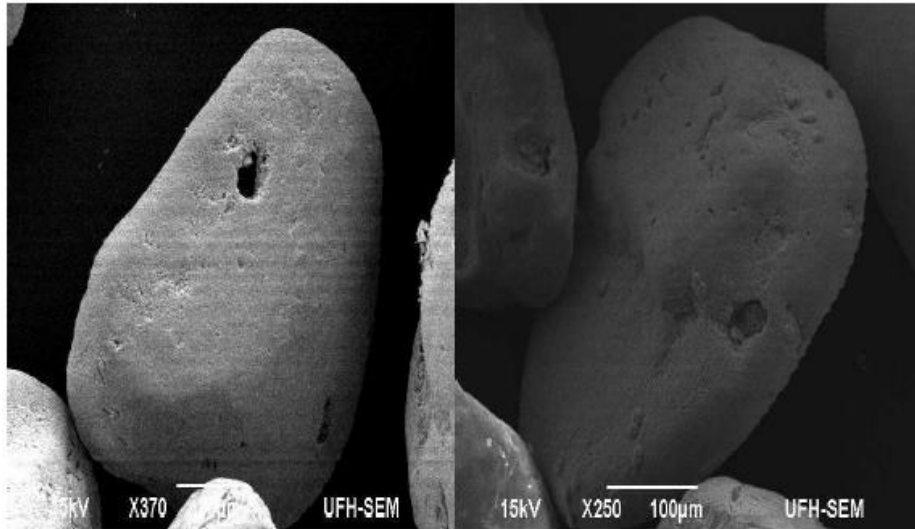


Figure 7.8: SEM photomicrograph showing a small rounded boring hole on the grain surface (left grain), also a dissolution hole on the right grain, which is much shallower.

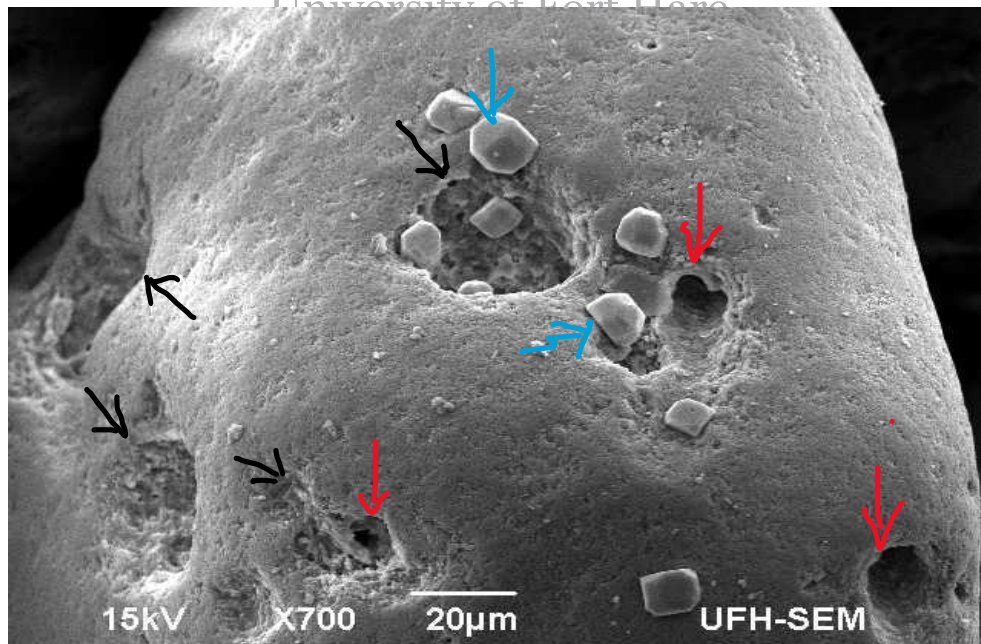


Figure 7.9: SEM photomicrograph showing rounded boring holes on the grain surface created by organism (such as worms) through corrosion and boring (red arrows). Also showing dissolution

holes created by chemical dissolution which are more irregular in shape and relative shallow in depth (black arrows) compared to boring holes. Note also secondary mineral (blue arrow) precipitated on the grain surface and in the dissolution holes.

7.7 Mineral recrystallization

Mineral recrystallization, by definition, is a process by which crystal reforms its crystal structure and size while keeping its fundamental mineral and chemical composition (Folk, 1965). Drury and Urai (1990) defined recrystallization as microstructural alteration during diagenesis, deformation and metamorphism of rocks. Fine minerals and micro-granular can recrystallize into coarse textures under higher temperature and pressure through recrystallization.

During recrystallization, grain alteration takes place in terms of size and shape. The relationship between crystalline grain-size and inter-crystal pore spaces is inversely proportional; when crystal grain-size increases, the inter crystalline pore space reduces.

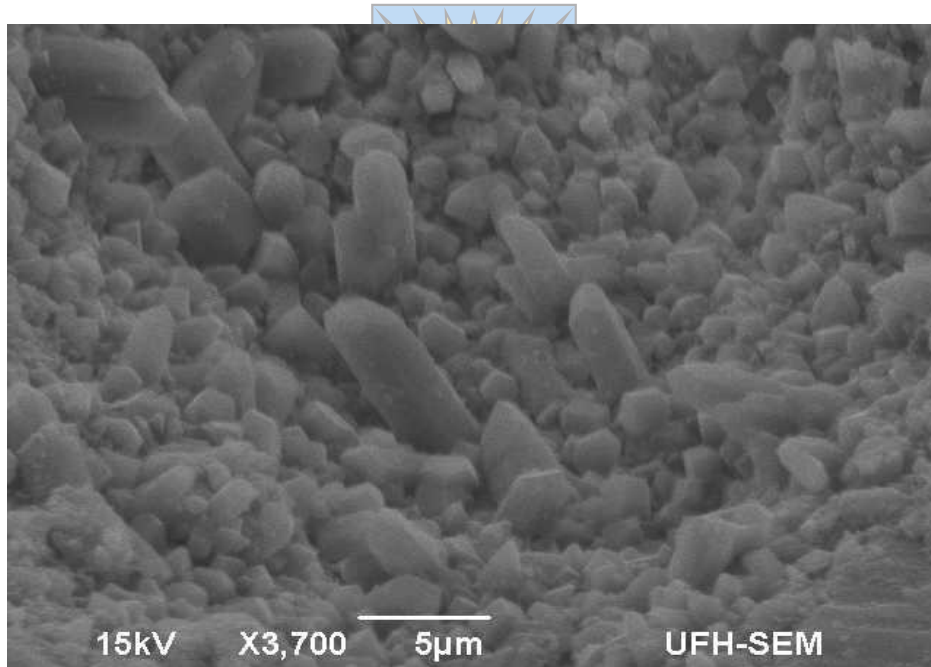


Figure 7.10: SEM photomicrograph showing recrystallization of quartz on the grain surface.

CHAPTER 8: SEDIMENTARY STRUCTURES

8.1 Introduction

A group of sedimentary structures had been found on the coast areas of Knysna and Plettenberg Bay. The formation of these sedimentary structures were closely linked to hydrodynamic conditions and thus are good indicators for hydrodynamic energy and depositional environment (Pettijohn & Potter, 1964; Johnson, 1976; Bevis, 2013). Sedimentary structures can be classified as physical, chemical and biological categories based on their origins and formation mechanisms (Pettijohn & Potter, 1964; Selley, 1988).

8.2 Flow regime

Flow regimes are typically a fluid flow, which generates various sedimentary structures at diverging velocities and speeds, called bedforms. It is categorized into the upper and lower flow regimes. The natural progression is from a flatbed to some sediment movement, ripples, and small dunes in the lower regime. At the upper flow regime forms large dunes, flattened beds, and antidunes (Jordan & Grotzinger, 2012; Kuriqi et al., 2019).

The Froude number, Fr , is a dimensionless value that defines numerous flow regimes of open channel flow. It is a ratio of inertial and gravitational forces.

- Gravity (numerator)- moves water downhill
- Inertia (denominator)- reflects its willingness to do so

$$F = \frac{U}{\sqrt{gD}}$$

U is the water/fluid velocity, D is the hydraulic depth (cross-sectional areas of flow/top width), and g is the acceleration due to gravity.

The Froude number is a measurement of bulk flow characteristics such as waves, sand bedforms, flow/depth interactions at cross-section or between boulders. It divides two discrete types of fluid flow; however, each flow regime creates certain bedforms and sedimentary structures, as shown in Figure 8.1. If the Froude number equals or greater than 1, a critical flow has resulted. By definition, the critical flow is unstable and often sets up standing waves between supercritical and

subcritical flow (Selley, 2000). If it is less than 1, the lower flow regime indicates that the waves can locomote upstream and propagate cross-bedded and cross-laminated sand, creating ripples and small dunes. However, if the Froude number is greater than 1, that means the waves can not locomote upstream in the upper flow regime. Therefore, the lower regime is defined as streaming, tranquil/slow, and subcritical flow because it is in a lower energy state instead, the upper flow regime is defined as fast/rapid flow, shooting and supercritical flow because it is in a higher energy state (Selley, 2000). Therefore, sedimentary structures can be used as an indicator for hydrodynamic environment.

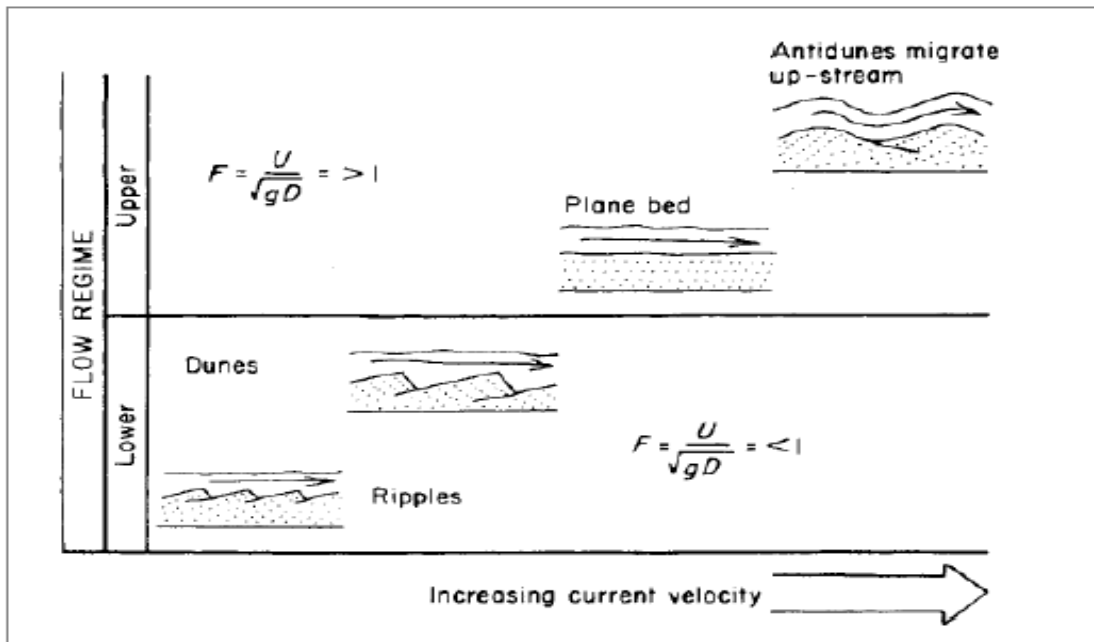


Figure 8.1: Sedimentary structures formed in different flow regimes (after Selley, 2000).

The sedimentary structures found during the fieldwork are discussed below. However, these sedimentary structures include the sand-dune, ripple marks, air escape hole structure, swash-line, lobe structure, planar lamination, lenticular bedding, cross-bedding, and etc.

8.3 Beach sedimentary-structures

8.3.1 Ripple mark and dune

When a wind or water current moves direct to loose sands, the sands are dragged along the flow bottom and accumulated up to form ripples and dunes. The fundamental difference between a ripple and dune is size and crest height, with dune being more large and the crest higher than about 10 cm (Selley, 2000). The wind created ripple marks are regularly identified by low amplitude compared to the ripples created by water which have a greater amplitude (Willard, 1935). Both ripples and dunes are crucial because they are frequently conserved in the sedimentary record.

The asymmetrical ripples and dunes are quite formed when there is a unique orientation of the current flow, as along a river bottom. Then, the symmetrical ripples or bidirectional dunes form when currents move in two directions, where waves wash back and forth in a marine environment. In addition, the preserved ripples and dunes consequently provide a hint as to whether waves or unidirectional currents controlled a particular sand pavement.

Ripples are formed up of two sides: the lee and the stoss sides (Figure 8.2). The stoss side in the ripple was a gentle slope, and currents uniformly flow up the stoss side down to the lee side. Along with the lee side in the ripple, which has a steep slope, the current flow meets the ripple. In conclusion, these two sides assist in determining the flow direction.

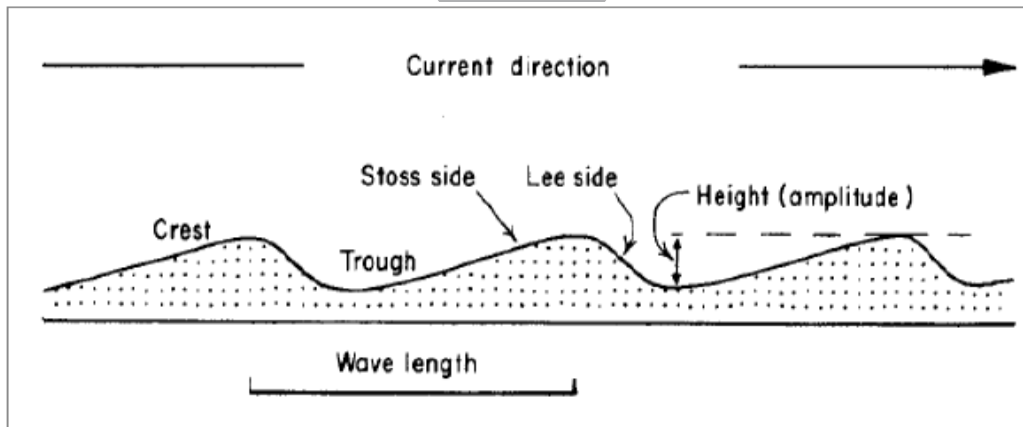


Figure 8.2: The stoss and the lee side of a ripple and the current flow direction (Selley, 2000).

The categorization of the ripples is based on their formation, including catenary, straight, sinuous, lunate/lingnoid, and rhomboid ripple marks (Nichols, 2009). Analysis and description of these ripple marks were spotted in the field.

8.3.1.1 Catenary ripples

The catenary ripples created the curvy cross-laminae with a unidirectional plunge; however, they also dip in an angle to the flow.



Figure 8.3: Catenary ripples created by variation of the strong currents in the Sanctuary beach, Plettenberg Bay.

8.3.1.2 Straight ripples

Straight ripples were caused by the cross-laminae flow but dipped in the same direction and lay in the same plane. Straight ripples are imbalanced and dissipative at all momentum motions (Baas et al., 2018). Current flow, to some extent, can split the straight ripples equally.



Figure 8.4: Straight ripples formed when a ripple crest is split by current flowing in the Lookout beach, Plettenberg Bay.

8.3.1.3 Sinuous ripples

The sinuous ripples generated curvy cross-laminae and dipped in a flow angle. Trough cross-lamination is formed through sinuous ripples. However, with this type of ripple, all laminae flows are generated at an angle to the flow and downstream. The unidirectional current additionally creates these laminae. These ripples display a ripple crest that is not long but short, and a alter in direction. Sinuous ripples produce curvy cross-laminae and dip within the end of the flow.



Figure 8.5: Sinuous ripples created by the interfering process of the second time of ripples in the Central beach, Plettenberg Bay.

8.3.1.4 Lunate/linguoid ripples

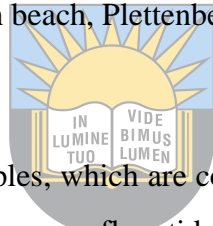
The lunate/linguoid ripples migrate curved cross-laminae are created mainly in the trough-shaped low areas between adjacent ripple forms resulting in a pattern of trough cross-lamination (Nichols, 2009). Linguoid ripples have arched lee slope surfaces, like sinuous and catenary ripples, ensuing in a lamina. Linguoid ripples form a downstream angle to the flow. Lunate ripples also called crescent ripples, are much like linguoid ripples but with curved stoss sides instead of the lee slope. The rest of the components are similar. As linguoid ripples form, curve cross laminae are shaped particularly in trough-shaped low regions among adjoining ripple forms. These ripples have curved slopes that form the dip at an angle to the flow and downstream.



Figure 8.6: Lunate/linguoid ripples created by very fast flow on the beach. Note also the flat top of these ripples, caused by erosion of ripple crest in a very shallow water environment in the Beacon beach, Plettenberg Bay.

8.3.1.5 Rhomboid marks

Rhomboid marks are rhombohedral ripples, which are commonly found on the intertidal zone or swash zone on a beach environment. There are flow tide and ebb tide moving along beach slope, flow tide creates a line of ripple marks, and ebb tide creates another line of ripple marks in a different angle, thus the two lines of ripples result an interfered diamond-shaped rhombohedral mark down the beach slope figure (8.7). Rhomboid marks are produced only in a very shallow, high energy water environment, and is a good indicator for beach or shallow tidal zone.

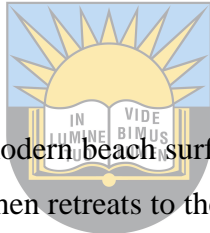


University of Fort Hare
Together in Excellence



Figure 8.7: Rhomboid marks are rhombohedra formed by tidal flow and ebb currents down a beach slope in the Lookout beach, Plettenberg Bay.

8.3.2 Groove mark



Groove mark is frequently found in a modern beach surface figure (8.9). It occurs when the tidal water flows rapidly into the beach and then retreats to the sea resulting in a bubble burst from the water at the beach, causing bursts and erosion along the surface and fossilized along the bedding surface after deposition figure (8.8). Groove mark indicates a strong erosion process caused by shallow water.



Figure 8.8: Groove marks caused by strong water erosion along beach surface in the Robberg beach, Plettenberg Bay.

8.3.3 Swash line

A Swash line or fore-wash line is defined as a turbulent layer of water that finally reached and broken along the beach slope. When the flowing water finally exhausts its energy, it will dump all the carried materials such as pebbles, shell fragments and weeds on the beach slope, resulting in a dump line on the shore which is the swash line figure (8.9). Huge swash ordinarily forms on horizontal beaches and the swash event performs an outstanding role in creating surface structure marks which are good indicators for paleo-beach environment if remained in the geological record (Masselink & Puleo, 2006).



Figure 8.9: A swash line in Plettenberg beach (Hobie beach) after water reached the highest point, dumped all the materials and then retreated into sea.

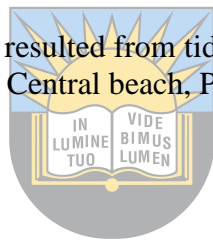
8.3.4 Disc-shaped pebble

The disc-shaped pebble is also common in the modern beach surface. This sedimentary structure is formed due to the tidal water pushing to the continental side, then retreating to the sea in a fast motion, resulting in routine abrasion and erosion of rock fragments becoming flat. Flat or disc

shaped pebbles are common in the beach environment, whereas river pebbles are more irregular shaped or equal three demencial.



Figure 8.10: The disc-shaped pebble resulted from tidal water of routine transportation and abrasion in the Central beach, Plettenberg Bay.



8.3.5 Burrows

Burrowing is a biological process caused by a variance of vertebrate and invertebrate species, differing throughout a set of bugs, worms, and algae. The burrows and bioturbation actions intensely affect physical and biogeochemical features and processes. Burrowing crustaceans modify the physical surroundings of all sedimentary environments, involving sand flats, salt marshes, mangroves, and coastal lagoons.



Figure 8.11: Photograph showing vertical burrows created by organism living in a shallow water environment in the Keurboomsriver Lagoon, Plettenberg Bay.

8.4 River sedimentary structures

8.4.1 Boring and bioturbation



Boring and bioturbation structures have been found on the river mouth in the Plettenberg and Knysna area, which are formed by the microfauna species that excavate holes and live fairly a sedentary live inside their holes and chambers. Others are mobile and dig or burrow through the loose sands or mud/soil. Some species can bore into hard detritus and remain various sized hole on the grain surface. Boring and bioturbation indicate active organic activities and shallow water environment where could be timeously emerged to surface.



Figure 8.12: Boring and bioturbation structures in the modern river surface formed by organisms in Knysna river mouth.

8.4.2 Planar lamination

The term planar lamination is frequently taken to demonstrate planar laminae that are more-or-less horizontal (within a few degrees) when initially deposited also have more-or-less parallel bounding surface. Laminae do differ in thickness laterally, varied from centimeter to millimeters (Boggs, 1987). Planar lamination has also been named horizontal lamination, and even a parallel lamination. They are a feature of river deposition within a relative circulation-restriction, lower energy environment.



Figure 8.13: Planar lamination in the river surface, elaborating a quiet water stage of lower energy environment at Keurbooms River (Plettenberg Bay).

8.4.3 Gravel pavement

The Knysna estuary is underlain by sediments of Knysna Formation (equal to Enon Formation) of conglomerates that are the basal unit of the Uitenhage Group. The sediments in the Knysna River mouth are subangular to subrounded, which means the water-energy was moderate initially, then later the water became relative fast eventually. Some of the sediments resulted from the weathering of the Table Mountain Group quartzite, and thus remained lots of metamorphic lithics in the loose sediments. The Udden-Wentworth scale classifies that the sediments in the Knysna river mouth range from 2-4 mm granules to 4-64 mm pebbles.

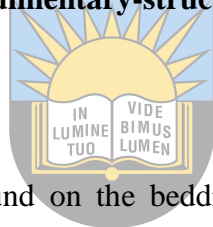


Figure 8.14: A photograph showing the gravel materials at Knysna river mouth.

8.5 Cretaceous Knysna Formation sedimentary-structures

8.5.1 Air escape holes

The air escape hole structure was found on the bedding surface of the Cretaceous Robberg Formation rocks. It is a rounded hole, which could be filled with sand and mud at later stage. When wet sediments exposed to subaerial, water escaped from the wet sediment remained a rounded hole at the surface. Air escape holes are usually larger than boring holes, and is a good indicator for a shallow fluvial, emerging water environment.



University of Fort Hare
Faculty of Education



Figure 8.15: Air escape-hole structure on bedding surface of the Cretaceous rock in Robberg Formation, Plettenberg Bay. Note the rounded air escape holes had been filled with sand and mud in the hole centre at later stage (left), while the holes at right side are empty due to the centre material was dissolved or taken off. Hammer head for scale (bottom right).



8.5.2 Bedding structure

Variable bedding structures were found in the Knysna Formation. Based on the bedding thickness, can classify bedding as thin bedded, medium bedded or thick bedded table (8.1). Based on the origin and shape, we can norminated them as lenticular bedding, tabular cross bedding, deformation bedding or load cast, and etc.

Table 8.1: Terminology of bed thickness (after Greensmith, 1989).

Scale	Thickness
Very thickly bedded (massive bedded)	>1m
Thickly bedded	30-100cm
Medium bedded	10-30cm
Thinly bedded	1-10cm
Thickly laminated	0.3-1 cm
Thinly laminated	< 0.3cm

8.5.2.1 Lenticular bedding

Lenticular bedding is identified as sedimentary succession revealing dynamical layers of mud and sand. It is created throughout the phase of slack water, wherever mud is ejected within the water on top of smaller formations of sand once the water rate reaches zero (at rest). The lenticular bedding is classified due to its massive quantities of mud relative to sand, while a flaser-bed consists mostly of sand. Thus, the sand formation inside the bedding exhibit a "lens-like" form, giving the sequence its revered name (Reineck & Wunderlich, 1968).



Together in Excellence

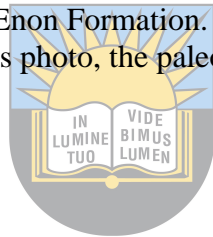
Figure 8.16: Lenticular bedding shows "lens-like" sandstone alternated with mudstone. The thickness of sandstone is unstable, and dies out on one side or both sides, Sundays River Formation.

8.5.2.2 Tabular cross-bedding

Tabular cross bedding is common in the Knysna and Enon Formations, the cross-beddings are parallel each other and dip toward one direction. Tabular cross bedding is a good indicator for paleocurrent direction, the dip direction of the cross bedding is the paleocurrent flow direction figure (8.17).



Figure 8.17 Tabular cross bedding in Enon Formation. The dip direction of the cross bedding indicates paleocurrent direction. In this photo, the paleocurrent was flowing from right to left.



8.5.2.3 Deformation bedding

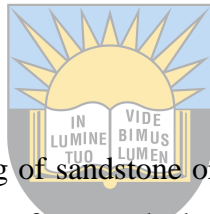
Due to unstable of wet sands and mud, the sand or mud bed could be deformed caused by tectonic movement, Earth quake or slipping along a slope. Figure 8.18 shows a deformation bedding in the Knysna Formation, indicating an event of quick sands and unstable environment.



Figure 8.18: Deformation bedding in the Knysna Formation.

8.5.2.4 Load cast

Load cast forms due to the down-sinking of sandstone or limestone into bottom mudstone. Load casts are lobes, lumps, and bulges that can form on the bottom bedding due to gravity loading. The casts take on the form of swellings, slight bulges, deep or rounded sacks, and highly irregular protuberance.



University of Port Harcourt
Together in Excellence



Figure 8.19: Load cast (middle) in the Cretaceous rocks of Knysna Formation.

Different sedimentary structures related to different formation mechanism and different formation environments. Some sedimentary structures can accurately reflect hydrodynamic condition or paleocurrent flow direction, thus sedimentary structures are useful tools to indicate geological setting and modern, or paleoenvironments.

The present is the key to the geological past, therefore all the sedimentary structures can be used in analysis of geological record in the history about its formation process, hydrodynamic condition and physical, chemical and biological environments. In the Cretaceous Knysna Formation, sedimentary structures, including tabular cross bedding, lenticular bedding and erosional surface, plus red-brownish coloured lithologies are assumed to be deposited by fluvial currents in an arid to semi-arid climate condition.

In addition, all beach structures and the cross-beds of the Cretaceous Knysna Formation belong to a lower flow regime field where the Froude number is less than 1 shown in figure (8.1).



University of Fort Hare
Together in Excellence

CHAPTER 9: COASTAL EROSION

9.1 Introduction

Coastal erosion is referred to as natural or coastal actions and human-induced impacts that erode land surfaces and lead to the loss of the beach, coastline, or dune material (Skaggs & McDonald, 1991). Coastal erosion can be further defined as removing weak rock materials and sediments on the shoreline because of the activities of waves, tides, currents and wind-driven flowings, plus alternative effects of storms. Rip currents, over-wash, storm surge, and storm waves are the exemple of fast, daily, short-term recurring, or yearly episodic phenomena that cause coastal erosion (Islam & Ryan, 2015). Hazardous weather actions (coastal surges, storms, and flooding) and tsunamis are often associated with important episodes of coastal erosion as a result of the waves and currents said to be much extreme. They are related to storm surge or tsunami flooding, which may enable waves and currents to strike landforms that are commonly out of their control. The economic consequences of infrastructure and property placed almost nearly to eroding coasts losing their natural protection by water and waves or being harmed due to damage of the soil upon which they were built are the key issues concerning coastal erosion (Bullock et al., 2017). Coastal areas of significant biological value include intertidal and mudflats, sand dunes, wetlands, salt marshes, coastal lagoons, and soft cliffs vulnerable to coastal erosion and flooding

9.2 Causes of erosion

However, because water is abundant and has many strengths, it is the major cause of soil erosion. Soil erosion mainly is made up of soil exposure to extreme winds, intense rainfall, and water runoff. Human events, involving farming and land cultivation, will expose the soil to erosion in numerous conditions (Mulvihill, 2021). The weather also influences erosion. Precipitation and water levels are affecting the soil, important temperature swings will create topsoil additional sensitivity to erosion, and expanded droughts will forbid plants from growing, exposing soil even additional (Mulvihill, 2021). Because wind may take up soil and blow it far away, it is also a major source of soil erosion. (IPCC, 2013). The sea is a powerful erosional force. Coastal erosion can modify the shape of entire coastlines by eroding rocks, dirt, or sand on the beach. Waves pound boulders into pebbles, then pebble into the sand, as part of the coastal erosion process. Sand is

moved far from beaches because of waves and currents, forcing the shoreline inland. Storm waves have the best effect, and hydraulic actions on coasts contain heavily articulated or bedded rock, issue to the quarrying or the hydraulic exacting of rock blocks (IPCC, 2013). The main wave erosional action is perhaps the abrasive result of sand and rocks eroded against coastlines (IPCC, 2013). Wave motion pulls particles back and forth, abrading the bedrock on the shore and abrading one another, changing pebbles into sand.

9.3 Impacts of erosion

Most soils are at risk of erosion, various are quite more susceptible than others. Quarrying and gulf formation, as an example, will extremely erode soils having coherent subsoils. Soil erosion minimizes the number and quality of soil ecosystems and cultivatable land (Mulvihill, 2021). Extreme soil erosion, if moved unmanaged, will cause the loss of food crops, damage community volatile and livelihoods, and even amendment ecosystems by decreasing biodiversity above, throughout, and more than the topsoil (Mulvihill, 2021). Some actions of erosion are extended flooding, enlarged sedimentation in the rivers and streams, depletion of nutrients within the soil, soil degradation, and, in intense cases, deforestation. Erosion decreases the regime availability for animals and plant biodiversity. Due to coastal environments are possible to be extremely sensitive to sea-level rise (Vestergaard, 1991). Recurrent landslides endanger the whole vegetation of geological formation slopes. Dune erosion conjointly causes the depletion of important coastal environments (Labuz, 2012). Sand dunes form on the far side of the direct impact of seawater, dune vegetation is a smaller amount at risk of sea-level rise than coastal vegetation.

9.4 Types of coastal erosion

9.4.1 Water erosion

The most major natural erosional agent is moving water. Coastal erosion is caused largely by the intensity of ocean waves; however, it is additionally formed due to the degradation or disintegration of sea cliffs formed by atmospheric agents like tide scour, rain, and frost. Water erosion is the discharge of soil because water and transportation of the eroded materials are removed from the position of the discharge (Mclovor, 2017). Rainwater erodes the surface and dulls soil creating activities like a gulf, and stream erosion, leading to flooding and sedimentation

downstream (Mclovor, 2017). Soil form, slope, soil water storage volume, underlying rock type, vegetation cover, rainfall severity, and time of entire impact impact the intensity of water erosion (Mclovor, 2017). Rainfall features, climate, topography, soil factors, and land use are vital parts influencing erosion. Natural water erosion is uncontrollable by humans and has no impact on soil fertility. Rainfall, melted snow, or runoff, in other words, natural processes, seem responsible. Some soil kind contain its natural erosion standard, determined by farming characteristics and environment. There are several kinds of water erosion, like; swash erosion which is a process caused by rain whereby raindrops are exposed to bare land and destroy the structure of the top layer. Sheet erosion is when rainfall intensity exceeds soil infiltration capacity, soil degradation by water occurs, resulting in the depletion of the fine-grained soil fragments containing organic matter and nutrients.



Figure 9.1: The photograph shows a tarred road washed away by water erosion in Durban.

9.4.2 Wind erosion

Wind erosion could be a natural occurrence during which wind generation moves the soil from another site to a different one. It is the potential to form substantial economic and environmental damage. A lightweight wind that soil fragments over the surface to a robust wind that pushes a major volume of soil fragments into the air to create dust storms are all exemplars of wind erosion. Whereas wind erosion is quite common in the deserts and on the beaches and coast's sand dunes, it also can take place in agricultural places because of specific land situations. Wind erosion of soils is one of the most important environmental and agriculture problems, affecting several fields (Movahedan et al., 2012). The resulting wind erosion management wants consideration in arid and semi-arid environments (Movahedan et al., 2012). Wind erosion destructions rely upon wind features like speed and time of the wind and therefore the amounts and kinds of transported fragments and surface layer characteristics (Lian-You et al., 2003). Wind erosion creates several harms to agricultural production and infrastructure (Lian-You et al., 2003).

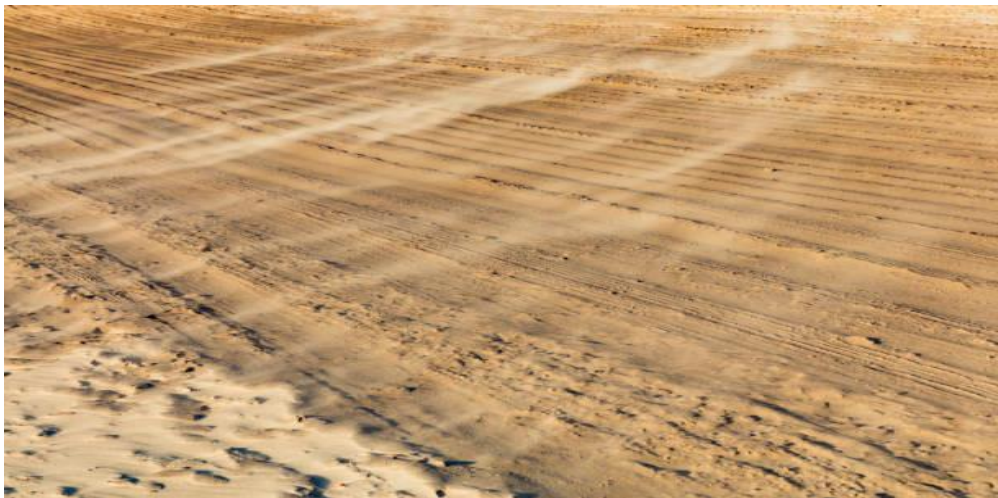


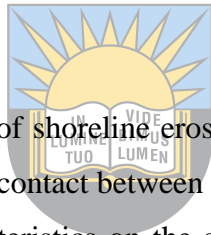
Figure 9.2: Photograph shows active wind erosion on a sandy beach resulting in tire tracks, PE in Colchester.

9.5 Damages of coastal erosion

Tropical storms and other natural phenomena produce erosion along all coastlines; however, the combination of storm surge at high tide combined with the additional effects of large waves often associated with landfalling tropical storms generates the most devastating conditions (Dahl & Stedman, 2013). Beach land can be lost due to scour if hard structures are installed to keep the

shoreline steady (Conathan et al., 2014). High erosion rates can be expected when the shoreline moves naturally, especially in areas of the coast that already have a low sediment budget and rapid shoreline migration (Conathan et al., 2014). Increased coastal erosion will occur when storm frequency and intensity increase in the future. Negative shoreline trends have a downstream influence on society, threatening human settlements, harbours, coastal recreation zones, wetlands, and marshes, among other things. As a result of climate change, these effects are predicted to worsen, resulting in rising sea levels. Beach erosion is a key consequence of rising sea levels, as it has a direct physical influence on numerous components of the coastal-resource system (Hanson & Lindh, 1993). The socioeconomic consequences on human activities or interests in the coastal zone are examples of secondary impacts (Hanson & Lindh, 1993). The preservation of the natural environment for future generations is a significant societal concern (Hanson & Lindh, 1993).

9.5.1 The shoreline erosion

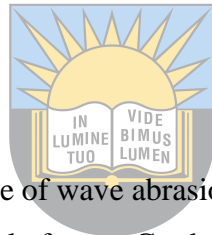


Water and wind are the major sources of shoreline erosion, affecting the shoreline change. The coastline is outlined because the line of contact between land, and therefore the water body is one among the foremost vital linear characteristics on the surface of the earth, that encompasses a dynamic nature (Niya et al., 2013). Natural characteristics like sediment supply, sea level, and wave energy are the first effects of coastal modifications. In distinction, human actions are stimulants influencing unbalanced situations that expand the standard of changes (Yadav et al., 2017). Coastal erosion influences shorelines with differing rates and is probably going to extend by the sea-level rise and accumulated storm actions. It happens primarily by the wind, waves, and long-shore currents, which can transport sand from the shore and deposit it in different regions (Yadav et al., 2017). The sand is often deposited to a different beach or the deeper ocean floor, to the ocean trench, or onto the landslide of a sand dune (Yadav et al., 2017).



Figure 9.3: Photograph shows shoreline erosion along the beach in Durban, South Africa.

9.5.2 The wave-cut platform cliff



The wave-cut platform increases because of wave abrasion, and the beaches shield the shore from abrasion and protect the formation of platforms. Gradually, this geological formation creates a cliff, which functions as a protecting barrier, protecting any type of erosion. Sinking relation to sea level on the coast has formed associate retreated coastline of moderate discharge with associate heavy of beaches, lagoons, barrier islands, and marshes, formed a lot of by deposition over erosion (DiPietro, 2018). Shore platforms are generally gently or horizontal sloping surfaces endorsed by a cliff, eroded in sediment or bedrock at the shore (Stephenson & Kirk, 2005). The erosional source of those surfaces is obvious as a result of the slit across and revealing geological features. Shore platforms have long been categorized due to a tripartite scheme regarding elevation with the tide (Stephenson & Kirk, 2005). Therefore high-tide, intertidal, and sub-tidal platforms are known. Another grouping utilizes the two main typical profile structures or the sloping or horizontal platforms (Stephenson & Kirk, 2005).



Figure 9.4: Photograph shows the wave-cut platform on the cliff resulting in shoreline erosion, Keurbooms River Lagoon.



University of Fort Hare
Together in Excellence

CHAPTER 10: MITIGATION METHODS FOR COASTAL EROSION

10.1 Introduction

This chapter provides the management strategies based on engineering geology approach to protect coastal erosion. Management strategies need to consist of knowledge, equipment, techniques, and institutional instruments to reduce or remove coastal erosion-associated influences (Shin et al., 2019). These ought to have the greatest advantage to decreasing society's susceptibility precisely to coastal erosion-hazards. Storm and sea-level rise action, surface erosion, and marine erosion of the toe and face of the sandbank all contribute to coastal erosion.

Coastal erosion is a frequent issue influencing around 75% of the world's coastline (Pilkey & Cooper, 2014). Coastal dangers are primarily related to risks such as coastal erosion, waves, excessive winds, flooding, storm inundation, and human actions on along the coast (Thior et al., 2019). Coastal erosion is dynamic, meaning the dune system interacts often and is continually changing in response to variations in wind and wave climate or sea level change. Yet, land stability and vegetation cover are among the criteria. The ecosystem rehabilitation technique, in which sustainable ecosystems are built, is more appropriate. Apart from vegetation restoration and succession, ecosystem development includes the establishment of distinctive landforms and land cover; therefore, consideration must be given to the other components of the system. Several countries have utilized a variety of techniques to fight coastal susceptible. As an example, a range of coastal protection structures like groins, breakwaters, seawalls, and jetties (Angnuureng et al., 2013; Laibi et al., 2014).

10.2 Hard engineering solution

10.2.1 Groins

Groins could be the main frequent engineering exercise for preventing the coast from erosion. By definition, a groin is a barrier-type construction that traps via blocking longshore sand transit on a range of beaches, involving covered shorelines and open coasts figure (10.1). Groins are built perpendicular to the beach and stretch in the backshore within the littoral zone. They are typically made of concrete, timbers, steel, or rock. The percentage of littoral movement that the groin stops

determine whether a building is classed as intensity, moderate, or low energy. The groin lowers the sediment supply to the down movement beach by collecting sand, perhaps starting or speeding up erosion on the groin's down movement side. The rapid erosion will occur in beach habitat depletion and shrinking. These engineering forms are installed as complete systems to affect shoreline sediment transportation as an outcome of longshore currents. Those structures to be constructed are as porous structures comprising blocks of calcareous rocks acquired from tertiary rocks taken close by quarries.

Some are created from geotextile bags, concrete tetrapods, concrete rests, tires, and corals. The detrimental influence of groins in many areas is the movement of sediment on the coast within the down movement confined on the up movement side of the development, making a sand shortage and increasing erosion rates on the down movement side (Bush et al., 1996). The utilization of groins are to decrease coastal erosion experiencing urban or timely necessary (necessary decent to be prevented) areas, is the main-known technique practiced in the geographical region, from Senegal to Nigeria (UNESCO-IOC, 2012).

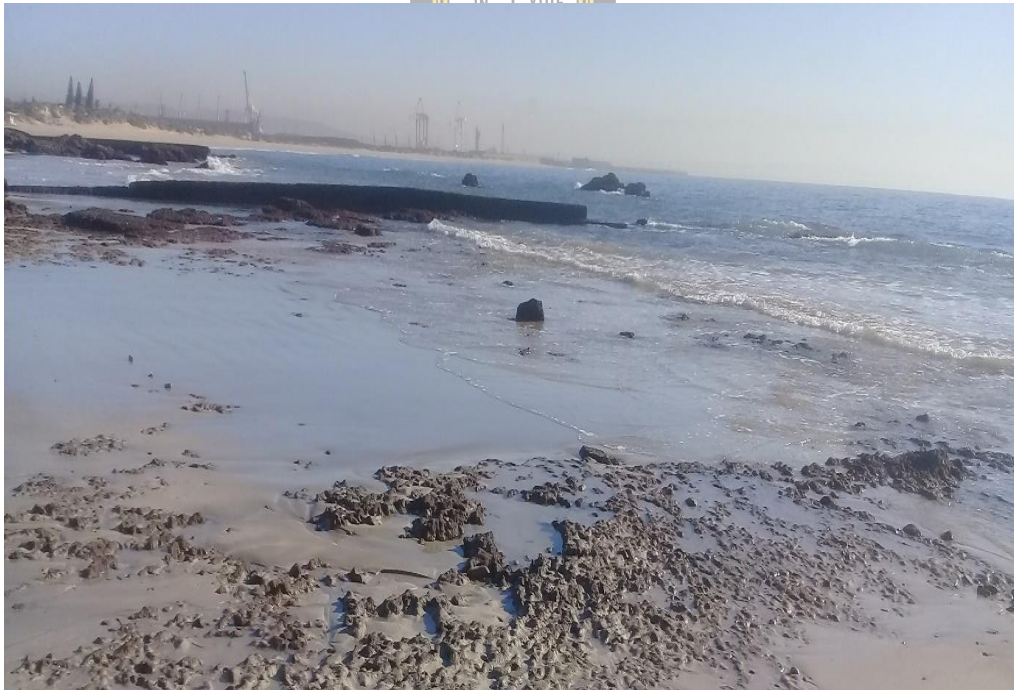
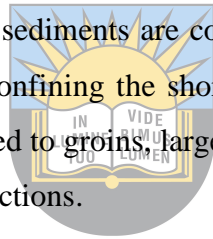


Figure 10.1: Photograph demonstrating a series of smaller groins in Port Elizabeth, South Africa.

10.2.2 Jetties

Jetties provide positive stabilization of the river mouths or tidal inlets, controlling the construction of difficult characteristics, like channel siltation. A jetty platform was erected into the sea on wooden or concrete piles to protect a navigation channel and allow ships to berth. It doesn't normally feature a shore-protection function (instead, breakwaters do). Parallel jetties typically delimit a navigation canal. Jetties will impact sediment transport and ecological processes along the coast. Jetties are generally built to "guard" forms constructed on the beach, removing sand (Horton et al., 2009). They are sometimes created to divert rivers and streams. Other times, they're built to provide shelter for boats in calm waters. In numerous situations, seawalls, jetties, breakwaters, and groins have produced down-coast erosion concerns, resulting in costs that far outweigh the cost of the structure itself (Horton et al., 2009). These constructions are normally structured to deflect sediment that moved alongshore so that they can stop sediment accumulation in estuaries or inlets. Huge portions of sediments are confined in the up movement of the jetty. However, like technique develops in confining the shoreline down movement of the jetty. For jetties are almost overlonger as compared to groins larger sediment deplete to very deep water is quite extra encountered through storm actions.



University of Fort Hare
Together in Excellence

10.2.3 Breakwaters

Breakwaters are known as offshore constructions composed to deflect and decrease wave influence reaching the coast. Breakwaters are classified as the third main frequent engineering operation for protecting the coastal areas worldwide. In some countries across the West Africa, breakwaters are applied at the harbours to decrease wave effects on the ship. In most cases, breakwaters are installed diagonally to the coastline to decrease or remove wave energy and bring deposition on beaches landward. Togo experienced various coastal management difficulties that concerned pollution, shoreline dynamics, flooding, and probability outcomes of rising sea-level.

10.2.4 Seawalls

The seawall will be outlined as a form of coastal protection designed wherever the ocean and related coastal constructions directly affect the coastal landforms. The most influential of an environment-friendly seawall includes its ability to allow a bigger stage of protection throughout coastal retreat or flooding. It helps because of the margin between the land and therefore the ocean, guaranteeing that no erosion will occur. Additionally, seawalls do not protect such massive areas, notably if vertical seawalls are well planned, reducing the development price. Seawalls are often possible to be constructed on open coasts to protect against ocean wave climates compared to bulkheads because they are created to endure a lot of wave energy. Cast-in-place concrete is the most typical material used; different materials, like wood, is scarcely used to assist redirect or divert wave energy, these forms may be vertical, curved, or stepped (Board, 2007).



Figure 10.2: Photograph displaying a coastal seawall to protect infrastructures along Knysna Coast.

10.2.5 Revetments

Revetment is construction to shield a fine property like a coastal slope or dune or furnish extra safety to actual protection like the seawall or dike (Bayle et al., 2020). Revetments protect the slope features of the beach. They are usually made of one or other layers of graded rip rap; however, they can be made of solid-cemented concrete matting, wood (wire mesh baskets, stone-

filled), and some materials (Board, 2007). Whilst properly designed and constructed revetments will successfully stop erosion, many projects are built haphazardly with minimal planning utilizing available resources (building rubble, concrete, and some waste materials) structures exist.



Figure 10.3: Photograph showing revetment of dolosse blocks in Port Elizabeth, South Africa.

University of Fort Hare
Together in Excellence

10.2.6 Rock armour (rip-rap)

Access to the beach is difficult due to rock armour, which forces tourists to scramble over it or take extensive diversions. Rip-rap is another name for rock armour. It comprises hundreds of massive granite boulders that operate as a barrier between land and water. The wave energy is deflected and absorbed by its downward slope arrangement. Wave scouring does not occur at the base because the water flows through the gaps, and pressure is relieved, making them particularly effective (Pak & Madj, 2011). The building of armour layers with set slope angle(s), thickness, and layer porosity is envisioned in traditional rock armouring design approaches. The median unit weight, or upper and lower limiting weights, describes the armour units inside the layer. However, such simple descriptors do not fully quantify the armour layer's hydraulic performance or stability levels (Bradbury & Allsop, 1987).



Figure 10.4: Photograph demonstrating riprap structures with pebble-and-boulder quartzite along the riverbank at Knysna.



Some other hard engineering solutions can protect coastal erosion along coastal regions, for example, dike, storm surge barrier, and closure dam. Dikes are used in low-lying areas tilted to coastal floods conduct on due to the seawater, commonly throughout high wave situations. They are not speculated to protect beaches that will seem before of the structure or any connected, unprotected beach. There are several low-lying regions on the coast of West Africa. The development of dikes needs to be of considerable help in protecting the inside and also the population. These coastal protection forms will protect estuaries, tidal inflows, and rivers from irregular storm surge occurrence (Appelquist et al., 2016). The basic demerit of the storm surge barrier is that it is capital intensive due to extreme maintenance prices. This coastal management resolution entails excessive capital charges for application and preservation.

10.3 Soft engineering solution

10.3.1 Dune restoration/vegetation

Dune rehabilitation is known as the restoration of artificial either natural dunes to acquire advantages from coastal protection. To naturally reconstruct a dune, it is essential to first control whether there is enough extent of windblown sand available. Proximate accumulation around sand fences or the familiar situation of adjoining dunes can reveal the availability of wind-blown sand.

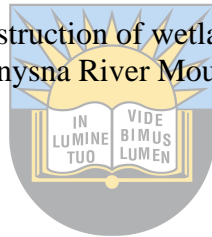


Figure 10.5: Photograph illustrating dunes rehabilitation managing coastal erosion in Central Beach, Plettenberg Bay.

The vegetation on the riverbanks and dunes helps restrict wind speed across the surface and trap and hold sand. Planting vegetation helps stabilize dunes and supports dune recovery; therefore, it is good to do it after a storm (Board, 2007). It forms a barrier all over the seaward front of current dunes that storm surges could undermine. Selected species will be able to resist silting, salt, and wind. The grass protection can enhance self-assistance after it has formed. Normally survey and, if necessary, the plantation will be needed. Marram grass planting-enormous nurseries of marram grass are planted on flat, open sandy areas, and the grass is collected using an under-cutting process (Board, 2007).



Figure 10.6: Photograph showing reconstruction of wetlands in the riverbanks to prevent erosion, Knysna River Mouth.



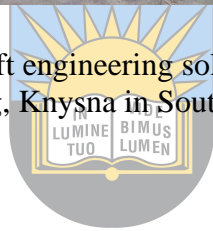
10.3.2 Beach nourishment

Beach nourishment has been practiced through numerous coastal components in West Africa. To keep far away from the approaching damages of human settlements, and disruption of socio-economic events on the Island of Lagos, man-made beach nourishment was completed till a possible answer was once constructed. A beach sand nourishment, conjointly associated with a sand refilling or beach fill, could be a coastal engineering and management project that mechanically enlarges the measuring of the above-water beach using off-site sand (Dean, 2003). Sandy nourishment is highly used in coastal environments to help business enterprises like tourists and protect infrastructure from erosion and coastal flooding (Dean, 2003). Nourishments may be created using many sediment types derivation from inland or marine origin (cobbles, sand, cohesive clays). They will be placed on the above-water beach (beach nourishment) or engulf nearshore beach profile (shore-face nourishment) (Liu et al., 2016).

Even on the soft engineering solution, several strategies exist to protect coastal erosion, such as fluvial sediment management, land claim, ecosystem-based management, and cliff stabilization.



Figure 10.7: Photograph showing soft engineering solution (beach nourishment) to prevent flooding, Knysna in South Africa.



University of Fort Hare
Together in Excellence

CHAPTER 11: DISCUSSION AND CONCLUSION

The oldest rocks in the Plattenberg Bay and Knysna area is the Table Mountain quartzite of Cape Supergroup, which is overlain by Knysna Formation that is equal to Enon Formation of Cretaceous age. An unconformity separated Knysna Formation with the basement of Table Mountain quartzite. The modern sediments of loose sands and soft mud distribute along coastline beach and river mouth, which linked to and reflected different hydrodynamic conditions and environmental zones. Stratigraphy of the Knysna Formation, it is composed mainly of clast-supported conglomerate with subsidiary sandstones and mudrocks. The pebbles of the clast-supported conglomerate are subrounded to subangular, reflecting short distance of transportation, and most probably of a braided stream of fluvial origin. The red-brownish colouration of the whole sequence is consistent with the fluvial formation.

Grain size analysis is a useful tool to study hydrodynamic condition and to analyse formation environment. Several factors can affect the grain-size distribution, such as transportation distance from the source area, parent rocks, topography, and transport media, etc. The hydraulic energy of the environment defines the grain size distribution of siliciclastic sediments. The classification of the grain-size analysis was based on the Udden-Wentworth scale, which was a world-wide used scale for grain size classification of sediments and sedimentary rocks. The gravel, sand, silt, and clay are the major-size classes used to identify these sediments according to the Udden-Wentworth scale. The river sediments vary from 3 ϕ (defines as fine sand) to -1 ϕ (granule gravel), whereas the grain-size distribution of the beach sediments is dominated by 3 ϕ (fine sands) and 2 ϕ (medium sands), meaning the river sands were more variable in size while beach sands were more uniform.

River sediments

Area	Grain-size	Sorting value	Skewness value	Kurtosis value	Explanation of sediments
Keurboomsriver (Plettenberg Bay)	1.80	0.8	0.06	1.085	Medium-grained, poorly-sorted, near symmetrical, and mesokurtic.
Knysna River Mouth	1.60	1.29	0.12	0.66	Medium-grained, very poorly-sorted, strongly coarse-skewed, and platykurtic.

Beach sediments in Plettenberg Bay

Area	Grain-size	Sorting value	Skewness value	Kurtosis value	Explanation of sediments
Beacon Beach	2.35	0.45	-0.008	0.97	Fine-grained, well-sorted, near symmetrical, and mesokurtic.
Robberg Beach	2.36	0.49	-0.202	1.064	Fine-grained, well-sorted, coarse-skewed, and mesokurtic.
Central Beach	2.43	0.41	-0.106	0.90	Fine-grained, well-sorted, near symmetrical, and platykurtic.
Hobie Beach	2.51	0.43	0.000	0.766	Fine-grained, well-sorted, near symmetrical, and platykurtic.
Wedge Beach	2.53	0.32	0.024	0.878	Fine-grained, very well-sorted, near symmetrical, and platykurtic.
Sanctuary Beach	2.46	0.40	-0.064	0.704	Fine-grained, well-sorted, near symmetrical, and platykurtic.
Lookout Beach	2.43	0.45	-0.11	1.104	Fine-grained, well-sorted, strongly coarse-skewed, and mesokurtic.


 University of Fort Hare
 Together in Excellence

The relationship between mean and sorting shows that beach sands are frequently fine-grained and very well-sorted to well-sorted; whereas the river sediments are medium-grained with more variable in sizes and moderately sorted to moderate well-sorted. Furthermore, compared to the river sediments, the beach sediments are more fine skewed, while river sands are more coarse-skewed. The beach sediments show a positive relationship between sorting and skewness, whereas river sediments show a negative relationship between sorting and skewness. Further, river sediments are more scattered in sizes, although with dominantly medium-grained. The graphic mean versus kurtosis reveals that river sediments are mesokurtic in nature and beach sands are platykurtic to mesokurtic in nature. Most beach sediments are fine-grained, and the river sediments are mostly medium-grained. The sorting of the beach sediments is much better than river sediments. Also, the river sediments are strongly coarse-skewed compared to those of beach sediments which are more fine skewed.

As noted by studies of SEM and microscopic thin sections, quartz is the dominant mineral in all the sediments. Quartz, calcite, aragonite, muscovite, and organic pellets are among the six main mineral group in the research area. Quartz, sourced from inland and brought into the beach by river streams and sourced from the quartzite of the Cape Supergroup. It took more than a half of the total mineral percentages. Quartz, feldspar, lithics and muscovite were mainly sourced from inland, while calcite, aragonite (mostly shell fragment and coral fragment), Foraminifera and organic pellets were mainly sourced from sea side. XRD analysis of mineral compositions is assistant with the finding of SEM and Microscope studies.

The scanning electron microscope (SEM) analyses give detailed information about the grain surface texture of the detrital grains. The SEM results exhibited that many grains have V-shaped pits, upturned pits caused by mechanical crashing, crystal precipitation and recrystallization of calcite, quartz, salt, and clay by chemical precipitation; whereas dissolution pits and pores were results from chemical dissolution of unstable minerals at a new burial environment. Activities by organisms, particularly the micro-organisms like worms and algae produced boring holes and bioturbation, The grain surface textures can reflect the geological process, transportation media and energy conditions. Chemical, mechanical and biogenic processes acted on the grains can remain useful clue for revealing hydrodynamic condition (hydraulic energy), chemical Eh and pH environment and organic activities in the grain transportation and deposition history.

Sedimentary structures are one of most useful features for interpreting depositional environments, including hydrodynamic energy, aeolian influence and water flow direction, and etc. Various ripple marks and dunes such as catenary ripples, straight ripples, sinuous and lunate ripples can reflect hydrodynamic conditions; whereas rhomboid ripples can only formed in a tidal environment. The bioturbation and boring hole reflect an active organic activity environment.

Erosion is a natural coastal activity that leads to sediment redistribution throughout the coastal system and the production of distinctive coastal landscapes such as coastal cliffs and sharpened dunes in erosive areas and spits and wide beaches in deposition areas. The Coastal hazard can assess various management choices and serve as a foundation for building a complete coastal management strategy. As coastal profiles adjust when sea level rise, coastal erosion rates will generally increase. The coastline will normally retreat if this process continues as part of the dynamic coastal landscape development. Damming rivers can worsen coastal erosion, resulting in

sediment deficiencies in delta areas and surrounding beaches and locations within the coast. Coastal erosion is dynamic, meaning the dune system interacts often and changes over time in response to changes in wind and wave actions. Flood and coastline retreat are the most worse hazards in the coast, which had caused serious damage in the past in the study area.

To combat coast erosion and to protect infrastructure and human properties and safety in the coast, a number of engineering projects have been suggested for this task. Vegetation, breakwaters, groins, jetties, vertical walls, rock armour, shoreline hardening, and revetments are common examples of coastal erosion protection structures. Considering vulnerability of coastal environment, establishment of an integrated management system/strategy to combat erosion and damage of coast properties is of significant importance in the Plettenberg Bay and Knysna area.



University of Fort Hare
Together in Excellence

RECOMMENDATIONS

Further investigation needs to be done on the stratigraphic correlations of the Knysna Formation with Enon Formation. More detailed investigation on the coast erosion and mitigation are needed to ascertain which method is more effective to combat hazard and to protect coast retreat and damage of infrastructure and human safety. An integrated coast management system/strategy is required to monitor the coast erosion and protection aspects in the Plettenberg Bay and Knysna area in the future.



University of Fort Hare
Together in Excellence

REFERENCES

- Aagaard, T., 2014.** Sediment supply to beaches: cross-shore sand transport on the lower shoreface. *J. Geophys. Res. Earth Surf.* 119, 913–926. doi: 10.1002/2013JF003041.
- Al-Ghadban, A.N., 1990.** Holocene sediments in a shallow bay, southern coast of Kuwait, Arabian Gulf. *Mar. Geol.*, 92, 237-254.
- Almond, J., 2013.** Palaentological specialist assessment: combined field-based and desktop study. 59pp. Natura ViVa cc, Cape Town.
- Alsharhan, A., & El-Sammak, A., 2004.** Grain-size analysis and characterization of sedimentary environments of the United Arab Emirates coastal area. *Journal of coastal Research*, pp. 464-477.
- Andrews, P., & Van Der Lingen, G., 1968.** Environmentally significant sedimentologic characteristics of beach sands. *Journal Geology and Geophysics*, 12, 119-137. New Zealand.
- Angnuureng, D.B., Appeaning, A.K., Wiafe, G., 2013.** Impact of sea defense structures on Downdrift coasts: the case of Keta in Ghana. *Acad J Environ Sci* 1(6):104–121.
- Anthony, E. J., Brunier, G., Besset, M., Goichot, M., Dussouillez, P., & Nguyen, V. L., 2015.** Linking rapid erosion of the Mekong River delta to human activities. *Scientific reports*, 5(1), 1-12.
- Anthony, E.J., Masselink, G., & Gehrels, R., 2014.** Coastal Environments: (Eds.) Dynamics, Climate Change and Management, Wiley-Springer, pp. 52-78
- Appelquist, L.R., Balstrøm, T., & Halsnæs, K., 2016.** Managing climate change hazards in coastal areas: The Coastal Hazard Wheel decision-support system. Main Manual. Nairobi, Kenya: United Nations Environment Programme, UNEP Job No. DEP/2029/NA.
- ARC, 2000.** Auckland regional council, 2000. Technical Publication No. 130. Coastal Erosion Management Manual.
- Atherstone, W., 1857.** Geology of Uitenhage. Eastern Cape Province Monthly Magazine, 1, 518-532.
- Avramidis, P., Samiotis A., Kalimani E., Papoulis D., Lampropoulou P., & Bekiari V., 2012.** Sediment characteristics and water physicochemical parameters of the Lysimachia Lake, Western Greece, *Environ Earth Sci.*, 70 (1): 383-392.

- Baas, J.H., Baker, M.L., Malarkey, J., Bass, S.J., Manning, A.J., Hope, J.A., & Davies, A.G., 2018.** Redefining ‘Clean’ Sand By Integrating Field And Laboratory Data On Mixed Sand–Clay–EPS Rippled-Bed Transport.
- Bagnold, R.A., 1941.** The physics of blown sand and desert dunes London: Methuen. Progress in Physical Geography, 18(1), 91-96.
- Baiyegunhi, C., Liu, K., & Gwavava, O., 2017.** Grain size statistics and depositional pattern of the Ecca Group sandstones, Karoo Supergroup in the Eastern Cape Province, South Africa. 9, pp. 554–576.
- Barclay, K.M., Gingras, M.K., Packer, S.T., & Leighton, L.R., 2020.** The role of gastropod shell composition and microstructure in resisting dissolution caused by ocean acidification. *Marine Environmental Research*, 162, p.105105.
- Barnard, P. L., & Warrick, J. A., 2010.** Dramatic beach and nearshore morphological changes due to extreme flooding at a wave-dominated river mouth. *Mar. Geol.* 271, 131–148. doi: 10.1016/j.margeo.2010.01.018.
- Barragan, J.M., Andreis, M., 2015.** Analysis and trends of the world's coastal cities and agglomerations. *Ocean Coast. Manage* 114, 11-20.
- Bayle, P., Blenkinsopp, C., Conley, D., Masselink, G., Beuzen, T., & Almar, R., 2020.** Performance of a dynamic cobble berm revetment for coastal protection under increasing water level. *Coast Eng* (in press).
- Becke, B., 2003.** The Tourism Industry in Plettenberg Bay. Plettenberg Bay Ratepayers Review 2002-2003: Avonwold House. Paarl Printers.
- Bevis, K.A., 2013.** The Geology of Sedimentary Rocks. Department of Geology, Hanover College, Hanover.
- Bird, E.C.F., 1985.** Coastline Changes. A Global Review. 219pp.
- Bish, D. L., & Post, J. E., 1993.** Quantitative mineralogical analysis using the Rietveld full-pattern fitting method. *American Mineralogist*, 78(9-10), 932-940.
- Blatt, H., Middleton, G.V., & Murray, R.C., 1972.** Origin of sedimentary rocks.

- Blott, S. J., & Pye, K., 2001.** GRADSTAT: A grain size distribution and statistics package for the analysis of unconsolidated sediments. *Earth surfaces processes and landforms*, 26, 1237-1248.
- Blumberg, D.G., & Greeley, R., 1993.** Field studies of aerodynamic roughness length. *Journal of Arid Environments*, 25(1), 39-48.
- Board, O.S., & National Research Council, 2007.** Mitigating shore erosion along sheltered coasts. National Academies Press.
- Botero, L., & Salzwedel, H., 1999.** Rehabilitation of the Cienaga Grande de Santa Marta, a mangrove-estuarine system in the Caribbean coast of Colombia. *Ocean. Coast. Manage* 42, 243-256.
- Bradbury, A.P. and Allsop, N.W.H., 1987.** Durability of rock armour on coastal structures. In *Coastal Engineering 1986* (pp. 1769-1782).
- Bruun, P., 1962.** Sea Level Rise as a Cause for Shore Erosion. *Jl. of Waterways and Harbour Division*, ASCE. No.88. ww I.
- Bruun, P., 1983.** Review of Conditions for uses of the Bruun Rule of Erosion. *Dock and Harbour Authority*, 54, pp.753.
- Bui, E., Mazullo, J., & Wilding, L., 1990.** Using quartz grain size and shape analysis to distinguish between aeolian and fluvial deposits in the Dalila Bosso of Niger (West Africa). *Earth Science Processes and Landforms*, 14, 157-166.
- Bullock, J., Haddow, G. & Coppola, D.P., 2017.** Introduction to emergency management. Butterworth-Heinemann.
- Bush, D., Pilkey, O.H., Neal, W., 1996.** Living by the Rules of the Sea. Duke University Press, Durham.
- Callaghan, D.P., Nielsen, P., Short, A.D., & Ranasinghe, R., 2008.** Statistical simulation of wave climate and extreme beach erosion. *Coastal Engineering* 55 (5), 375–390.
- Chauhan, R., Ramanathan, A.L., & Adhya, T.K., 2014.** Patterns of seasonal variability in granulomeres characteristics of Bhitarkanika Mangrove-estuarine complex, East coast of India. *India of Geo-Marine Sciences*, 3: 1083-1090.
- Chunnett, E., 1965.** Siltation problems in the Knysna estuary. Pretoria: CSIR. (Report MEG 353).



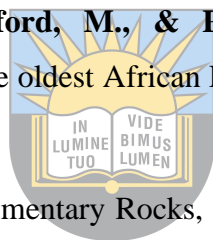
University of Fort Hare
Together in Excellence

- Coetzee, J., Adams, J., & Bate, G., 1997.** A botanical importance rating of selected Cape. *Water SA*, 23, 81-93.
- Conathan, M., Buchanan, J., & Polefka, S., 2014.** *The Economic Case for Restoring Coastal Ecosystems*. Center for American Progress and Oxfam America, 54 pp.
- Cooper, J. A. G., 1993.** Sedimentation in a river dominated estuary. *Sedimentology* 40, 979–1017. doi: 10.1111/j.1365-3091.1993.tb01372.x.
- Cooper, M.R., 1983.** The ammonite genus *Umaganiceras* in the Sundays River Formation. *Transactions of the Geological Society of South Africa* 86(1):63-64.
- CSIR, 1989.** Report on the investigation of siltation in the Green Hole, Knysna and technical evaluation of remedial measures. CSIR Report EMA-C 8920. Stellenbosch. 28pp plus figures.
- Dahl, T.E., & Stedman, S.-M., 2013.** Status and trends of wetlands in the coastal watersheds of the Conterminous United States 2004 to 2009. U.S. Department of the Interior, Fish and Wildlife Service, and NOAA National Marine Fisheries Service, 46 pp.
- Dann, S.E., 2002.** *Reactions and Characterization of SOLIDS*. Royal Society of Chemistry, USA.
- David, J.C., 1970.** Information contained in sediment-size analysis. *Mathematical Geology*, 2(2), 105-112.
- De Vries, S., De Schipper, M., Stive, M., & Ranasinghe, R., 2010.** SEDIMENT EXCHANGE BETWEEN THE SUB-AQUEOUS AND SUB-AERIAL COASTAL ZONES. *Coastal Engineering*, 2.
- Dean, R. G., 2003.** Beach Nourishment: A Short Course. In *Soft Shore Protection* (pp. 349-394). Springer, Dordrecht.
- Deline, P., Gruber, S., Delaloye, R., Fischer, L., Geertsema, M., Giardino, M., Hasler, A., Kirkbride, M., Krautblatter, M., Magnin, F. & McColl, S., 2015.** Ice loss and slope stability in high-mountain regions. In *Snow and ice-related hazards, risks and disasters* (pp. 521-561). Academic Press.
- Dickinson, W., 1974.** Plate Tectonics and Sedimentation. In: Dickinson, W.R., Ed., *Tectonics and Sedimentation*, Soc. Econ.Paleon.Mineral., Special Pub, 22: 1-27.

- Dingle, R., Siesser, W., & Newton, A., 1983.** Mesozoic and Tertiary geology of southern Africa. Rotterdam, Balkema, 375p.
- Dingle, R.V., 1973.** Mesozoic palaeogeography of the southern Cape, South Africa. *Palaeogeography, Palaeoclimatology, Palaeoecology*, 13(3), 203-213.
- Dinis, Y., 2018.** Sedimentology of the lower Uitenhage Group in the Middle to Late Mesozoic Oudtshoorn Basin, South Africa. MSc thesis, University of Cape Town (Unpublished).
- DiPietro, J.A., 2018.** *Geology and Landscape Evolution: General Principles Applied to the United States.* Elsevier.
- Dong, Z., Liu, X., & Wang, X., 2002.** Aerodynamic roughness of gravel surfaces. *Geomorphology*, 43(1-2), 17-31.
- Drury, M.R., & Urai, J.L., 1990.** Deformation-related recrystallization processes. *Tectonophysics*, 172(3-4), 235-253.
- Du Toit, A., 1956.** *The Geology of South Africa (Third Edition).* Oliver and Boyd, Edinburgh.
- Duvenage, I., & Morant, P., 1984.** Keurbooms / Bitou System (CMS 19) & Piesang (CMS 18). Report No. 31. In: *Estuaries of the Cape. Part II. Synopses of available information on individual systems.* (A. Heydorn, & J. Grindley, Eds.) CSIR Research Report 430. CSIR, Stellenbosch. 64 pp.
- Duvenhage, I., 1983.** Getyrvieroppervlaktes van sommige getyrviere aan die Kaapse kus. NRIO Internal Report, Stellenbosch. 172pp.
- Dyer, K., 1986.** *Coastal and Estuaries Sediment Dynamics.* New York: John Wiley and Sons.
- Dziadkowiec, J., 2019.** Interactions between Confined Calcite Surfaces in Aqueous Solutions: A surface forces apparatus study.
- East, A. E., Stevens, A. W., Ritchie, A. C., Barnard, P. L., Campbell-Swarzenski, P., & Collins, B. D., 2018.** A regime shift in sediment export from a coastal watershed during a record wet winter, California: implications for landscape response to hydroclimatic extremes. *Earth Surf. Process. Landf.* 43, 2562–2577. doi: 10.1002/esp.4415.
- Edwards, A., 2001.** Grain Size and Sorting in Modern Beach Sands. *Journal of Coastal Research*, West Palm Beach, Florida, 17(1), 38-52.

- Engelbrecht, L., Coertze, F., & Snyman, A., 1962.** Die geologic van die gebied tussen PE en Alexandria, Kaaprovinsie. Explanation of 1: 125 000 scale Sheets 3325D PE and 3326C Alexandria, Geological Survey of South Africa, 54p.
- Essien, N., Ilori, A., Okon, E., & Njoku, S., 2016.** Textural characteristics and depositional processes of sediments from a 47 Km transect in the Niger Delta, Southern Nigeria. *Journal of Geography, Environment and Earth Science International*, 7(1), 1-11.
- Folk, R.L., & Ward, W., 1957.** Brazos river bar: a study in the significance of grain size parameters. *Journal of Sedimentary Petrology*, 27, 3-26.
- Folk, R.L., 1965.** Some aspects of recrystallisation in ancient limestones. In: *Dolomitization and Limestone Diagenesis* (Eds L.C. Pray & R.G. Murray). Spec. Publ. Soc. Econ. Paleont. Miner. Tulsa, OK, 13: 14-48.
- Folk, R.L., 1966.** A Review of Grain-size Parameters. *The Journal of International Association of Sedimentologists*. University of Texas, Austin, Texas (U.S.A.), 6(2).
- Folk, R.L., 1974.** *Petrology of sedimentary rocks*: Hemphill Publishing Company, Austin TX, 182.
- Fouche, J., Bate, K., & Van der Merwe, R., 1992.** Plate tectonic setting of the Mesozoic Basins, southern offshore, South Africa: A review. In: *De Wit, M.J.; Ransome, I.G.D (Eds.). Inversion Tectonics of the Cape Fold Belt, Karoo and Cretaceous Basins of southern Africa*. A.A. Rotterdam Balkema, 33-48.
- Friedman, G.M., 1961.** Distinction between dune, beach, and river sands from their textural characteristics. *Journal of Sedimentary Petrology*, 31(4), 514-529.
- Friedman, G.M., 1967.** Dynamic processes and statistical parameters compared for size frequency distribution of beach and river sands. *Journal of Sedimentary Petrology*, 37, 327-354.
- Frost, S., 1996.** Early Cretaceous alluvial palaeosols (Kirkwood Formation, Algoa Basin, South Africa) and their palaeoenvironmental and palaeoclimatological significance. MSc thesis. University of Rhodes, Grahamstown (Unpublished).

- Gao, W., Shao, D., Wang, Z.B., Nardin, W., Yang, W., & Sun, T., 2018.** Combined Effects of Unsteady River Discharges and Wave Conditions on River Mouth Bar Morphodynamics. *Geophys. Res. Lett.* 45, 903–912. doi: 10.1029/2018GL080447.
- Gingras, M., & Pemberton, S., 2015.** Bioturbation: Reworking sediments for Better or Worse. University of Alberta Edmonton. Alberta, Canada.
- Gingras, M., Bann, K., MacEachern, J., & Pemberton, S., 2009.** A Conceptual Framework for the Application of Trace fossils” In MacEachern, J.A., Bann, K.L., Gingras, M.K., and Pemberton, S.G. (Eds.): *Applied Ichnology*. Tulsa: Society for Sedimentary Geology, short course notes, 52: 1-26.
- Giosan, L., & Bhattacharya, J.P., 2005.** River Deltas-Concepts, Models, and Examples. *SEPM* (eds). Tulsa: Society for Sedimentary Geology. doi: 10.2110/pec.05.83.
- Gomez, B., Martxxnez-Delclos, X., Bamford, M., & Philippe, M., 2002.** Taphonomy and palaeoecology of plant remains from the oldest African Early Cretaceous amber locality. *Lethaia* 35, 300-308.
- Greensmith, J.T., 1989.** *Petrology of the Sedimentary Rocks*, (7th Ed). University College, University of London.
- Griffith, J.C., 1967.** *Scientific Methods in analysis of sediments*. McGraw-Hill. New York USA.
- Grindley, J., 1985.** Estuaries of the Cape, Part II: Synopses of available information on individual systems. Knysna (CMS13). Report No. 30. CSIR Research Report 429. 80 pp.
- Grippio, A., 2015.** Stratigraphy. PhD thesis. Department of Earth Sciences. Santa Monica College. Los Angeles, California.
- Gust, D., Biddle, K., Phelps, D., & Uliana, M., 1985.** Associated Middle to Late Jurassic volcanism and extension in Southern South America. *Tectophysics*, 116(3-4), 223-253.
- Gutman, A., 1979.** Low-cost shoreline protection in Massachusetts. *Coastal Structures*, 79, 373–387.
- Haider, S., 2016.** Sediments grain size analysis from the Eastern Makran coastline area, Pakistan. *Journal of Biodiversity and Environmental Sciences*, 9, 40-56.



University of Fort Hare
Together in Excellence

- Hajek, E.A., Huzurbazar, S.V., Mohrig, D., Lynds, R.M., & Heller, P.L., 2010.** Statistical Characterization of Grain size Distributions in Sandy Fluvial Systems. *Journal of Sedimentary Research*, 80: 184-192.
- Hambrey, M.J. & Glasser, N.F., 2005.** Glaciers. Sedimentary processes. *Encyclopedia of geology*. Elsevier Academic Press, Amsterdam [etc.], 4, p.676.
- Hanson, H. & Lindh, G., 1993.** Coastal erosion: An escalating environmental threat. *Ambio*, pp.188-195.
- Harrison, T., Hohls, D., Meara, T., & Webster, M., 2001.** South African Estuaries: Catchment Land-Cover National Summary Report (Prepared for Department of Environmental Affairs & Tourism).
- Harvey, N., Gross, A., Jose, F., Savarese, M., & Missimer, T. M., 2021.** Geomorphological impact of Hurricane Irma on Marco Island, Southwest Florida. *Natural Hazards*, 106(1), 1-17.
- Haughton, S., 1928.** The geology of the country between Grahamstown and Port Elizabeth. Explanation of Cape Sheet 9 (Port Elizabeth), Geological Survey of South Africa, 50p.
- Hicks, D. M., & Inman, D. L., 1987.** Sand dispersion from an ephemeral river delta on the Central California coast. *Mar. Geol.* 77, 305–318. doi: 10.1016/0025-3227(87)90119-8.
- Hill, R., 1972.** The geology of the northern Algoa Basin, Port Elizabeth. Unpublished MSc. thesis, University of Stellenbosch, 62p.
- Hodel, K.L., Reimnitz, E., & Barnes, P.W., 1988.** Microtextures of quartz grains from modern terrestrial and subaqueous environments, North Slope of Alaska. *Journal of Sedimentary Research*, 58(1), 24-32.
- Holzforster, F., 2007.** Alluvial Fan system in the Late Mesozoic Oudtshoorn Basin and their implications for basin development. *Beringeria*, 37, 81-93.
- Horton, B.P., Peltier, W.R., Culver, S.J., Drummond, R., Engelhart, S.E., Kemp, A.C., Mallinson, D., Thieler, E.R., Riggs, S.R., Ames, D.V. and Thomson, K.H., 2009.** Holocene sea-level changes along the North Carolina Coastline and their implications for glacial isostatic adjustment models. *Quaternary Science Reviews*, 28(17-18), pp.1725-1736.

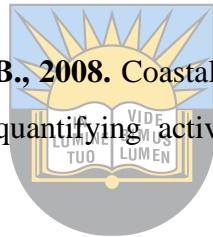
- Ingersoll, R.V., 1990.** Actualistic sandstone petrofacies: Discriminating modern and ancient source rocks. *Geology*, 18, 733-736.
- IPCC, 2013: Climate Change 2013: The Physical Science Basis.** Contribution of Working Group I to the Fifth Assessment Report of the Intergovernmental Panel on Climate Change [Stocker, T.F., D. Qin, G.-K. Plattner, M. Tignor, S.K. Allen, J. Boschung, A. Nauels, Y. Xia, V. Bex and P.M. Midgley (eds.)]. Cambridge University Press, Cambridge, United Kingdom and New York, NY, USA, 1535 pp
- Islam, T. & Ryan, J., 2015.** Hazard mitigation in emergency management. Butterworth-Heinemann.
- Jacobs, E., 1992.** Lithostratigraphy of the Knysna Formation. South African Committee for Stratigraphy Lithostratigraphic Series 17, Government Printer, Pretoria.
- Jew, A.D., Druhan, J.L., Ihme, M., Kovscek, A.R., Battiato, I., Kaszuba, J.P., Bargar, J.R., & Brown Jr, G.E., 2022.** Chemical and reactive transport processes associated with hydraulic fracturing of unconventional oil/gas shales. *Chemical reviews*, 122(9), pp.9198-9263.
- Jin, D., Hoagland, P., Au, K.D., Qiu, J., 2015.** Shoreline change, seawalls, and coastal property values. *Ocean. Coast. Manage* 114, 185-193.
- John, E. J., 1984.** Study of Coastal Erosion and Planning and Design of Related Defence Works on the West Coast of India. Ph. D. Thesis submitted to Mysore University. Department of Applied Mechanics and Hydraulics, KREC Surathkal, pp.330.
- Johnson, M., 1994.** Thin section grain size analysis revisited. *Sedimentology*, 41, 985-999.
- Johnson, M., 1994.** Uitenhage In: Johnson, M.R (Ed.). *Lericon of South African Stratigraphy. Part 1: Phanerozoic Units*, South African Committee for Stratigraphy. Council for Geosciences, South Africa, 42pp.
- Johnson, M.R., 1976.** Stratigraphy and sedimentology of the Cape and Karoo sequences in the Eastern Cape Province. PhD thesis, Rhodes University, Grahamstown, xiv-335.
- Jordan, T.H., & Grotzinger, J.P., 2012.** *The Essential Earth* (2nd ed.). New York: W.H. Freeman. ISBN 9781429255240. OCLC 798410008.

- Joubert, P., & Johnson, M., 1998.** Abridged lexicon of South Africa stratigraphy. South African Committee for Stratigraphy (SACS), Council for Geoscience, Pretoria, 160p.
- Kanori, Y., 1980.** Surface textures of quartz grains from fault gouges (Pt. II). Formational age and fracturing mode. Repts. of the Central Electricity Board, Res. Rept, 381007, 1-35.
- Katemaunzanga, D., & Gunter, C., 2009.** Lithostratigraphy, sedimentology and provenance of the Balfour Formation, Beaufort Group in the Fort Beaufort Alice area, Eastern Cape Province, South Africa. *Acta Geologica Sinica (English Edition)*, 83(5), 902-916.
- Kitchin, F.L., 1908.** The invertebrate fauna and palaeontological relationships of the Uitenhage Series. *Annals of the South African Museum* 7(2):21-250, pls. 2-11.
- Komar P.D., 1998.** Beach processes and sedimentation. New Jersey: Prentice-Hall.
- Koutsoukus, E., 2005.** Stratigraphy: Evolution of the Concept. In: E.A.M. Koutsoukus (ed.), applied stratigraphy, 3-19, Springer.
- Krinsley, D. H., & Doornkamp, J.C., 2011.** Atlas of quartz sand surface textures. Cambridge University Press.
- Krumbein, W., & Pettijohn, F., 1938.** Manual of sedimentary petrography. Appleton Century-Crofts, Inc., New York, 230-233.
- Krumbein, W., 1934.** Size frequency distribution of sediments. *Journal of Sedimentary Research*, 4(2), 65-77.
- Kuenzi, W. D., Horst, O. H., & McGehee, R. V., 1979.** Effect of volcanic activity on fluvial-deltaic sedimentation in a modern arc-trench gap, southwestern Guatemala. *Geol. Soc. Am. Bull.* 90, 827–838.
- Kuriqi, A., Pinheiro, A. N., Sordo-Ward, A., & Garrote, L., 2019.** Flow regime aspects in determining environmental flows and maximising energy production at run-of-river hydropower plants. *Applied Energy*, 256, 113980.
- Łabuz, T.A., 2012.** Coastal response to climatic changes: Discussion with emphasis on southern Baltic Sea. *Landform Analysis* 21:43-55

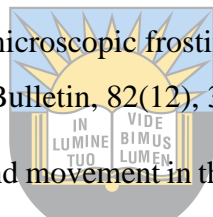


University of Fort Hare
Together in Excellence

- Laïbi, R.A., Anthony, E.J., Almar, R., Castelle, B., Sénéchal, N, Kestenare., E., 2014.** Longshore drift cell development on the human-impacted Bight of Benin sand barrier coast, West Africa. *J Coast Res* 70(SI): 78–83.
- Leng, Y.B., Huang, J.T., & Wang, R., 2005.** Theon-line acoustic sediment concentration instrument developed for model Yellow River. In *Proceedings of the 2nd international Yellow River Forum on keeping healthy life of the river*, 36-39.
- Lian-You, L., Shang-Yu, G., Pei- Jun, S., Xiao-Yan, L., & Zhi-Bao, D., 2003.** Wind tunnel measurements of adobe abrasion by blown sand: profile characteristics in relation to wind velocity and sand flux, *Journal of Arid Environments* 53(3), 351-363
- Lima, M., Coelho, C., Veloso-Gomes, F., & Roebeling, P., 2020.** An integrated physical and cost-benefit approach to assess groins as a coastal erosion mitigation strategy. *Coastal Engineering*, 156, 103614.
- Limber, P. W., Patsch, K. B., & Griggs, G. B., 2008.** Coastal sediment budgets and the littoral cutoff diameter: a grain size threshold for quantifying active sediment inputs. *Journal of Coastal Research*, (24 (10024)), 122-133.
- Liu, G., Cai, F., Qi, H., Zhu, J., Lei, G., Cao, H., & Zheng, J., 2019.** A method to nourished beach stability assessment: The case of China. *Ocean & Coastal Management*, 177, 166-178.
- Liu, K., & Greyling, E.H., 1996.** Grain-size distribution and cementation of the Cretaceous Mzamba Formation of Eastern Cape, South Africa: a case study of a storm-influenced offshore sequence. *Sedimentary Geol.*, 107 (1), 83-98.
- Lock, B., Shone, R., Coates, A., & Hatton, C., 1975.** Mesozoic Network-Type sedimentary basins within the Cape Fold Belt of South Africa. *Proceedings of the 9th International Congress of Sedimentology, Nice*, 2, pp. 217-225.
- Lucchi, F.R., & Casa, G.D., 1968.** Surface textures of desert quartz grains. A new attempt to explain the origin of desert frosting. *Giornale di Geologia*,(2), 36, 751-776.
- Madhavaraju, J.M., Lee, Y.I., Armstrong-Altrin, J.S., & Hussain, S.M., 2006.** Microtextures on detrital quartz grains of upper MaastrichtianDanian rocks of the Cauvery Basin, southeastern India: implications for provenance and depositional history. *Geosci J* 10:23–34.

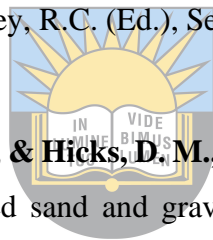


- Mahaney, W.C., 1995.** Glacial crushing, weathering and diagenetic histories of quartz grains inferred from scanning electron microscopy. *Glacial environments*, 1, 487-506.
- Maity, S.K., & Maiti, R., 2016.** Understanding the sediment sources from mineral composition at the lower reach of Rupnarayan River, West Bengal, India—XRD-based analysis. *GeoResJ*, 9, 91-103.
- Mangor, K., Drønen, N. K., Kærgaard, K. H., & Kristensen, S. E., 2004.** Shoreline management guidelines.
- Maree, B., 2000.** Structure and status of the intertidal wetlands of the Knysna Estuary. In: *The Knysna Basin Project 1995- 1998* (eds) Hodgson AN, Allanson BR. *Transaction of the Royal Society of South Africa* 55: 1-237.
- Margolis, S., & Kennett, J.P., 1971.** Cenozoic paleoglacial history of Antarctica recorded in Sub-antarctic deep-sea cores: *American Journal of Science*, 271: 1–36.
- Margolis, S.V., & Krinsley, D.H., 1971.** Submicroscopic frosting on eolian and subaqueous quartz sand grains. *Geological Society of America Bulletin*, 82(12), 3395-3406.
- Marker, M., 2000.** A descriptive account of sand movement in the Knysna Estuary. In: *The Knysna Basin Project 1995- 1998* (eds) Hodgson AN, Allanson BR. *Transaction of the Royal Society of South Africa* 55: 1-237.
- Masselink, G., & Puleo, J.A., 2006.** Swash-zone morphodynamics. *Continental Shelf Research*, 26: 661–680.
- Masselink, G., Austin, M., Tinker, J., O’Hare, T., & Russell, P., 2008.** Cross-shore sediment transport and morphological response on a macrotidal beach with intertidal bar morphology, Truc Vert, France. *Mar. Geol.* 251, 141–155. doi: 10.1016/j.margeo.2008.01.010.
- McGlinchey, D., 2005.** *Characterisation of bulk solids*. CRC Press, 231.
- McIvor, I., Youjun, H., Daoping, L., Eyles, G. & Pu, Z., 2017.** *Agroforestry: conservation trees and erosion prevention*.
- McLachlan, I., & McMillan, I., 1979.** Microfaunal biostratigraphy, chronostratigraphy and history of Mesozoic and Cenozoic deposits on the coastal margin of South Africa. *Geological Society of South Africa Special Publication*, 6, 161–181.

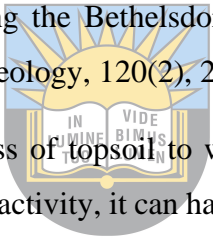


University of Fort Hare
Together in Excellence

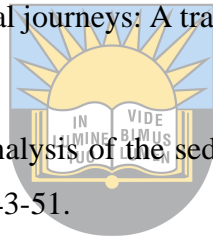
- McLachlan, I.R., & McMillan, I.K., 1976.** Review and stratigraphic significance of southern Cape Mesozoic palaeontology. *Transaction of the Geological Society of South Africa* 79, 197-212.
- McLaren, P., & Bowles, D., 1985.** The effects of sediment transport on grain size distributions. *Journal of Sedimentary Research*, 55-64.
- McMillan, I. K., 2010.** The foraminifera of the Portlandian (late Jurassic) Bethelsdorp Formation of the onshore Algoa Basin, Eastern Cape province: Their stratigraphic position compared with other early graben infill successions of the South African continental margin. *Les Rosalines*.
- McMillan, I.K., 2003.** The Foraminifera of the Late Valanginian to Hauterivian (Early Cretaceous) Sundays River Formation of the Algoa Basin, Eastern Cape Province, South Africa. *Annals of the South Africa Museum* 106, 1-274.
- McMillan, I.K., Brink, G.I., Broad, D.S. & Maier, J.J., 1997.** Late Mesozoic sedimentary basins off the south coast of South Africa. In: Selley, R.C. (Ed.), *Sedimentary basins of the World*, Elsevier, 3, pp. 319–376.
- Measures, R. J., Hart, D. E., Cochrane, T. A., & Hicks, D. M., 2020.** Processes controlling river-mouth lagoon dynamics on high-energy mixed sand and gravel coasts. *Mar. Geol.* 420:106082. doi: 10.1016/j.margeo.2019.106082.
- Milliman, J. D., & Farnsworth, K. L., 2013.** *River discharge to the coastal ocean: a global synthesis*. Cambridge University Press.
- Milliman, J. D., & Syvitski, J. P., 1992.** Geomorphic/tectonic control of sediment discharge to the ocean: the importance of small mountainous rivers. *The Journal of Geology*, 100(5), 525-544.
- Moiola, R.J., Weiser, D., 1968.** Textural parameters: an evaluation. *Journal of Sedimentary Petrology*, 38, 45-53.
- Montgomery, C., 2010.** *Environmental geology* (9th ed.). McGraw-Hill.
- Moore, D.M. & Reynolds, R.C. Jr., 1997.** *X-ray Diffraction and the Identification and Analysis of Clay Minerals*, 2nd Edition. Oxford University Press, New York, 378 pp.
- Movahedan, M., Abbasi, N. & Keramati, M., 2012.** Wind erosion control of soils using polymeric materials. *Eurasian Journal of Soil Science*, 1(2), pp.81-86.



University of Fort Hare
Together in Excellence

- Muir, R., 2018.** Recalibrating the breakup history of SW Gondwana: The first U-Pb chronostratigraphy for the Uitenhage Group, South Africa. PhD. Thesis. University of Cape Town.
- Muir, R.A., Bordy, E.M., & Prevec, R., 2015.** Lower Cretaceous deposit reveals first evidence of a postwildfire debris flow in the Kirkwood Formation, Algoa Basin, Eastern Cape, South Africa. *Cretaceous Research*, 56, 161–179.
- Muir, R., Bordy, E., Reddering, J., & Viljoen, J., 2017a.** Lithostratigraphy of the Enon Formation (Uitenhage Group), South Africa. *South Africa Journal of Geology* 2017., 120(2), 273-280.
- Muir, R.A., Bordy, E.M., Reddering, J.S.V., & Viljoen, J.H.A., 2017b.** Lithostratigraphy of the Enon Formation (Uitenhage Group), South Africa. *South African Journal of Geology*, 120.2, 273-280. doi:10.2113/gssajg.120.273.
- Muir, R.A., Bordy, E.M., Reddering, J.S.V., Viljoen, J.H.A., 2017b.** Lithostratigraphy of the Enon Formation (Uitenhage Group), including the Bethelsdorp, Colchester and Swartkops member, South Africa. *South Africa Journal of Geology*, 120(2), 281-293.
- Mulvihill, K., 2021.** Soil erosion 101. The loss of topsoil to wind, rain, and other forces is a natural process, but when intensified by human activity, it can have negative environmental, societal, and economic impact.
- 
 University of Fort Hare
Together in Excellence
- Neal, W. J., Pilkey, O. H., Cooper, J. A. G., & Longo, N. J., 2018.** Why coastal regulations fail. *Ocean & coastal management*, 156, 21-34.
- Nelson, S., 2015.** Geologic Time. *Physical Geology*. Tulane University. 1-16.
- Nelson, S., 2015.** Sediment and Sedimentary Rocks. *Physical Geology*. Tulane University. 1-10.
- Nichols, G., 2009.** *Sedimentology and stratigraphy*, 2nd ed., John Wiley & Sons Ltd, Chichester, West Sussex, United Kingdom, 419.
- Nienhuis, J. H., Ashton, A. D., & Giosan, L., 2015.** What makes a delta wave-dominated? *Geology* 43, 511–514. doi: 10.1130/G36518.1.
- Nienhuis, J. H., Ashton, A. D., Edmonds, D. A., Hoitink, A. J. F., Kettner, A. J., Rowland, J. C., & Törnqvist, T. E., 2020.** Global-scale human impact on delta morphology has led to net land area gain. *Nature*, 577(7791), 514-518.

- Nienhuis, J. H., Ashton, A. D., Nardin, W., Fagherazzi, S., & Giosan, L., 2016.** Alongshore sediment bypassing as a control on river mouth morphodynamics. *J. Geophys. Res. Earth Surf.* 121, 664–683. doi: 10.1002/2015JF003780.
- Niu, X., Yan, D., Zhuang, X., Liu, Z., Li, B., Wei, X., Xu, H., & Li, D., 2018.** Origin of quartz in the lower Cambrian Niutitang Formation in south Hubei Province, upper Yangtze platform. *Marine and Petroleum Geology*, 96, pp.271-287.
- Niya, A.K., Alesheikh, A.A., Soltanpor, M. & Kheirkhahzarkesh, M.M., 2013.** Shoreline change mapping using remote sensing and GIS. *International Journal of Remote Sensing Applications*, 3(3), pp.102-107.
- Nordstrom, J. M., 2004.** The influence of thermal stability and angle of incidence on the acceleration of up a slope. *Journal of wind engineering and industrial aerodynamics*, 15, 231-242.
- Norman, N., & Whitfield, G., 2006.** Geological journeys: A traveller's guide to South Africa's rocks and landforms. Struik.
- Okeyode, I., & Jibiri, N., 2013.** Grain size analysis of the sediments from Ogun River, south western Nigeria. *Earth Science Research*. 2(1): 43-51.
- Okrusch, M., & Frimmel, H.E., 2020.** Sediments and sedimentary rocks. In *Mineralogy* (pp. 417-452). Springer, Berlin, Heidelberg.
- Ortiz, A. C., & Ashton, A. D., 2016.** Exploring shoreface dynamics and a mechanistic explanation for a morphodynamic depth of closure. *J. Geophys. Res. Earth Surf.* 121, 442–464. doi: 10.1002/2015JF003699.
- Otunola, B., & Liu, K., 2019.** Granulometric and depositional characteristics of sandstones from Knysna and Robberg Formations, South Africa. *Journal of Engineering and Applied Sciences*, 14(1), 114-123.
- Pak, A., & Majd, F., 2011.** Integrated coastal management plan in free trade zones, a case study. *Ocean & coastal management*, 54(2), 129-136.



University of Fort Hare
Together in Excellence

- Parthasarathy, P., Ramesh, G., Ramasamy, S., Arumugam, T., Govindaraj, P., Narayanan, S., & Jeyabal, G., 2016.** Sediment dynamics and depositional environment of Coleroon river sediments, Tamil Nadu, Southeast coast of India. *Journal of Coastal Sciences*, 3, 1-7.
- Passega, R., 1964.** Grain size representation by C-M pattern as a geological tool. *Journal of Sedimentary Petrology*, 34, 830-847.
- Pedrerros, R., Howa, H.L., & Michel, D., 1996.** Application of grain size trend analysis for the determination of sediment transport pathways in intertidal areas. *Marine geology*, 135: 35-49.
- Pettijohn, F., & Potter, P., 1964.** Atlas and glossary of primary sedimentary structures: Springer-Verlag, Berlin-Gottingen, Heidelberg, 370.
- Phillips, C., Hales, T., Smith, H., & Basher, L., 2021.** Shallow landslides and vegetation at the catchment scale: A perspective. *Ecological Engineering*, 173, 106436.
- Phillips, J., 1927.** Fossil *Widdringtonia* in lignite of the Knysna Series, with a note on fossil leaves of several other species. *South African Journal of Science*, 24, 188-197.
- Pilkey, O.H., & Cooper, A.G., 2014.** *The Last Beach*. Duke University Press, Durham. Donnelly, J.P., Cleary, P., Newby, P., Ettinger, R., 2004. Coupling instrumental and geological records of sea-level change: evidence from southern new England of an increase in the rate of sea-level rise in the late 19th century. *Geophys. Res. Lett.* 31, 234-350.
- Pratellesi, M., Ciavola, P., Ivaldi, R., Anthony, E. J., & Armaroli, C., 2018.** River-mouth geomorphological changes over > 130 years (1882–2014) in a small Mediterranean delta: Is the Magra delta reverting to an estuary?. *Marine Geology*, 403, 215-224.
- Pye, K., & Croft, D., 2007.** Forensic analysis of soil and sediment traces by scanning electron microscopy and energy-dispersive X-ray analysis: An experimental investigation. *Forensic Science International*, 165(1), 52-63.
- Rangel-Buitrago, N., & Posada, P., 2005.** Geomorphology and erosive processes in the north coast of Cordoba department, colombian caribbean (sector Paso Nuevocristo rey). *Bol. Invest. Mar. Cost.* 34, 101-119

- Rangel-Buitrago, N., Anfuso, G., & Williams, A.T., 2015b.** Coastal erosion along the Caribbean coast of Colombia: magnitudes, causes and management. *Ocean. Coast. Manage* 114, 129-144.
- Rangel-Buitrago, N., Anfuso, G., Ergin, A., & Williams, A.T., 2015a.** Assessing and Managing the Coastal Scenery. *Blue Solutions from Latin America and the Wider Caribbean*. GTZ, Berlin.
- Rangel-Buitrago, N., Stancheva, M., & Anfuso, G., 2011.** Effects of coastal armouring in the bolivar department (caribbean sea of Colombia). *Probl. Geo.* 1-2, 97-106.
- Rashedi, S., & Siad, A., 2016.** Grain size Analysis and Depositional Environment for Beach sediments along Abu Dhabi Coast, United Arab Emirates. *International Journal of Scientific & Technology Research*, 5, 106-115.
- Reddering, J. S. V., 2000.** Sedimentary facies, sequences and depositional environments of the Mesozoic Robberg formation in its type area, South Africa (Vol. 126). Council for Geoscience.
- Reddering, J. S., & Esterhuysen, K., 1987.** Prediction of the effects of reduced river discharge on the estuaries of the south-eastern Cape Province, South Africa. *South African Journal Science*, 84, 726-730.
- Reddering, J., & Esterhuisen, K., 1987.** Sediment dispersal in the Knysna estuary: environmental management considerations. *South African Journal of Geology*, 90(4), 448-457.
- Reddering, J., & Esterhuizen, K., 1984.** Sedimentation of the Knysna estuary. ROSIE Report No. 9. Univ of Port Elizabeth, Dept. of Geology. 79 pp.
- Reddering, J., & Rust, I., 1997.** Fluvial sedimentology. Paper delivered at the 6th International conference - Sedimentology of the Keurbooms Estuary and the Robberg formation, Plettenberg Bay. University of Cape Town, Cape Town.
- Reddering, J., 1994.** Supply of land-derived sediment and its dispersal in the Knysna Estuary: an environmental appraisal. Council for Geoscience, Geological Survey Report No: 1994-0024. Pretoria 62pp.
- Reddering, J.S.V., 1999.** The effects of proposed municipal water extraction from rivers in the Plettenberg Bay area on their estuarine sediment dynamics. Appendix A-3: Estuarine

Sedimentation. In: Plettenberg Bay Coastal Catchments Study. Second Phase. Keurbooms River Estuary. (M. Luger, & N. Shand., Eds.) DWAF Report No. PK 000/00/1699.

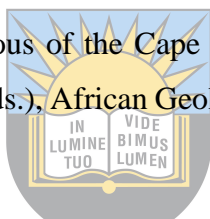
Reddering, J.S.V; Esterhuisen, K., 1983. Management proposals to counter undesirable sediment accumulation in the Keurbooms Estuary. *Trans.geol.soc. S.Afr*, 86, 87-91.

Reineck, H.E., & Wunderlich, F., 1968. Classification and origin of flaser and lenticular bedding. *Sedimentology*, 11(1-2), 99-104.

Reynolds, R.C., 1989. Principles and techniques of quantitative analysis of clay minerals by X-ray powder diffraction. Pp. 4-36 in: *Quantitative Mineral Analysis of Clays* (D.R. Pevear and EA. Mumpton, editors). CMS Workshop Lectures, 1. The Clay Minerals Society, Bloomington, Indiana.

Richard, C.S., 2000. *Applied sedimentology* (2nd Ed.). Academic Press, San Diego, 523.

Rigassi, D.A., & Dixon, G.E., 1972. Cretaceous of the Cape Province, Republic of South Africa. In: Dessauvage, T.F.J., Whiteman, A.J. (Eds.), *African Geology*. Geology Department, University of Ibadan, Nigeria, pp. 513-527.



Robert, A.M., Emese, M.B., & Rose, P., 2015. Lower Cretaceous deposit reveals first evidence of a post-wildfire debris flow in the Kirkwood Formation, Algoa Basin, Eastern Cape, South Africa. *Cretaceous Research*, 56, p. 161-179.

Roosenboom, A., 1978. Sedimentafvoer in Suider-Afrikaanse Riviere. *Water SA*, 4(1), 14-17.

Ross, C.S., & Kerr, P.F., 1931. The clay minerals and their identity. *Journal of Sedimentary Research*, 1(1), 55-65.

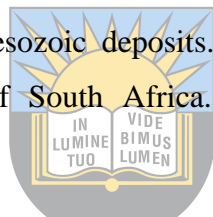
Sallenger Jr, A. H., 2011. Hurricanes, sea level rise, and coastal change. In *The Proceedings of the Coastal Sediments 2011: In 3 Volumes* (pp. 15-28).

Sallenger, A. H., Stockdon, H. F., Fauver, L., Hansen, M., Thompson, D., Wright, C. W., & Lillycrop, J., 2006. Hurricanes 2004: An overview of their characteristics and coastal change. *Estuaries and Coasts*, 29(6), 880-888.

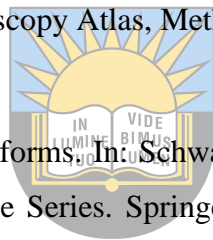
Selley, R., 1988. *Applied Sedimentology*. London: Academic Press, xii-466.

Selley, R.C., 2000. *Applied Sedimentology* (2nd Ed.). San Diego: Academic Press, 523.

- Serra, O., 2008.** Well Logging Handbook. Editions TECHNIP Publisher. Doctorate Degree in Geology: ENSPM Engineer. Paris, France.
- Shin, E.C., Kim, S.H., Hakam, A. and Istijono, B., 2019.** Erosion problems of shore line and counter measurement by various geomaterials. In MATEC Web of Conferences (Vol. 265, p. 01010). EDP Sciences.
- Shone, R., 1976.** The sedimentology of the Mesozoic Algoa Basin. Unpublished MSc. thesis, University of Port Elizabeth, 48p.
- Shone, R.W., 1976.** The sedimentology of the Mesozoic Algoa Basin. M.Sc. thesis. University of Port Elizabeth (Unpublished).
- Shone, R.W., 1978.** A case for lateral gradation between the Kirkwood and Sundays River formations, Algoa Basin. Transactions of the Geological Society of South Africa, 81, 319–326.
- Shone, R.W., 2006.** Onshore post-Karoo Mesozoic deposits. In: Johnson, M.R., Anhaeusser, C.R., Thomas, R.J. (Eds.), The geology of South Africa. Geological Society of South Africa, Marshalltown, pp. 541-552.
- Simms, A.R., Anderson, J.B., & Blume, M., 2006.** Barrier- island aggradation via inlet migration: Mustang Island, Texas: Sedimentary Geology, 187:105-125.
- Skaggs, L.L. & McDonald, F.L., 1991.** National Economic Development Procedures Manual. Coastal Storm Damage and Erosion. ARMY ENGINEER INST FOR WATER RESOURCES ALEXANDRIA VA.
- Skoog, D.A., Holler, F.J., & Crouch, S.R., 2007.** Principles of Instrumental Analysis. Sixth Edition, Thomson Brooks/Cole, USA.
- Snyder, R.L., & Bish, D.L., 1989.** Quantitative analysis. Pp. 101-144 in: Modern Powder Diffraction (D.L. Bish & J.E. Post, editors). Reviews in Mineralogy, 20, Mineralogical Society of America, Washington, USA, 101-144.
- Sowmya, K., Sri, M.D., Bhaskar, A.S., & Jayappa, K.S., 2019.** Long-term coastal erosion assessment along the coast of Karnataka, west coast of India. International Journal of Sediment Research, 34(4), 335-344.



- Spath, L.F., 1930.** On the Cephalopoda of the Uitenhage beds. *Annals of the South African Museum* 28(2):131-157, pls. 13-15, 1 text fig.
- Srivastava, A.K., & Mankar, R.S., 2009.** Grain Size Analysis and Depositional Pattern of Upper Gondwana Sediments (Early Cretaceous) of Salbardi Area, Districts Amravati, Maharashtra and Betul, Madhya Pradesh. *Journal Geological Society of India*, 73, 393-406.
- Srivastava, A.K., Ingle, P.S., Lunge, H.S., & Khare, N., 2012.** Grain-size characteristics of deposits derived from different glacial environments of the Schirmacher Oasis, East Antarctica. *Geologos*, 18(4), 251-266.
- Srivastava, A.K., Khare, N., & Ingle, P.S., 2010.** Textural characteristics, distribution pattern and provenance of heavy minerals in glacial sediments of Schirmacher Oasis, East Antarctica. *Journal of the Geological Society of India*, 75, 393-402.
- Steinmetz, R., 1984.** Scanning Electron Microscopy Atlas, Method in Exploration series: The American Association of Petroleum Geologists.
- Stephenson W., & Kirk R., 2005.** Shore Platforms. In: Schwartz M.L. (eds) *Encyclopedia of Coastal Science*. Encyclopedia of Earth Science Series. Springer, Dordrecht. https://doi.org/10.1007/1-4020-3880-1_288.
- Stewart, H.B., 1958.** Sedimentary reflection on depositional environment, in San Miguel lagoon, Baja California, Mexico, *AAPG Bull.*, 42, 2567-2618.
- Su, N., Song, F., Qiu, L., & Zhang, W., 2021.** Diagenetic evolution and densification mechanism of the Upper Paleozoic tight sandstones in the Ordos Basin, Northern China. *Journal of Asian Earth Sciences*, 205, p.104613.
- Subba Rao, M., 2002.** Study of Coastal Erosion along Karnataka Coast. *ISH Journal of Hydraulic Engineering*, 8(2), 23-33. doi:10.1080/09715010.2002.10514713
- Subrahmanya, K. R., & Rao, B. R. J., 1991.** Marine geological aspects of Dakshina Kannada coast: Perspective on Dakshina Kannada and Kodagu. *Mangalore University Decennial Volume*, Mangalore, 201-220.

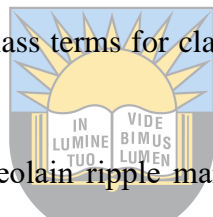


University of Fort Hare
Together in Excellence

- Sutherland, R.A., & Lee, C., 1994.** Discrimination between coastal sub-environments using textural characteristics. *Sedimentology*, 41, 1133-1145.
- Thior, M., Sané, T., Dièye., E-HB, Sy., O, Cissokho., D., Ba, B.D., Descroix, L., 2019.** Coastline dynamics of the northern lower Casamance (Senegal) and southern Gambia littoral from 1968 to 2017. *J Afr Earth Sci* 160:103611. <https://doi.org/10.1016/j.jafrearsci.2019.103611>.
- Trask, P., 1932.** *Origin and Environment of Source Sediments of Petroleum*. Gulf Publishing Company: Houston, 323.
- Udden, J., 1914.** Mechanical composition of clastic sediments. *Geological Society of America Bulletin*, 25, 655-744.
- UNESCO-IOC, 2012.** A Guide on adaptation options for local decisionmakers: guidance for decision making to cope with coastal changes in West Africa. <https://unesdoc.unesco.org/ark:/48223/pf0000216603>.
- Vallejo, P.P., Vasquez, L.F., Correa, I., Bernal, G., Alcantara-Carrio, J., & Palacio, B., 2016.** Impact of terrestrial mining and intensive agriculture in pollution of estuarine surface sediments: spatial distribution of trace metals in the Gulf of Uraba. *Colomb. Pull. Bull.* 111 (1-2), 311-320.
- Van der Linde, C., 2007.** Sediment supply processes and patterns in the Enon Formation, Gamtoos Basin, Eastern Cape, South Africa. Unpublished MSc. thesis, University of Cape Town, 82p.
- Van der Merwe, I., 1998.** *The Knysna and Tsitsikamma forests. Their history, ecology and management.* Department of Water Affairs and Forestry, Pretoria, 152pp.
- Vestergaard, P., 1991.** Morphology and vegetation of a dune system in SE Denmark in relation to climate change and sea-level rise. *Landsc Ecol* 6:77-87
- Vilardy, S.P., Gonzalez, J.A., Martín-Lopez, B., & Montes, C., 2011.** Relationships between hydrological regime and ecosystem services supply in a Caribbean coastal wetland: a social-ecological approach. *Hydrol. Sci. J.* 56 (8), 1423-1435.
- Viljoen, J. H. A., 1992.** The stratigraphy of the Heidelberg/Riversdale Mesozoic Basin. In *Conference on inversion tectonics of the Cape Fold Belt* (pp. 77-84).



- Vitousek, S., Barnard, P. L., Fletcher, C. H., Frazer, N., Erikson, L., & Storlazzi, C. D., 2017.** Doubling of coastal flooding frequency within decades due to sea-level rise. *Scientific reports*, 7(1), 1-9.
- Von Breitenbach, F., 1974.** Southern Cape forests and trees. Government Printers, Pretoria. R.S.A, 328pp.
- Warrick, J. A., 2020.** Littoral sediment from rivers: Patterns, rates and processes of river mouth morphodynamics. *Frontiers in Earth Science*, 355.
- Warrick, J. A., Stevens, A. W., Miller, I. M., Harrison, S. R., Ritchie, A. C., & Gelfenbaum, G., 2019.** World's largest dam removal reverses coastal erosion. *Scientific reports*, 9(1), 1-12.
- Wei, Z., Dalrymple, R. A., Xu, M., Garnier, R., & Derakhti, M., 2017.** Short-crested waves in the surf zone. *J. Geophys. Res. Oceans* 122, 4143–4162. doi: 10.1002/2016JC012485.
- Wentworth, C., 1922.** A scale of grade and class terms for clastic sediments. *The Journal of Geology*, 30(5), 377-392.
- Willard, B., 1935.** An “antidune” phase of aeolian ripple marks. Topographic and Geologic Survey, Harrisburg, Pennsylvania. *Journal of Sedimentary Petrology*, 5: 133-136.
- Winter, H., 1973.** Geology of the Algoa Basin, South Africa. In: Blant, G. (Editor), *Sedimentary basins of the African coasts, Part 2, South and East Coast*. Association of African Geological Surveys, Paris, 17–48.
- Xu, J.X., 2002.** Implication of relationships among suspended sediment size, water discharge and suspended sediment concentration: the Yellow River basin, China. *Catena*, 49: 289-307.
- Zhou, X., Liu, D., Bu, H., Deng, L., Liu, H., Yuan, P., Du, P. & Song, H., 2018.** XRD-based quantitative analysis of clay minerals using reference intensity ratios, mineral intensity factors, Rietveld, and full pattern summation methods: A critical review. *Solid Earth Sciences*, 3(1), pp.16-29.
- Zwamborn, J., 1980.** Small-craft harbour and launching sites. Preliminary evaluation. Volume IV: South coast Groot Kei River to Cape Point, Part 1, Groot Kei to Knysna. CSIR Report No. T/SEA 8012, Stellenbosch.



Zwell, L., & Danko, A.W., 1975. Applications of X-ray diffraction methods to quantitative chemical analysis. *Applied Spectroscopy Reviews*, 9(1), 167-221.



University of Fort Hare
Together in Excellence

APPENDICES

APPENDIX A: GRAIN SIZE ANALYS

From sample P2-P9 are the river sediments from Plettenberg Bay (Keurbooms River), sample K2-K3 are also the river sediments from Knysna estuary, however, they are poorly and moderately sorted. Sample P15-P50 are the beach sediments from Plettenberg Bay and are well-sorted sediments.

A.1 Sample P2

Aliquot mass = 216.67g

Table A.1: Retained and cumulative percentage for Sample P2.

Sieve size (ϕ)	Mass retained (g)	% retained	Cumulative %
-1	3.4	1.57	1.57
0	3.34	1.54	3.11
1	10.4	4.8	7.91
2	88.89	41.05	48.96
3	107.5	49.64	98.6
4	2.32	1.07	99.67
5	0.7	0.32	99.99
Total mass	216.55		

Error = 0.06%

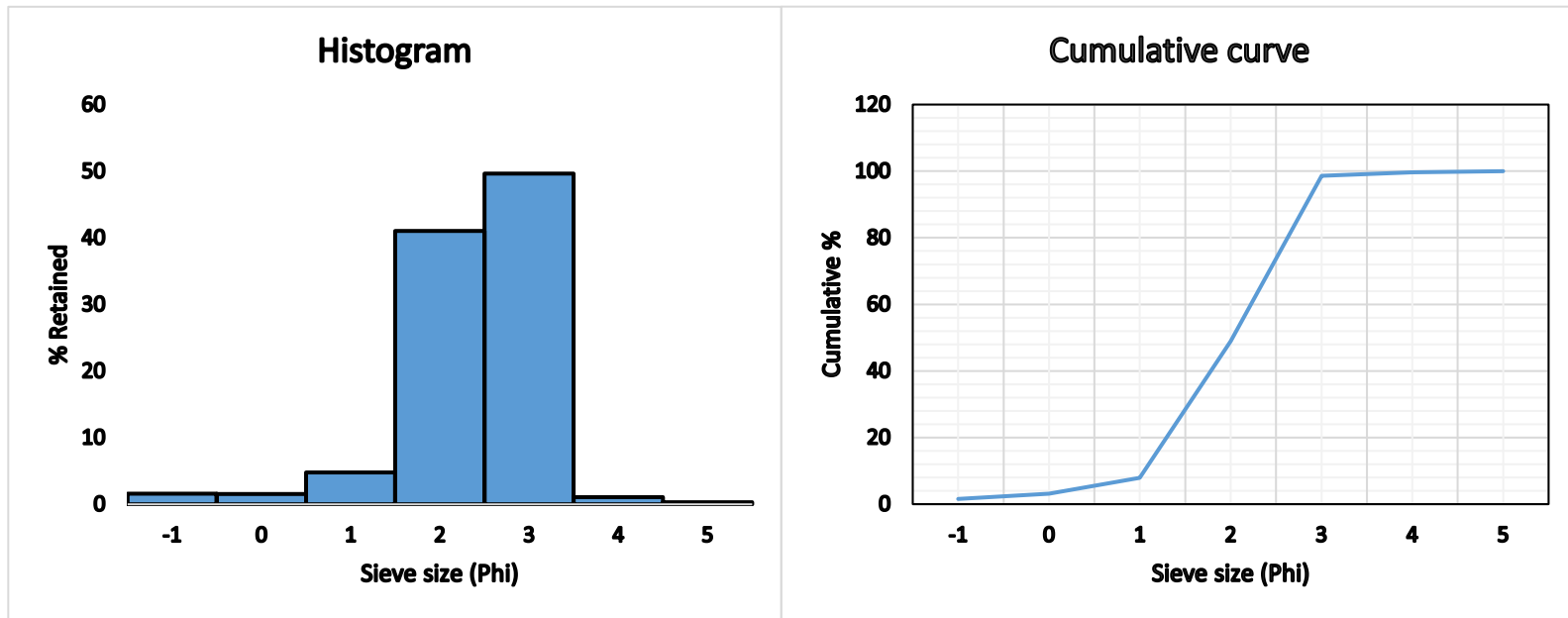


Figure A.1: Histogram (left) and cumulative curve (right) for P2.

The dominant sediment grain size range is 3 ϕ (0.125 mm), 2 ϕ (0.25mm), 1 ϕ followed by 0 ϕ and -1 ϕ in P2, and according to the Wentworth scale this grain size range fall into fine and medium sand class and therefore fine and medium sand is dominant in P2.

A.2 Sample P3

Aliquot mass = 236.65g

University of Fort Hare
Together in Excellence

Table A.2: Retained and cumulative percentage for Sample P3.

Sieve size (ϕ)	Mass retained (g)	% retained	Cumulative %
-1	0.08	0.03	0.03
0	0.58	0.25	0.28
1	7.99	3.39	3.67
2	110.03	46.45	50.12
3	16.4	49.35	99.47
4	0.73	0.31	99.78
5	0.06	0.03	99.81
Total mass	235.87		

Error = 0.33%

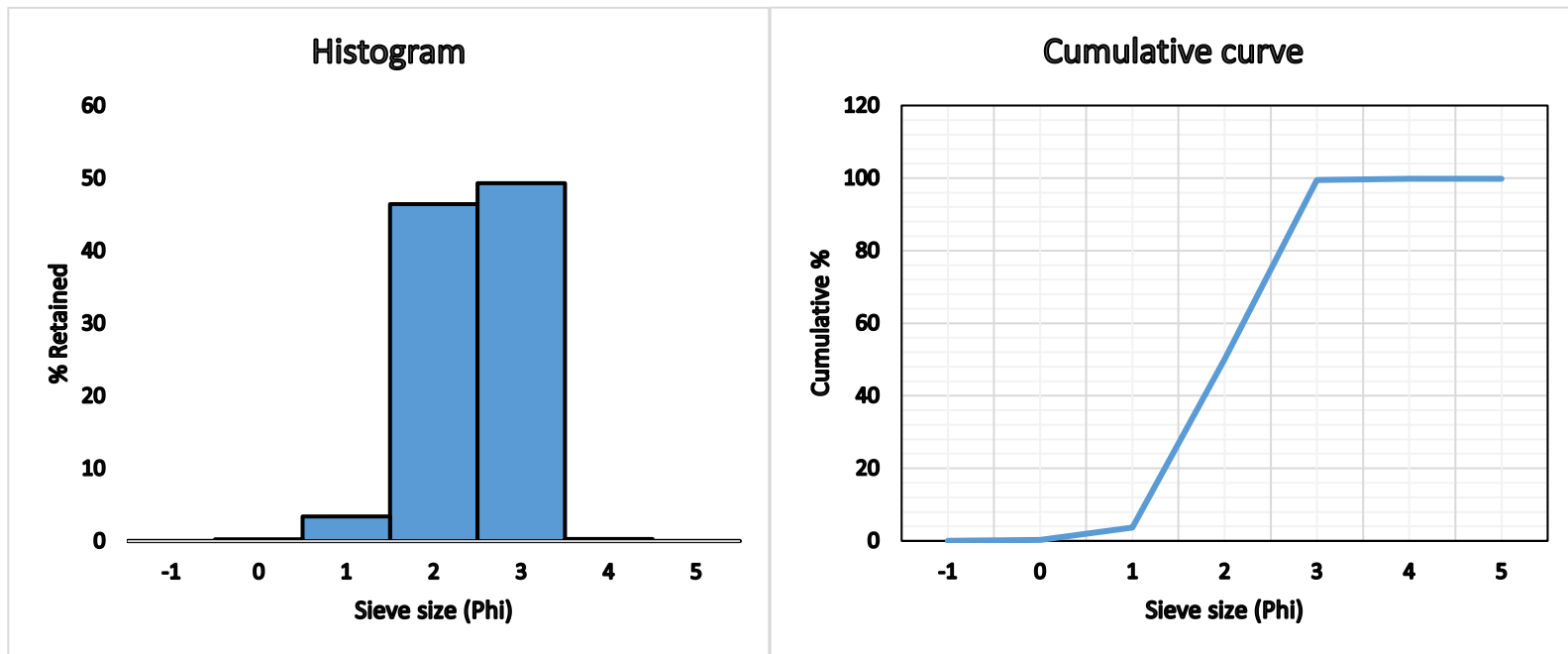


Figure A.2: Histogram (left) and cumulative curve (right) for Sample P3.

The dominant sediment grain size range is 3 ϕ (0.125 mm) and 2 ϕ (0.25mm) followed by 1 ϕ (0.5), and according to the Wentworth scale this grain size range fall into fine and medium sand class and therefore fine and medium sand is dominant in Sample P3, with some seashells.

University of Fort Hare
Together in Excellence

A.3 Sample P4

Aliquot mass = 255.01g

Table A.3: Retained and cumulative percentage for Sample P4.

Sieve size (ϕ)	Mass retained (g)	% retained	Cumulative %
-1	2.21	0.87	0.87
0	1.4	0.55	1.42
1	13.88	5.44	6.86
2	158.03	61.99	68.85
3	78.75	30.89	99.74
4	0.56	0.22	99.96
5	0.1	0.04	100
Total mass	254.93		

Error = 0.03%

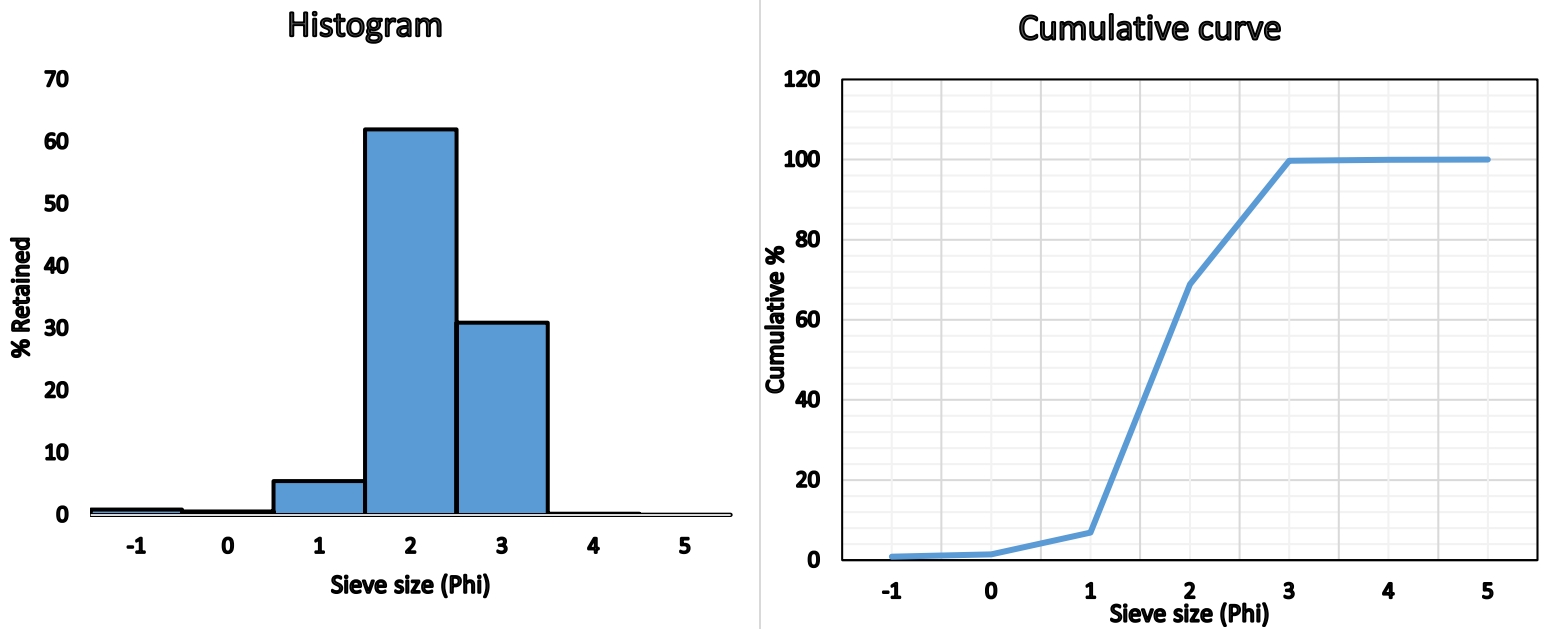


Figure A.3: Histogram (left) and cumulative curve (right) for Sample P4.

The dominant sediment grain size range is 2 ϕ (0.25mm) and 3 ϕ (0.125 mm) followed by a small percentage at 1 ϕ (0.5mm). According to the Wentworth scale this grain size range fall into medium sand and fine sand class is dominant in Sample P4, with minor coarser sands.

University of Fort Hare
Together in Excellence

A.4 Sample P6

Aliquot mass = 207.7g

Table A.4: Retained and cumulative percentage for Sample P6.

Sieve size (ϕ)	Mass retained (g)	% retained	Cumulative %
-1	17.02	8.22	8.22
0	10.92	5.28	13.5
1	8.24	3.98	17.48
2	29.59	14.3	31.78
3	124.27	60.05	91.83
4	6.21	3	94.83
5	10.71	5.17	100
Total mass	206.96		

Error = 0.36%

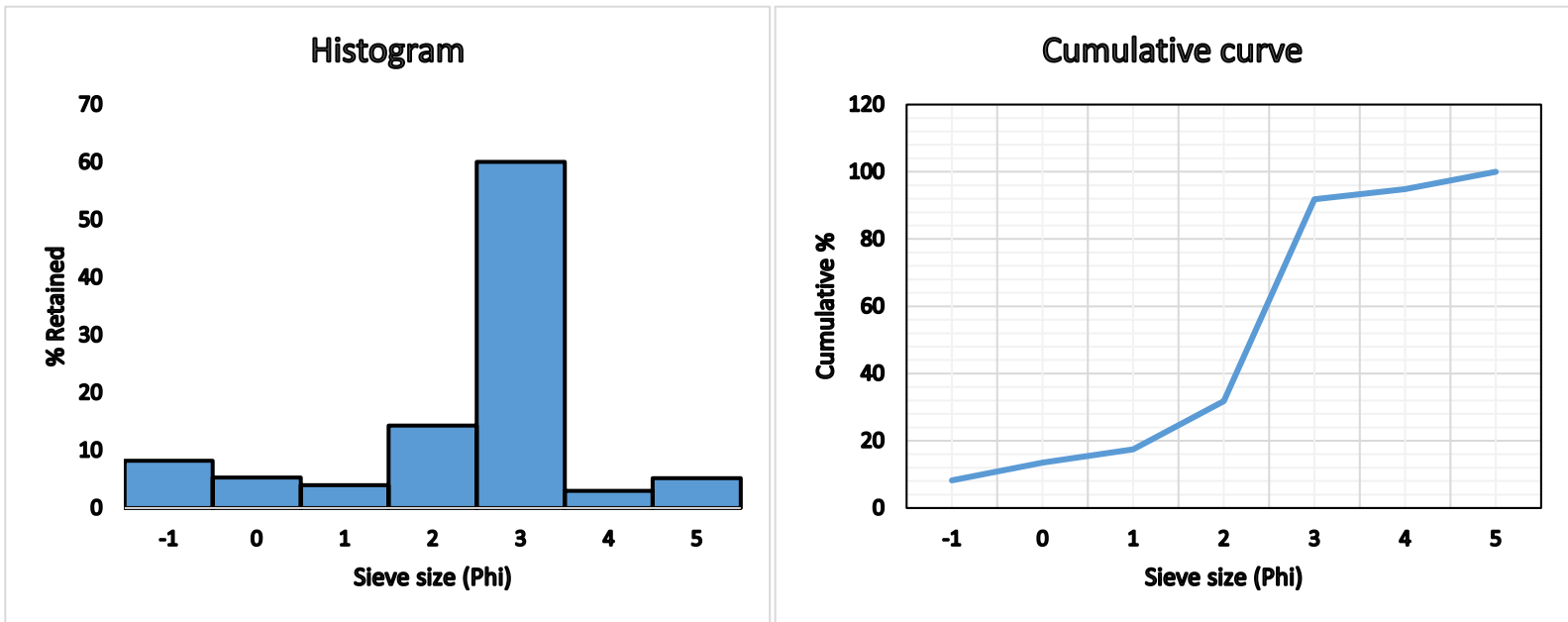


Figure A.4: Histogram (left) and cumulative curve (right) for Sample P6.

The dominant sediment grain size range is 3 ϕ (0.125 mm) followed by a considerable percentage of grain size range of 2 ϕ (0.25 mm) and scattered from very coarse sands to fine sands of wide range mixture. Actually there are coarse root and shell fragments in side.

A.5 Sample P9

Aliquot mass = 252.42g

University of Fort Hare
Together in Excellence

Table A.5: Retained and cumulative percentage for sample P9.

Sieve size (ϕ)	Mass retained (g)	% retained	Cumulative %
-1	23.92	9.49	9.49
0	13.13	5.21	14.7
1	10.8	4.29	18.99
2	57.04	22.64	41.63
3	127.72	50.69	92.32
4	5.77	2.29	94.61
5	13.56	5.38	99.99
Total mass	251.94		

Error = 0.19%

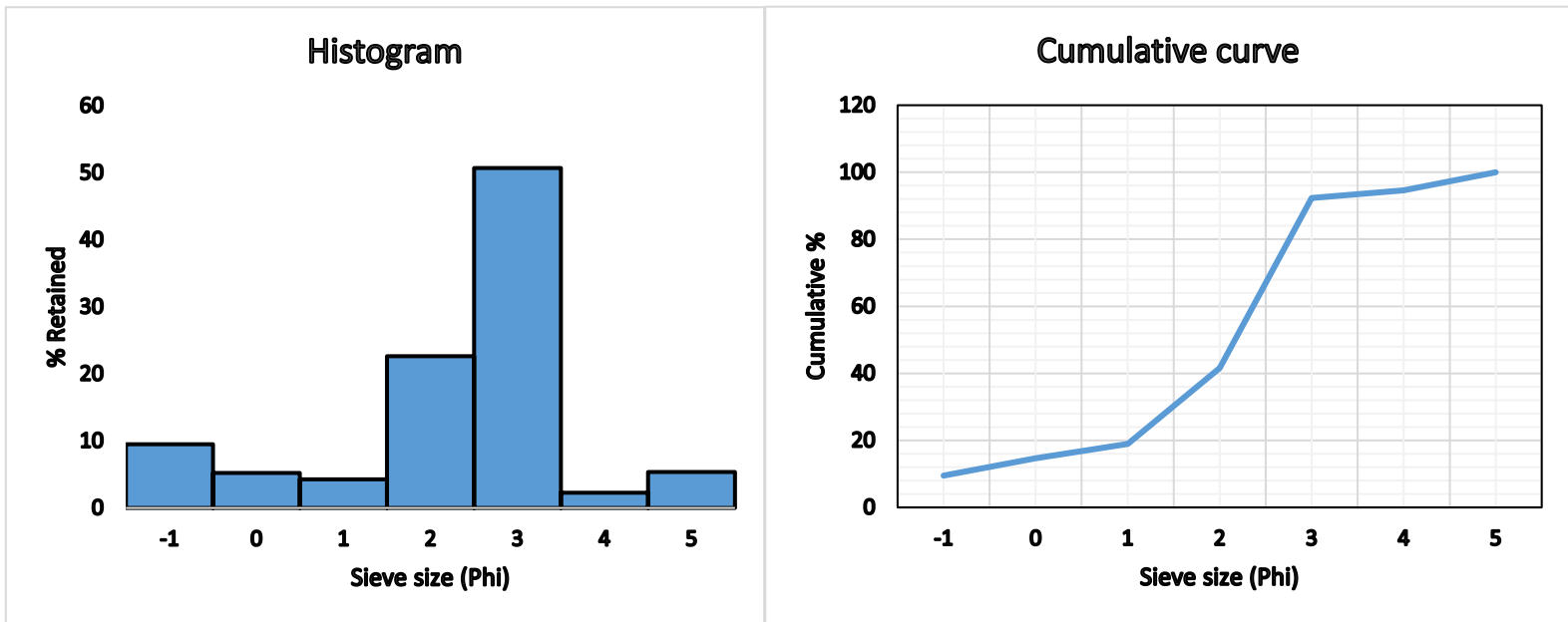
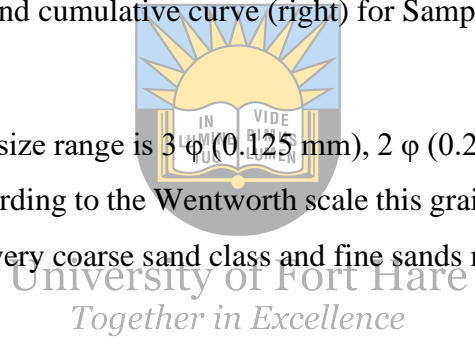


Figure A.5: Histogram (left) and cumulative curve (right) for Sample P9.

The dominant sediment grain size range is 3 ϕ (0.125 mm), 2 ϕ (0.25mm), but scattered from -1 ϕ to 5 ϕ in Sample P9, and according to the Wentworth scale this grain size range fall into fine sand and medium sand with some very coarse sand class and fine sands mixture.



A.6 Sample K2

Aliquot mass = 323.65g

Table A.6: Retained and cumulative percentage for sample K2.

Sieve size (ϕ)	Mass retained (g)	% retained	Cumulative %
-1	64.18	19.85	19.85
0	19.08	5.9	25.75
1	13.45	4.16	29.91
2	29.5	9.13	39.04
3	166.25	51.43	90.47
4	13.19	4.08	94.55
5	17.62	5.45	100

Total mass	323.27		
------------	--------	--	--

Error = 0.12%

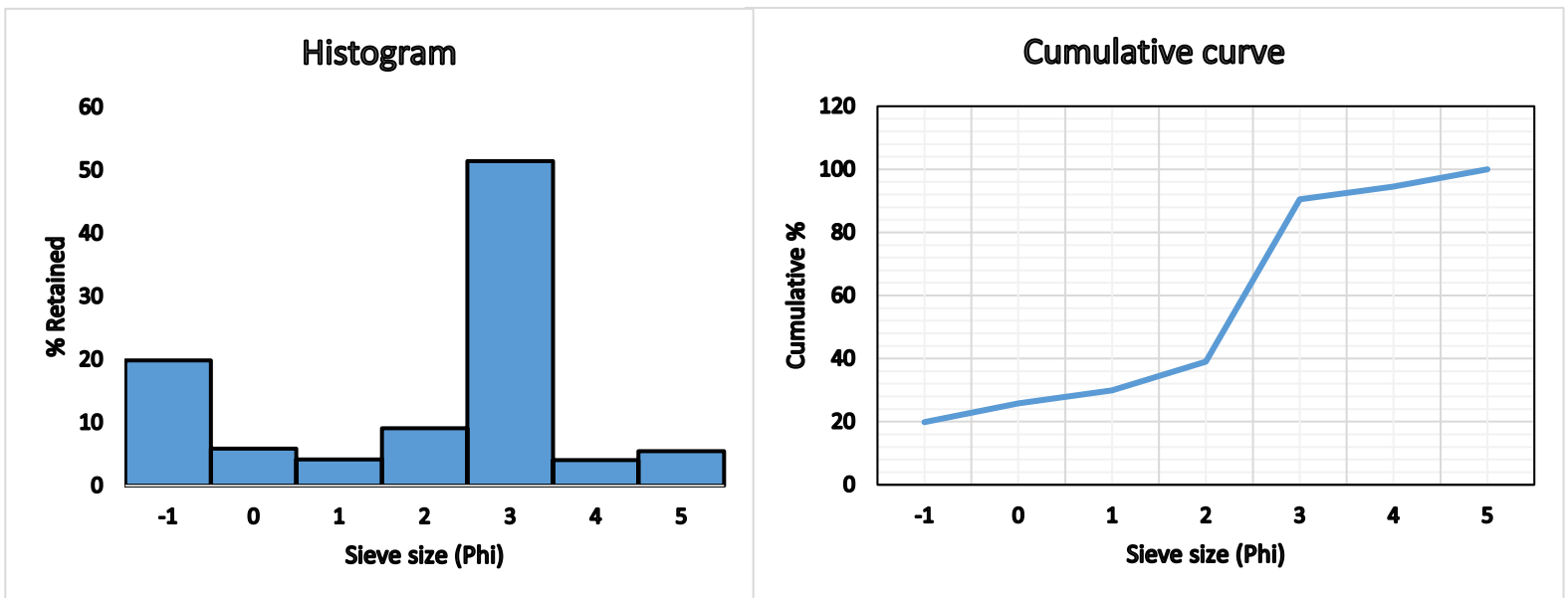


Figure A.6: Histogram (left) and cumulative curve (right) for Sample K2.

The dominant sediment grain size range is 3 ϕ (0.125 mm) followed by a considerable percentage of grain size range of -1 ϕ (2 mm) and small percentages at 2 ϕ , with equal 0 ϕ and 5 ϕ and equal 1 ϕ and 4 ϕ . According to the Wentworth scale this grain size range fall into fine sand and very coarse sand class and therefore fine sand and very coarse is dominant, with some coarse silt.

A.7 Sample K3

Aliquot mass = 328.35g

Table A.7: Retained and cumulative percentage for sample K3.

Sieve size (ϕ)	Mass retained (g)	% retained	Cumulative %
-1	74.91	22.84	22.84
0	19.57	5.97	28.81
1	12.13	3.7	32.51
2	31.9	9.73	42.24
3	162.29	49.48	91.72

4	13.46	4.1	95.82
5	13.7	4.18	100
Total mass	327.96		

Error = 0.12%

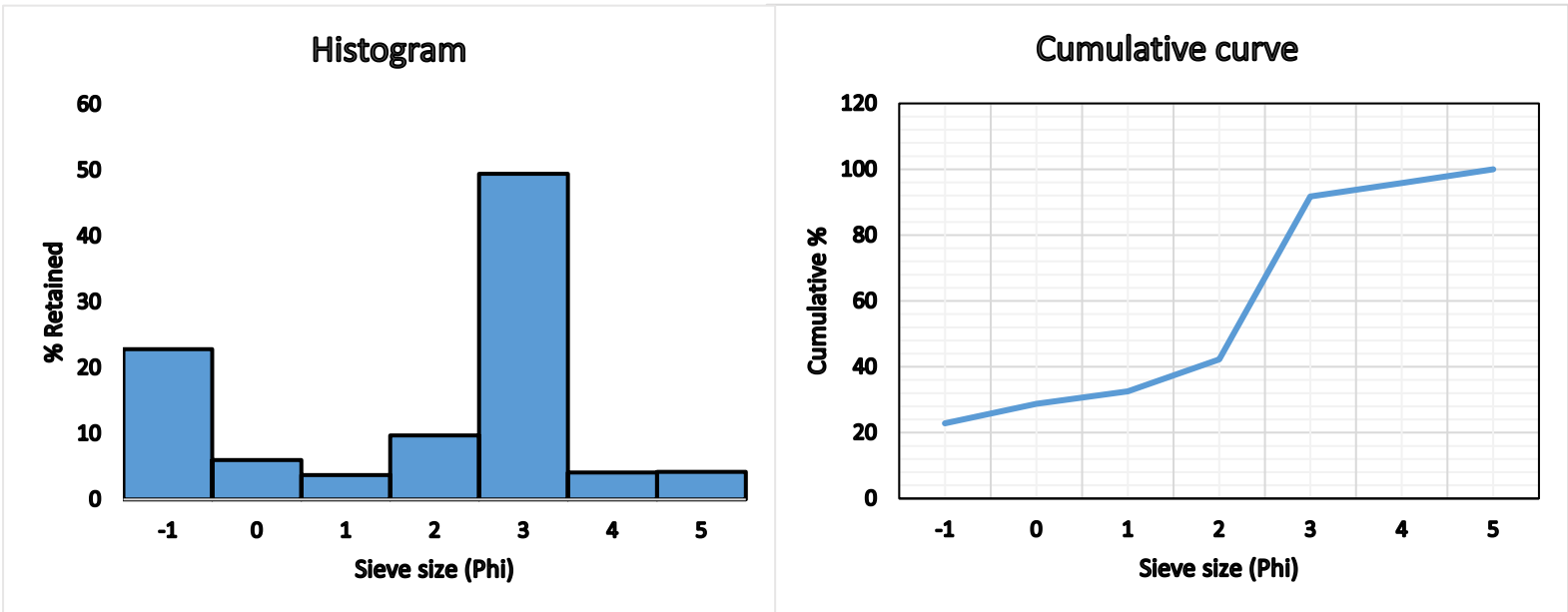


Figure A.7: Histogram (left) and cumulative curve (right) for Sample K3.

The dominant sediment grain size range is 3 ϕ (0.125 mm) followed by a considerable percentage of grain size range of -1 ϕ (2 mm) and small percentages at 2 ϕ , 0 ϕ and equal 1 ϕ , 4 ϕ and 5 ϕ . According to the Wentworth scale this grain size range fall into fine sand and very coarse sand class and therefore fine sand and very coarse is dominant, with some coarse silt, no seashells.

A.8 Sample P15

Aliquot mass = 342.09g

Table A.8: Retained and cumulative percentage for sample P15.

Sieve size (ϕ)	Mass retained (g)	% retained	Cumulative %
-1	3.09	0.9	0.9
0	0.8	0.23	1.13
1	0.98	0.29	1.42
2	12.41	3.63	5.05
3	320.88	93.92	98.97

4	2.23	0.65	99.62
5	1.27	0.37	99.99
Total mass	341.66		

Error = 0.13%

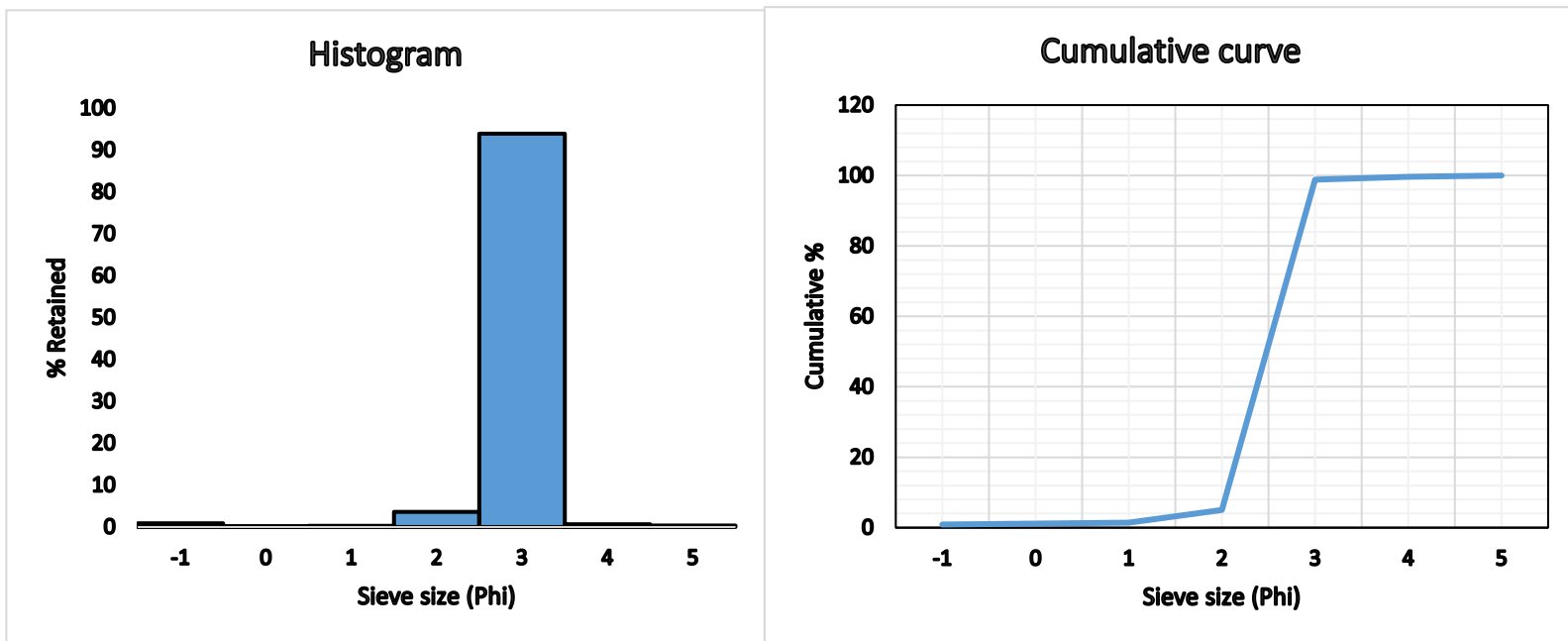


Figure A.8: Histogram (left) and cumulative curve (right) for Sample P15.

University of Fort Hare
Together in Excellence

The dominant sediment grain size range is 3 ϕ (0.125 mm) followed by small percentages of grain size range of 2 ϕ (0.25 mm), and according to the Wentworth scale this grain size range falls into fine sand and medium sand class and therefore fine and medium sands are dominant in sample P15, and there are no seashells present.

A.9 Sample P16

Aliquot mass = 331.93g

Table A.9: Retained and cumulative percentage for sample P16.

Sieve size (ϕ)	Mass retained (g)	% retained	Cumulative %
-1	0.25	0.06	0.06
0	1.42	0.43	0.49
1	4.48	1.35	1.84

2	67.22	20.26	22.1
3	257.94	77.76	99.86
4	0.4	0.12	98.98
5	0	0	99.98
Total mass	331.71		

Error = 0.07%

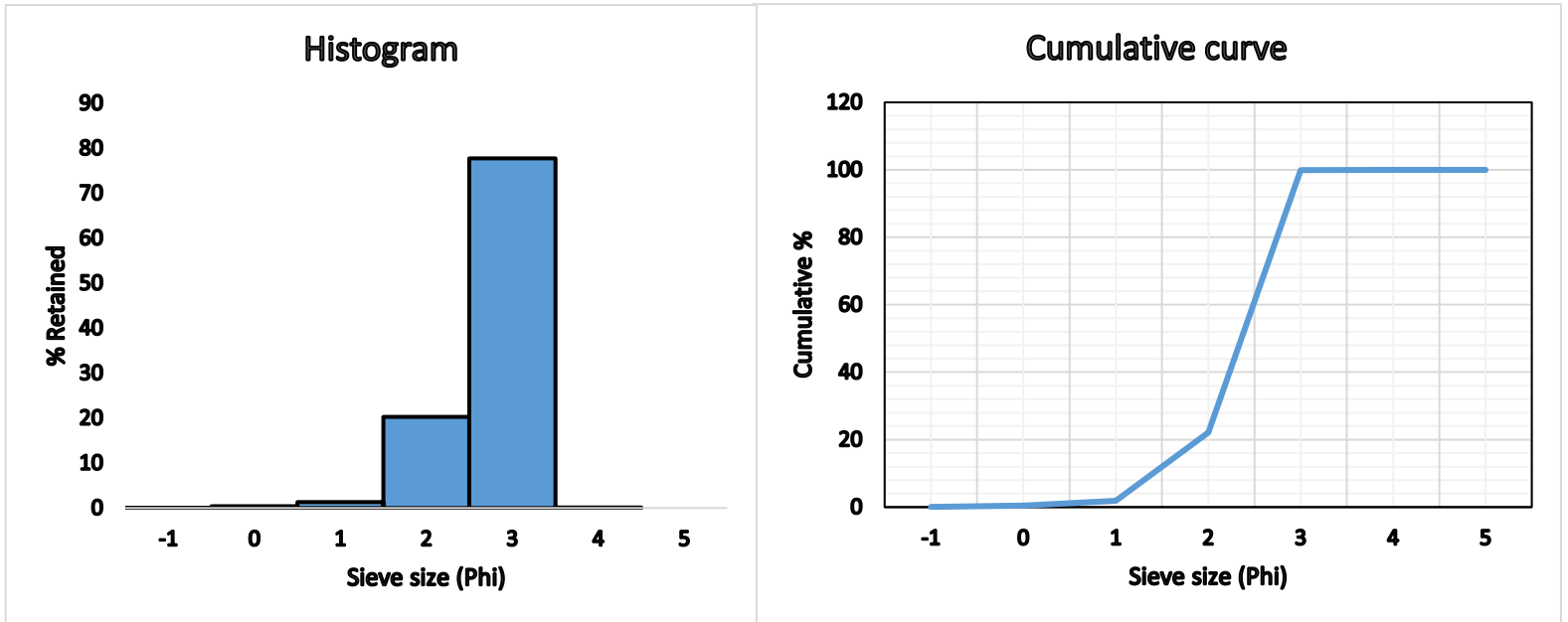


Figure A.9: Histogram (left) and cumulative curve (right) for Sample P16.

The dominant sediment grain size range is 3 ϕ (0.125 mm) followed by a considerable percentages of grain size range of 2 ϕ (0.25 mm) and a small percentage at 1 ϕ , and according to the Wentworth scale this grain size range fall into fine sand and medium sand class, thus fine and medium sand is dominant in sample P16 and there are no seashells present.

A.10 Sample P17

Aliquot mass = 332.08g

Table A.10: Retained and cumulative percentage for sample P17.

Sieve size (ϕ)	Mass retained (g)	% retained	Cumulative %
-1	0.35	0.11	0.11
0	0.6	0.18	0.29
1	1.41	0.43	0.72

2	28.75	8.67	9.39
3	300	90.5	99.89
4	0.4	0.12	100.01
5	0	0	100.01
Total mass	331.51		

Error = 0.17%

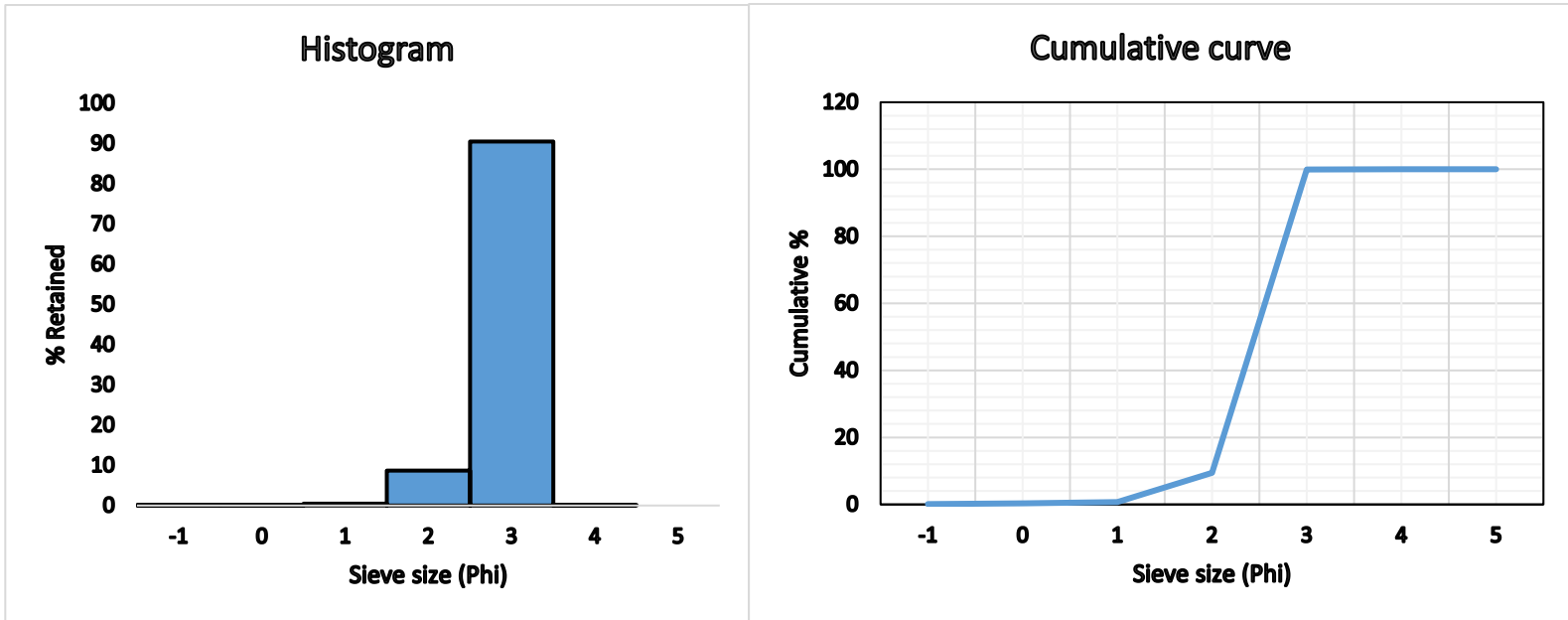


Figure A.10: Histogram (left) and cumulative curve (right) for Sample P17.

The dominant sediment grain size range is 3 ϕ (0.125 mm) followed by small percentages of grain size range of 2 ϕ (0.25 mm), and according to the Wentworth scale this grain size range fall into fine sand and medium sand class, hence fine and medium sand is dominant in sample P16 and there are some seashells present.

A.11 Sample P18

Aliquot mass = 369.97g

Table A.11: Retained and cumulative percentage for sample P18.

Sieve size (ϕ)	Mass retained (g)	% retained	Cumulative %
-1	0.04	0.01	0.01
0	0	0	0.01
1	0.08	0.02	0.03

2	67.07	18.14	18.17
3	302.3	81.76	99.93
4	0.27	0.07	100
5	0	0	100
Total mass	369.76		

Error = 0.01%

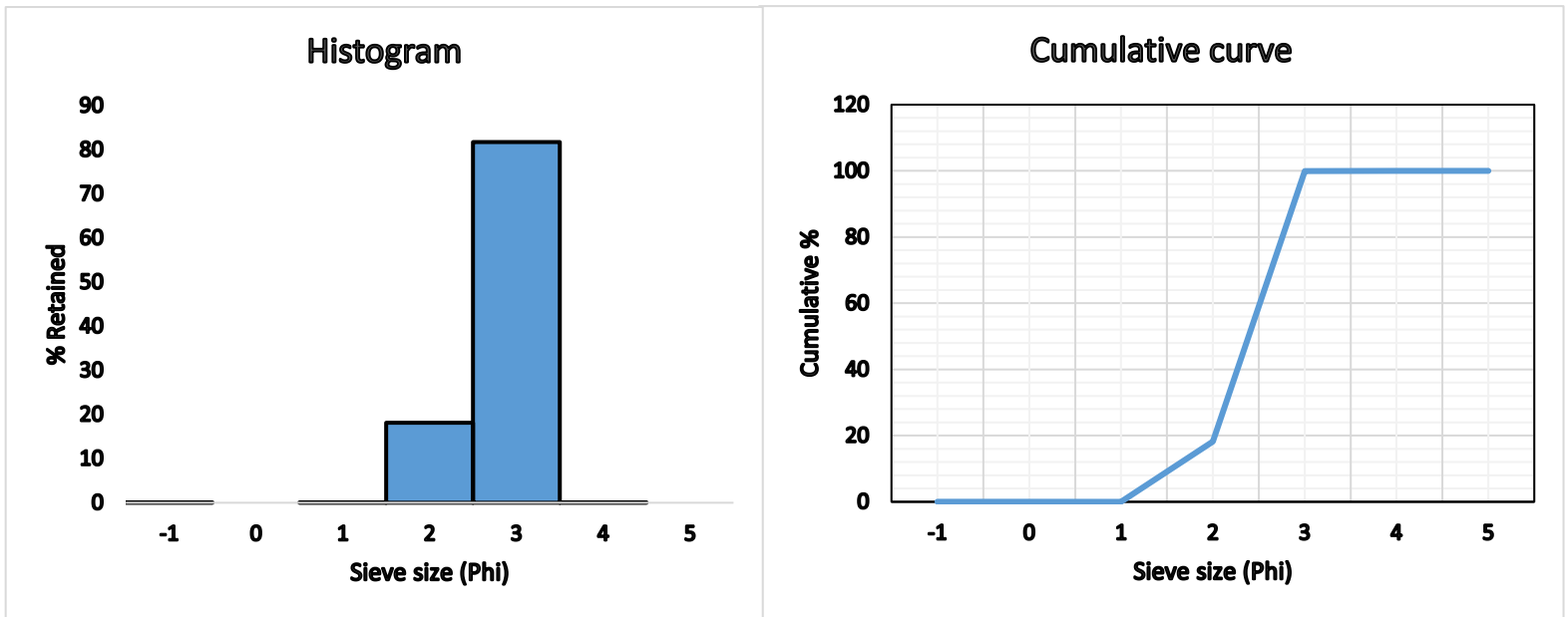


Figure A.11: Histogram (left) and cumulative curve (right) for Sample P18.

The dominant sediment grain size range is 3 ϕ (0.125 mm) followed by small percentages of grain size range of 2 ϕ (0.25 mm), and according to the Wentworth scale this grain size range fall into fine sand and medium sand class, hence fine and medium sand is dominant in sample P18 and there are no seashells present.

A.12 Sample P19

Aliquot mass = 387.6g

Table A.12: Retained and cumulative percentage for sample P19.

Sieve size (ϕ)	Mass retained (g)	% retained	Cumulative %
-1	0.11	0.03	0.03
0	0.05	0.01	0.04
1	0.09	0.02	0.06

2	150.01	38.73	38.79
3	236.83	61.14	99.93
4	0.25	0.06	99.99
5	0	0	99.99
Total mass	387.34		

Error = 0.07%

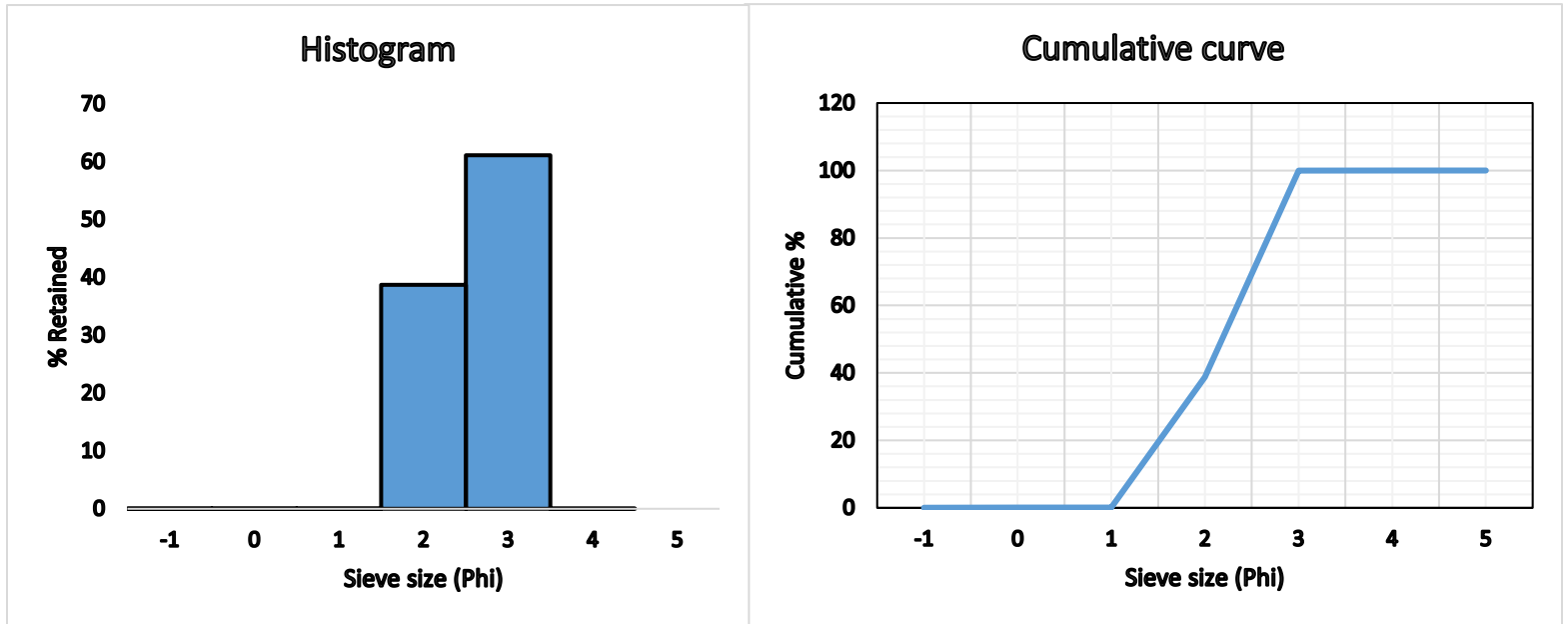


Figure A.12: Histogram (left) and cumulative curve (right) for Sample P19.

The dominant sediment grain size range is 3 ϕ (0.125 mm) followed by a considerable percentages of grain size range of 2 ϕ (0.25 mm), and according to the Wentworth scale this grain size range fall into fine sand and medium sand class and therefore fine and medium sand is dominant in sample P19 and there are no seashells present.

A.13 Sample P20

Aliquot mass = 284.52g

Table A.13: Retained and cumulative percentage for sample P20.

Sieve size (ϕ)	Mass retained (g)	% retained	Cumulative %
-1	3.03	1.07	1.07
0	3.22	1.13	2.2
1	3.57	1.26	3.46

2	23.4	8.23	11.69
3	244.17	85.91	97.6
4	2.5	0.88	98.48
5	4.33	1.52	100
Total mass	284.22		

Error = 0.11%

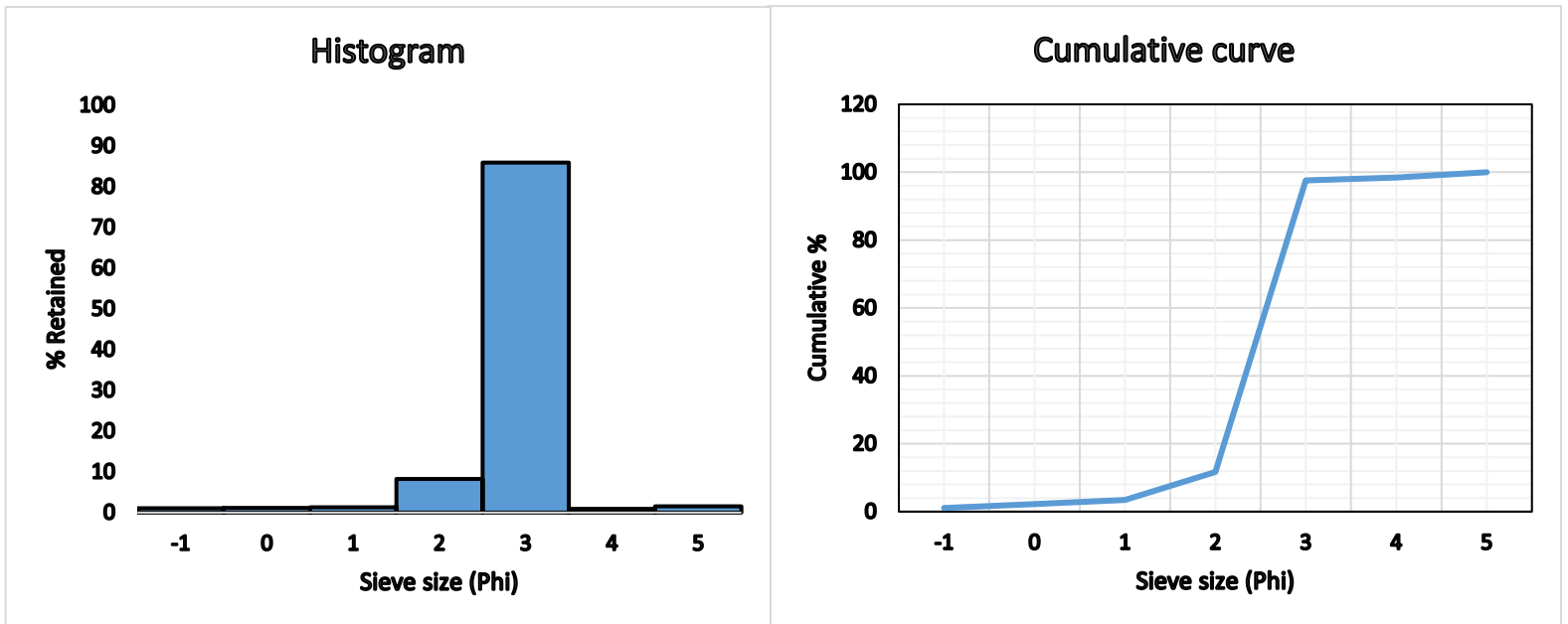


Figure A.13: Histogram (left) and cumulative curve (right) for Sample P20.

The dominant sediment grain size range is 3 ϕ (0.125 mm) followed by a considerable percentages of grain size range of 2 ϕ (0.25 mm) and according to the Wentworth scale this grain size range fall into fine sand and medium sand class and therefore fine and medium sand is dominant in sample P20, with some coarse silt, and there are no seashells present.

A.14 Sample P21

Aliquot mass = 251.65g

Table A.21: Retained and cumulative percentage for sample P21.

Sieve size (ϕ)	Mass retained (g)	% retained	Cumulative %
-1	0.49	0.19	0.19
0	0.74	0.29	0.49
1	3.39	1.35	1.83

2	68.66	27.3	29.13
3	178.04	70.8	99.93
4	0.16	0.06	99.99
5	0	0	99.99
Total mass	251.48		

Error = 0.07%

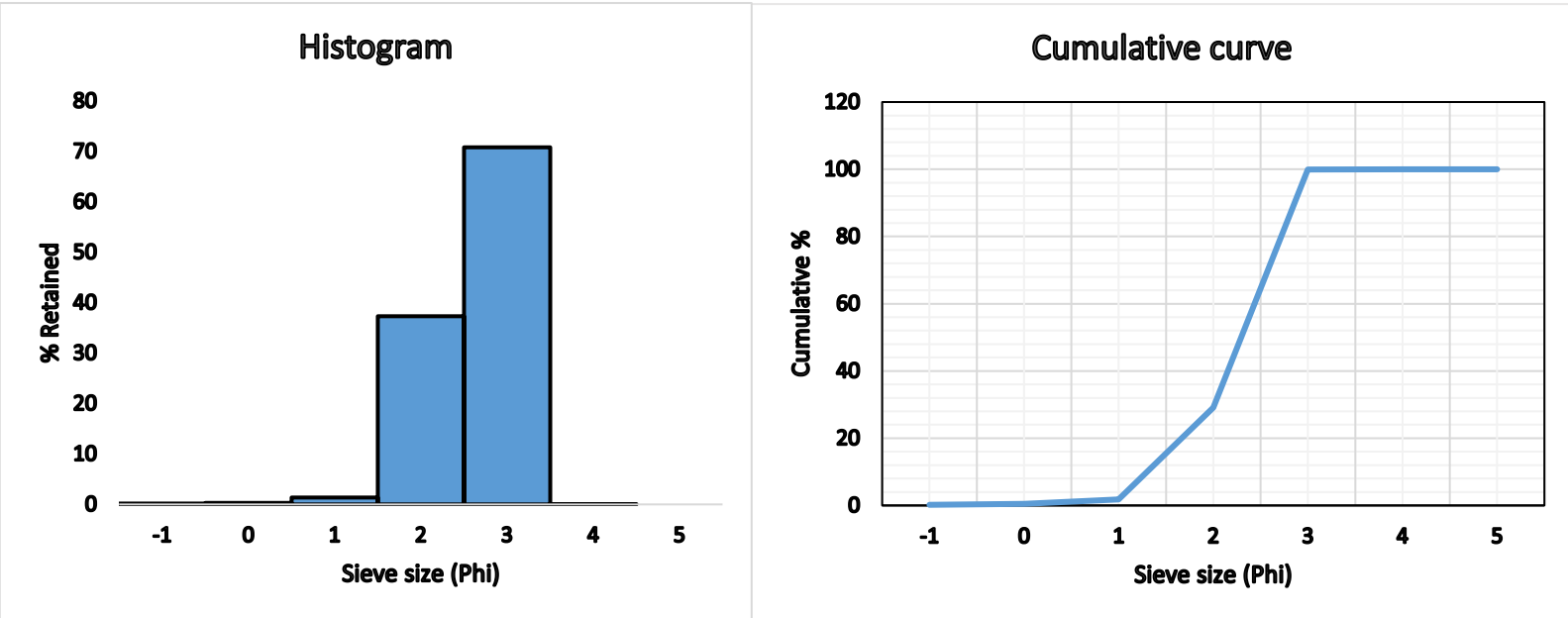


Figure A.14: Histogram (left) and cumulative curve (right) for Sample P21.

The dominant sediment grain size range is 3 ϕ (0.125 mm) followed by a considerable percentages of grain size range of 2 ϕ (0.25 mm) and a small percentage at 1 ϕ , and according to the Wentworth scale this grain size range fall into fine sand and medium sand class, thus fine and medium sand is dominant in sample P21 and there are no seashells present.

A.15 Sample P22

Aliquot mass = 304.01g

Table A.15: Retained and cumulative percentage for sample P22.

Sieve size (ϕ)	Mass retained (g)	% retained	Cumulative %
-1	0	0	0
0	0.13	0.04	0.04
1	0.51	0.17	0.21

2	44.75	14.73	14.94
3	258.12	84.98	99.92
4	0.23	0.08	100
5	0	0	100
Total mass	303.74		

Error = 0.09%

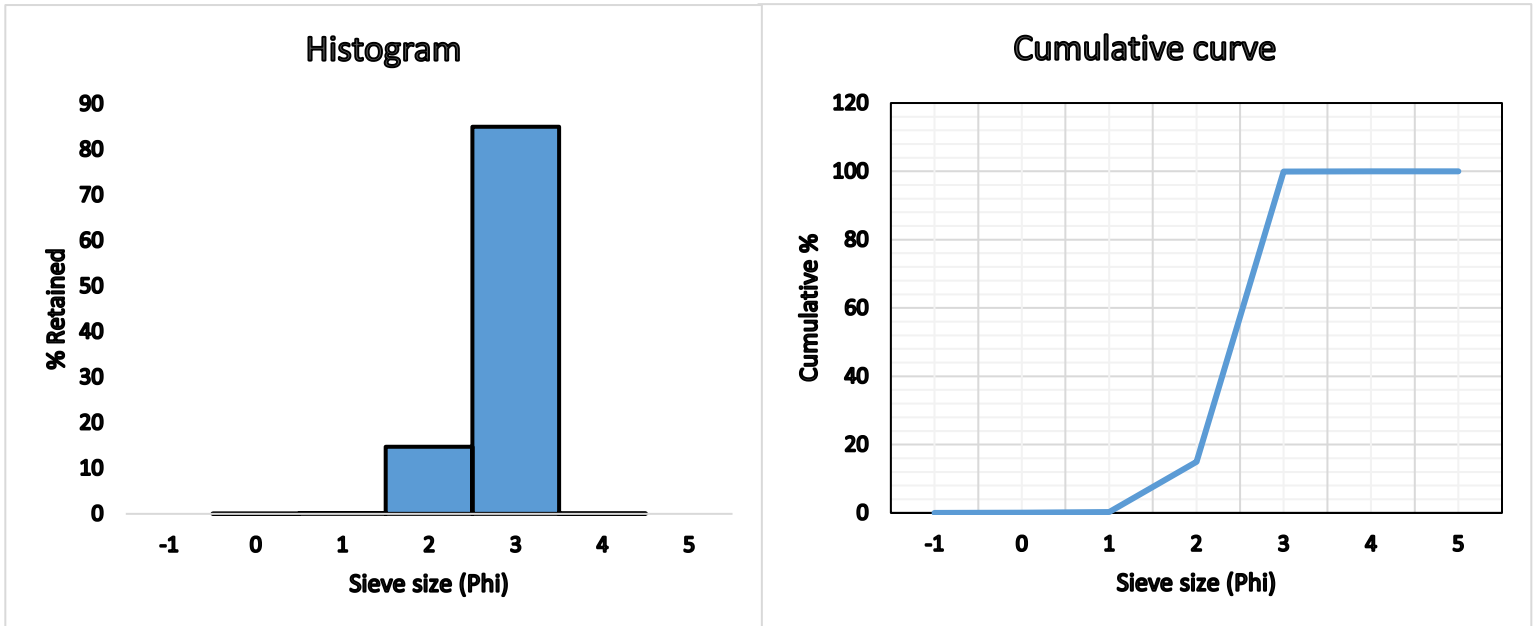


Figure A.15: Histogram (left) and cumulative curve (right) for Sample P22.

The dominant sediment grain size range is 3 ϕ (0.125 mm) followed by small percentages of grain size range of 2 ϕ (0.25 mm), and according to the Wentworth scale this grain size range fall into fine sand and medium sand class and hence fine and medium sand is dominant in sample P22 and there are some seashells present.

A.16 Sample P23

Aliquot mass = 252.35g

Table A.16: Retained and cumulative percentage for sample P23.

Sieve size (ϕ)	Mass retained (g)	% retained	Cumulative %
-1	0	0	0
0	0	0	0
1	0	0	0

2	4.63	1.84	1.84
3	246.51	97.87	99.71
4	0.73	0.29	100
5	0	0	100
Total mass	251.87		

Error = 0.19%

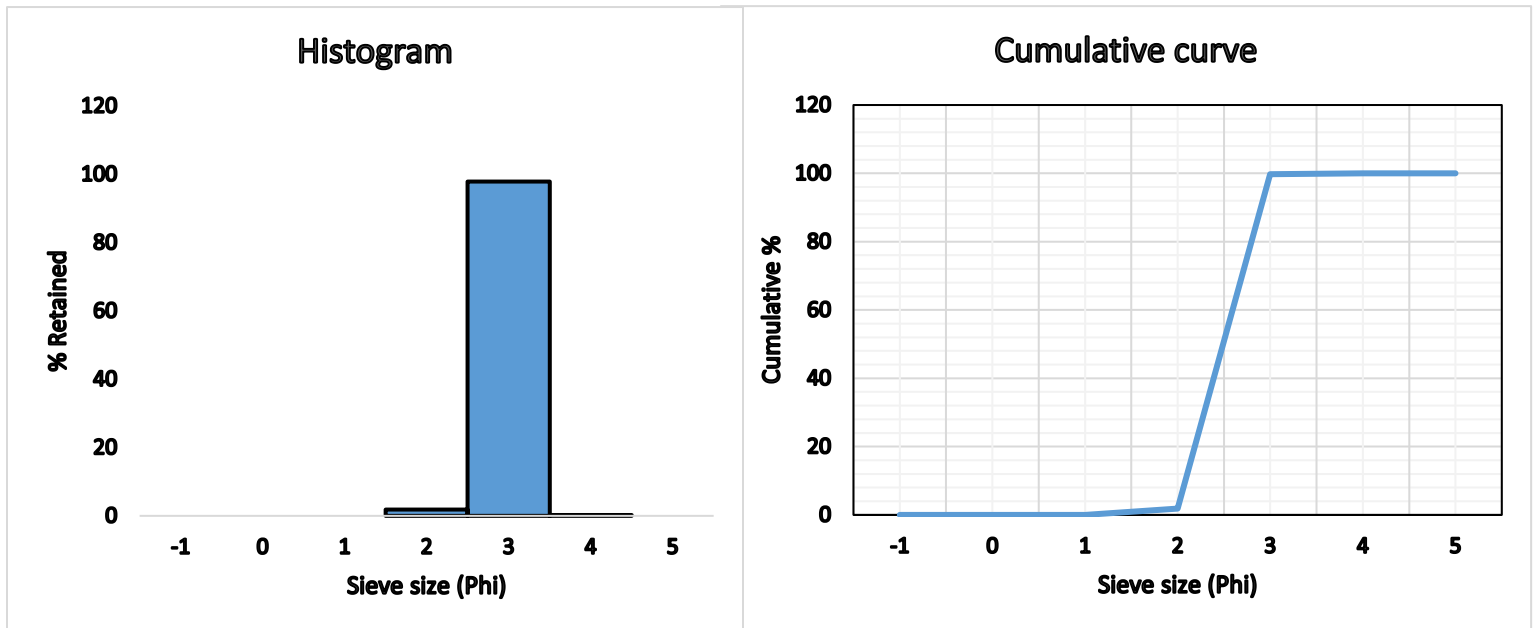


Figure A.16: Histogram (left) and cumulative curve (right) for Sample P23.

The dominant sediment grain size range is 3 ϕ (0.125 mm) in sample P23, and according to the Wentworth scale this grain size range fall into fine sand class and therefore fine sand is dominant in sample P23 and there are no seashells present.

A.17 Sample P24

Aliquot mass = 426.4g

Table A.17: Retained and cumulative percentage for sample P24.

Sieve size (ϕ)	Mass retained (g)	% retained	Cumulative %
-1	0.2	0.05	0.05
0	0.1	0.02	0.07
1	0.1	0.02	0.09

2	18.99	4.46	4.55
3	405.31	95.15	99.7
4	1.18	0.28	98.98
5	0.08	0.02	100
Total mass	425.96		

Error = 0.1%

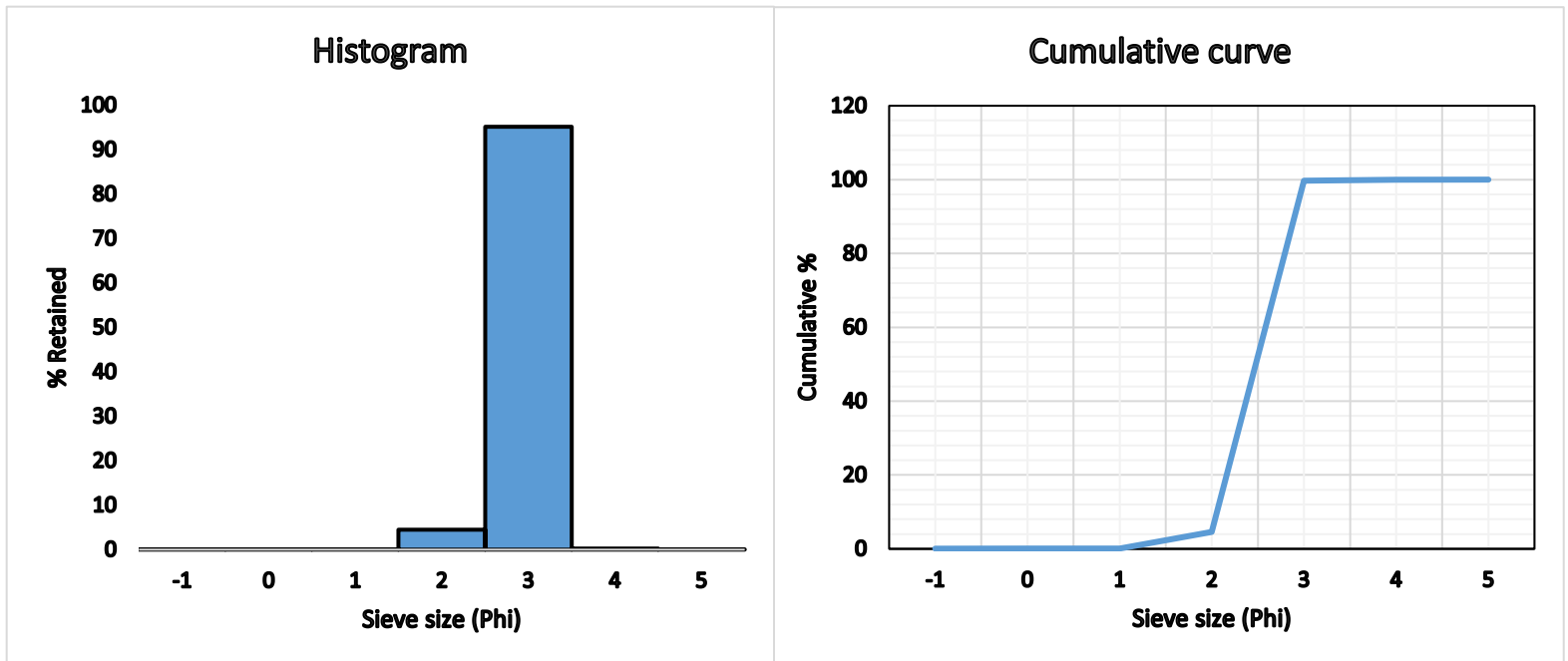


Figure A.17: Histogram (left) and cumulative curve (right) for Sample P24.

The dominant sediment grain size range is 3 ϕ (0.125 mm) and small quantity of 2 ϕ (0.25) in sample P24, and according to the Wentworth scale this grain size range fall into fine sand and medium sand class and hence fine sand and medium sand is dominant, and there are no seashells present.

A.18 Sample P25

Aliquot mass = 336.89g

Table A.18: Retained and cumulative percentage for sample P25.

Sieve size (ϕ)	Mass retained (g)	% retained	Cumulative %
-1	2	0.59	0.59
0	2.15	0.64	1.23

1	3.98	1.18	2.41
2	11.68	3.47	5.88
3	309.72	92.04	97.92
4	2.75	0.82	98.74
5	4.24	1.26	100
Total mass	336.52		

Error = 0.11%

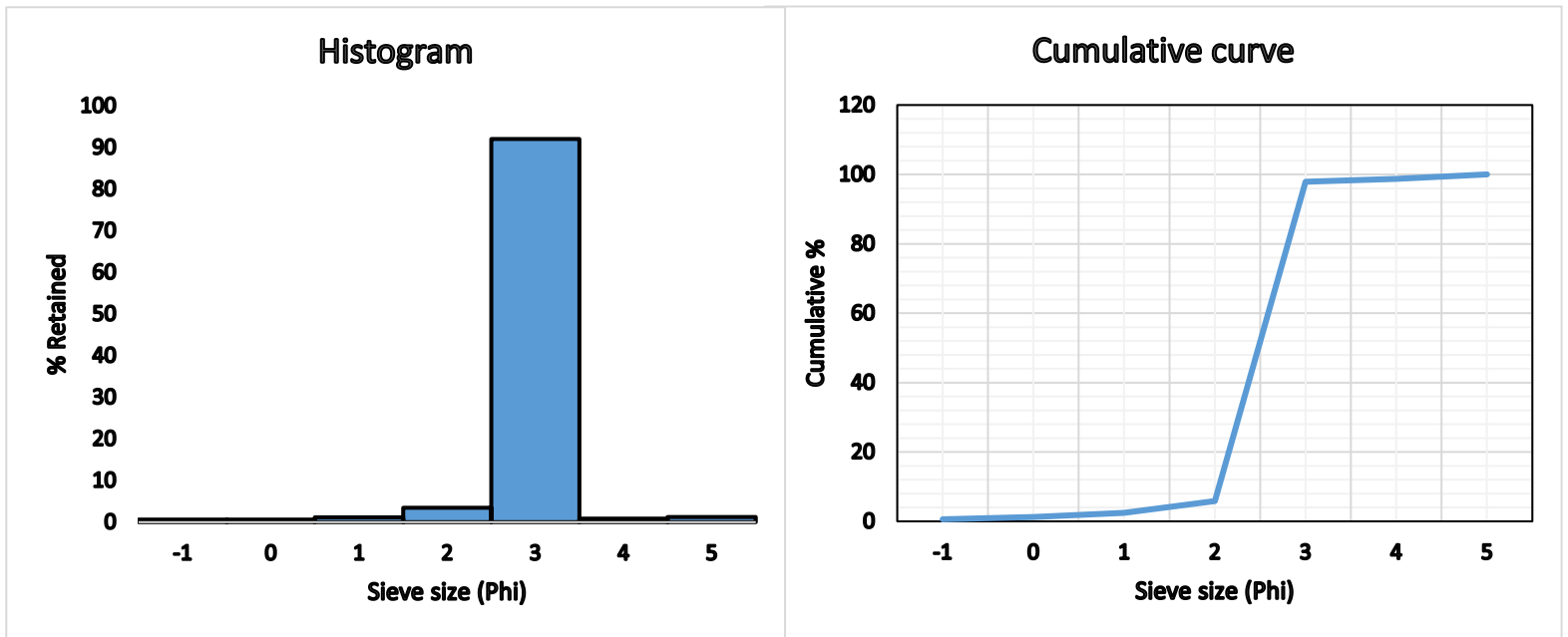


Figure A.18: Histogram (left) and cumulative curve (right) for Sample P25.

The dominant sediment grain size range is 3 ϕ (0.125 mm) and small quantity of 2 ϕ (0.25) in sample P25, and according to the Wentworth scale this grain size range fall into fine sand and medium sand class and hence fine sand and medium sand is dominant, with some coarse silt and there are no seashells present.

A.19 Sample P26

Aliquot mass = 377.08g

Table A.19: Retained and cumulative percentage for sample P26.

Sieve size (ϕ)	Mass retained (g)	% retained	Cumulative %
-1	0.65	0.17	0.17
0	1.96	0.52	0.69
1	4.43	1.18	1.87
2	25.32	6.73	8.6
3	342.54	90.98	99.58
4	1.6	0.42	100
5	0	0	100
Total mass	376.5		

Error = 0.15%

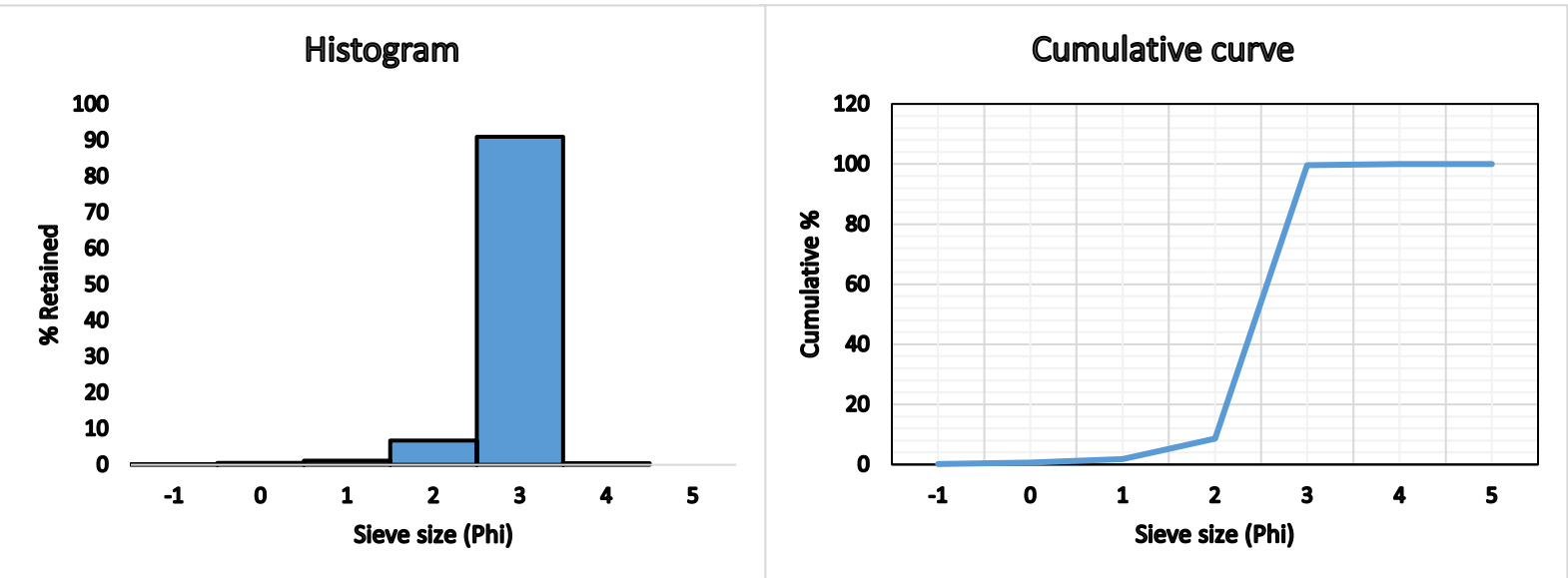


Figure A.19: Histogram (left) and cumulative curve (right) for Sample P26.

The dominant sediment grain size range is 3 ϕ (0.125 mm) and small quantity of 2 ϕ (0.25) in sample P26, and according to the Wentworth scale this grain size range fall into fine sand and medium sand class and hence fine sand and medium sand is dominant, and there are no seashells present.

A.20 Sample P27

Aliquot mass = 305.91g

Table A.20: Retained and cumulative percentage for sample P27.

Sieve size (ϕ)	Mass retained (g)	% retained	Cumulative %
-1	0.55	0.18	0.18
0	1.05	0.34	0.52
1	3.08	1.01	1.53
2	10.79	3.53	5.06
3	288.37	94.36	99.42
4	1.75	0.57	99.99
5	0	0	99.99
Total mass	305.59		

Error = 0.1%

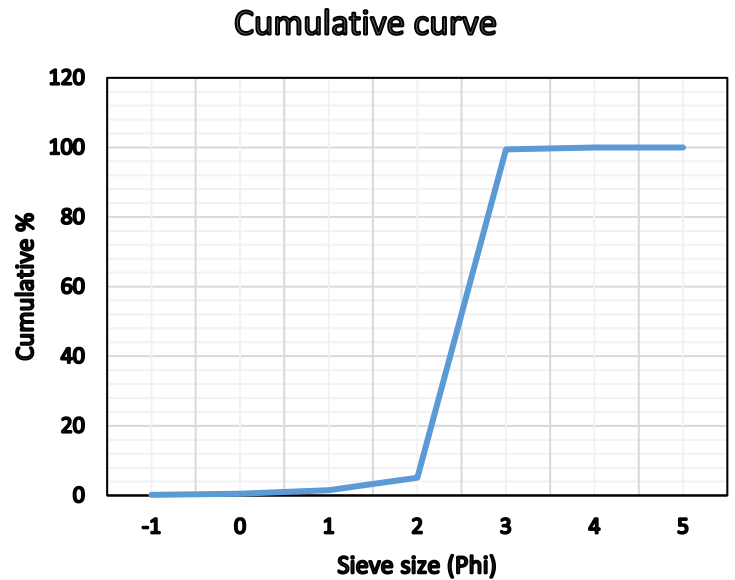
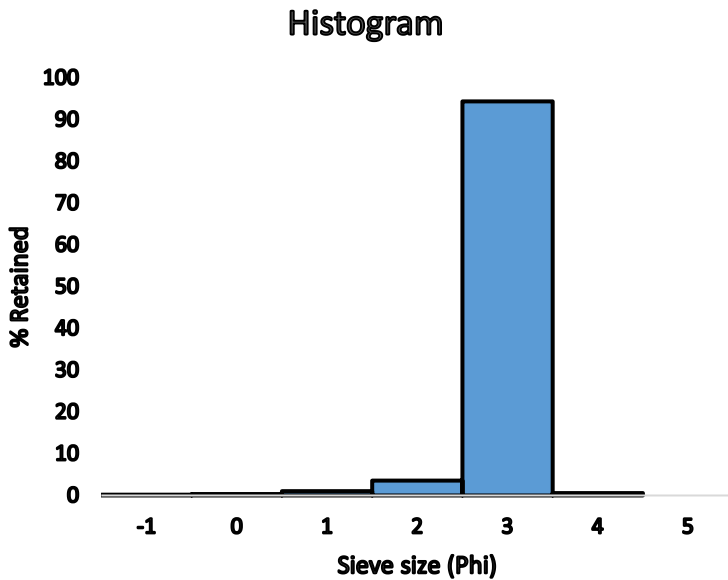


Figure A.20: Histogram (left) and cumulative curve (right) for Sample P27.

The dominant sediment grain size range is 3 ϕ (0.125 mm) and small quantity of 2 ϕ (0.25) in sample P27, and according to the Wentworth scale this grain size range fall into fine sand and medium sand class and hence fine sand and medium sand is dominant, and there are seashells present.

A.21 Sample P28

Aliquot mass = 260.54g

Table A.21: Retained and cumulative percentage for sample P28.

Sieve size (ϕ)	Mass retained (g)	% retained	Cumulative %
-1	0	0	0
0	0	0	0
1	0	0	0
2	1.92	0.74	0.74
3	256.8	98.69	99.43
4	1.48	0.57	100
5	0	0	100
Total mass	260.2		

Error = 0.13%

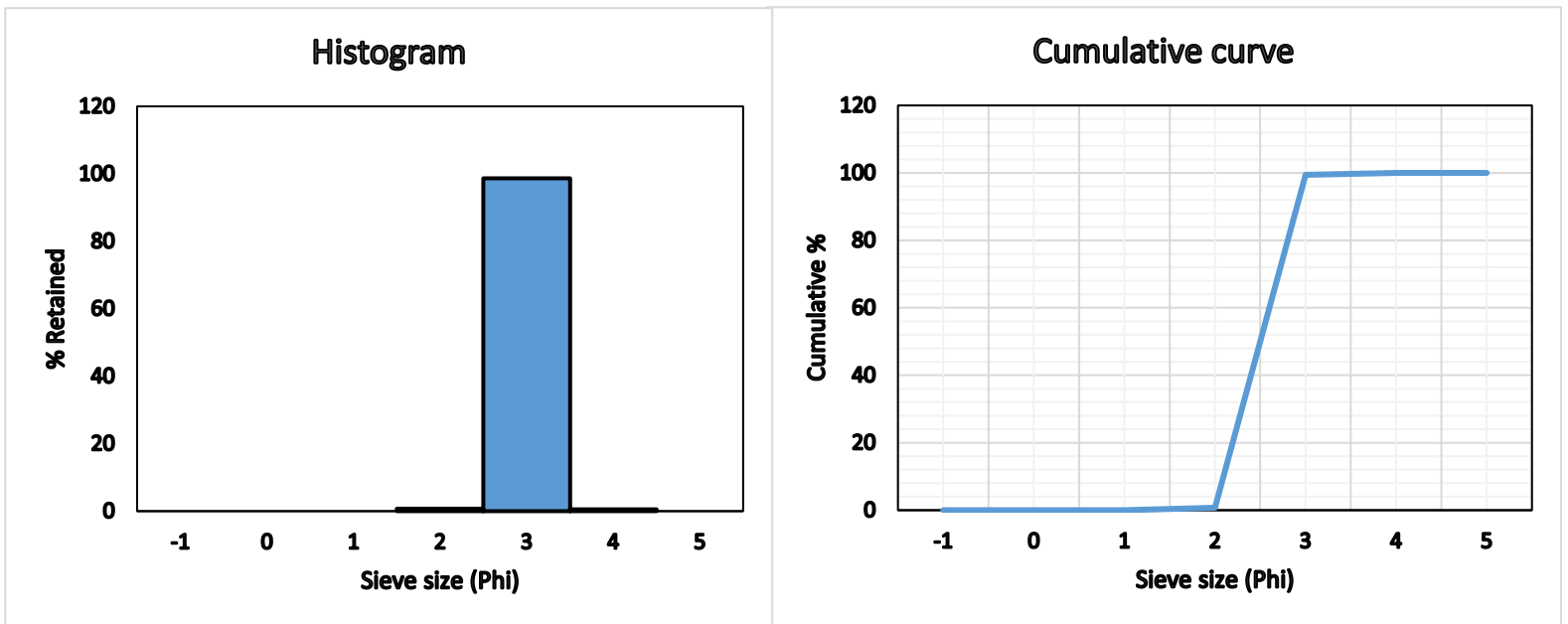


Figure A.21: Histogram (left) and cumulative curve (right) for Sample P28.

The dominant sediment grain size range is 3 ϕ (0.125 mm) in sample P28, and according to the Wentworth scale this grain size range fall into fine sand class and therefore fine sand is dominant in sample P28 and there are no seashells present.

A.22 Sample P29

Aliquot mass = 254.96g

Table A.22: Retained and cumulative percentage for sample P29.

Sieve size (ϕ)	Mass retained (g)	% retained	Cumulative %
-1	1.19	0.47	0.47
0	0.26	0.1	0.57
1	0.29	0.11	0.68
2	8.14	3.2	3.88
3	243.56	95.67	99.55
4	1	0.39	99.94
5	0.14	0.05	99.99
Total mass	254.58		

Error = 0.15%

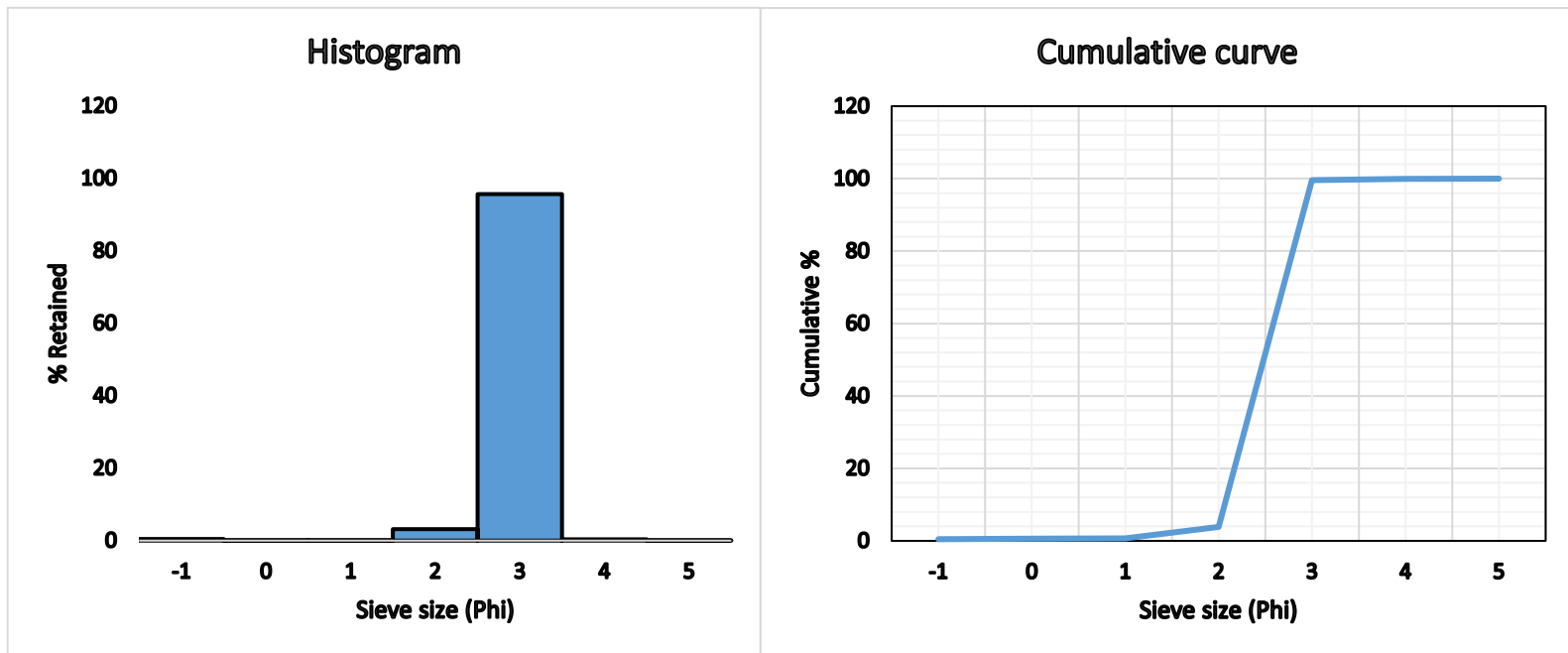


Figure A.22: Histogram (left) and cumulative curve (right) for Sample P29.

The dominant sediment grain size range is 3 ϕ (0.125 mm) and small quantity of 2 ϕ (0.25) in sample P29, and according to the Wentworth scale this grain size range fall into fine sand and medium sand class and hence fine sand and medium sand is dominant, and there are no seashells present.

A.23 Sample P30

Aliquot mass = 257.99g

Table A.23: Retained and cumulative percentage for sample P30.

Sieve size (ϕ)	Mass retained (g)	% retained	Cumulative %
-1	0	0	0
0	0	0	0
1	0.06	0.02	0.02
2	8.52	3.31	3.33
3	247.9	96.25	99.58
4	0.94	0.36	99.94
5	0.15	0.06	100
Total mass	257.57		

Error = 0.16%

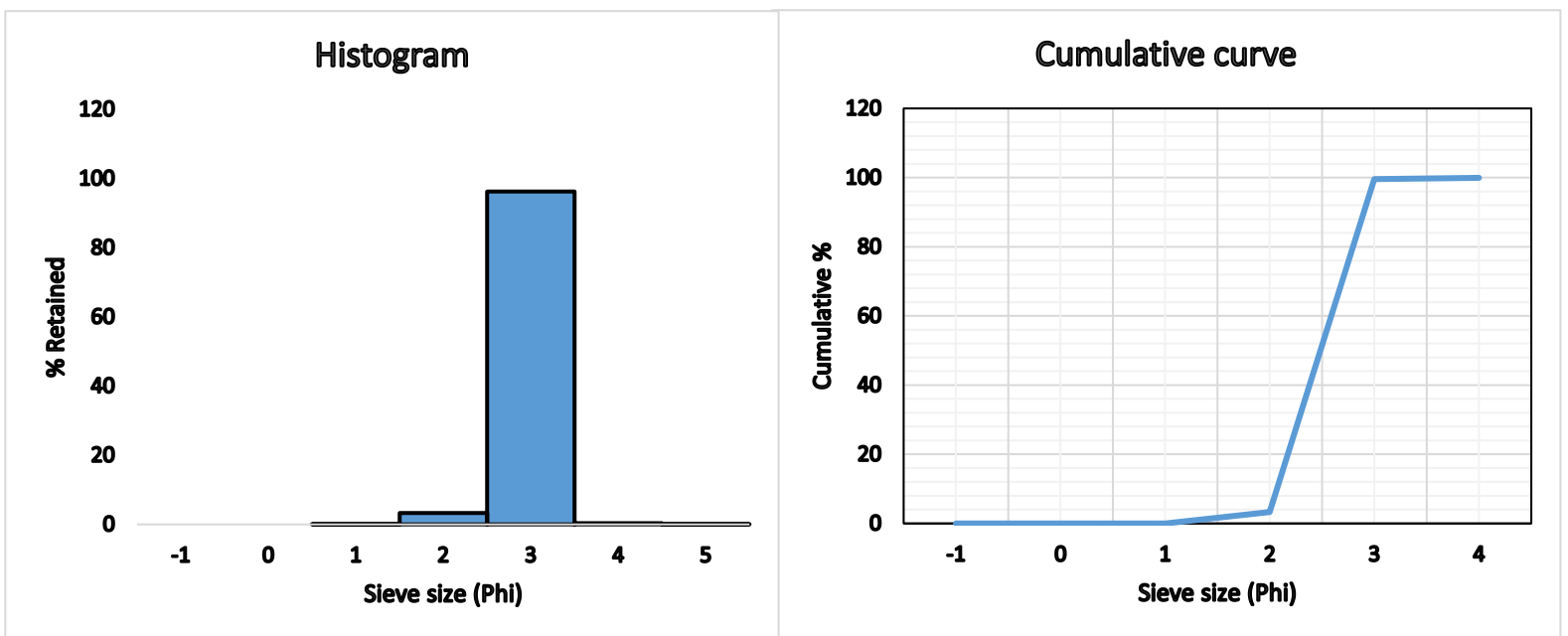


Figure A.23: Histogram (left) and cumulative curve (right) for Sample P30.

The dominant sediment grain size range is 3 ϕ (0.125 mm) and small quantity of 2 ϕ (0.25) in sample P30, and according to the Wentworth scale this grain size range fall into fine sand and medium sand class, thus fine sand and medium sand is dominant, with some coarse silt and there are no seashells present.

A.24 Sample P31

Aliquot mass = 199.61g

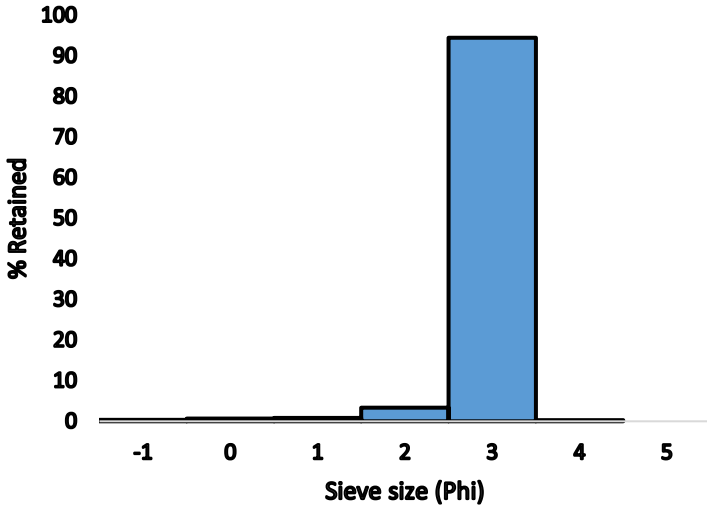
Table A.24: Retained and cumulative percentage for sample P31.

Sieve size (ϕ)	Mass retained (g)	% retained	Cumulative %
-1	0.8	0.4	0.4
0	1.3	0.65	1.05
1	1.7	0.85	1.9
2	6.65	3.34	5.24
3	188.38	94.5	99.74
4	0.52	0.26	100
5	0	0	100
Total mass	199.35		

Error = 0.13%



Histogram



Cumulative curve

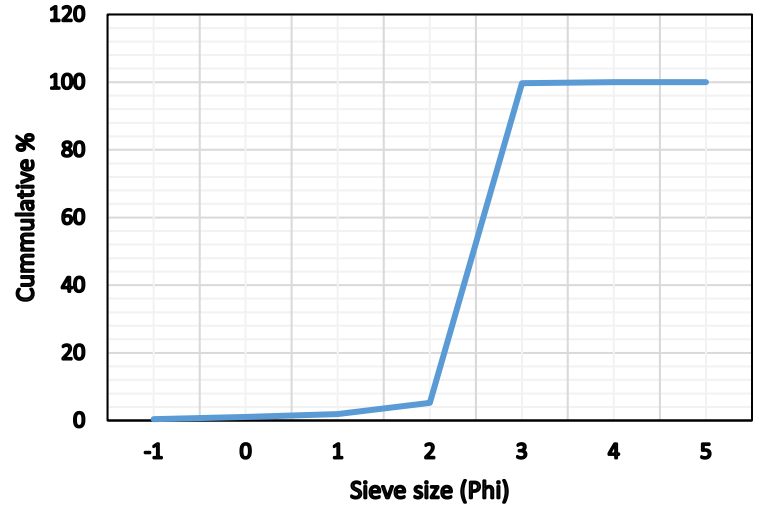


Figure A.24: Histogram (left) and cumulative curve (right) for Sample P31.

The dominant sediment grain size range is 3 ϕ (0.125 mm) and small quantity of 2 ϕ (0.25) in sample P31, and according to the Wentworth scale this grain size range fall into fine sand and medium sand class and hence fine sand and medium sand is dominant, and there are no seashells present.

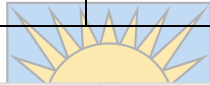
A.25 Sample P32

Aliquot mass = 275.89g

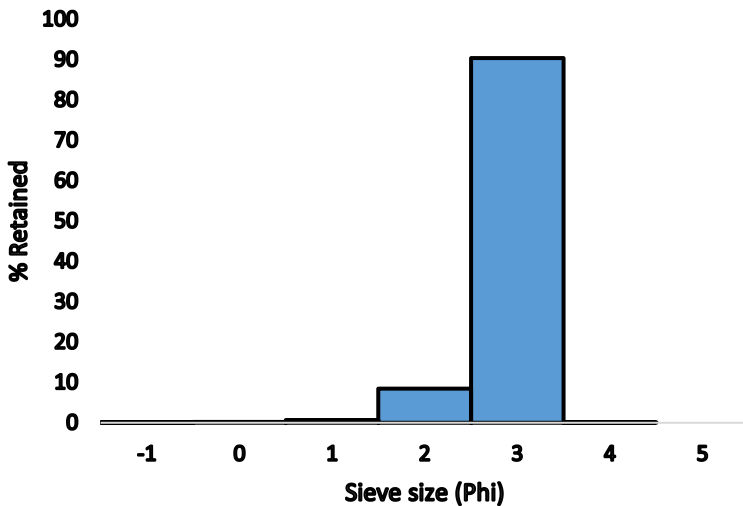
Table A.25: Retained and cumulative percentage for sample P32.

Sieve size (ϕ)	Mass retained (g)	% retained	Cumulative %
-1	0.3	0.11	0.11
0	0.63	0.23	0.34
1	1.8	0.65	0.99
2	23.4	8.49	9.48
3	248.97	90.36	99.84
4	0.42	0.15	99.99
5	0	0	99.99
Total mass	275.52		

Error = 0.14%



Histogram



Cumulative curve

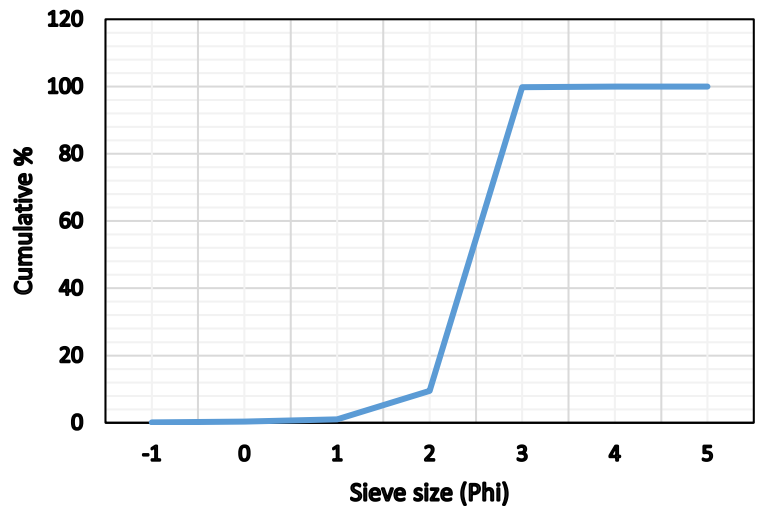


Figure A.25: Histogram (left) and cumulative curve (right) for Sample P32.

The dominant sediment grain size range is 3 ϕ (0.125 mm) and small quantity of 2 ϕ (0.25) in sample P32, and according to the Wentworth scale this grain size range fall into fine sand and medium sand class and hence fine sand and medium sand is dominant, and there are no seashells present.

A.26 Sample P33

Aliquot mass = 203.4g

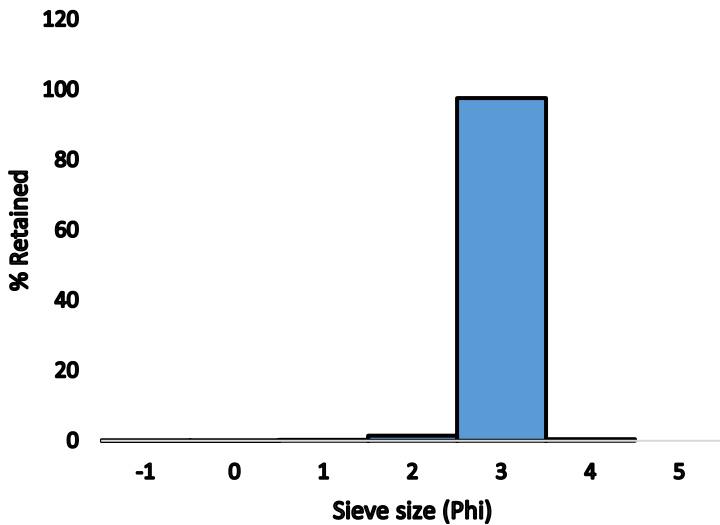
Table A.26: Retained and cumulative percentage for sample P33.

Sieve size (ϕ)	Mass retained (g)	% retained	Cumulative %
-1	0.25	0.12	0.12
0	0.25	0.12	0.24
1	0.52	0.26	0.5
2	3.03	1.49	1.99
3	198.38	97.59	99.58
4	0.84	0.41	99.99
5	0	0	99.99
Total mass	203.27		

Error = 0.06%



Histogram



Cumulative curve

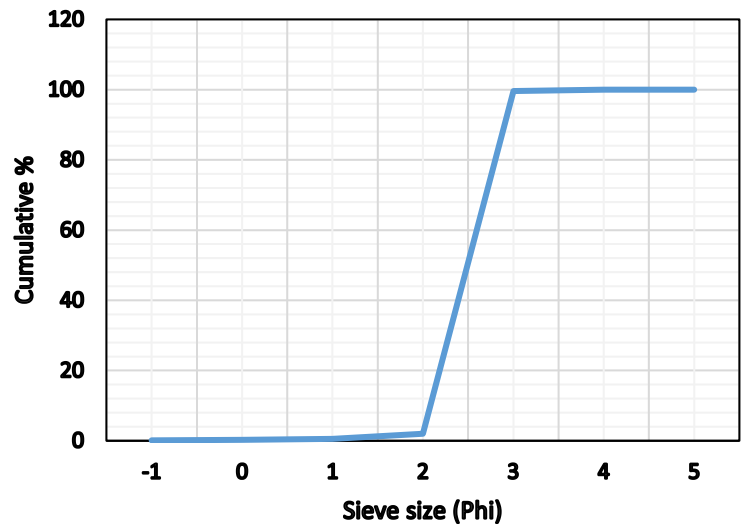


Figure A.26: Histogram (left) and cumulative curve (right) for Sample P33.

The dominant sediment grain size range is 3 ϕ (0.125 mm) in sample P33, and according to the Wentworth scale this grain size range fall into fine sand class and therefore fine sand is dominant and there are some seashells present.

A.27 Sample P34

Aliquot mass = 309.18g

Table A.27: Retained and cumulative percentage for sample P34.

Sieve size (ϕ)	Mass retained (g)	% retained	Cumulative %
-1	0.09	0.03	0.03
0	0.25	0.08	0.11
1	0.9	0.29	0.4
2	23.52	7.62	8.02
3	282.75	91.55	99.57
4	1.23	0.4	99.97
5	0.09	0.03	100
Total mass	308.83		

Error = 0.11%

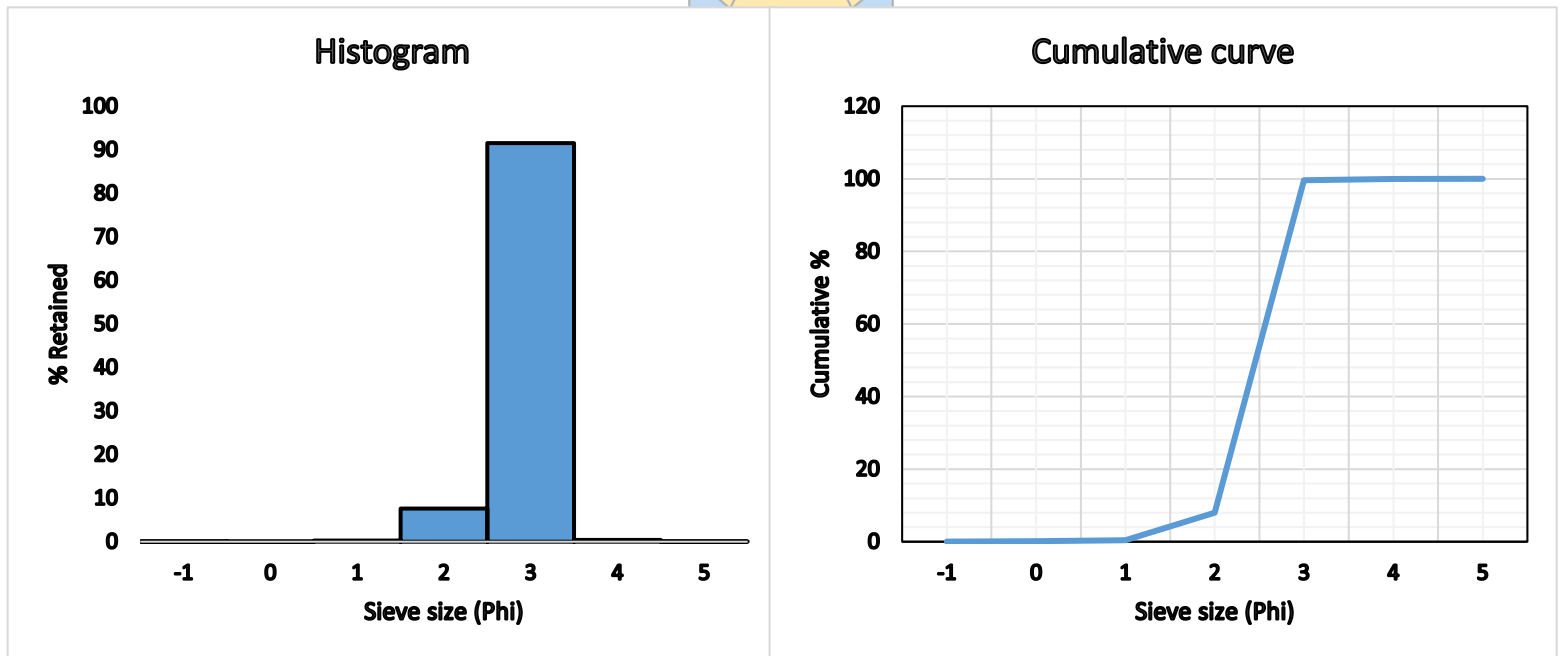


Figure A.27: Histogram (left) and cumulative curve (right) for Sample P34.

The dominant sediment grain size range is 3 ϕ (0.125 mm) and small quantity of 2 ϕ (0.25) in sample P34, and according to the Wentworth scale this grain size range fall into fine sand and medium sand class and thus fine sand and medium sand is dominant, with some coarse silt and there are no seashells present.

A.28 Sample P35

Aliquot mass = 227.98g

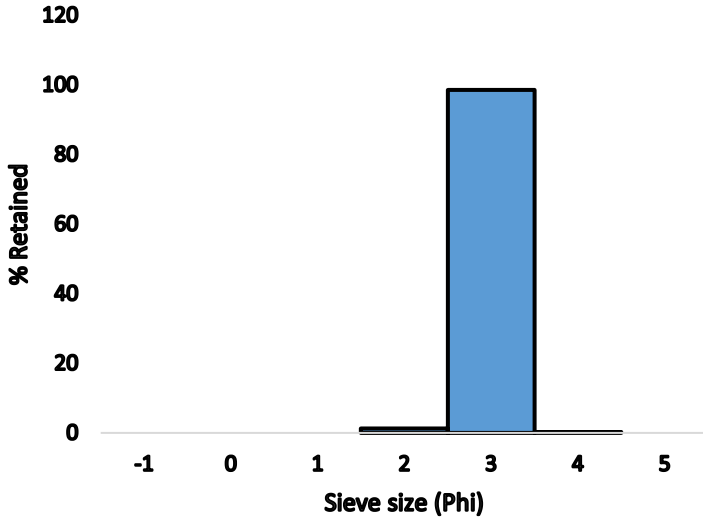
Table A.28: Retained and cumulative percentage for sample P35.

Sieve size (ϕ)	Mass retained (g)	% retained	Cumulative %
-1	0	0	0
0	0	0	0
1	0	0	0
2	2.8	1.23	1.23
3	224.45	98.53	99.76
4	0.54	0.24	100
5	0	0	100
Total mass	227.79		

Error = 0.08%



Histogram



Cumulative curve

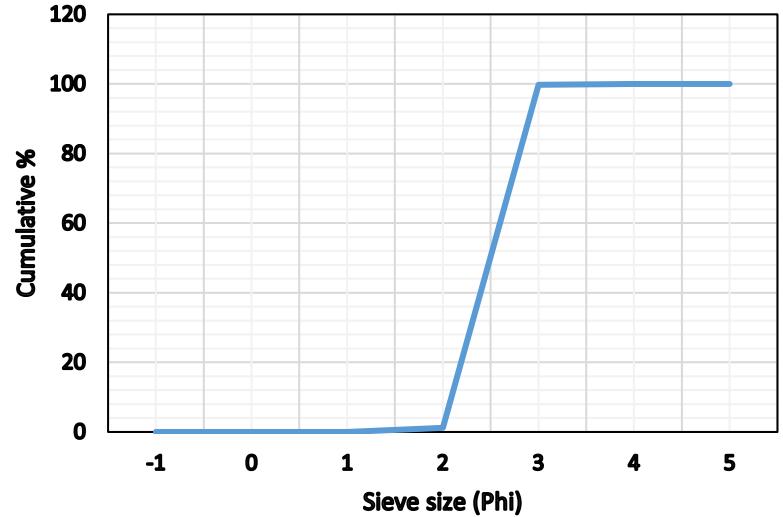


Figure A.28: Histogram (left) and cumulative curve (right) for Sample P35.

The dominant sediment grain size range is 3 ϕ (0.125 mm) in sample P35, and according to the Wentworth scale this grain size range fall into fine sand class and therefore fine sand is dominant in sample P35 and there are no seashells present.

A.29 Sample P36

Aliquot mass = 240.55g

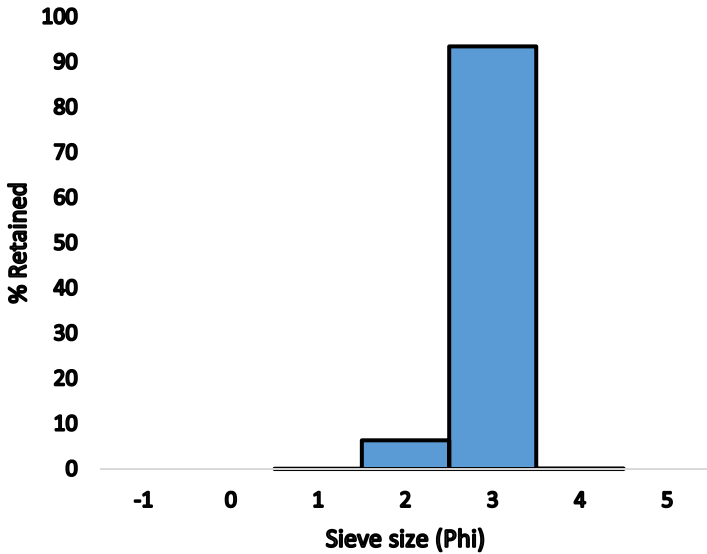
Table A.29: Retained and cumulative percentage for sample P36.

Sieve size (ϕ)	Mass retained (g)	% retained	Cumulative %
-1	0	0	0
0	0	0	0
1	0.1	0.04	0.04
2	15.28	6.36	6.4
3	224.65	93.49	99.89
4	0.26	0.11	100
5	0	0	100
Total mass	240.29		

Error = 0.11%



Histogram



Cumulative curve

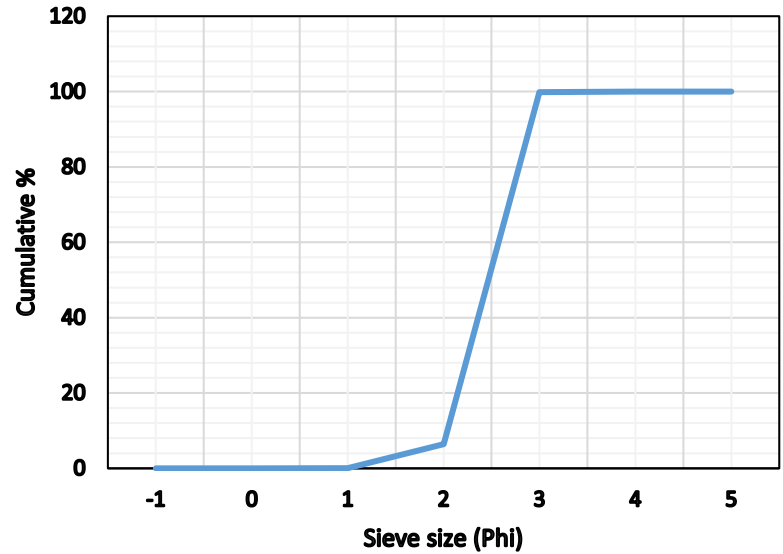


Figure A.29: Histogram (left) and cumulative curve (right) for Sample P36.

The dominant sediment grain size range is 3 ϕ (0.125 mm) and small quantity of 2 ϕ (0.25) in sample P36, and according to the Wentworth scale this grain size range fall into fine sand and

medium sand class and hence fine sand and medium sand is dominant, and there are no seashells present.

A.30 Sample P37

Aliquot mass = 293.47g

Table A.30: Retained and cumulative percentage for sample P37.

Sieve size (ϕ)	Mass retained (g)	% retained	Cumulative %
-1	4.47	1.52	1.52
0	2.68	0.91	2.43
1	2.05	0.7	3.13
2	9.6	3.27	6.4
3	273.8	93.33	99.73
4	0.78	0.27	100
5	0	0	100
Total mass	293.38		

Error = 0.03%

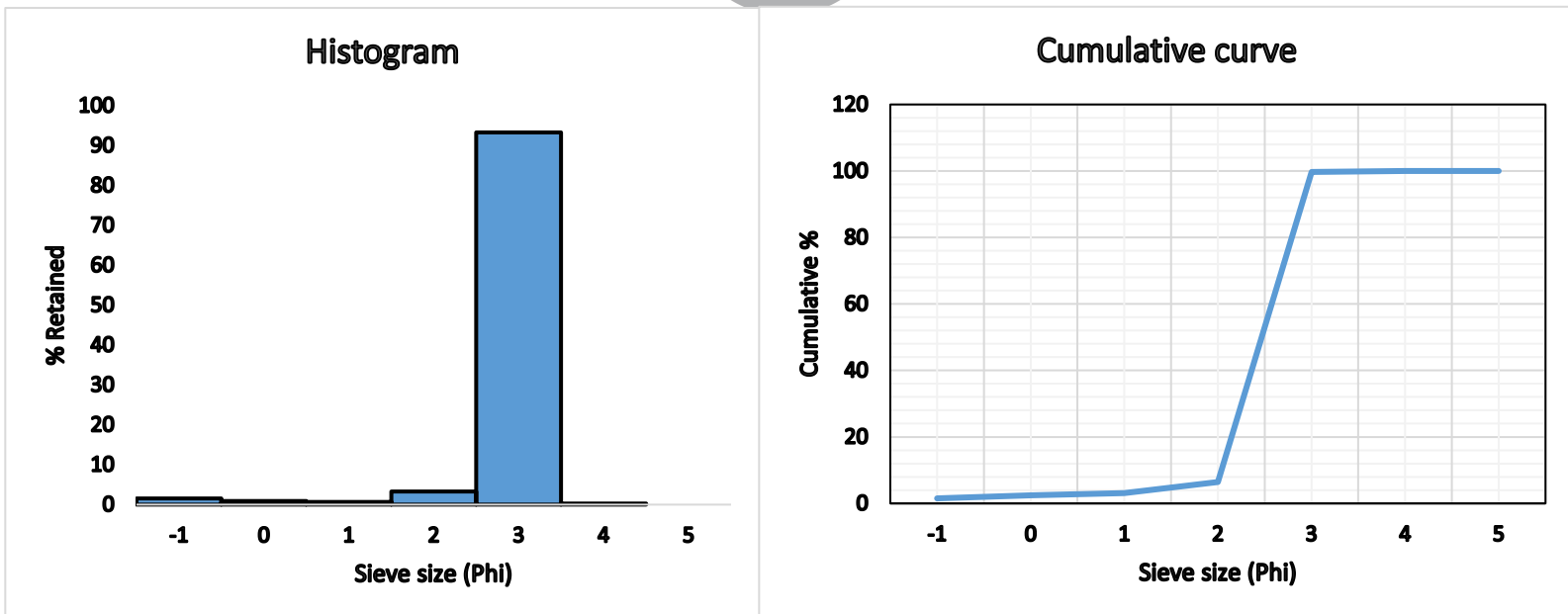
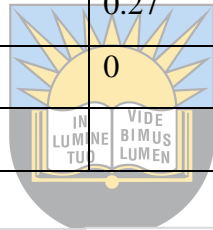


Figure A.30: Histogram (left) and cumulative curve (right) for Sample P37.

The dominant sediment grain size range is 3 ϕ (0.125 mm) and small quantity of 2 ϕ (0.25) in sample P37, and according to the Wentworth scale this grain size range fall into fine sand and medium sand class, thus fine sand and medium sand is dominant, and there are no seashells present.

A.31 Sample P38

Aliquot mass = 239.8g

Table A.31: Retained and cumulative percentage for sample P38.

Sieve size (ϕ)	Mass retained (g)	% retained	Cumulative %
-1	0.2	0.08	0.08
0	0	0	0.08
1	0.15	0.06	0.14
2	10.6	4.42	4.56
3	228.1	95.19	99.75
4	0.58	0.24	99.99
5	0	0	99.99
Total mass	239.63		

Error = 0.07%

University of Fort Hare

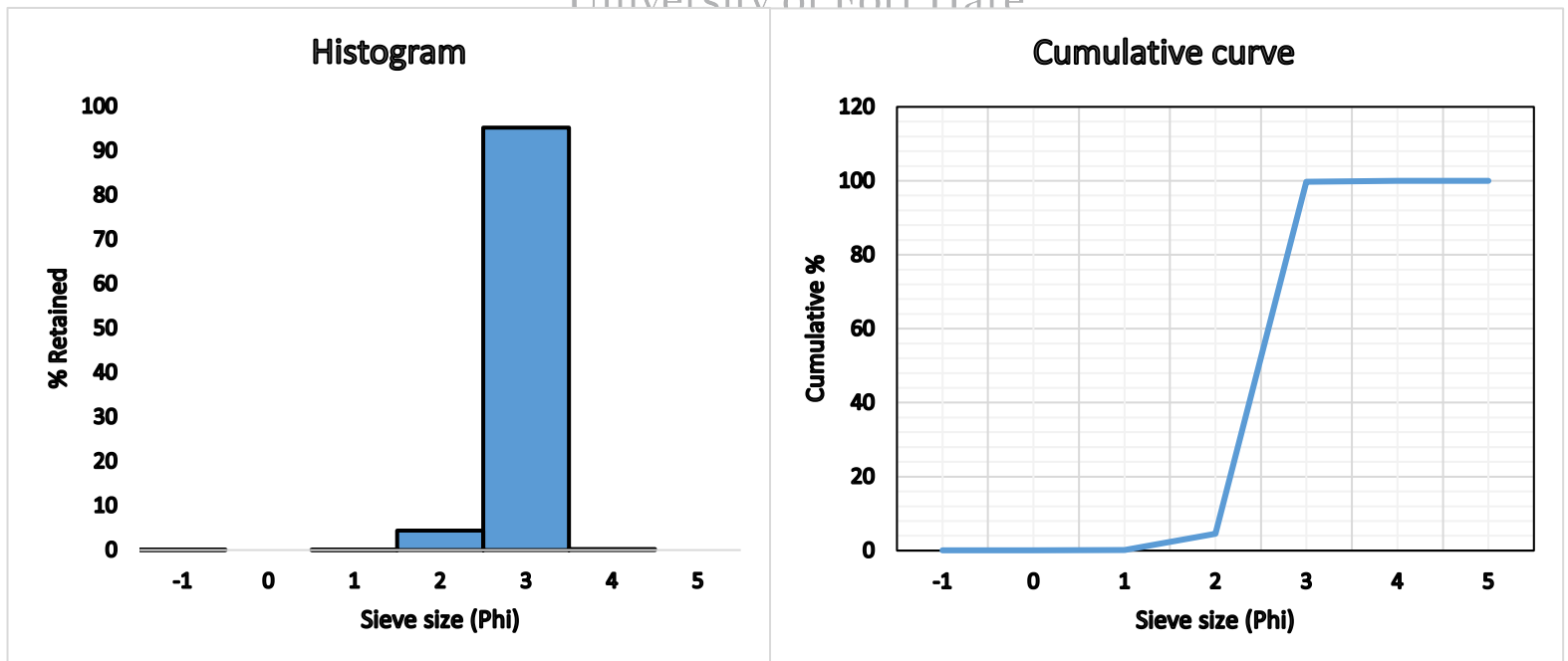


Figure A.31: Histogram (left) and cumulative curve (right) for Sample P38.

The dominant sediment grain size range is 3 ϕ (0.125 mm) and small quantity of 2 ϕ (0.25) in sample P38, and according to the Wentworth scale this grain size range fall into fine sand and medium sand class and hence fine sand and medium sand is dominant, and there are some seashells present.

A.32 Sample P39

Aliquot mass = 243.36g

Table A.32: Retained and cumulative percentage for sample P39.

Sieve size (ϕ)	Mass retained (g)	% retained	Cumulative %
-1	1.2	0.49	0.49
0	0.65	0.27	0.76
1	0.95	0.39	1.15
2	5.16	2.12	3.27
3	234.1	96.29	99.56
4	1.07	0.44	100
5	0	0	100
Total mass	243.13		

Error = 0.09%

University of Fort Hare
Together in Excellence

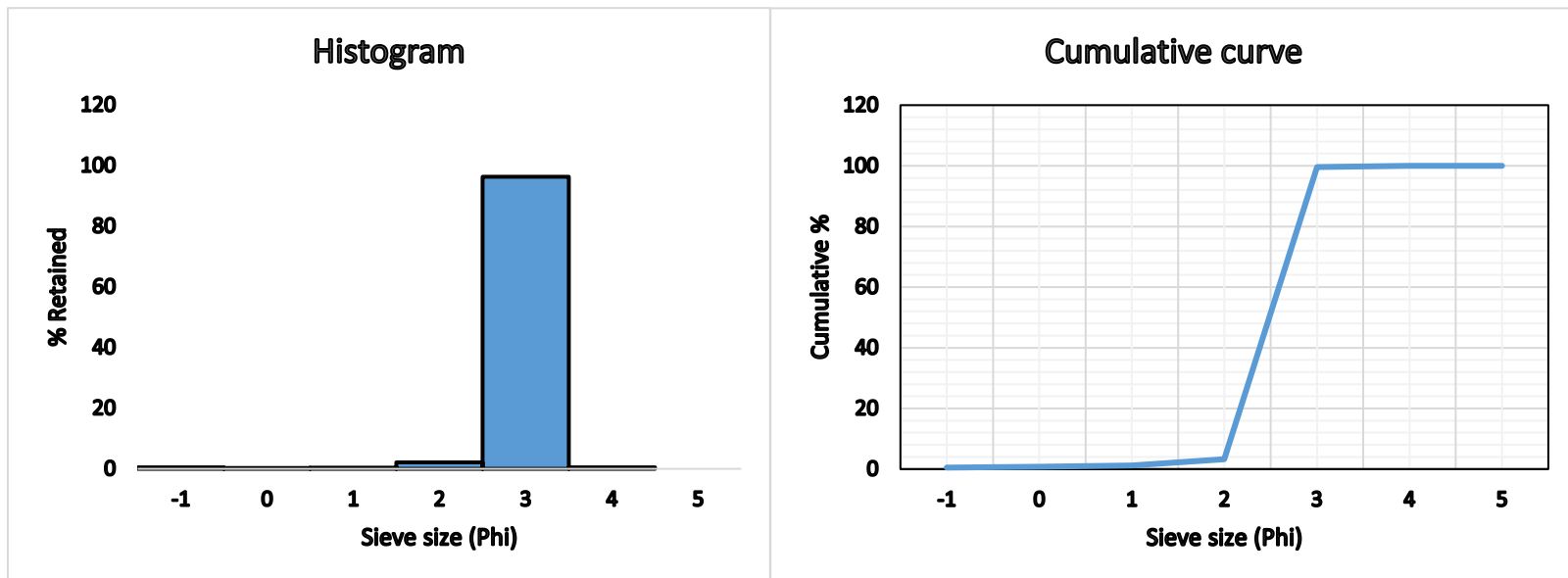


Figure A.32: Histogram (left) and cumulative curve (right) for Sample P39.

The dominant sediment grain size range is 3 ϕ (0.125 mm) in sample P39, and according to the Wentworth scale this grain size range fall into fine sand class and therefore fine sand is dominant in sample P39 and there are no seashells present.

A.33 Sample P40

Aliquot mass = 344.63g

Table A.33: Retained and cumulative percentage for sample P40.

Sieve size (ϕ)	Mass retained (g)	% retained	Cumulative %
-1	0.85	0.25	0.25
0	1.62	0.47	0.72
1	5.15	1.5	2.22
2	89.6	26.03	28.25
3	246.75	71.68	99.93
4	0.25	0.07	100
5	0	0	100
Total mass	344.22		

Error = 0.12%

University of Fort Hare

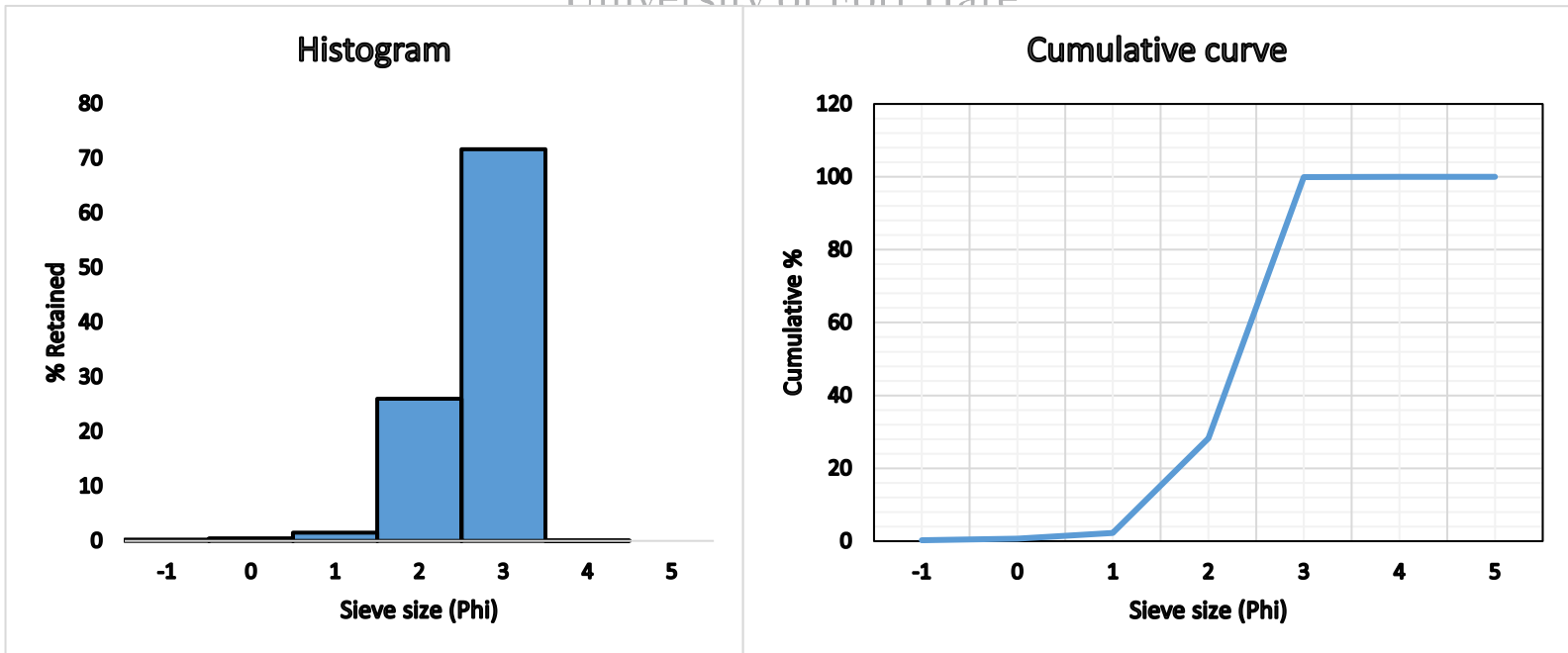


Figure A.33: Histogram (left) and cumulative curve (right) for Sample P40.

The dominant sediment grain size range is 3 ϕ (0.125 mm) and small quantity of 2 ϕ (0.25) in sample P40, and according to the Wentworth scale this grain size range fall into fine sand and medium sand class, thus fine sand and medium sand is dominant, and there are no seashells present.

A.34 Sample P41

Aliquot mass = 273.66 g

Table A.34: Retained and cumulative percentage for sample P41.

Sieve size (ϕ)	Mass retained (g)	% retained	Cumulative %
-1	7.43	2.72	2.73
0	11.06	4.06	6.78
1	9.43	3.46	10.24
2	25.16	9.23	19.47
3	199.05	73.09	92.56
4	17.71	6.50	99.06
5	2.46	0.90	99.96
Total mass	272.30		

Error = 0.4%

University of Fort Hare

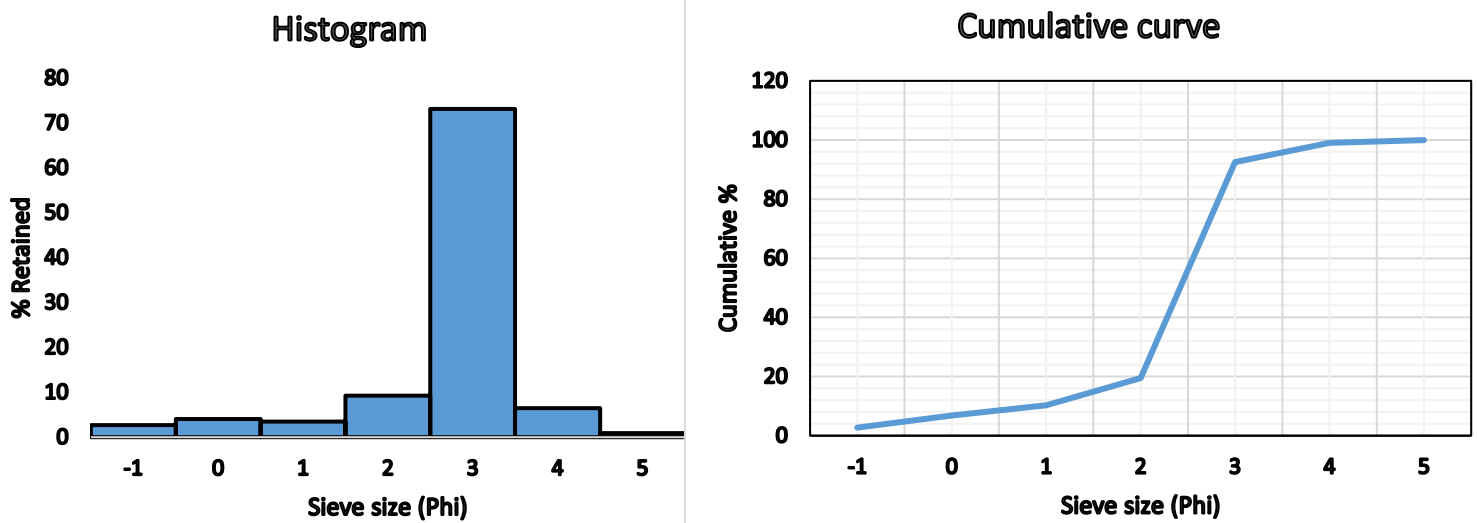


Figure A.34: Histogram (left) and cumulative curve (right) for Sample P41.

The dominant sediment grain size range is 3 ϕ (0.125 mm) followed by 2 ϕ (0.25 mm) and small percentages of the remaining sieves. According to the Wentworth scale this grain size range fall

into fine sand and medium sand class and therefore fine sand and medium sand is dominant in sample P41, with some coarse silt and no seashells present.

A.35 Sample P42

Aliquot mass = 196.77 g

Table A.35: Retained and cumulative percentage for sample P42.

Sieve size (ϕ)	Mass retained (g)	% retained	Cumulative %
-1	0	0	0
0	0.	0	0
1	0.15	0.08	0.08
2	4.32	2.21	2.29
3	190.98	97.58	99.87
4	0.16	0.08	99.95
5	0.10	0.05	100
Total mass	195.71		

Error = 0.5%

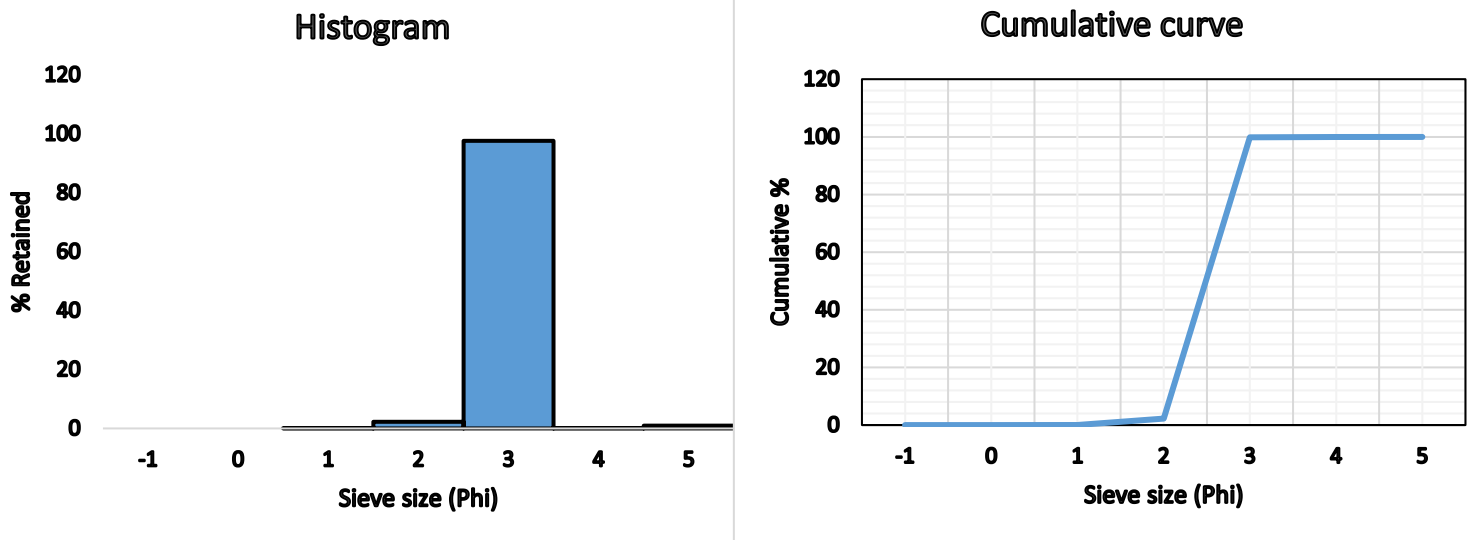
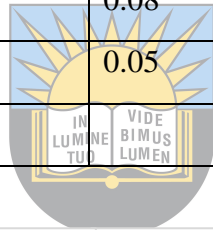


Figure A.35: Histogram (left) and cumulative curve (right) for Sample P42.

The dominant sediment grain size range is 3 ϕ (0.125 mm) in sample P42, and according to the Wentworth scale this grain size range fall into fine sand class and therefore fine sand is dominant in sample P42 and there are no seashells present.

A.36 Sample P43

Aliquot mass = 224.23g

Table A.36: Retained and cumulative percentage for sample P43.

Sieve size (ϕ)	Mass retained (g)	% retained	Cumulative %
-1	4.08	1.82	1.82
0	1.02	0.46	2.28
1	0.88	0.39	2.67
2	2.4	1.07	3.74
3	214.48	95.72	99.46
4	1.22	0.54	100
5	0	0	100
Total mass	224.08		

Error = 0.07%

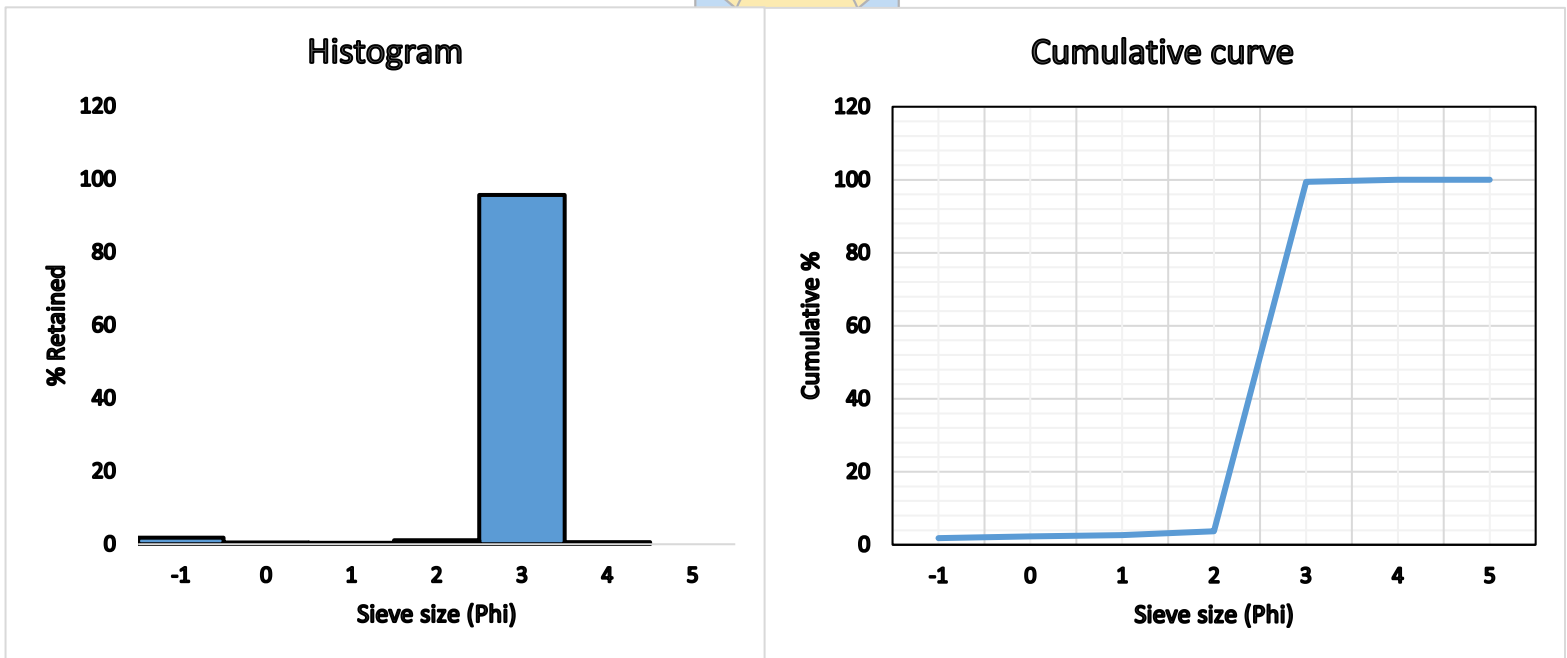


Figure A.36: Histogram (left) and cumulative curve (right) for Sample P43.

The dominant sediment grain size range is 3 ϕ (0.125 mm) in sample P43, and according to the Wentworth scale this grain size range fall into fine sand class and therefore fine sand is dominant in sample P43 and there are no seashells present.

A.37 Sample P44

Aliquot mass = 269.01g

Table A.37: Retained and cumulative percentage for sample P44.

Sieve size (ϕ)	Mass retained (g)	% retained	Cumulative %
-1	0.06	0.02	0.02
0	0.11	0.04	0.06
1	0.45	0.17	0.23
2	21.77	8.1	8.33
3	245.83	91.49	99.82
4	0.47	0.17	99.99
5	0	0	99.99
Total mass	268.69		

Error = 0.12%

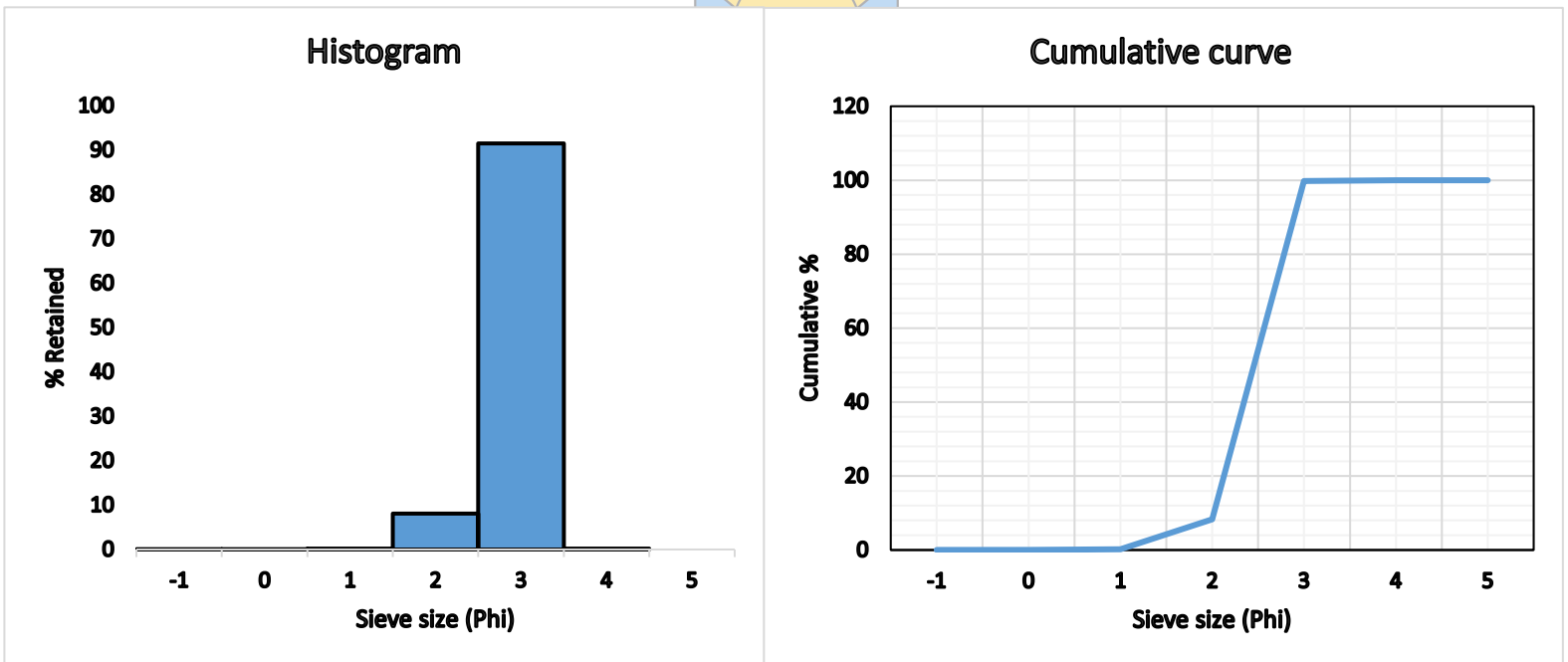
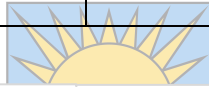


Figure A.37: Histogram (left) and cumulative curve (right) for Sample P44.

The dominant sediment grain size range is 3 ϕ (0.125 mm) and small quantity of 2 ϕ (0.25) in sample P44, and according to the Wentworth scale this grain size range fall into fine sand and medium sand class, and thus fine sand and medium sand is dominant, and there are some seashells present.

A.38 Sample P45

Aliquot mass = 296.55g

Table A.38: Retained and cumulative percentage for sample P45.

Sieve size (ϕ)	Mass retained (g)	% retained	Cumulative %
-1	0.13	0.04	0.04
0	0	0	0.04
1	0.17	0.06	0.1
2	17.69	5.97	6.07
3	277.88	93.79	99.86
4	0.4	0.14	100
5	0	0	100
Total mass	296.27		

Error = 0.09%

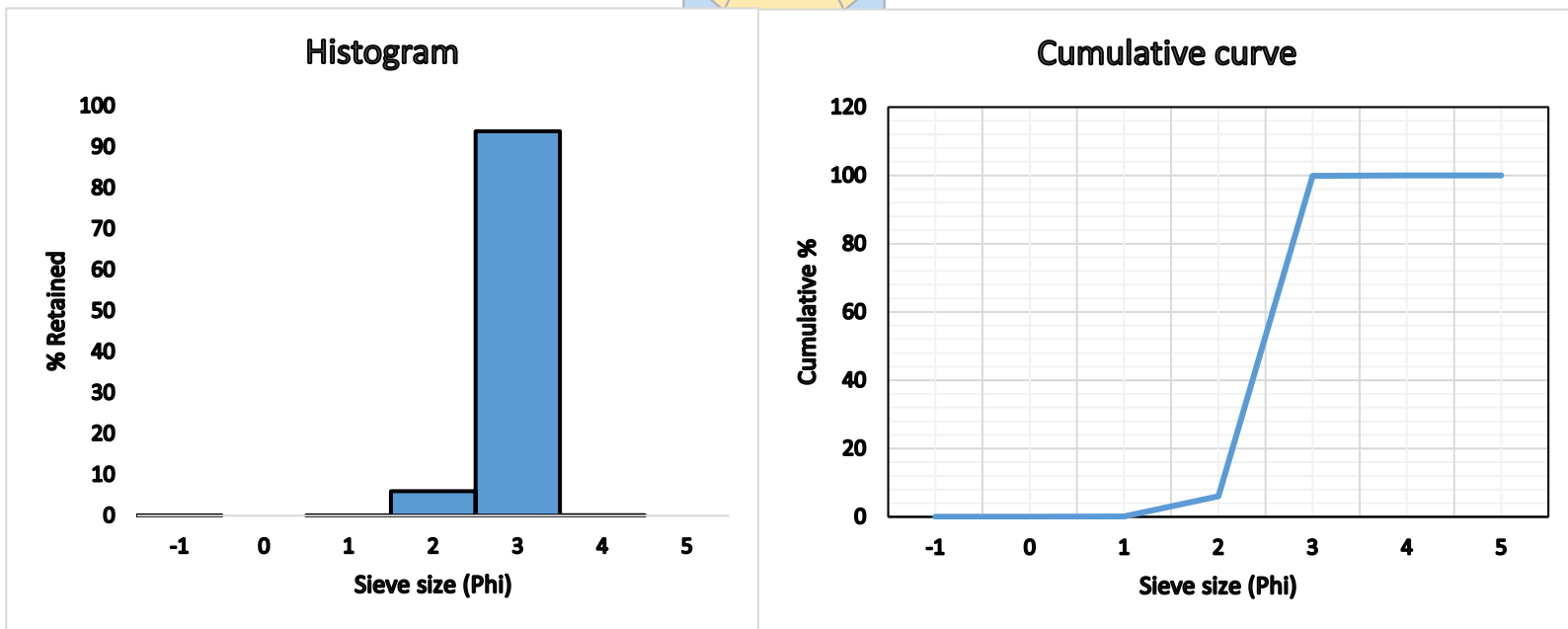
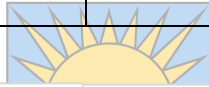


Figure A.38: Histogram (left) and cumulative curve (right) for Sample P45.

The dominant sediment grain size range is 3 ϕ (0.125 mm) and small quantity of 2 ϕ (0.25) in sample P45, and according to the Wentworth scale this grain size range fall into fine sand and medium sand class and hence fine sand and medium sand is dominant, and there are some seashells present.

A.39 Sample P46

Aliquot mass = 323.17g

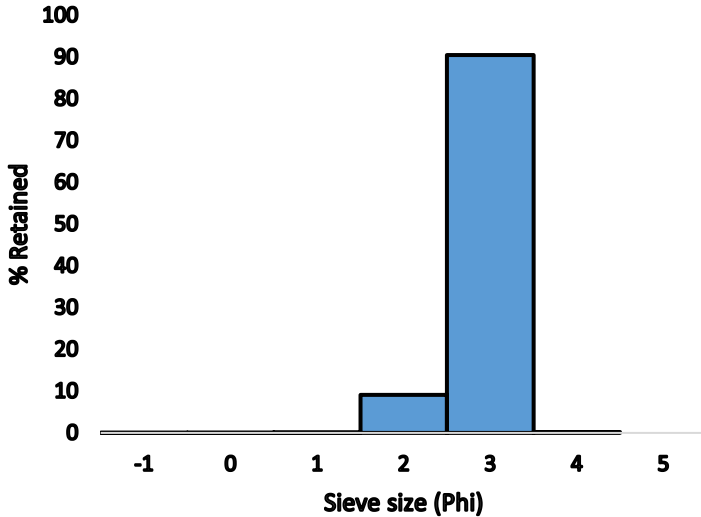
Table A.39: Retained and cumulative percentage for sample P46.

Sieve size (ϕ)	Mass retained (g)	% retained	Cumulative %
-1	0.28	0.09	0.09
0	0.15	0.05	0.14
1	0.37	0.11	0.25
2	29.32	9.08	9.33
3	292.18	90.49	99.82
4	0.6	0.19	100.01
5	0	0	100.01
Total mass	322.9		

Error = 0.08%



Histogram



Cumulative curve

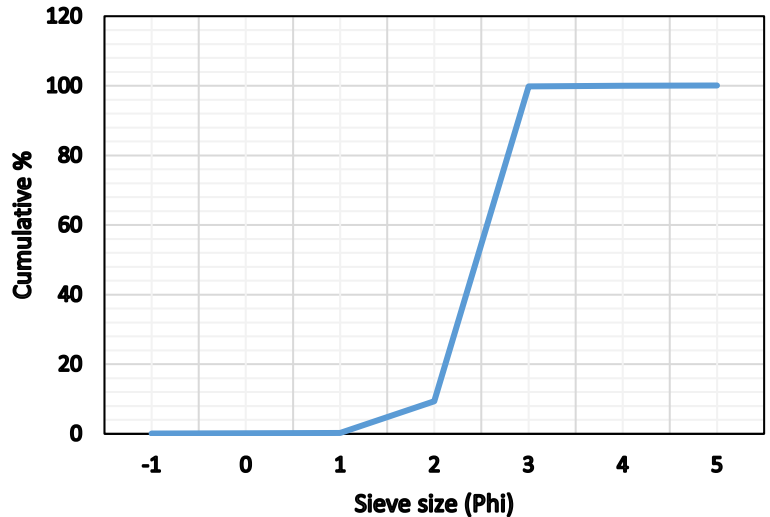


Figure A.39: Histogram (left) and cumulative curve (right) for Sample P46.

The dominant sediment grain size range is 3 ϕ (0.125 mm) and small quantity of 2 ϕ (0.25) in sample P46, and according to the Wentworth scale this grain size range fall into fine sand and medium sand class, thus fine sand and medium sand is dominant, and there are no seashells present

A.40 Sample P47

Aliquot mass = 284.75g

Table A.40: Retained and cumulative percentage for sample P47.

Sieve size (ϕ)	Mass retained (g)	% retained	Cumulative %
-1	0	0	0
0	0	0	0
1	0.08	0.03	0.03
2	14.18	4.98	5.01
3	269.9	94.85	99.86
4	0.4	0.14	100
5	0	0	100
Total mass	284.56		

Error = 0.07%

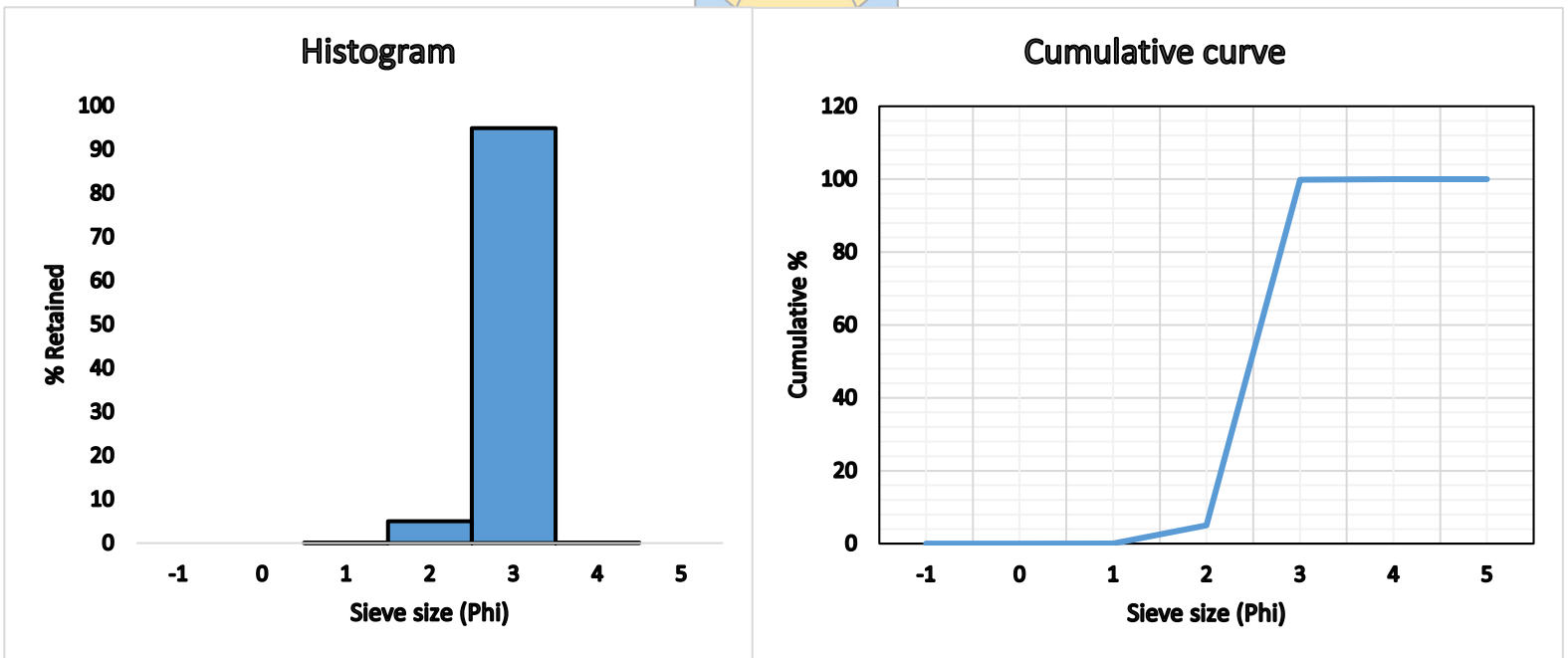


Figure A.40: Histogram (left) and cumulative curve (right) for Sample P47.

The dominant sediment grain size range is 3 ϕ (0.125 mm) followed by small percentages of grain size range of 2 ϕ (0.25 mm), and according to the Wentworth scale this grain size range fall into fine sand and medium sand class, hence fine and medium sand is dominant in sample P47 and there are no seashells present.

A.41 Sample P48

Aliquot mass = 307.45g

Table A.41: Retained and cumulative percentage for sample P48.

Sieve size (ϕ)	Mass retained (g)	% retained	Cumulative %
-1	0.77	0.25	0.25
0	0.8	0.26	0.51
1	7.05	2.3	2.81
2	99.73	32.48	35.29
3	198.57	64.66	99.95
4	0.17	0.06	100.01
5	0	0	100.01
Total mass	307.09		

Error = 0.12%

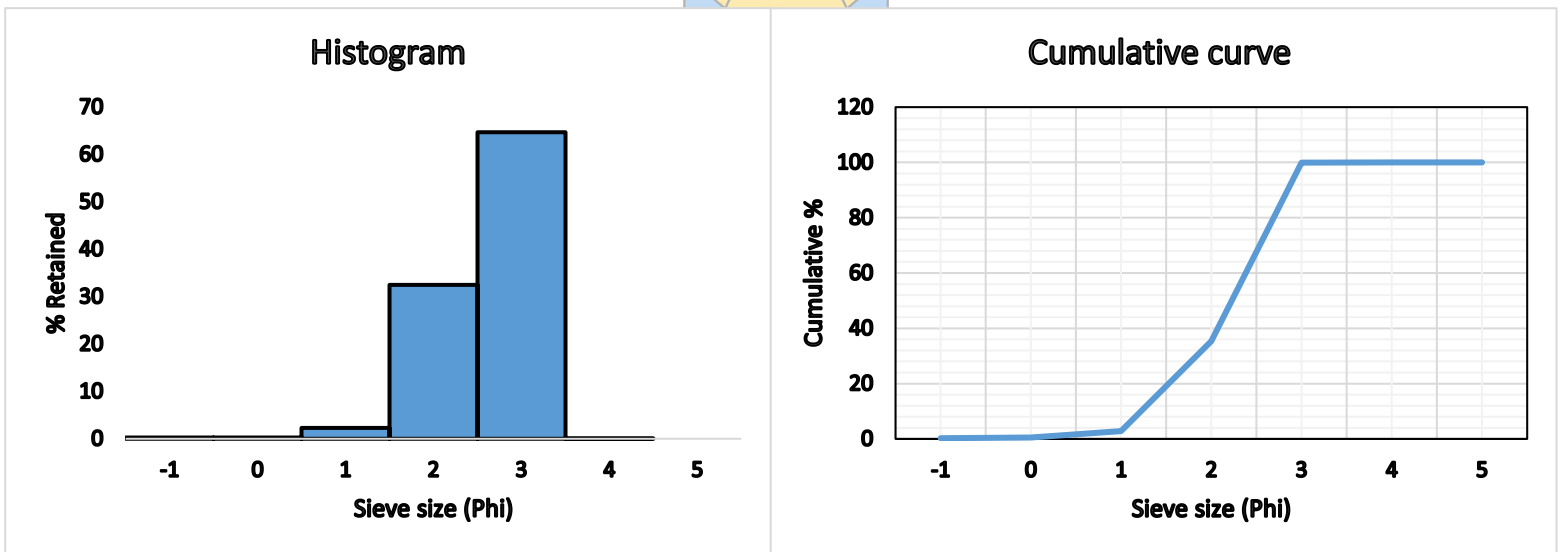
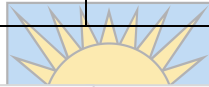


Figure A.41: Histogram (left) and cumulative curve (right) for Sample P48.

The dominant sediment grain size range is 3 ϕ (0.125 mm) followed by a considerable percentages of grain size range of 2 ϕ (0.25 mm) and a small percentage at 1 ϕ , and according to the Wentworth scale this grain size range fall into fine sand and medium sand class, and therefore fine and medium sand is dominant in sample P48 and there are no seashells present.

A.42 Sample P49

Aliquot mass = 265.4g

Table A.42: Retained and cumulative percentage for sample P49.

Sieve size (ϕ)	Mass retained (g)	% retained	Cumulative %
-1	0.87	0.33	0.33
0	0.95	0.36	0.69
1	1.45	0.55	1.24
2	24	9.06	10.3
3	237.2	89.58	99.88
4	0.33	0.12	100
5	0	0	100
Total mass	264.8		

Error = 0.23%

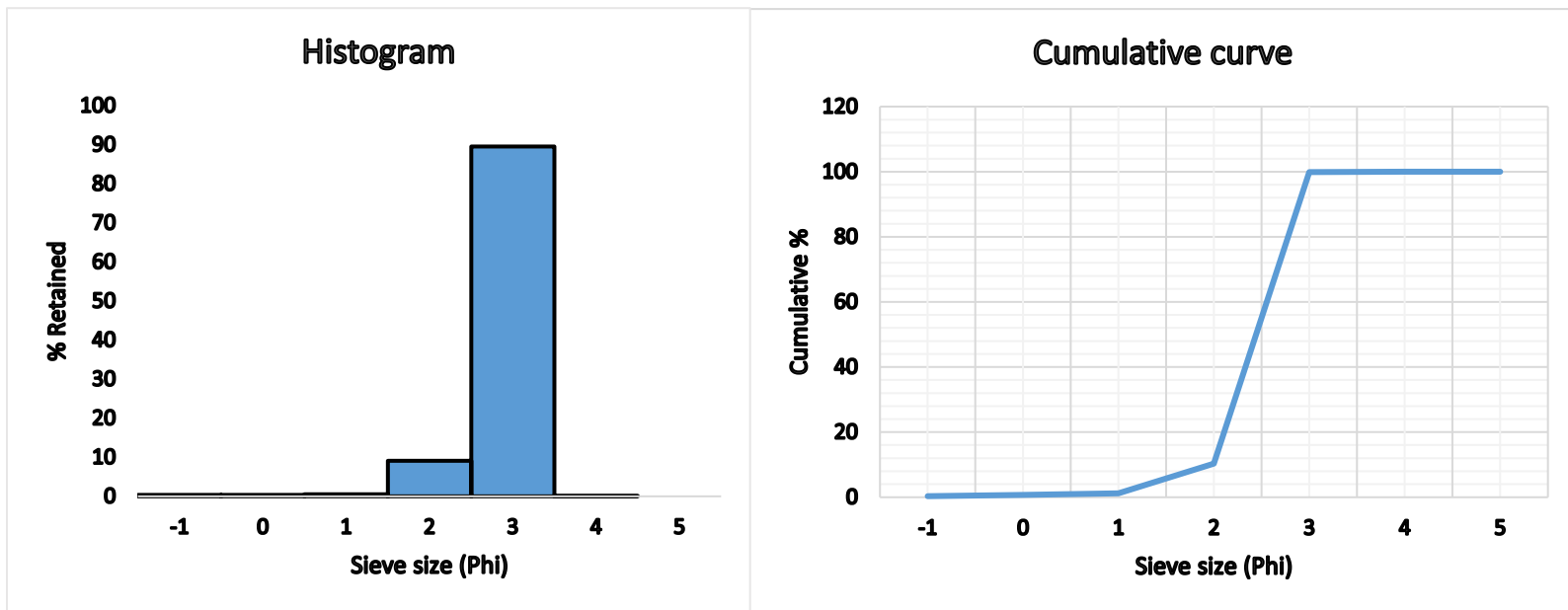


Figure A.42: Histogram (left) and cumulative curve (right) for Sample P49.

The dominant sediment grain size range is 3 ϕ (0.125 mm) followed by small percentages of grain size range of 2 ϕ (0.25 mm), and according to the Wentworth scale this grain size range fall into fine sand and medium sand class and therefore fine and medium sand is dominant in sample P49, and there are some seashells present.

A.43 Sample P50

Aliquot mass = 299.43g

Table A.43: Retained and cumulative percentage for sample P50.

Sieve size (ϕ)	Mass retained (g)	% retained	Cumulative %
-1	0	0	0
0	0	0	0
1	0	0	0
2	9.48	3.17	3.17
3	289.1	96.64	99.81
4	0.57	0.19	100
5	0	0	100
Total mass	299.15		

Error = 0.09%

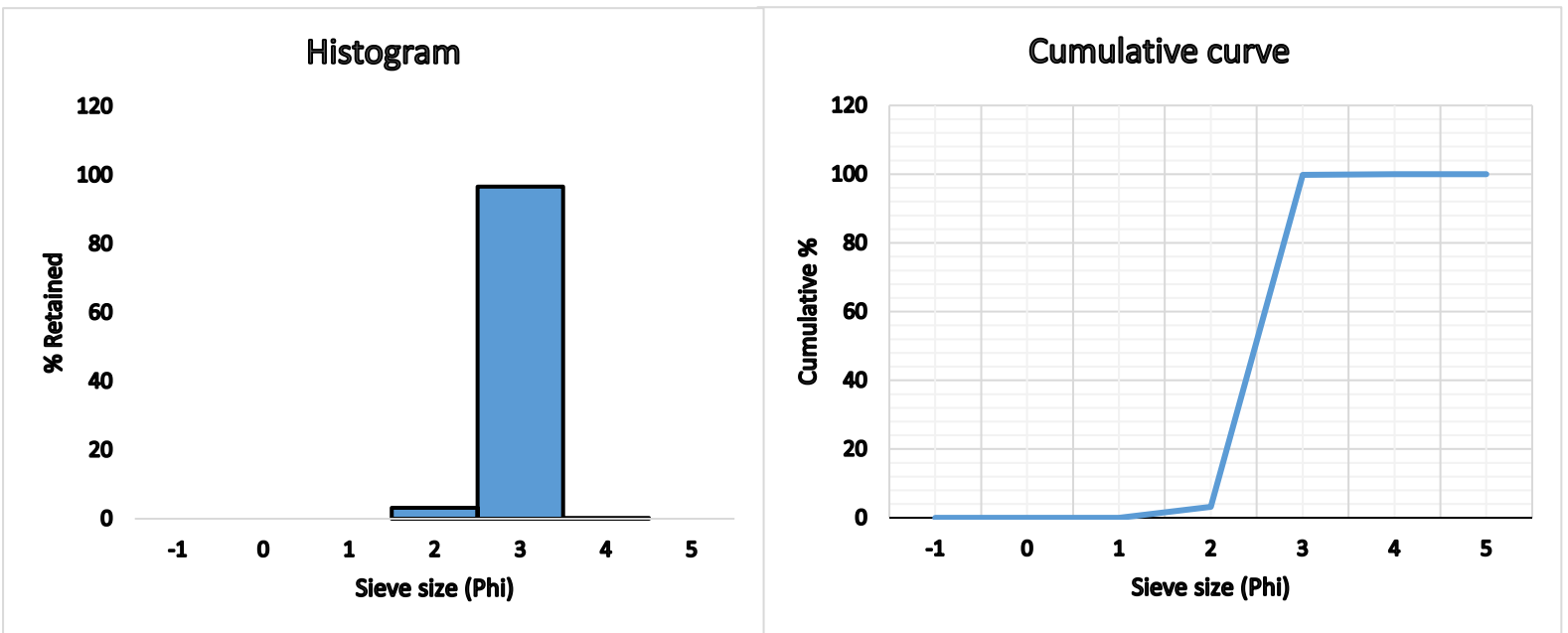


Figure A.43: Histogram (left) and cumulative curve (right) for Sample P50.

The dominant sediment grain size range is 3 ϕ (0.125 mm) followed by a considerable percentages of grain size range of 2 ϕ (0.25 mm) and according to the Wentworth scale this grain size range fall into fine sand and medium sand class and thus fine and medium sand is dominant in sample P50 and there are no seashells present.